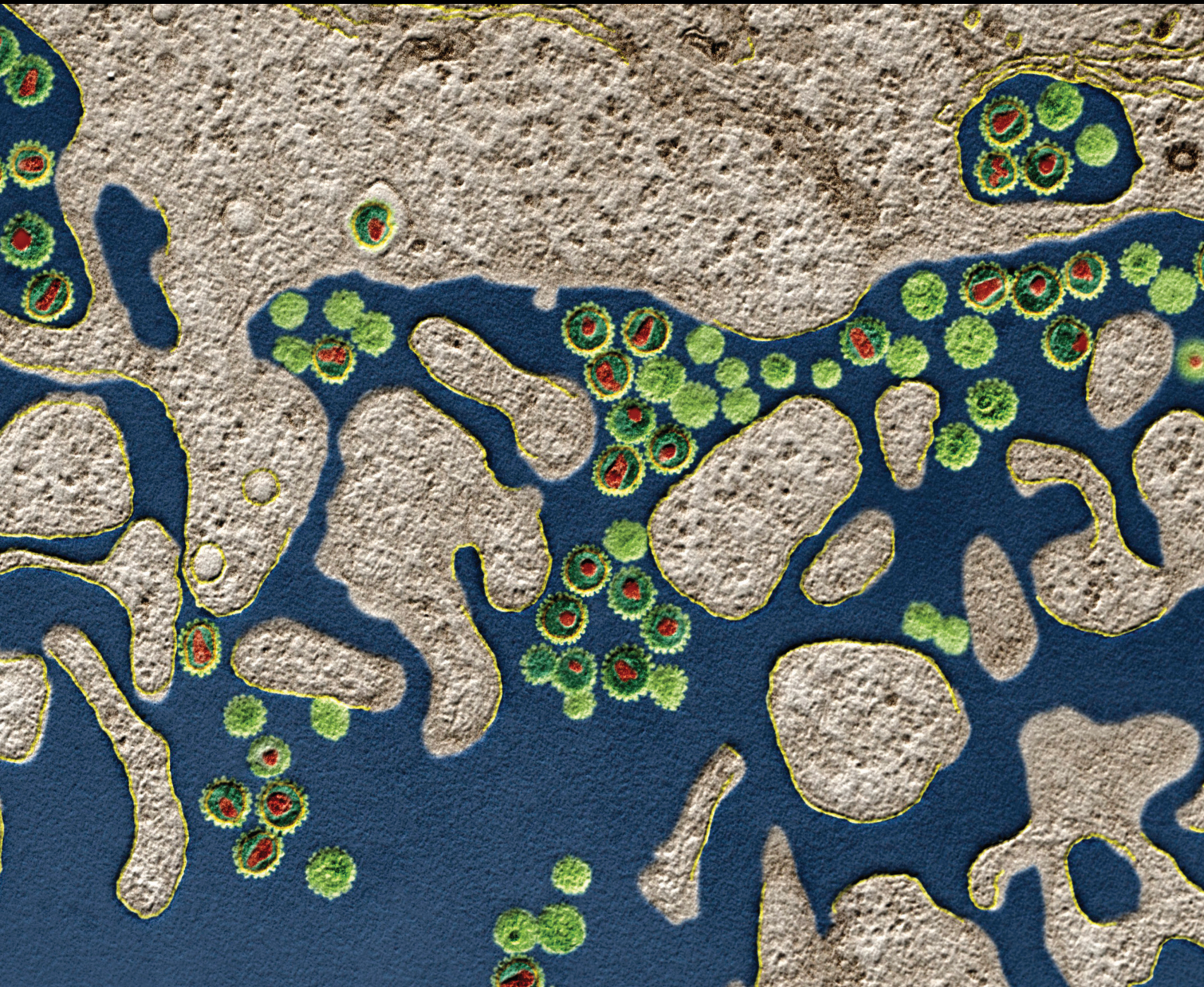# Immune System and Chronic Diseases 2021

Lead Guest Editor: Margarete D. Bagatini
Guest Editors: Charles Elias Asmann, Cristina R. Reschke, and Fabiano Carvalho

Immune System and Chronic Diseases 2021

Immune System and Chronic Diseases 2021

Lead Guest Editor: Margarete D. Bagatini
Guest Editors: Charles Elias Asmann, Cristina R. Reschke, and Fabiano Carvalho

Contents

Research Article

Recovery from Liver Failure and Fibrosis in a Rat Portacaval Anastomosis Model after Neurointermediate Pituitary Lobectomy

Martín Muñoz-Ortega [ID],[1] **Noé Macías-Segura,**[2] **Javier Ventura-Juárez** [ID],[3]
Manuel Enrique Ávila-Blanco,[3] **Leonardo D. Ponce-Damian,**[2] **Daniel González-Blas,**[4]
Esperanza Sánchez-Alemán,[3] **and Andrés Quintanar-Stephano** [ID][2]

[1]*Departamento de Química, Centro de Ciencias Básicas, Universidad Autónoma de Aguascalientes, Aguascalientes, PC 20100, Mexico*
[2]*Departmento Fisiología y Farmacología, Centro de Ciencias Básicas, Universidad Autónoma de Aguascalientes, Aguascalientes, PC 20100, Mexico*
[3]*Departamento de Morfología, Centro de Ciencias Básicas, Universidad Autónoma de Aguascalientes, Aguascalientes, PC 20100, Mexico*
[4]*Departamento de Patología, Hospital General ISSSTE, Aguascalientes, PC 20010, Mexico*

Correspondence should be addressed to Andrés Quintanar-Stephano; aquinta@correo.uaa.mx

Liver diseases, including cirrhosis, viral hepatitis, and hepatocellular carcinoma, account for approximately two million annual deaths worldwide. They place a huge burden on the global healthcare systems, compelling researchers to find effective treatment for liver fibrosis-cirrhosis. Portacaval anastomosis (PCA) is a model of liver damage and fibrosis. Arginine vasopressin (AVP) has been implicated as a proinflammatory-profibrotic hormone. In rats, neurointermediate pituitary lobectomy (NIL) induces a permanent drop (80%) in AVP serum levels. We hypothesized that AVP deficiency (NIL-induced) may decrease liver damage and fibrosis in a rat PCA model. Male Wistar rats were divided into intact control (IC), NIL, PCA, and PCA+NIL groups. Liver function tests, liver gene relative expressions (IL-1, IL-10, TGF-β, COLL-I, MMP-9, and MMP-13), and histopathological assessments were performed. In comparison with those in the IC and PCA groups, bilirubin, protein serum, and liver glycogen levels were restored in the PCA+NIL group. NIL in the PCA animals also decreased the gene expression levels of IL-1 and COLL-I, while increasing those of IL-10, TGF-β, and MMP-13. Histopathology of this group also showed significantly decreased signs of liver damage with lower extent of collagen deposition and fibrosis. Low AVP serum levels were not enough to fully activate the AVP receptors resulting in the decreased activation of cell signaling pathways associated with proinflammatory-profibrotic responses, while activating cell molecular signaling pathways associated with an anti-inflammatory-fibrotic state. Thus, partial reversion of liver damage and fibrosis was observed. The study supports the crucial role of AVP in the inflammatory-fibrotic processes and maintenance of immune competence. The success of the AVP deficiency strategy suggests that blocking AVP receptors may be therapeutically useful to treat inflammatory-fibrotic liver diseases.

1. Introduction

Liver diseases (e.g., cirrhosis, viral hepatitis, and hepatocellular carcinoma) create an enormous burden on the global healthcare system, accounting for approximately two million deaths per year. In Mexico, it is the third leading cause of death in men and seventh in women [1]. Currently, research into new treatments for liver diseases is of great importance.

Liver disease and fibrosis are the result of chronic inflammatory processes, which are independent of its etiology (e.g., drugs, alcohol history, hepatitis virus B and C, obesity, and autoimmunity). Liver inflammation and fibrosis are initiated in response to permanent liver damage with excessive accumulation of collagen overdegradation [2–5]. During the initial stage, liver damage induces the release of proinflammatory cytokines like IL-1, TNF-α, and IL-8 [2, 3, 6]. If

the liver damage persists, the inflammatory response includes infiltration of lymphocytes, plasma cells, polymorphonuclear cells, histiocytes, fibroblast, and development of regeneration nodules, vascular distortion, and fibrosis [3]. During persistent inflammation, the hepatic stellate cells (HSCs) are activated by different kind of factors: cytokines (IL-1, TNF-α, and IL-8), growth factors (TGF-β, PDGF, and ET-1), and factors from the endothelial cells, Kupffer's cells, hepatocytes, and platelets. All these factors induce differentiation of HSCs into myofibroblasts with properties such as proliferation, contraction, fibrogenesis, and expression of type I collagen (Col1al) and alpha-smooth muscle actin (α-SMA) [2, 4], thus making HSCs one of the main responsible factors for liver fibrosis and liver failure. Currently, liver fibrosis treatment is done to revert fibrosis and to restore the liver functions [2, 7–10].

There are several models of experimental fibrosis-cirrhosis, which have physio-pathogenic characteristics of the human cirrhosis. Some models of the experimental liver fibrosis are induced by (1) CCl_4 administration for eight weeks, (2) acetaminophen administration for ten weeks, (3) ethanol administration for more than ten weeks, (4) hypercaloric diets for more than 12 weeks [5, 7, 8, 11], and (5) portacaval anastomosis (PCA) [12–14].

In rats, PCA induces a decrease in serum albumin, hyperbilirubinemia, and increased serum levels of bile acids, alkaline phosphatase (AP), aspartate aminotransferase (AST), alanine aminotransferase (ALT), lactate dehydrogenase (LDH), creatinine, urea, and ammonium [13–15] with clear signs of liver histopathological damage such as hepatocytic necrosis and apoptosis, portal inflammation, biliary proliferation, steatosis, and fibrosis. All these observations indicate that the PCA model reproduces the clinical and histopathological signs of chronic liver disease [13–15].

In recent years, neuro-immune-endocrine interactions in inflammatory diseases have allowed for a better understanding of pathological regulatory processes. In this context, arginine vasopressin (AVP), also called antidiuretic hormone, synthesizes in the paraventricular and supraoptic nuclei of the hypothalamus, passes through the axons to the posterior lobe of the pituitary gland (neurohypophysis), and releases into the blood. Corticotropin-releasing hormone (CRH) and AVP of the hypothalamic paraventricular parvocellular neurons play an important role in coordinating hypothalamic-pituitary-adrenal axis activity during stress, inflammation, and autoimmune diseases [16, 17]. AVP also has several other activities that include diuresis inhibition, contraction of vascular smooth muscle cells, and liver glycogenolysis. AVP is also involved in several brain functions that affect memory, anxiety, and depression [18, 19]. Presently, most of the evidence indicates that AVP acting directly on different cells of the immune system is a proinflammatory hormone [20–23]. We have shown that animals that underwent surgical removal of the neurohypophysis (NIL) showed a permanent decrease in AVP and oxytocin (OXT) blood levels (80% and 90% below the normal ranges, respectively) [24]. Experiments from others [25] and from our lab have demonstrated that decreased AVP serum levels (NIL-induced) diminish humoral and cellular immune responses [20, 21, 26, 27]. Profibrogenic properties of AVP on the heart, liver, and kidney have been demonstrated [28–32]. In addition, we have reported that AVP deficiency promotes the reduction of collagen deposits in a CCl_4 cirrhosis hamster model and restores the balance between metalloproteinases and tissue inhibitors of metalloproteinases (TIMPs) [33]. All this evidence supports that AVP is a major player in the regulation of immune responses and fibrosis; however, less is known on cell and molecular mechanisms through AVP deficiency may modulate the immune responses. Thus, in this work, we study the effects of AVP deficiency (NIL-induced) on liver inflammation, tissue damage, and fibrosis in the PCA rat model.

2. Materials and Methods

2.1. Animals. Male Wistar rats (*Rattus norvegicus*) at 6-8 weeks old (200-250 g body weight) from our Animal Care Facility were used. Animals were treated according to the Institutional Normative Welfare Standards of the Autonomous University of Aguascalientes and the official Mexican regulations (NOM-062-ZOO-1999). Experimental protocols were approved by the Institutional Bioethics Committee.

Animals were maintained in a 12 h/12 h light/dark cycle and 21-22°C room temperature and fed with Purina Rat Chow (Ralston Purina Company, St. Louis, MO, USA). Food and water were provided *ad libitum*. The rats were divided into the following four groups (4-6 animals/group): (1) intact control (IC), (2) NIL, (3) PCA, and (4) PCA+NIL. In the PCA+NIL group, NIL surgery was performed three weeks after PCA. Figure 1 shows the experimental schedule.

2.2. Portacaval Anastomosis (PCA). PCA was performed at week 0 in the PCA and PCA+NIL groups (Figure 1). The PCA microsurgery technique used was an adaptation of those described by Aller et al. [13] and Padilla-Sánchez [34]. Rats were anesthetized with a mixture of ketamine (80%) and xylazine (20%) (Cheminova, Mexico) (1 μL/g of body weight/i.p.), and a laparotomy was performed to access the abdominal organs. Under stereomicroscope (Zeiss OPMI-19 FC at 6x magnification), the portal vein was dissected, followed by the right kidney vein and the inferior cava vein. The cava vein was dissected from above the left kidney vein to where the cava vein is covered by the liver lobule. The right kidney vein and the ends of the isolated cava vein were transiently occluded by a gentle pull of removable threads. On the left side of the dissected cava, a window was opened and washed with heparin-saline solution (1%) (Inhepar, Heparina, Pisa, Mexico). The dissected portal vein was temporarily occluded with a surgical clip at its union with the splenic vein, and the vein was tied and cut below the knot at the hilum liver level. The remnant vein blood was washed with heparin-saline solution. The open end of the portal vein was then anastomosed with the cava vein window. The PCA was performed in less than 15 min. After surgery, the animals were placed in a recovery box with clinical oxygen and controlled temperature. For infection prevention, animals were injected with penprocillin (6000 IU, i.m.) (Pisa, Mexico) once a day for three days.

Bleeding and euthanized

(i) Serum aliquots for liver function tests: AST, ALT, TB, BUN, Alb, TP, and AP

Liver samples:

(i) RNA later for inflammatory and fibrogenic factors expression: COL-1, MMP-13, MMP-9, TGF-β, IL-10, IL-1

(ii) Liver slides stained with H-E, Masson trichrome and Sirius red for histopathological and collagen content studies

(iii) Glycogen content.
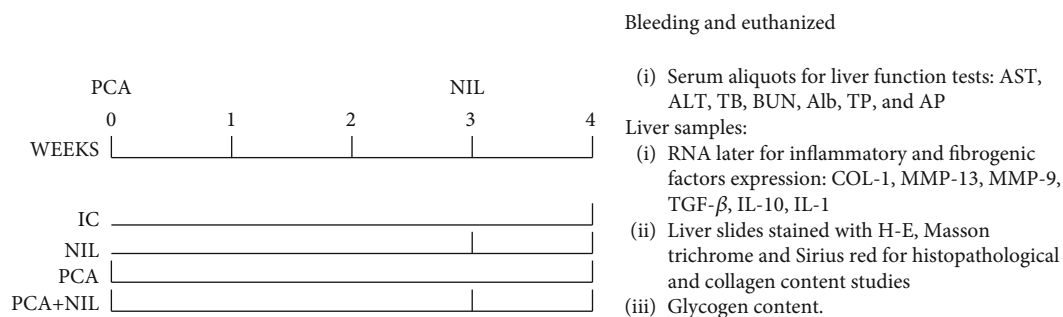
FIGURE 1: Experimental schedule. Rats were divided into intact control (IC), neurointermediate pituitary lobectomy (NIL), portacaval anastomosis (PCA), and the PCA+NIL groups. PCA and NIL surgeries were performed at weeks 0 and 3, respectively. At week 4, all animals were anesthetized, bled, and euthanized. Serum aliquots were used for assessing functional liver test, tissue liver samples were used to assess inflammatory and fibrogenic factors expression, histopathological studies and collagen and glycogen contents. $n = 4 - 6$ animals/group.

For analgesia, sodium metamizole (Pharmalife, Mexico) (10 mg/kg i.m.) was administrated once daily for three days. After anesthesia recovery, the animals were put in cages with food and water *ad libitum*.

2.3. Neurointermediate Pituitary Lobectomy (NIL).

NIL surgeries were performed on the NIL and PCA+NIL groups at week 3 of the experiment (see experimental schedule in Figure 1).

The method employed has been described in our previous work [35]. Fifteen minutes prior to anesthesia, 0.06 mg atropine/s.c. (Atropisa, Pisa, Mexico) was injected to prevent excessive airway secretion. Animals were anesthetized with a mixture of ketamine 80% and xylazine 20% (1 μL/g body weight/i.p.). Removal of the neurointermediate pituitary lobe (neural and intermediate lobes) was performed under a dissecting microscope (Zeiss OPMI-19 FC at 6x magnification) through the parapharyngeal-transoccipital-sphenoidal approach. After direct viewing of the neurointermediate lobe, it was gently aspirated using a bent needle as follows. The neck was shaved, and the animal was placed into dorsal decubitus on the operating table. With the upper incisor fork, the head was fixed to the table, while the legs were fastened with threads to the lateral edges of the table. The trachea was cannulated through the snout. The surgical approach to the pituitary gland included the following steps: (1) asepsis and cutting of the skin on the anterior aspect of the neck, (2) identification of the left digastric muscle, (3) blunt separation of the digastric muscle central tendon, (4) placement of retractors to get a wider view of the bottom of the opening, (5) identification of the distal end of the pterygoid process and the long neck muscles, (6) identification and cleaning of the basioccipital and basisphenoid bones, (7) display of the occipital-sphenoid joint, (8) trepanation of the skull in the center of the occipital-sphenoid joint until the pituitary capsule can be viewed, (9) cutting of the pituitary capsule at its most posterior end, (10) elevation of the adenohypophyseal lobe and visual identification of the intermediate and neural lobes of the hypophysis, and (11) gentle aspiration of the neurointermediate lobe with a bent needle.

The total time of the surgery was within 15 min, and animals were fully recovered within 40 min. For infection prevention, animals were injected with penprocillin after the surgery (6000 IU, i.m./3 days). For analgesia, sodium metamizole (10 mg/kg/i.m./2 days) was used.

All groups were euthanized at the fourth week of experimentation. Before euthanasia, animals were anesthetized with sodium pentobarbital (Maver, China), bled from the abdominal aorta, and the serum was aliquoted and frozen at −70°C until the liver function tests. Samples of liver tissue were immediately immersed in RNA later (Invitrogen, Thermo Fisher Scientific, USA) and processed to determine pro- and anti-inflammatory and pro- and antifibrogenic gene expression (relative levels). For histopathological study, liver tissue samples were fixed in 10% neutral formalin solution in paraffin, cut into 5 μm thick slices, mounted on slides, and stained with hematoxylin-eosin (HE) for histopathological study and Masson's trichrome and Sirius Red stains for fibrosis area and collagen content estimation [36]. Fuji software was used to determine the percentage of fibrosis area [37] from Sirius Red-stained slides observed under polarized light at 400x magnification. The histopathological study was performed under a Nikon light microscope Optiphot-2.

2.4. Liver Function Tests.

Serum samples were defrosted, and the following markers of hepatic function were assessed: AST, ALT, AP, LDH, total bilirubin, total protein, albumin, and urea serum levels. All tests were performed using kits from Spinreact (Girona, Spain) following the manufacturer's instructions. Samples were read in a spectrophotometric semiautomatic bts-350 analyzer (Biosystems, Quezon City, Philippines).

2.5. RNA Isolation and Determination of Gene Expression by Real-Time qPCR.

Total RNA was isolated from 100 mg of liver samples with the Jena Bioscience Isolation System (Jena Bioscience, Jena, Germany), following the manufacturer's protocol. Total RNA was quantified with a NanoDrop 2000 (Thermo Scientific, Waltham, MA, USA). Reverse transcription was performed with 1 μg of total RNA using the GoScript Reverse Transcription System (Promega) for real-time quantitative PCR, which was analyzed using qPCR GreenMaster with UNG-clear (Jena Bioscience, Jena, Germany) in a StepOne machine (Applied Biosystems)

TABLE 1: Oligonucleotide sequences.

Gene	Oligonucleotide-F	Oligonucleotide-R	Accession number
IL-1	5′-CTGTGACTCGTGGGATGATG-3′	5′-GGGATTTTGTCGTTGCTTGT-3′	NM_031512.2
IL-10	5′-GAATTCCCTGGGAGAGAAGC-3′	5′-CGGGTGGTTCAATTTTTCAT-3′	NM_012854.2
TGF-β	5′-GACTCTCCACCTGCAAGACCA-3′	5′-CGGGTGACTTCTTTGGCGTA-3′	AY550025.1
COL-1	5′-TTGACCCTAACCAAGGATGC-3′	5′-CACCCCTTCTGCGTTGTATT-3′	NM_053356.1
MMP-9	5′-CAGAAGCCCAAGGAAGAGTG-3′	5′-AGACCCACAGGAAACCACAG-3′	AJ438266.1
MMP-13	5′-ATCCCAGCTTAGGGCTCAAT-3′	5′-GGGAAAACAGCTACGCTGAG-3′	AY135636.1
β-Actin	5′-GTCGTACCACTGGCATTGTG-3′	5′-GCTGTGGTGGTGAAGCTGTA-3′	XM_032887061.1

(a)

(b)

(c)

FIGURE 2: Effects of neurointermediate pituitary lobectomy (NIL), portacaval anastomosis (PCA), and PCA+NIL on total proteins (a), albumin (b), and urea (c) serum levels. The intact control (IC) group served as reference. (a) $^*p < 0.05$: NIL vs. PCA+NIL. (b) $^*p < 0.05$: IC vs. PCA and $^{**}p < 0.01$ NIL vs. PCA. (c) Nonstatistical (NS) differences between groups were observed. It was evaluated with analysis of variance test with the Tukey post hoc values, which are expressed as the mean ± SD.

under the following conditions: 50°C for 2 min, 95°C for 3 min, 40 cycles of 95°C for 45 sec, and 60°C for 45 sec. Oligonucleotides were designed to target type I collagen (COL-I), MMP-13, MMP-9, TGFβ, IL-10, IL-1, and β-actin (as a reference control) (Table 1). Relative expression level was normalized with β-actin as reference gene, and differences were determined using the $2^{-\Delta\Delta Ct}$ method.

2.6. Statistical Analyses. All data were evaluated for Gaussian distribution using the Kolmogorov-Smirnov normality test. Multiple comparisons between the groups were performed for each parameter. One-way ANOVA and Tukey's post

hoc test for parametric data or the Kruskal-Wallis test and Dunn's post hoc test were performed for nonparametric data, according to the Kolmogorov-Smirnov normality test. Two-way ANOVA was performed to analyze differences in total area of fibrosis between the groups (green and red); $p < 0.05$ were considered significant in all cases. All statistical analyses were performed using GraphPad Prism 7.0 software.

3. Results

3.1. Liver Function Assessment. As shown in Figure 2(a), serum levels of total proteins in the NIL group were not
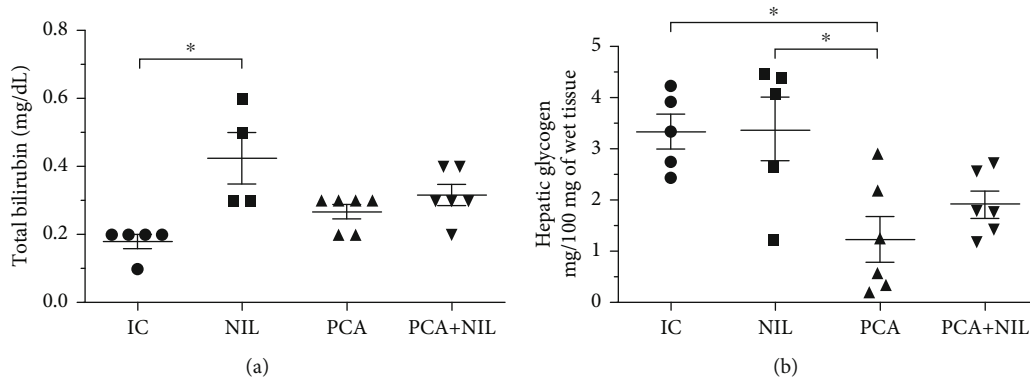
FIGURE 3: Effects of neurointermediate pituitary lobectomy (NIL), portacaval anastomosis (PCA), and PCA+NIL on (a) total bilirubin serum levels and (b) hepatic glycogen. $^*p < 0.05$ IC vs. NIL. The intact control (IC) group served as reference. It was evaluated with analysis of variance test with the Tukey post hoc values, which are expressed as the mean ± SD.
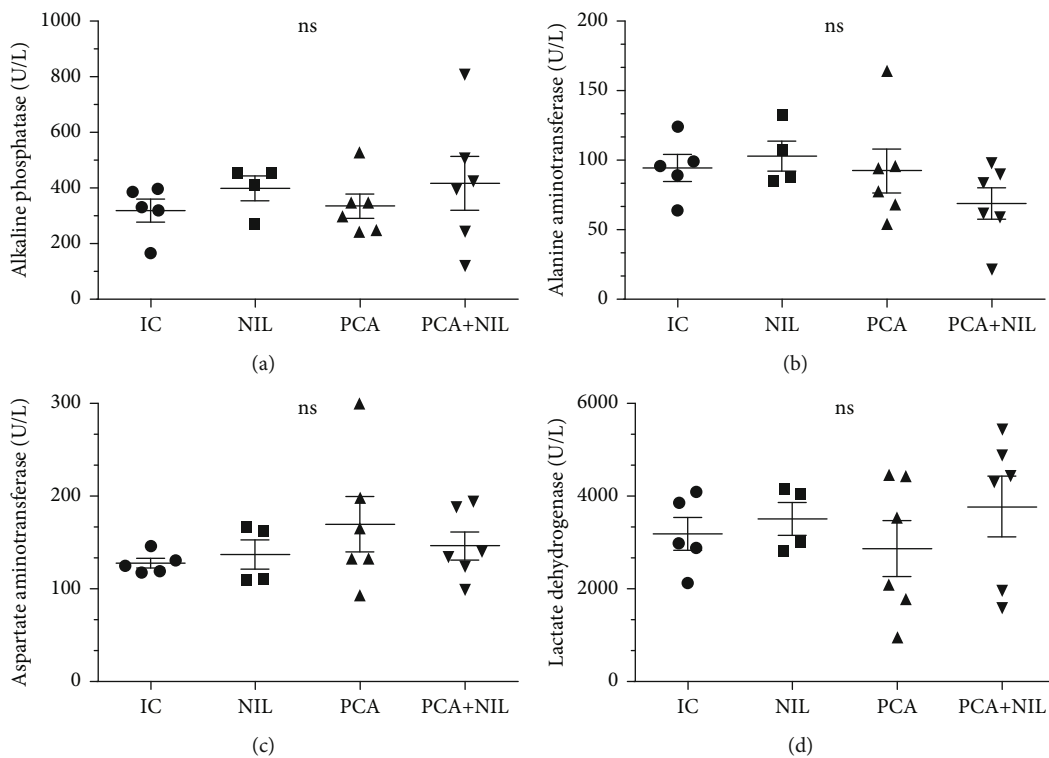
FIGURE 4: Effects of neurointermediate pituitary lobectomy (NIL), portacaval anastomosis (PCA), and PCA+NIL on (a) alkaline phosphatase (AP), (b) aspartate aminotransferase (AST), (c) alanine aminotransferase (ALT), and (d) lactate dehydrogenase (LDH) serum levels. Nonstatistical differences between groups were apparent. The intact control (IC) group served as reference. It was evaluated with analysis of variance test with the Tukey post hoc values, which are expressed as the mean ± SD.

significantly different from the IC group. PCA induced a significant decrease in total proteins ($p < 0.05$) as compared with those in the NIL group, whereas the NIL surgery restored the serum proteins to normal in the PCA+NIL group (NS: NIL vs. NIL+PCA). The albumin serum levels were not significantly different in the IC, NIL, and PCA +NIL groups, while a significant decrease in the serum albumin occurred in the PCA group ($p < 0.05$ and $p < 0.01$: PCA vs. IC and NIL, respectively; Figure 2(b)). In the PCA+NIL group, the AVP deficiency caused a mild recovery in the

albumin serum levels (NS: IC and NIL vs. PCA+NIL; Figure 2(b)). Compared with the IC group, NIL, PCA, and PCA+NIL did not affect the urea serum levels (Figure 2(c)).

In comparison with the IC group, no significant changes in total bilirubin serum levels occurred in the PCA and PCA +NIL groups. The NIL surgery alone caused a significant increase in the bilirubin serum levels in the NIL group ($p < 0.05$: IC vs. NIL) (Figure 3(a)). In comparison with the IC and NIL groups, the PCA surgery alone induced a significant decrease in the glycogen content ($p < 0.05$: IC and NIL

(a)

(b)

(c)
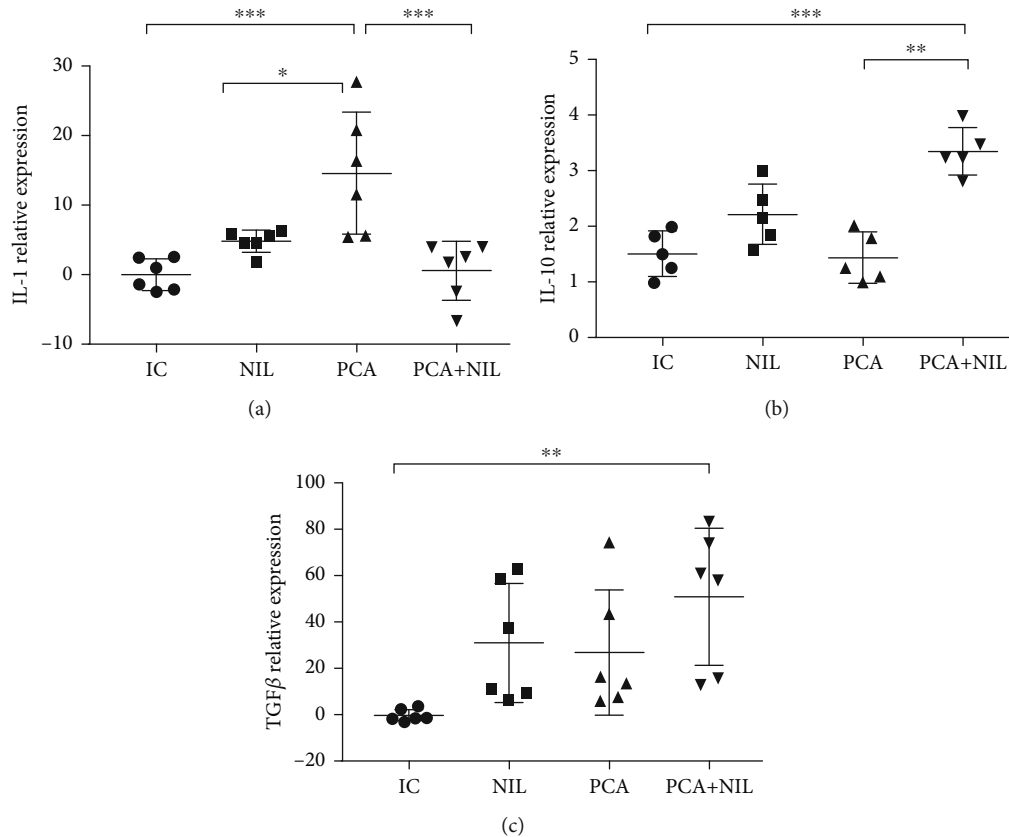
Figure 5: Effects of neurointermediate pituitary lobectomy (NIL), portacaval anastomosis (PCA), and PCA+NIL on the relative expression of (a) IL-1, (b) IL-10, and (c) TGF-β. (a) ***$p < 0.001$: IC vs. PCA, *$p < 0.05$: NIL vs. PCA, and ***$p < 0.001$: PCA vs. PCA+NIL. (b) *** $p < 0.001$ IC vs. PCA+NIL. (c) **$p < 0.01$: IC vs. PCA+NIL. The intact control (IC) group served as reference. It was evaluated with analysis of variance test with the Kruskal-Wallis test and Dunn's post hoc values, which are expressed as the mean ± SD.

vs. PCA group), whereas the NIL to the PCA+NIL group caused a mild recovery in the glycogen content (NS: IC, NIL, and PCA vs. PCA+NIL group) (Figure 3(b)).

The serum levels of the enzymes AP, AST, ALT, and LDH were not significantly affected by the different experimental conditions (Figures 4(a), 4(b), 4(c), and 4(d)). In summary, as shown in Figures 2, 3, and 4, four weeks of PCA is a model of liver damage, where the pathophysiological changes do not develop concurrently.

The relative gene expression levels of proinflammatory cytokine IL-1 and anti-inflammatory cytokines IL-10 and TGF-β showed that in comparison with the IC group, PCA induced a significant increase in IL-1 level ($p < 0.001$: IC vs. PCA), NIL surgery did not affect the IL-1 expression level, while the PCA+NIL group showed a diminution of the IL-1 expression levels to basal levels (Figure 5(a)). Compared with the IC, NIL, and PCA groups, the expression levels of the anti-inflammatory cytokines IL-10 and the TGF-β were significantly higher in the PCA+NIL group ($p < 0.001$ and $p < 0.01$; IC vs. PCA+NIL, respectively; Figures 5(b) and 5(c)).

The relative gene expression levels of COLL-I, MMP-9, and MMP-13 showed that while PCA induced a significant increase of the COL-I expression level ($p < 0.01$: IC vs. PCA), the PCA+NIL group showed a decrease in COLL-I expression level, although not to the IC group levels ($p < 0.05$: IC vs. PCA+NIL group; Figures 6(a), 6(b), and 6(c)).

The MMP-9 was not significantly expressed in the NIL, PCA, and PCA+NIL groups compared with the IC group (Figure 6(b)). While the NIL and PCA+NIL groups showed significantly increased MMP-13 expression levels ($p < 0.001$: IC vs. NIL and PCA+NIL, respectively), no significant differences were found between the expression levels in the IC vs. PCA groups (Figure 6(c)).

3.2. Effects of NIL, PCA, and PCA+NIL on the Liver Histopathology. The livers from all the groups showed histopathological changes in response to different experimental conditions. Table 2 summarizes the main stromal and cellular changes found in the different experimental groups. Figure 7 shows liver slides stained with HE method at 20x magnification. As shown in Figure 7(a), a normal pattern of the blood sinusoids and tissue morphology from an IC group show normal liver lobules and triads: hepatic artery (asterisk), bile ducts (arrow), and portal vein (arrowhead). No inflammatory infiltrates, necrosis, or fibrosis was observed (Table 2). The NIL group (Figure 7(b)) showed a similar normal histological pattern as the IC group (Table 2). The PCA group showed significant changes in the morphology of liver structures, mainly in the periportal zone, with a significant
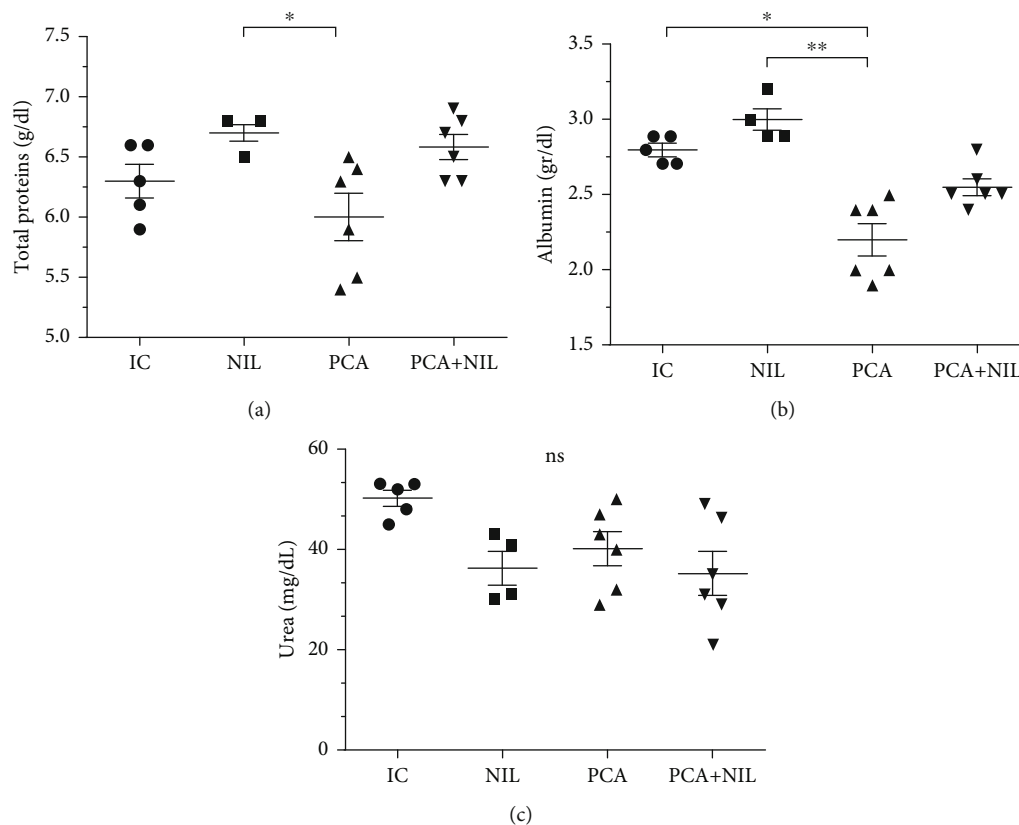
(a)

(b)

(c)
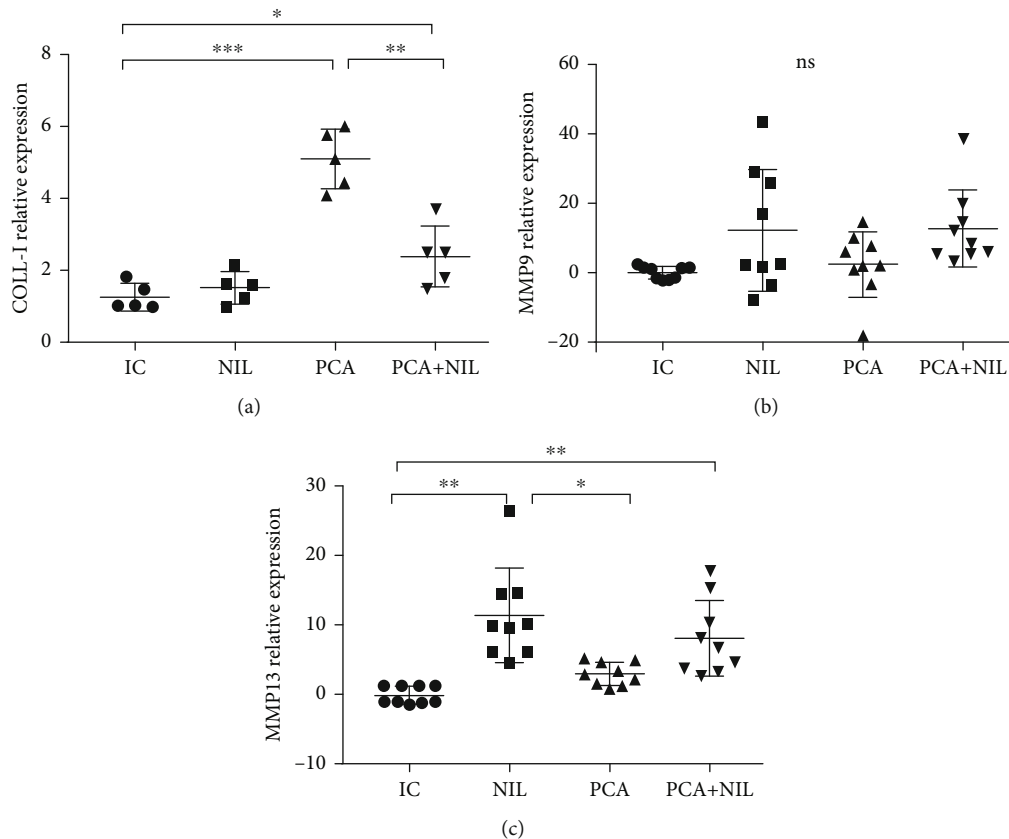
FIGURE 6: Effects of neurointermediate pituitary lobectomy (NIL), portacaval anastomosis (PCA), and PCA+NIL on the relative expression of (a) collagen type 1 (COLI), (b) metalloproteinase-9 (MMP-9), and (c) metalloproteinase-13 (MMP-13). (a) $^*p < 0.05$: IC vs. PCA-NIL and $^{**}p < 0.01$: IC vs. PCA. (b) Nonstatistical differences between groups were apparent. (c) $^{**}p < 0.01$: IC vs. NIL, $^{**}p < 0.01$: IC vs. PCA+NIL, and $^*p < 0.05$: NIL vs. PCA. The intact control (IC) group served as reference. It was evaluated with analysis of variance test with the Kruskal-Wallis test and Dunn's post hoc values, which are expressed as the mean ± SD.

TABLE 2: Table of parameters of magnitude of cell damage and stroma.

| Experimental group | Stromal changes | | | Cell changes | | |
	Arterial wall thickening	Collagen fibers	Inflammatory infiltrate	Pleomorphism	Binucleation	Balonization
IC	-	-	-	-	-	-
PCA	++	+++	++	++	++	+++
NIL	-	-	-	-	-	-
PCA+NIL	++	+	+	++	+	++

-: parameter not found in histological preparations; +: magnitude of damage found in histological preparations.

thickening around the bile ducts (arrows), artery walls (asterisks), and portal veins (arrowhead) caused by increased collagen deposits (Figure 7(c)). Some inflammatory infiltrations were occasionally observed (Table 2). The PCA+NIL group showed a partial reversion in the stroma and cell patterns as compared to the PCA and IC groups (Figure 7(d)) (Table 2). The periportal area showed the restored morphological pattern of the hepatocytes and sinusoids and the slimming of the portal vein wall (arrowhead).

Masson's trichrome staining method to assess the distribution of collagen fibers (blue) in the several liver groups showed major histopathological changes mainly in the periportal area of the PC and PC+NIL groups (Figure 8). The IC

(Figure 8(a)) and NIL (Figure 8(b)) groups showed a thin pattern of collagen distribution around the portal vein (arrowhead). The effects of PCA were observed as an increased collagen deposition around the triad vessels and mildly into the surrounding liver parenchyma (asterisk in Figure 8(c)). In addition, isolated inflammatory infiltrates were observed (arrow). In comparison with the APC group (Figure 8(c)), the PCA +NIL group (Figure 8(d)) showed decreased collagen deposits around the triad and liver parenchyma (asterisk). All photographs were taken at 20x magnification.

The slides stained with Sirius Red and analyzed under polarized light to assess the collagen types and areas of fibrosis showed normal basal distribution of type III collagen

(a)

(b)

(c)

(d)
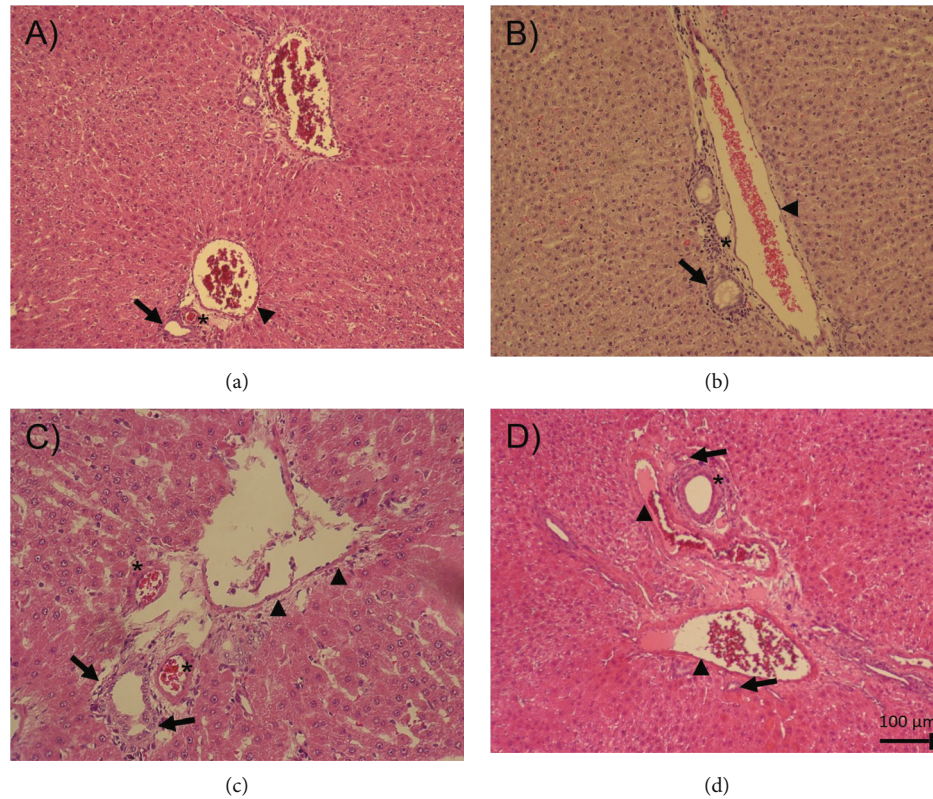
Figure 7: Liver slides HE stained from the IC, NIL, PCA, and PCA+NIL groups. (a) Slide from an IC animal. Normal pattern of the liver lobules, triads (hepatic artery ∗), bile ducts (arrow), portal vein (arrowhead), and blood sinusoids are apparent. Neither inflammatory infiltrates nor necrosis or fibrosis is present. (b) The NIL group. Similar normal structural patterns of the IC liver morphology are discernible. (c) PCA slide. Evident morphological changes are noted in the periportal zone, increased collagen deposits, thickening of the bile ducts (arrows), artery walls (∗), and portal veins (arrowhead). (d) PCA+NIL slide. A restored morphological pattern of hepatocytes and sinusoids (∗) is apparent, as well as slimming of the portal vein wall (arrowhead). All images taken at 20x magnification. $n = 5 - 6$ animals/group.

(mainly yellow and green colors) in the periportal area from an IC group (Figure 9(a)). The NIL group showed similar distribution of collagen, although thinner than that observed in the IC group (Figure 9(b)). In the PCA group, (Figure 9(c)) large changes in the distribution and type of collagens were observed such as increased fibrosis in the periportal area type III collagen (green, asterisk), thickness of the triad vessels, and increased collagen invasion into the surrounding liver parenchyma (arrow). PCA+NIL animal showed a decreased amount of collagen invading the liver parenchyma (type III collagen) and a significant diminution of the periportal fibrotic area (asterisk; Figure 9(d)). To assess the percentage of liver fibrosis, the ImageJ software program was used [36, 37]. On comparing the percentage area of fibrosis among the different groups, NIL surgery showed no effect on the percentage of fibrosis as compared to the IC group (Figure 9(e)). In contrast, the PCA group developed a significant increase in the fibrotic area ($p < 0.001$: IC vs. PCA, Figure 9(e)). The PCA+NIL group showed significantly lower percentage ($p < 0.01$: PCA vs. PCA+NIL group, Figure 9(e)).

Previously, it was demonstrated that NIL induced an immediate but transient increase in water intake and urine output (*diabetes insipidus*) for 2-4 weeks and a permanent drop in AVP serum levels. AVP assessed at 3, 15, 45, and 90 days after NIL were on average 2.4 ± 0.16 pg/mL versus 10.6 ± 0.08 pg/mL of their respective control groups [24]. Similar low AVP serum levels were also reported 3 and 8 weeks after NIL surgery [38].

4. Discussion

In the present work, PCA as a model of chronic liver disease is supported by the decreased circulating levels of total proteins and albumin, decreased liver glycogen level, the increased relative expression levels of IL-1 and COLL-I genes, nonsignificant changes in gene expression levels of MMP-13 and IL-10, and the significant increase in periportal (triads) and Rappaport parenchymal 1 and 2 fibrosis. This information, along with those previous findings of Aller et al. [13], Vázquez-Martínez et al. [14], and Gandhi et al. [39], reinforces that PCA is a paradigm of chronic liver damage.

The stimulating role of AVP in fibrotic process has been demonstrated in several clinical and experimental conditions. *In vitro*, AVP stimulates the mesangial cell proliferation, hypertrophy, type IV collagen production, and increased concentration of TGF-β, which are inhibited by the selective V1a AVP receptor antagonist (YM218) [30].
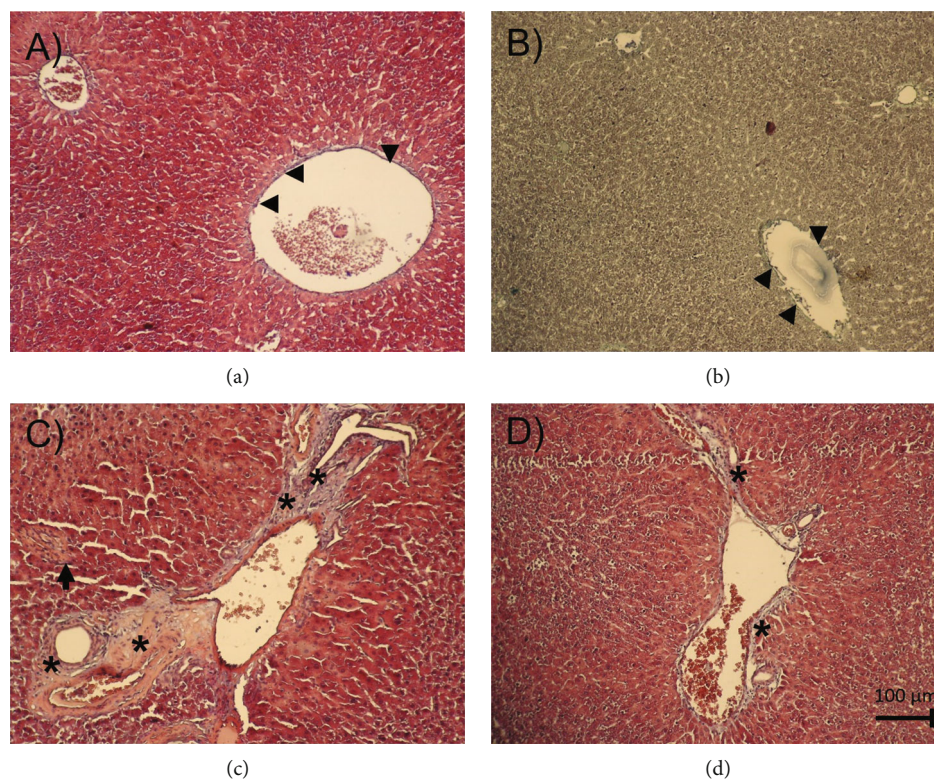
Figure 8: Liver slides stained with Masson's trichrome to identify collagen distribution (blue) in the several experimental groups. In (a) from an IC and (b) from a NIL group, a thin pattern of collagen fibers is distributed around the triad (hepatic artery, bile duct, and portal vein) (arrowhead). (c) PCA liver slide. An increase in collagen distribution around the vessels of the triad and a mild invasion into the liver parenchyma is observed (∗). In addition, isolated foci of inflammation are observed (arrow). (d) PCA+NIL liver slide. In comparison with the PCA group, the collagen distribution around the triad and liver parenchyma is less apparent (∗). All photographs are taken at 20x magnification.

Experiments in rats and human observational studies suggest that AVP may play a role in the genesis and exacerbation of renal damage and chronic renal insufficiency [32]. Yan-Hong et al. [29] described the effect of AVP on cardiac fibroblast differentiation into collagen producer myofibroblasts, and Niu et al. [28] found a synergistic effect of angiotensin (fragments 1-7) and AVP on proliferation and collagen synthesis in rat cardiac fibroblasts. The presence of V1a and V2 AVP receptors in immune system cells and its stimulatory role during inflammatory responses has also been demonstrated [40]. AVP V1a receptors were present in blood monocytes, macrophages, splenic lymphocytes, and B cells; V2 AVP receptors in peripheral blood cell cultures; and V1b receptors in the thymus and spleen cells. Furthermore, the V1a AVP receptors in HSCs and their activation and differentiation into collagen producer myofibroblasts were demonstrated by Bataller et al. [31], whereas the presence of V1a and V2 AVP receptors and their activation by AVP in hepatocytes and cholangiocytes were described by Dünser and Westphal [41]. Together, this information strongly supports that AVP is directly involved in innate and acquired immunity, as well as in the activation and development of the fibrotic process. This view is supported by the present results in the AVP-deficient animals.

In the NIL group, AVP deficiency increased both total bilirubin serum levels and relative gene expression levels of the MMP-13, with no significant effects on the remaining biochemical and histopathological parameters. Although the mechanism by which AVP deficiency (NIL-induced) causes hyperbilirubinemia is not known, a possible explanation for this may be that AVP in the liver is involved in hepatocyte ureogenesis, glycogenolysis, neoglucogenesis, and cell regeneration through its V1a receptors [41], while the V2 AVP receptors regulate the biliary epithelium functions [42]. It is known that AVP stimulates efflux of the bile salts taurocholate and glycocholate in suspended hepatocytes, via its association with the AVP V1 receptors on hepatocyte membranes [43, 44]. It is also known that several hepatobiliary organic anion-transporting polypeptide systems (Oatps in rodents) located in the basolateral membrane extract chemicals from sinusoidal blood into the hepatocytes, while canalicular transporters mediate the movement of chemicals into the lumen of the bile canaliculus, including the bile acids and unconjugated bilirubin (in rodents) [45]. Therefore, we speculate that the hyperbilirubinemia in the NIL group may be due to the low AVP circulating levels, which were not enough to activate the AVP receptor signaling mechanisms that mediate the hepatocyte bilirubin excretion. Further experiments must be conducted to evaluate this possibility.

Results also show that one week of AVP deficiency in the PCA+NIL animals caused the following effects: (i) reversion

(a)

(b)

(c)

(d)

(e)
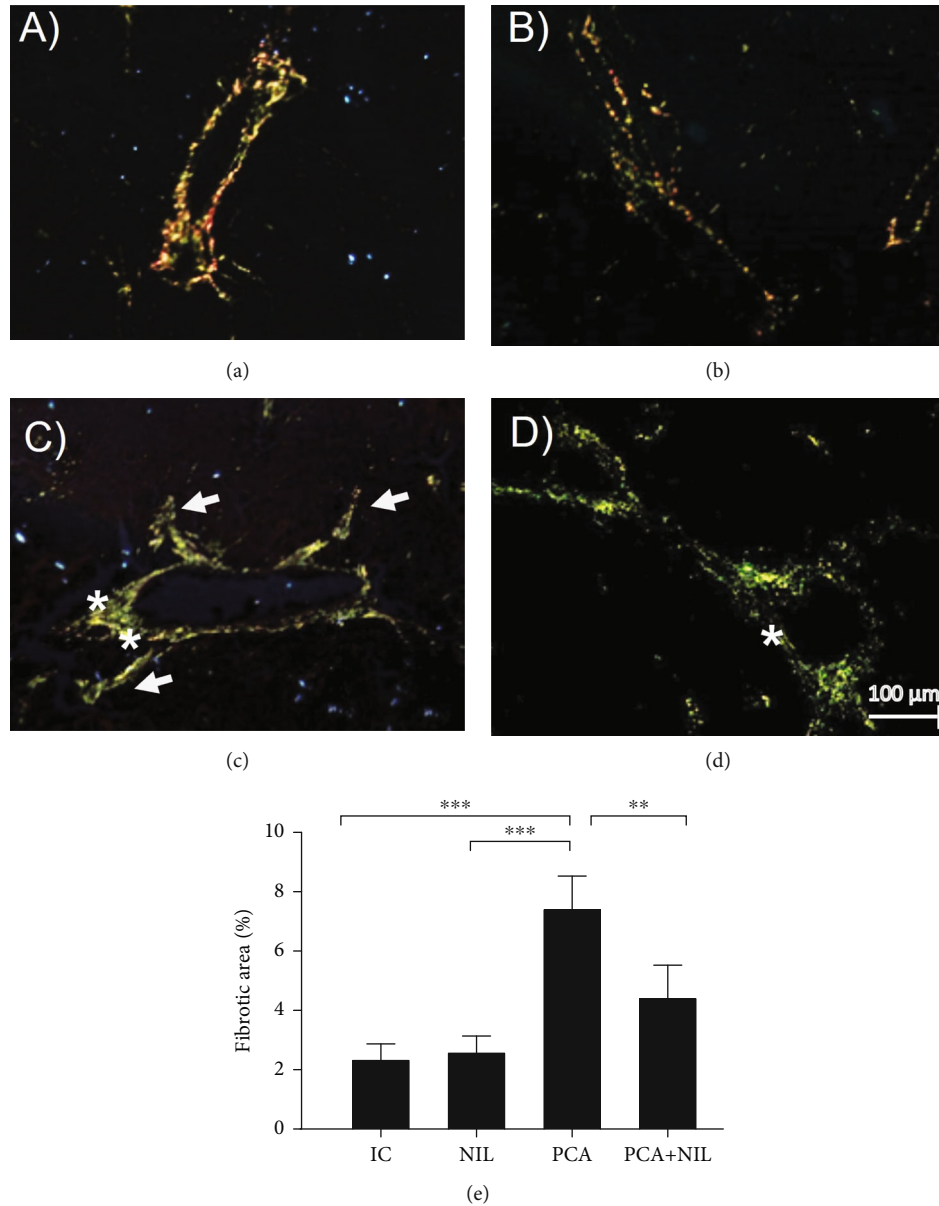
FIGURE 9: Liver slides stained with Sirius Red analyzed under polarized light to assess the area of fibrosis. (a) Periportal area from an IC animal. Normal distribution of type III collagen (mainly green color) is observed. (b) NIL liver slide. Similar distribution of collagens of the IC group is apparent. (c) PCA liver slide. Increase in collagen type I (red) and III (yellow) distribution is observed in the periportal area, with thickening of the triad vessels. Also, an increased collagen invasion into the surrounding liver parenchyma (∗) is apparent. (d) PCA+NIL. It shows regression of type I collagen, mainly in the periportal area (∗). (e) Comparisons of percentage of the fibrosis areas in the several experimental groups. Observe that between the IC and NIL groups, similar percentages of fibrosis are apparent. In contrast, the PCA animals developed a significant increase in the fibrotic area (∗∗$p < 0.001$: IC vs. PCA). In the PCA+NIL group, the percentage of fibrosis was significantly decreased as compared with the PCA group (∗$p < 0.01$: PCA vs. PCA+NIL group), indicating reversible effect of AVP deficiency on liver fibrosis. It was evaluated with analysis of variance test with the Tukey post hoc values, which are expressed as the mean ± SD. Pictures are taken at 20x magnification.

of some of the altered metabolic parameters to normal (total proteins and serum albumin and liver glycogen content), (ii) increase in the anti-inflammatory IL-10 gene expression level, (iii) decrease of both COLL-I gene expression level and deposition of type I collagen, and (iv) increase in MMP-13 gene expression level and depressed liver fibrosis (assessed by histopathology). The anti-inflammatory and antifibrotic role of IL-10 has been associated with the control of inflammation in many organs with clinical diseases and experimentally induced fibrosis [46, 47]. Currently, the administration of IL-10 is considered as a tentative pharmacological tool in the treatment of liver inflammation and fibrosis [46, 48]. Considering all the previous observations, present results can be partially explained as follows: the

low levels of AVP (NIL-induced) are not enough to activate the AVP receptors of the immune cells and HSCs, resulting in a decreased activation of the cell signaling pathways associated with the proinflammatory-profibrotic responses (IL-1, COLL-1). Simultaneously, the AVP deficiency activates cell signaling pathways associated with an anti-inflammatory-antifibrotic state (IL-10 and MMP-13), thus favoring a decreased liver inflammatory response and less activation of the HSCs and fibrosis, favoring liver recovery. This possibility is supported by our previous work on NIL-cirrhotic hamsters, in which both overexpression of MMP-13 and decreased expression level of TIMP-2 were accompanied by a significant regression in liver cirrhosis [33].

In response to acute and chronic liver injury, TGF-β is activated from the ECM deposits and then expressed and released from various cell types. The presence of V1a AVP and TGF-β receptors in the HSCs and its activation by inducing transdifferentiation of HSCs into collagen producer myofibroblasts have been demonstrated previously [31, 49]. In cooperation with other signaling pathways (reactive oxygen species (ROS), platelet-derived growth factor (PDGF), and connective tissue growth factor (CTGF)), the TGF-β signaling is considered the key fibrogenic factor in liver fibrosis [49]. In the present study, despite significant increase of TGF-β gene expression levels in the PCA+NIL animals, the inflammatory-fibrotic process (PCA-mediated) was downregulated. A possible explanation for this may be that the increased expression level of TGF-β combined with the inhibition in the expression of the IL-1 and COLL-1 (proinflammatory-profibrotic factors) was overcome by anti-inflammatory-antifibrotic factors (IL-10 and MMP-13). However, further experiments are required to establish this interpretation.

The effects of NIL on the adenohypophyseal hormone secretions have been reported [50–53]. Based on the literature and our previous work, the short- and long-term effects of the NIL surgery on several adenohypophyseal hormone secretions might be differentially regulated; thus, the main hormone secretory changes in response to NIL occur for a short time, returned to basal conditions after a few weeks, including the ability of the pituitary cells to respond to different physiological challenges [50–53]. In our studies, the effects of NIL on GH and TSH secretions decreased after 3 weeks of NIL and reverted to normal levels after eight weeks after surgery, whereas PRL, FSH, LH, and ACTH always showed normal ranges [27, 38, 53, 54]. Furthermore, to assess the viability of the physiological reactivity of the hypothalamic-pituitary-thyroid axis, NIL rats were simultaneously subjected to thyroidectomy. Results showed that NIL-thyroidectomized rats responded with a significant increase in TSH secretion levels, accompanied by significant changes in pituitary thyrotrophs, which underwent hypertrophy, hyperplasia, and development of thyroidectomy cells [53, 55]. These results suggest that short- and long-term endocrine effects of NIL on adenohypophyseal hormonal secretion are transient and that the regulatory hypothalamic-adenohypophyseal mechanisms for hormone secretions in the NIL animals were able to adapt to the permanent diminution of AVP and OT serum levels.

5. Conclusions

From the present study, we conclude that PCA is a good model to study chronic liver damage. The inflammatory and fibrotic effects of PCA are partially reverted by the AVP deficiency (NIL-induced) through both decreased expression of inflammatory-fibrotic factors and increased expression of the anti-inflammatory-antifibrotic factors, resulting in a decreased fibrosis and improvement in liver functions. Present results support the view that AVP plays a direct role in the regulation of the immune system and fibrotic process. Further experiments are required in order to obtain better insight regarding cell and molecular mechanisms through the AVP deficiency which stimulate or inhibit the cell signal pathways involved in the anti-inflammatory and antifibrotic processes responsible of improvement liver damage.

Abbreviations

PCA: Portacaval anastomosis
AVP: Arginine vasopressin
OXT: Oxytocin
NIL: Neurointermediate pituitary lobectomy
HSCs: Hepatic stellate cells
IL-Iβ: Interleukin-1β
IL-10: Interleukin-10
TGF-β: Transforming growth factor-β
MMP: Matrix metalloproteinase
AST: Aspartate aminotransferase
ALT: Alanine aminotransferase
TNF-α: Tumor necrosis factor-α
IL-8: Interleukin-8
PDGF: Platelet-derived growth factor
ET-1: Endothelin-1
α-SMA: Alpha-smooth muscle actin
CCl$_4$: Carbon tetrachloride
AP: Alkaline phosphatase
LDH: Lactate dehydrogenase
Ig: Immunoglobulin
TIMPs: Tissue inhibitors of metalloproteinases
HE: Hematoxylin & eosin
COLL-I: Type I collagen
GH: Growth hormone
PRL: Prolactin
CRH: Corticotropin-releasing hormone
ACTH: Corticotropin
TSH: Thyrotropin
FSH: Follicle-stimulating hormone
LH: Luteotropic hormone.

Data Availability

The data that support the findings of this study are available from the corresponding author, AQS, upon reasonable request.

Disclosure

Noé Macías-Segura's present address is Departamento de Inmunología, Facultad de Medicina y Hospital Universitario

"Dr. José Eleuterio González", Universidad Autónoma de Nuevo León, Monterrey, PC 64460, Mexico.

Conflicts of Interest

The authors declare that they have no conflicts of interest.

Acknowledgments

References

[1] A. A. Mokdad, A. D. Lopez, S. Shahraz et al., "Liver cirrhosis mortality in 187 countries between 1980 and 2010: a systematic analysis," *BMC Medicine*, vol. 18, no. 12, p. 145, 2014.

[2] S. L. Friedman, "Mechanisms of hepatic fibrogenesis," *Gastroenterology*, vol. 134, pp. 1655–1669, 2008.

[3] E. Huang, N. Peng, F. Xiao, D. Hu, X. Wang, and L. Lu, "The roles of immune cells in the pathogenesis of fibrosis," *International Journal of Molecular Sciences*, vol. 21, p. 5203, 2020.

[4] A. P. Holt, M. Salmon, C. D. Buckley, and D. H. Adams, "Immune interactions in hepatic fibrosis," *Clinics in Liver Disease*, vol. 12, pp. 861–882, 2008.

[5] R. P. Tamayo, "Is cirrhosis of the liver experimentally produced by CC14 an adequate model of human cirrhosis?," *Hepatology*, vol. 3, pp. 112–120, 1983.

[6] H. Popper, "Pathologic aspects of cirrhosis. A review," *The American Journal of Pathology*, vol. 87, p. 228, 1977.

[7] R. Afrin, S. Arumugam, A. Rahman et al., "Curcumin ameliorates liver damage and progression of NASH in NASH-HCC mouse model possibly by modulating HMGB1-NF-κB translocation," *International Immunopharmacology*, vol. 44, pp. 174–182, 2017.

[8] Q. Bai, H. Yan, Y. Sheng et al., "Long-term acetaminophen treatment induced liver fibrosis in mice and the involvement of Egr-1," *Toxicology*, vol. 382, pp. 47–58, 2017.

[9] M. Parola and M. Pinzani, "Liver fibrosis: pathophysiology, pathogenetic targets and clinical issues," *Molecular Aspects of Medicine*, vol. 65, pp. 37–55, 2019.

[10] T. Tsuchida and S. L. Friedman, "Mechanisms of hepatic stellate cell activation," *Nature Reviews. Gastroenterology & Hepatology*, vol. 14, pp. 397–411, 2017.

[11] A. Kojima-Yuasa, M. Goto, E. Yoshikawa et al., "Protective effects of hydrolyzed nucleoproteins from salmon milt against ethanol-induced liver injury in rats," *Marine Drugs*, vol. 14, p. 232, 2016.

[12] J.-L. Arias, M.-A. Aller, F. Sánchez-Patan, and J. Arias, "The inflammatory bases of hepatic encephalopathy," *European Journal of Gastroenterology & Hepatology*, vol. 18, pp. 1297–1310, 2006.

[13] M. A. Aller, V. Martinez, M. T. Corcuera et al., "Liver impairment after portacaval shunt in the rat: the loss of protective role of mast cells?," *Acta Histochemica*, vol. 114, pp. 301–310, 2012.

[14] O. H. Vázquez-Martínez, H. Valente-Godínez, A. Quintanar-Stephano et al., "Reduced liver lipid peroxidation in subcellular fractions is associated with a hypometabolic state in rats with portacaval anastomosis," *Oxidative Medicine and Cellular Longevity*, vol. 2019, 13 pages, 2019.

[15] C. García, E. Gine, M.-A. Aller et al., "Multiple organ inflammatory response to portosystemic shunt in the rat," *Cytokine*, vol. 56, pp. 680–687, 2011.

[16] F. A. Antoni, "Vasopressinergic control of pituitary adrenocorticotropin secretion comes of age," *Frontiers in Neuroendocrinology*, vol. 14, pp. 76–122, 1993.

[17] M. Harbuz, G. Conde, O. Marti, S. Lightman, and D. Jessop, "The hypothalamic-pituitary-adrenal axis in autoimmunity," *Annals of the New York Academy of Sciences*, vol. 823, pp. 214–224, 1997.

[18] M. A. Gülpınar and B. Ç. Yegen, "The physiology of learning and memory: role of peptides and stress," *Current Protein and Peptide Science*, vol. 5, pp. 457–473, 2004.

[19] S. Jard, "Vasopressin receptors: a historical survey," in *Vasopressin and Oxytocin*, H. H. Zingg, C. W. Bourque, and D. G. Bichet, Eds., pp. 1–13, Springer, New York, NY, 1998.

[20] A. Quintanar-Stephano, E. Abarca-Rojano, R. A. Jarillo-Luna et al., "Hypophysectomy and neurointermediate pituitary lobectomy decrease humoral immune responses to T-independent and T-dependent antigens," *Journal of Physiology and Biochemistry*, vol. 66, pp. 7–13, 2010.

[21] V. Viñuela-Berni, B. Gómez-González, and A. Quintanar-Stephano, "Blockade of arginine vasopressin receptors prevents blood-brain barrier breakdown in experimental autoimmune encephalomyelitis," *Scientific Reports*, vol. 16, p. 467, 2020.

[22] J. Szmydynger-Chodobska, L. M. Fox, K. M. Lynch, B. J. Zink, and A. Chodobski, "Vasopressin amplifies the production of proinflammatory mediators in traumatic brain injury," *Journal of Neurotrauma*, vol. 27, pp. 1449–1461, 2010.

[23] L. Ferrier, C. Serradeil-le Gal, A. M. Schulte et al., "Proinflammatory role of vasopressin through V1b receptors in hapten-induced experimental colitis in rodents: implication in IBD," *American Journal of Physiology-Gastrointestinal and Liver Physiology*, vol. 299, no. 6, pp. G1298–G1307, 2010.

[24] G. M. Villanueva-Rodríguez, A. Organista-Esparza, V. Biñuela-Berni et al., "Effects of Arginine Vasopressin deficiency on Basal Mean Arterial Blood Pressure in Normal and Spontaneously Hypertensive Rats," *The FASEB Journal*, vol. 30, 1 Supplement, p. 955.7, 2016.

[25] V. K. Patchev, K. T. Kalogeras, P. Zelazowski, L. I. Wilder, and P. C. Chrousos, "Increased-plasma concentrations, hypothalamic content, and in vitro release of arginine vasopressin in inflammatory disease-prone, hypothalamic corticotropin-

releasing hormone-deficient Lewis rats," *Endocrinology*, vol. 131, no. 3, pp. 1453–1457, 1992.

[26] A. Quintanar-Stephano, K. Kovacs, and I. Berczi, "Effects of neurointermediate pituitary lobectomy on humoral and cell-mediated immune responses in the rat," *Neuroimmunomodulation*, vol. 11, pp. 233–240, 2004.

[27] I. Berczi, A. Quintanar-Stephano, E. C. Villalobos-Hernández, R. Campos-Rodríguez, and K. Kovacs, "The healing power of vasopressin," *Advances in Neuroimmune Biology*, vol. 3, pp. 217–224, 2012.

[28] X. Niu, Y. Xue, X. Li et al., "Effects of angiotensin-(1-7) on the proliferation and collagen synthesis of arginine vasopressin–stimulated rat cardiac fibroblasts: role of mas receptor-calcineurin-NF-κB signaling pathway," *Journal of Cardiovascular Pharmacology*, vol. 64, pp. 536–542, 2014.

[29] F. Yan-Hong, D. Hui, P. Qing et al., "Effects of arginine vasopressin on differentiation of cardiac fibroblasts into myofibroblasts," *Journal of Cardiovascular Pharmacology*, vol. 55, pp. 489–495, 2010.

[30] A. Tahara, J. Tsukada, Y. Tomura, T. Yatsu, and M. Shibasaki, "Vasopressin increases type IV collagen production through the induction of transforming growth factor-beta secretion in rat mesangial cells," *Pharmacological Research*, vol. 57, no. 2, pp. 142–150, 2008.

[31] R. Bataller, J. M. Nicolas, P. Gines et al., "Arginine vasopressin induces contraction and stimulates growth of cultured human hepatic stellate cells," *Gastroenterology*, vol. 113, pp. 615–624, 1997.

[32] D. Bolignano and C. Zoccali, "Vasopressin beyond water: implications for renal diseases," *Current Opinion in Nephrology and Hypertension*, vol. 19, pp. 499–504, 2010.

[33] A. Quintanar-Stephano, J. Ventura-Juárez, E. Sánchez-Alemán et al., "Liver cirrhosis reversion is improved in hamsters with a neurointermediate pituitary lobectomy," *Experimental and Toxicologic Pathology*, vol. 69, pp. 496–503, 2017.

[34] L. Padilla-Sánchez, *Microvascular End-To-Side Portacaval Anastomosis (Sun Lee)*, Servicio de Cirugía Experimental. Centro Médico Nacional, México, 2013, November 20 I.S.S.S.T.E. https://www.youtube.com/watch?v=1YXQKcQA0ec.

[35] A. Quintanar-Stephano, R. Chavira-Ramírez, K. Kovacs, and I. Berczi, "Neurointermediate pituitary lobectomy decreases the incidence and severity of experimental autoimmune encephalomyelitis in Lewis rats," *The Journal of Endocrinology*, vol. 184, no. 1, pp. 51–58, 2005.

[36] L. C. U. Junqueira, W. Cossermelli, and R. Brentani, "Differential staining of collagens type I, II and III by Sirius Red and polarization microscopy," *Archivum Histologicum Japonicum*, vol. 41, no. 3, pp. 267–274, 1978.

[37] J. I. Schindelin, E. Arganda-Carreras, V. Frise et al., "Fiji: an open-source platform for biological-image analysis," *Nature Methods*, vol. 9, no. 7, pp. 676–682, 2012.

[38] A. Organista-Esparza, V. Viñuela-Berni, M. Tinajero-Ruelas et al., "Effects of the neurointermediate pituitary lobectomy (NIL) on pituitary hormones blood level in the rat," *The FASEB Journal*, vol. 2016, pp. 1248.6–1248.6, 2016.

[39] C. R. Gandhi, N. Murase, V. M. Subbotin et al., "Portacaval shunt causes apoptosis and liver atrophy in rats despite increases in endogenous levels of major hepatic growth factors," *Journal of Hepatology*, vol. 37, no. 3, pp. 340–348, 2002.

[40] A. Quintanar-Stephano, A. Organista-Esparza, R. Chavira-Ramírez, R. Campos-Rodríguez, I. Berczi, and K. Kovacs, "Arginine vasopressin: an immunoregulatory hormone," in *Insights to Neuroimmune Biology 2nd ed*, pp. 85–106, Elsevier, 2016.

[41] M. W. Dünser and M. Westphal, "Arginine vasopressin in vasodilatory shock: effects on metabolism and beyond," *Current Opinion in Anesthesiology*, vol. 21, no. 2, pp. 122–127, 2008.

[42] R. Mancinelli, A. Franchitto, S. Glaser et al., "Vasopressin regulates the growth of the biliary epithelium in polycystic liver disease," *Laboratory Investigation*, vol. 96, no. 11, pp. 1147–1155, 2016.

[43] D. A. Gewirtz, J. K. Randolph, and I. D. Goldman, "Induction of taurocholate release from isolated rat hepatocytes in suspension by α-Adrenergic agents and vasopressin: implications for control of bile salt secretion," *Hepatology*, vol. 4, no. 2, pp. 205–212, 1984.

[44] W. F. Kuhn, D. M. Heuman, Z. Reno Vlahcevic, and D. A. Gewirtz, "Receptor-mediated stimulation of taurocholate efflux from the rat hepatocyte and the ex vivo perfused rat liver," *European Journal of Pharmacology*, vol. 175, no. 2, pp. 117–128, 1990.

[45] J. E. Manautou, N. S. Campion, and L. M. Aleksunes, "Regulation of hepatobiliary transporters during liver injury," in *Comprehensive Toxicology (Second Edition)*, vol. 9, pp. 175–220, Elsevier, 2010.

[46] E. H. Steen, X. Wang, S. Balaji, M. J. Butte, P. L. Bollyky, and S. G. Keswani, "The role of the anti-inflammatory cytokine interleukin-10 in tissue fibrosis," *Advances in Wound Care*, vol. 1, no. 4, pp. 184–198, 2020.

[47] M. N. Shi, Y. H. Huang, W. D. Zheng, L. J. Zhang, Z. X. Chen, and X. Z. Wang, "Relationship between transforming growth factor beta1 and anti-fibrotic effect of interleukin-10," *World Journal of Gastroenterology*, vol. 21, no. 15, pp. 2357–2362, 2006.

[48] L.-J. Zhang and X.-Z. Wang, "Interleukin-10 and chronic liver disease," *World Journal of Gastroenterology*, vol. 12, no. 11, pp. 1681–1685, 2006.

[49] B. Dewidar, C. Meyer, S. Dooley, and N. Meindl-Beinker, "TGF-β in hepatic stellate cell activation and liver fibrogenesis-updated 2019," *Cell*, vol. 8, no. 11, p. 1419, 2019.

[50] I. Murai and N. Ben-Jonathan, "Chronic posterior pituitary lobectomy: prolonged elevation of plasma prolactin and interruption of cyclicity," *Neuroendocrinology*, vol. 43, no. 4, pp. 453–458, 2004.

[51] F. Mena, D. Aguayo, M. Vigueras, A. Quintanar-Stephano, G. Perera, and T. Morales, "Effect of posterior pituitary lobectomy on in vivo and in vitro secretion of prolactin in lactating rats," *Endocrine*, vol. 5, no. 3, pp. 285–290, 1996.

[52] R. E. Miller, H. Yueh-Chien, M. K. Wiley, and R. Hewitt, "Anterior hypophysial function in the posterior-hypophysectomized rat: normal regulation of the adrenal system," *Neuroendocrinology*, vol. 14, no. 3-4, pp. 233–250, 2004.

[53] A. Quintanar-Stephano, I. Villapando-Fierro, P. Damián-Matsumura et al., "Effects of protracted neurointermediate pituitary lobectomy on hormone secretion and number of each type of endocrine cell in the anterior pituitary lobe of rats," *Endocrine Pathology*, vol. 12, pp. 235–237, 2001.

[54] K. D. Fagin, S. G. Wiener, and M. F. Dallman, "ACTH and corticosterone secretion in rats following removal of the neurointermediate lobe of the pituitary gland," *Neuroendocrinology*, vol. 40, no. 4, pp. 352–362, 2004.

[55] R. Campos-Rodríguez, A. Quintanar-Stephano, R. A. Jarillo-Luna et al., "Hypophysectomy and neurointermediate pituitary lobectomy reduce serum immunoglobulin M (IgM) and IgG and intestinal IgA responses to Salmonella enterica serovar Typhimurium infection in rats," *Infection and Immunity*, vol. 74, no. 3, pp. 1883–1889, 2006.

Review Article

Self-Centered Function of Adaptive Immunity in Regulation of Immune Responses and in Tolerance

Silvana Balzar (ID)

Department of Clinical Microbiology, Polyclinic Breyer, Zagreb, Croatia

Correspondence should be addressed to Silvana Balzar; sbalzar@gmail.com

The search for common mechanisms underlying the pathogenesis of chronic inflammatory conditions has crystalized the concept of continuous dual resetting of the immune repertoire (CDR) as a basic principle of the immune system function. Consequently, outlined was the first dynamic comprehensive picture of the immune system function. The goal of this study is to elaborate on regulation of immune responses and mechanisms of tolerance, particularly focusing on adaptive immunity. It is well established that the T/B cell repertoire is selected and maintained based on interactions with self. However, their activation also requires interaction with a self-specific major histocompatibility complex (MHC) "code," i.e., the context of MHC molecules. Therefore, not only repertoire selection and maintenance but also the T/B cell activation and function are self-centered. Thus, adaptive effectors may be primarily focused on the state of self and maintenance of integrity of the self, and only to a certain degree on elimination of the foreign. As examples of such function are used immunologically poorly understood MHC-disparate settings typical for transplantation and pregnancy. Transplantation represents an extreme setting of strong systemic compartment-level adaptive/MHC-restricted immune responses. Described are clinically identified conditions for operational tolerance of MHC-disparate tissues/living systems in allotransplantation, which are in line with the CDR-proposed self-centered regulatory role of T/B cells. In contrast, normal pregnancy is coexistence of semiallogeneic or entirely allogeneic mother and fetus, but without alloreactivity akin to transplantation settings. Presented data support the notion that maintenance of pregnancy is a process that relies predominantly on innate/MHC-independent immune mechanisms. By the inception of hemotrophic stage of pregnancy (second and third trimester), both mother and child are individual living systems, with established adaptive immune repertoires. Although mother-fetus interactions at that point become indirect systemic compartment-level communications, their interactions throughout gestation remain within the innate realm of molecular-level adaptations.

1. Introduction

The concept of continuous dual resetting of the immune repertoire (CDR) as a basic principle of the immune system function outlines a comprehensive, dynamic picture of the immune system function that is governed by the randomness of interactions and uncertainty of outcomes [1]. The original paper focuses on applying CDR to describe common mechanisms underlying the pathogenesis of chronic inflammatory conditions and autoimmune diseases, including processes associated with both pathologic and aging-related immunosenescence. It also defines the elusive immu-

nological self and describes the dynamics of regulation of immune responses and tolerance [2]. This paper's intention is to further develop the notion that adaptive effectors represent a high-level regulatory mechanism to maintain integrity of a living system. Discussed will be the role of major histocompatibility complex (MHC) in the proposed primary focus of adaptive immunity on the state of self. Prominent examples of regulation of immune responses and maintenance of states of tolerance/integrity of a living system(s) will be used allogeneic settings inherent to both, transplantation and pregnancy. First segment of this paper will tackle the coexistence of MHC-disparate tissues in

transplantation and then proceed to analyze the physiologic setting that supports semiallogeneic or entirely allogeneic pregnancy.

This paper briefly outlines the segments of the CDR pertinent to discussed issues. However, broader familiarity with the CDR is advisable.

1.1. Getting Priorities Straight: Maintenance of Integrity Supersedes Elimination of the Foreign or Dangerous. The CDR puts immunity into a more general context of maintenance of organism's integrity instead of perceiving immune processes as a battle against the foreign or dangerous. It outlines a rather pacifistic picture of the immune system function: continuous molecular-level resetting/adjustments in response to molecular-level changes/disturbances instead of antagonizing them. Disturbances that may trigger the immune repertoire resetting include (a) interactions with the environment and (b) intrinsic changes of self. There is no inherent animosity against intruders or unknowns. Although perceived as such, the drive to destroy or kill often used to describe immune reactions is not congruent with nature's intrinsic mechanisms of adaptation. Instead, the main purpose of immune responses is about overcoming a disturbance (regardless of its nature) with minimum energy expenditure, and guiding innate responses (sometimes through actions of adaptive immunity) toward equilibrium/steady-states.

Such a seemingly subtle shift in understanding immunity has complex implications. This CDR-driven concept of integrity maintenance versus elimination/neutralization of everything sensed as a foreign is with an understanding that disturbances are not just the foreign. Disturbance can be also physiologic growth, hormonal effects, pregnancy, mechanical injury, etc. The system continues resetting toward more energy-efficient states, which are never the same as before. The change is continuous and a constant in living system's existence, and there is no going back to previous states. In response to disturbances, the system takes thermodynamically optimal path to acquire appropriate steady-states. Those steady-states may not be always perceived as states of health but are the optimum for given parameters and under given circumstances.

2. Transplantation

Despite significant advances in transplantation approaches, conditioning procedures that deplete immune system of recipients, continuous immunosuppression required in many patients, and paucity of reliable markers to guide clinicians in decisions about caring for their patients make transplantation a difficult process with uncertain outcomes. Operational tolerance that results in a stable long-term function without the need for immunosuppression remains difficult to achieve. Recent clinical studies demonstrate that induction of a stable mixed chimerism or inclusion of donor's liver in the combined transplantation with other parenchymal organs improve transplantation outcomes [3–9]. However, underlying immunological processes associated with tolerance remain unclear. The most limiting issue

is the lack of a general understanding of immunity, which would provide more grounded rationale for various transplantation approaches.

2.1. Conventional Adaptive Immunity in Maintenance of Integrity: the Importance of Knowing Thy Self. The CDR describes regulation of adaptive responses through fluctuations in the phenotype profile of a T cell receptor- (TCR) diverse T cell population activated in a particular adaptive response, so that immune response eventually enters the phase of repair and resolution [1]. How does understanding of the T cell function as focused on the maintenance of system's integrity makes a difference as compared to the perception of T cells as focused on a particular antigen and its elimination?

It is well established that T cell repertoire is selected based on interactions with self and therefore mirrors the self. This "self-obsession" continues as a requirement for homeostatic signaling from interactions with self (self-awareness), which is necessary in maintenance of T cell repertoire/specificities in the periphery [10]. Surprisingly, implementation of the CDR leads to a conclusion that not only T cell repertoire selection and its maintenance are self-centered, but the T cell function is self-centered as well: T cell repertoire, knowing/mirroring the self and responding only to MHC-restricted innate alerts, may primarily focus on the state of self (hence the MHC restriction of a self-based adaptive repertoire that is useless in a MHC-mismatched host). Here, it is important to keep in mind that the T cell repertoire selection in thymus proceeds through interactions between the MHC-bound self-antigens presented by thymic epithelial cells and the randomly assembled TCRs on newly formed T cells. The MHC is always a component of the molecular pattern that interacts with TCRs, i.e., TCRs recognize epitopes only in the MHC context. Therefore, MHC serves as a "code" that allows cognate interactions with T cells, but only with the code-matching antigen-presenting cells (APCs). The MHC code is unique to a particular living system, which implies that information exchanged through MHC-restricted communications is pertinent only to that particular living system and directed toward regulation of its integrity. Thus, such communication regulates innate immune responses in the context of self and toward maintenance of self's integrity. More precisely, as APC-delivered antigen presentation does not discriminate self/altered self from the foreign, activation of T cell specificities in response to foreign epitopes is due to cross-reactivity of the T cells' self-mirroring repertoire with the foreign, as well as with the APC-presented damaged self. Thus, T cell activity is determined by the self and proceeds in the context of self regardless whether elicited by a foreign or by the self-antigens. Innate mechanisms/effectors, guided and regulated by T/B cells, are actually doing the basic work—eliminating infectious agents, removing destructed tissue, etc. The self-regulating loop closes when innate signals, modulated by T/B cells' regulatory capacity (determined by their repertoire's granularity), eventually change the quality/intensity of integrated signaling toward T/B cells and terminate their engagement. So, it is the innate→adaptive→innate
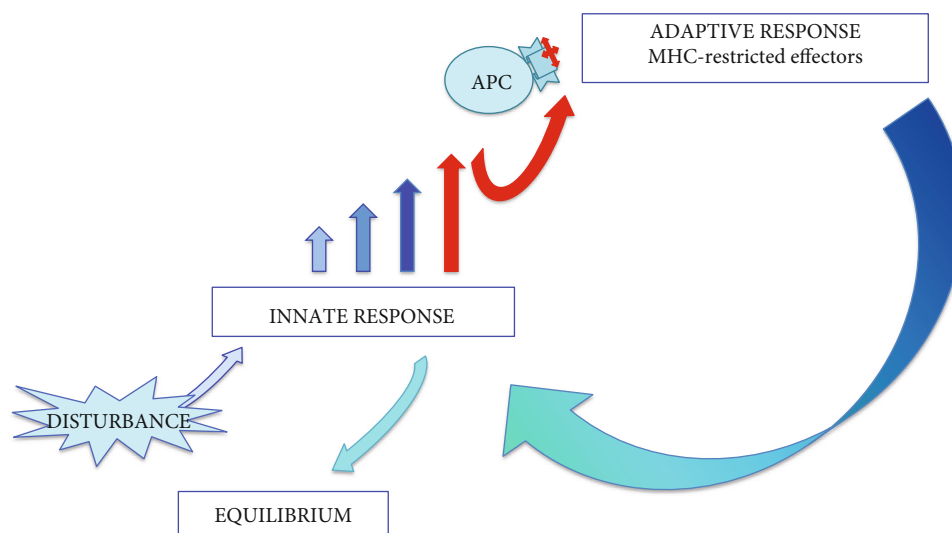
FIGURE 1: Activation of the innate-adaptive-innate regulatory loop. Innate signaling above the threshold activates adaptive responses (conventional T/B lymphocytes) to regulate innate responses toward resolution and new equilibrium states.

mutuality of signaling/interactions that eventually establish homeostasis (Figure 1).

How this view of immunity applies to transplantation? In a recipient, the presence of allotransplant is first sensed by innate mechanisms as a major disturbance in a system. It is not only the foreign but also the trauma caused by the procedure that could overwhelm the system and take it toward the loss of integrity/death. As immune reactions are triggered by mechanisms that do not distinguish between disturbances caused by the foreign or the damaged self, minimizing the injury during initial stages of transplantation (recipient's trauma by the diseased organ resection and graft attachment; graft's trauma by detachment and subsequent reperfusion injury) may be beneficial. Establishing an acceptable pace of innate reactions could allow appropriate time for resetting/adaptation to new circumstances on both recipient's and graft's sides. As regulatory mechanisms of adaptive responses are to engage later in the process, important element in successful regulation of innate responses would be a diverse repertoire of adaptive effectors on both, recipient's and donor's sides. The dynamics and outcomes of those processes are uncertain. However, some level of control of the pace of those initial innate and consequent adaptive processes may help the system to overcome such a major disturbance and gradually establish equilibrium states compatible with integrity of the newly created chimeric system.

As CDR posits, T/B cells' function is primarily to guide innate immune responses toward homeostasis, resolution, and repair. Their self-centered repertoire determines the system's ability to maintain integrity, i.e., through continuous resetting maintain the states of homeostasis. Being evolutionary developed only in most complex and highly organized living systems (yawed vertebrates) further supports the notion that the range of T cell phenotypes may represent a self-centered regulatory mechanism to maintain integrity of those most complex living megaorganisms. This view of T/B cell function may explain consequences of iatrogenic

or disease-induced lymphopenia. Lymphopenic patients become susceptible and often succumb to infections with microorganisms considered commensals or environmental flora (*Candida* species, *Pseudomonas aeruginosa*, and *Pneumocystis jirovecii*), possibly due to unregulated innate responses. Depleted T cell population, and thus reduced repertoire, may result in inability to regulate/channel innate responses toward maintenance of system's integrity. Similar effects of lymphopenia in a transplant recipient could jeopardize regulatory mechanisms required to establish equilibrium states and eventual graft tolerance. In addition, transplant's integrity (as explained below) may be similarly affected.

2.2. Maintenance of Integrity in Transplantation. How the proposed function of self-centered adaptive repertoire in maintenance of system's integrity can be applied to understand issues in transplantation? In a transplanted organ that lacks autochthon T cells and their MHC-matched APCs (T cells + MHC – matched APCs = TAPCs), transplant's disturbances (ischemic injury, innate alloreactions, etc.) remain unattended/unregulated, because the transplant is outside the "jurisdiction" of host's TAPCs. Transplant remains a stranger to host's TAPCs. Even when relative homeostasis can be established, specific regulatory mechanisms to preserve integrity of a transplant (would be in the domain of its own TAPCs) may not function appropriately, and integrity of a transplant may be brittle. Although survival can be prolonged, it would be in the context of host's integrity.

If the graft/transplant brings its own self-focused/integrity-preserving TAPCs into a host with functioning TAPCs (that regulate host's innate responses and watch over host's integrity), the resetting processes may be directed toward steady-states that would allow coexistence of both entities—the host and the transplanted organ. Such a setting may exist in liver transplantation. Liver, due to its complex function as an immunological barrier between the gut's mucosal compartment and the systemic compartment, has

its own resident population of lymphocytes and APCs. That puts liver in a position to regulate its own resetting processes toward maintaining its own integrity versus host's own immune mechanisms maintaining host's integrity. Although (allo)reactions (including host vs. graft and graft vs. host) may continue, regulatory mechanisms on both sides may eventually reach sustainable steady-states and allow both MHC-distinct entities to coexist. Liver's TAPCs, supported by their autochthon environment, are likely to continue their function even in a MHC-mismatched host. Spontaneous operational tolerance of liver transplants is indeed more common than with other parenchymal organ transplants [9].

The proposed benefit of having functional both host and donor TAPCs is demonstrated in a particular approach to transplantation of organs that, unlike liver, lack autochthon TAPCs. It has been recognized that establishing stable mixed chimerism in organ transplantation may reduce complications and help achieve tolerance [3–7]. Reports suggest that establishing stable mixed chimerism with infusion of donor haematopoietic stem cells (HSC)+T cells in a solid organ recipient can prevent rejection, eventually lead to cessation of immunosuppressive therapy and induction of transplant tolerance [3–5]. Preserved recipient's T cell repertoire, B cell lymphopoiesis, and myelopoiesis may be the source of recipient's replenished population of lymphocytes and APCs undergoing posttransplant resetting against the donor's molecular patterns. In the case of B cells, the resetting process may include de novo posttransplant repertoire selection/replenishment. The observed strong B cell signature in subjects with operationally tolerant kidney transplants originates from naïve and transitional B cells, which suggests that indeed newly derived B cell repertoire may be resetting against the newly present alloentity [11, 12]. At the same time, infused donor's HSC+T cells may be resetting against the recipient's environment, looking for the way to engraft and find a "home" for donor's TAPCs. Successful resetting processes may result in mixed chimerism, with both recipient's and donor's TAPCs providing maintenance of respective immunologically disparate entities that coexist within the recipient's body. The innate (allo)reactions on both sides would be regulated by the respective MHC-matching TAPCs, while functioning in the context of preserving integrity of the newly created chimeric megaorganism. While outcomes are uncertain, the CDR-postulated intrinsic lack of animosity toward the foreign and intrinsically regulated resetting processes toward energy-efficient steady-states may result in persistence/maintenance of integrity of a chimeric megaorganism. Indeed, contribution of both recipient and donor cells to the population of peripheral blood regulatory T cells (Tregs) has been recently reported in subjects with mixed chimerism post HSC transplantation [13].

Consistent with the CDR's understanding of graft tolerance and importance of having both donor and recipient MHC-matched TAPCs to maintain the integrity of a chimeric living system, the full donor chimerism associates with graft-versus-host disease, recipient's immunodeficiency and immune incompetence, suggesting that donor's leucocytes may not be appropriate/sufficient to maintain recipient's integrity [6, 7, 14].

It has been observed that tolerance can be lost after years of stable allograft function. In some subjects, the triggers were viral or bacterial infections, while others can develop immunologically driven rejection [15, 16]. Indeed, conclusions drawn from transplantation studies indicate that tolerance is an acquired and metastable condition [17]. These clinical observations are consistent with the CDR view of tolerance as a dynamic process maintained by a continuous resetting of the immune repertoire in a system whose function is governed by randomness of events and uncertainty of outcomes. Significant disturbances in the system (such as infection or even allograft biopsy procedure) may carry a risk of resetting processes that could trigger rejection. The rejection could be due to reduced regulation of reactions unrelated to the transplant itself (bystander effects due to cross-reactivity triggered by infection, transplant-unrelated injury), and also due to physiologic reduction in repertoire diversity related to aging [1]. Consistent with uncertainty of living system's function, those events could occur at any point in time.

As mentioned, equilibrium states are established by thermodynamically optimal mechanisms, which could include markers otherwise associated with pathology. Nevertheless, those may reflect equilibrium states still compatible with maintenance of integrity. In that context, biopsy-detectable indicators of continuing alloreactivity despite clinically evident operational tolerance may not be surprising or a sign of rejection. Therefore, routine biopsy to assess the state of a transplant may not be as useful/informative, particularly considering the risk that may carry. Perhaps looking for peripheral blood markers of innate activation reflective of the transplant-related resetting processes (and indicators of potentially significant disturbance leading to activation of adaptive reactions) may constitute a better warning system of possible rejection. As each patient's immune states are expected to be unique, personalized pre- and posttransplant "baselines" for future follow-up may need to be established. For that purpose, identifying the parameters most indicative of pretransplant immunological setting/background (may be influenced by gender, age, genetics etc.; ref. 1) and the posttransplant states may require multifactorial profiling/analyses of many patients.

While the "self-obsession" and self-awareness hint at basic requirements, what exactly constitutes the homeostatic signaling that gives a sense of home for lymphocyte/APC populations (and thus may create a refuge for donor cells that results in engraftment) is unknown [10]. As liver can be a home and a source of donor's TAPCs, perhaps an organ transplant with adjacent lymph nodes or lymphoid tissue could provide similar homing sites and a source of transplant-preserving donor TAPCs for maintenance of a stable mixed chimerism.

2.3. Concluding Remarks regarding Transplantation. Under appropriate conditions, immune interactions may result in acceptance of an allotransplant and persistence/maintenance of integrity of a chimeric organism. Having in mind that stochasticity and chaotic behavior govern the function of living systems, iatrogenic elimination of particular segments of

those processes may not be a good strategy to achieve better outcomes. Instead, supporting the living system's resetting mechanisms and directing them toward outcomes that would be less detrimental for system's integrity may be a more productive strategy. These issues may be of particular interest for approaches to modulate early posttransplant resetting processes. The goal would be to skew those initial "raw state" processes toward equilibrium states conducive to better clinical outcomes instead of allowing the system to take a direct "shortcut" toward acute situation-appropriate equilibrium states that may associate with unacceptable pathology, rejection, or loss of integrity/death [18].

The proposed self-centered function of conventional T/B cells represents an upper-tier regulatory mechanism that is engaged only under circumstances that require channeling innate responses toward maintenance of living system's integrity. Therefore, a diverse repertoire of T/B cells and MHC-matching APCs to regulate interactions and resetting processes of both entities in the newly created chimeric living system may be essential. That means that preserving adaptive repertoire of both the recipient and the donor may be necessary to acquire an immunosuppression-free operational tolerance. In that context, donor-specific antibodies may be a part of those regulatory processes and not necessarily an indicator of rejection. Indeed, while donor-specific anti-human leukocyte antigen (HLA) antibodies may associate with graft loss, they do not reliably predict allograft rejection [17]. Unlike with T cells (whose repertoire is limited by thymus involution), the B cell repertoire continues to be replenished throughout one's life, which makes them a more "adaptable" element of regulatory processes and tolerance. Also, antibodies, regardless of origin, may bind both donor's and recipient's epitopes and thus contribute to the regulation of immune responses.

Considering that the T cell repertoire is formed at the end of individual's growth/maturation (which also coincides with involution of thymus), transplant tolerance in humans is operational tolerance. It depends on repertoire's granularity/diversity [1]. The role of the thymus and central tolerance in humans could be potentially a factor only in very young children, while the thymus is still active. Proposals to reactivate the function of thymus in adults (and thus derive/select new Tregs) are disconcerting, as clinical data show that activation of thymus in adults associates with autoimmunity [19–21].

Association between the increase in Tregs and transplant tolerance has resulted in approaches to condition polyclonal T cells *in vitro* to acquire a regulatory phenotype and use those Tregs to induce transplant tolerance *in vivo*. Considering that the phenotype of all cells, including T cells, forms and fluctuates as a result of integrated signaling received from cells' environment, potential regulatory effect of *in vitro*-conditioned Tregs may not translate to *in vivo* setting.

3. Pregnancy

Immunologically, pregnancy is a puzzling physiologic phenomenon. Contrary to incompatibility between allogeneic tissues that makes transplantation such a challenging and uncertain process, a woman's body cradles and supports the growth of not only her own semiallogeneic fetus but, in gestational surrogacy, supports an allogeneic fetus created from other woman's oocyte. In transplantation, an allogeneic transplant can only rarely maintain its function without immunosuppression. Pregnancy, a basic physiologic event, readily supports the development of an MHC-disparate fetus. Mechanisms involved in that physiologic process are still poorly understood.

Per CDR, rather than acting against unknowns, immunity includes a molecular-level resetting process of adaptation to disturbances in the system. Maintenance of integrity (i.e., immunity) is a matter of adaptation to changes. Also, regardless whether (innately) detected changes are due to continuous changes of self or originating from the environment (including infectious agents and allogeneic interactions), there is no intrinsic animosity: reactions are self-regulated, and their outcomes depend on the living system's immune repertoire and its competency. Such a pacifistic understanding of immunity, as opposed to the presumption of intrinsic aggression against unknowns, allows for a different view of pregnancy, as well as transplant tolerance. Therefore, per CDR, pregnancy is a matter of adaptation to an allogeneic entity—conceptus/fetus.

3.1. Compartmentalization of the Immune System: the Importance of Sequestration of the Systemic Compartment.
An important element of the CDR to emphasize before discussing the immunological aspects of pregnancy is compartmentalization of the immune system. Compartmentalization is essential in maintenance of living system's integrity [1]. The surface-lining mucosal compartment (MC) functions as a barrier against the environment and keeps the systemic compartment (SC) sequestered/isolated. Equipped with a particular population of unconventional cells and innate mechanisms to interact with the environment, MC could be considered an immune-privileged site where more is "allowed" without triggering an adaptive response/engagement of the systemic effectors.

Figure 2 outlines the hierarchy in activation of effector mechanisms (in the domain of cellular immune responses) during the course of an immune response, which is clinically evident in typical dynamics of an acute inflammatory reaction. As a rule, and regardless whether the trigger is infection or a noninfectious injury/disturbance, early stages of an acute inflammatory reaction are marked by a prompt increase in neutrophils/granulocytes (left shift). Neutrophil/granulocyte recruitment and influx are an innate prompt reaction to a range of infectious or noninfectious disturbances in the system. While relatively short-lived, their role has been proven indispensable [22]. Although not as numerous as neutrophils, eosinophils and basophils (highlighted as "degranulators") emerge as unique innate cells that are engaged in immunologically challenging reactions triggered at mucosal surfaces (allergy, responses to parasites), and also in regulation of repair and profibrotic processes [23]. Mast cells, unlike granulocytes, constitute a resident population of cells distributed along epithelial and

*„Degranulators" – cells that contain granules filled with distinct array of mediators. Release of those mediators by degranulation is their most prominent mode of function.
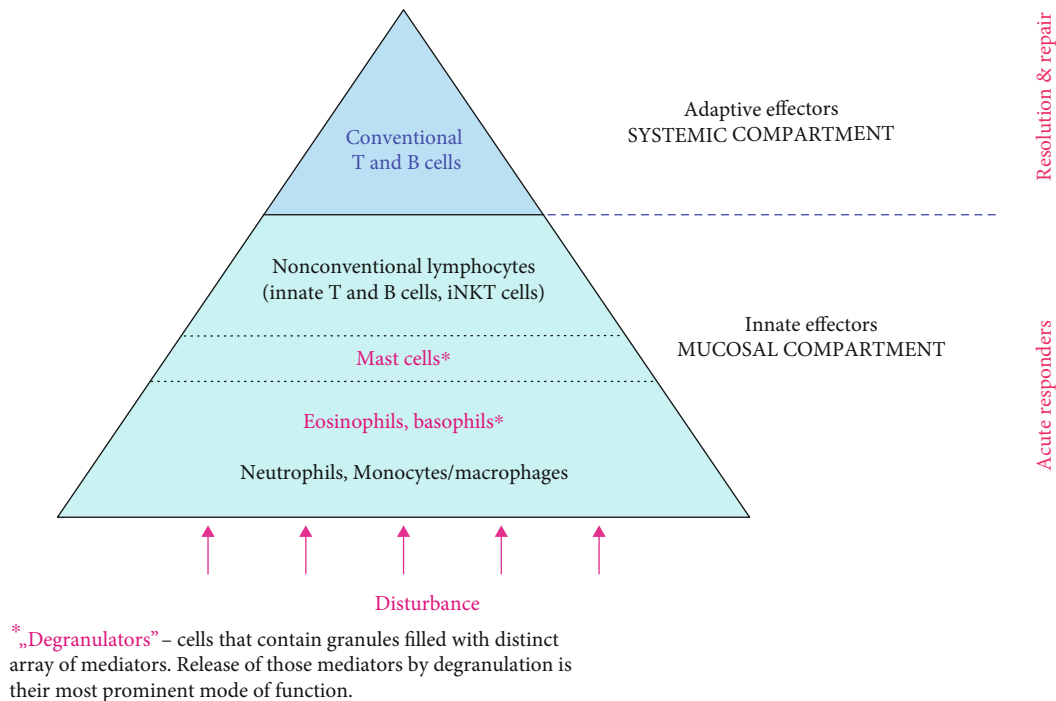
FIGURE 2: The engagement sequence pyramid of cellular immune effectors. Physiologic characteristics of immune cells, their timing of recruitment, number, and distribution are consistent with their function. Innate effectors are the first/acute responders. Conventional T/B cells (MHC-restricted adaptive effectors) are secluded within the systemic immune compartment (SC) and activated only when innate reactions reach a particular threshold, i.e., in later stages of an immune response.

endothelial surfaces. They are considered essential for homeostasis and barrier function of the mucosal immune compartment (MC) [24–26]. Nonconventional T/B cells represent an innate segment of local regulatory mechanisms that function within the MC. Unlike conventional T/B cells, they are directly activated by innate signals/interactions and are able to act promptly.

Eventual lymphocytosis (when adaptive arm of immunity is engaged) is established several days later and is considered a marker of late stages of an inflammatory reaction. Activation of conventional T cells is MHC-restricted. The highly regulated activation and clonal expansion make the conventional lymphocytes slow-reacting effectors reserved for processes that cannot be resolved solely by innate mechanisms, i.e., those innate processes that reach a threshold of signaling indicating significant disturbance in the system (Figure 1). Conventional T cells require interactions with APCs-activated cells capable to pre-process antigens and present those in the context of MHC molecules. Similarly restricted conventional B cells require cognate T cell help to undergo class switch and specificity maturation (somatic hypermutation).

Clinically, a drop in peripheral blood neutrophils and concomitant lymphocytosis associate with resolution and recovery. In infectious diseases, the drop in peripheral blood neutrophils coincides also with the specific disease-associated seroconversion and increase in immunoglobulin G levels. That typically occurs 7-10 days after initial symptoms of the disease. The timing of those routinely measurable effects is consistent with the CDR view: initial strong

innate reaction is subsequently regulated by T/B lymphocytes.

The sequestered SC is a home of adaptive T/B cell effectors. Their MHC-guided/focused responses are activated only when disturbances reach a threshold requiring a specificity-driven adaptive reaction (Figure 1). Those adaptive responses, through innate effectors, neutralize and repair the damage, thus regulating inflammatory reactions. Reliance on mucosal/innate protection, with seldom activation of the systemic compartment effectors/adaptive responses, reduces immune repertoire attrition (intrinsic to the CDR) and preserves regulatory capacity of the system. Unlike with transplantation, where recipient-donor interactions occur as a direct systemic event (surgery or parenteral introduction of heterologous cells is a harsh disturbance of the SC), appropriate compartmentalization of the immune system and strong MC may play a major role in implantation and maintenance of pregnancy.

Another important element in discussing the immunologic aspects of pregnancy is the role of glycosylation and glycation, in which CDR considers the driving force in growth, differentiation, immune repertoire development, and aging [1]. Here, the role of glycosylation will be considered related to appropriate decidualization and placentation processes, creation of an immunologically inert uterine environment, and its systemic impact on mother's immune status.

Finally, this study will address how fetal and maternal immune systems' interactions may shape the development of fetal immunity and affect mother's immune status.

3.2. First Trimester of Pregnancy—a Mucosal Event. It has been established that the first 10-12 weeks of pregnancy represent a histiotrophic phase, during which the carbohydrate moieties/glycoprotein-rich endometrial/decidual environment are the source of nutrients for the conceptus/fetus [27]. Preimplantation conditioning of endometrium includes a progesterone-driven glycosylation processes, with abundant secretion of highly glycosylated moieties. Histologic studies show uterine epithelium immersed in mucous secretion [27]. Mucous secretion at other mucosal surfaces (respiratory and digestive tract) functions as a protective and antigen-exclusion mechanism. It renders epithelial surfaces less reactive to environmental triggers, which modulates epithelial signaling to stromal cells and thus modulates the mucosal environment. That, in turn, shapes the phenotype and function of resident immune cells and regulates the influx of other cells involved in immune reactions/responses [1]. While other mucosal surfaces are directly exposed to the environment and their mucous secretion is triggered by exogenous stimuli, endometrium is largely protected from such exposures. Endometrial mucous secretion is endogenously (due to hormonal changes) induced to create a pregnancy-conducive environment.

The prominent glycosylation, so obvious in uterine epithelium/glands, may change decidual/stromal environment as well. The process of decidualization creates a particular tissue environment that modifies the phenotype and function of resident cells, including stromal cells, decidual natural killer (NK) cells, and macrophages. The placentation processes under such conditions are governed by appropriate interactions between decidual/stromal environment and both, maternal and fetal cells (trophoblast), and proceed to form an appropriate maternal-fetal interface [28, 29].

Glycosylation, an enzymatic addition of carbohydrate sequences to proteins and lipids, is known to differentially affect all molecular interactions—adhesion, receptor-ligand binding/signaling, innate signaling, etc. [30, 31]. The pregnancy-induced glycosylation may create an immunologically inert environment that is during the first trimester conducive to implantation, propagation of fetal trophoblast deeper into decidual layers, and formation of the placenta. Indeed, recent studies demonstrate differential glycosylation in specific phases of the menstrual cycle, implantation, and in placentation-associated pathology of pregnancy [32, 33]. In addition, reported is a complex role of glycan-binding galectins in placentation and pregnancy disorders [34, 35]. Also, baseline-altered glycosylation and/or glycation (due to aging or other altered glycosylation/glycation states such as diabetes, obesity, and chronic inflammatory conditions) could result in impaired placentation and unfavorable pregnancy outcomes. Indeed, murine reproductive decline in aged dames associates with altered uterine environment, blunted hormonal responsiveness, and thus deficient decidualization and placentation [36]. Those could be due to aging-associated changes in glycation/glycosylation [1].

Therefore, under physiologic conditions, adaptation to the invading alloentity during implantation may proceed regulated solely by innate mechanisms residing within the uterine mucosa. Those innate mechanisms include the molecular-level resetting and the local tissue-modulated interactions between the fetal trophoblast, decidual NK cells, and macrophages. From the CDR perspective, it is important for this mucosal process to remain within the innate realm of interactions and not to engage mother's SC/adaptive immune mechanisms (fetal immunity is at that point still limited to the innate). As emphasized before, adaptive responses are intrinsically autoreactive and thus could not only jeopardize the pregnancy/fetal survival but also hurt the mother.

3.3. Second and Third Trimester of Pregnancy: Communication of Maternal and Fetal Systemic Immune Compartments. The blood flow within the newly formed placenta is detectable around 12th week of pregnancy and marks the beginning of the hemotrophic phase of pregnancy [27]. Mother's blood bathes the large surface of intricately branched placenta. The layer of placental syncytiotrophoblast (STB) facing mother's side represents the barrier that from second trimester onward maintains molecular-level communication between the fetus and the mother. In addition to gas, nutrients, and waste exchange, trafficking includes various molecules (environmental particles and other environmental cues), inflammatory mediators, immunoglobulins, exosomes/extracellular vesicles, etc. [37, 38]. Also, a certain number of cells are exchanged between the mother and her developing child [39, 40].

During the histiotrophic phase, mother-fetus interactions are limited: mother's uterine mucosal environment resets against the proliferating and differentiating fetal trophoblast, and vice versa. With the placental blood flow established, the fetal STB begins its adaptation to systemic molecular patterns of mother's self. Also, mother's exposure to the STB is now direct/systemic—not through decidua/MC. In addition to mother-fetus interactions, the STB layer is to modulate interactions with molecular patterns of the environment that may break through mother's mucosal barrier (genital, respiratory, and gut mucosa and skin) and reach the blood circulation. Thus, the strength of mother's MC and its barrier function will directly affect the degree of fetal exposure to the environment. While modulated by STB, both mother's self and the foreign/environment may translate into molecular-level disturbances in the fetus and trigger the resetting processes pertinent to the fetal growth, its immune repertoire development, and maintenance of its integrity.

3.3.1. Fetal Immunity. Fetal immune system's T cell compartment begins to develop at 10 weeks of gestation [41]. That precedes the inception of placental blood flow and increased level of disturbances due to the more direct exposure of STB/fetus to mother's immune environment. The thymus-derived populations of T cells include conventional $\alpha\beta$ T cells, as well as the innate $\gamma\delta$ T cells, $\alpha\beta$ innate natural killer T cells (iNKT cells), and mucosa-associated innate T cells (MAIT cells) [42]. Innate T cells populate fetal mucosal tissues and mature before the postnatal microbial exposures [43]. Similar timing and distribution are observed for

myeloid lineages, including innate B1 and marginal zone B cells, monocytes, and macrophages [44].

3.3.2. *Mother's Immune Status.* A mother's entire body undergoes changes under the influence of pregnancy-induced hormonal environment. The number of various forms of steroid hormones increased in pregnancy (progestogens, estrogens), numerous forms of steroid hormones' receptors, and the well-recognized promiscuity in their interactions makes it difficult to clearly understand the role of hormonal setting typical for pregnancy. That includes the function of the most investigated and clearly essential progesterone [45]. Still, it is reasonable to infer that the progesterone-associated highly glycosylated local/uterine environment may be reflective of a similar pregnancy-induced systemic increase in glycosylation. Systemically increased glycosylation of molecular patterns involved in signaling, matrix composition, and cellular interactions could result in phenomena quite typical for pregnancy. For example, altered function of olfactory and gustatory receptors could result in altered sense of smell or taste in pregnancy; glycosylation-affected insulin receptors could associate with insulin resistance and gestational diabetes; altered epitopes of tissue structural elements could underlie amelioration of rheumatoid arthritis symptoms that is known to occur during pregnancy, etc. Similarly, increased glycosylation may result in generally different tissue/immune environment, which can shift the signaling toward a predominantly Th2 realm of humoral responses, another common feature of pregnancy. Although a Th2 pattern of responses is known to be prominent also in nonpregnant women, in pregnancy, it is considered part of a tolerogenic environment that protects the pregnancy [46]. Indeed, pregnancy may associate with somewhat blunted responses to certain pathogens and increased susceptibility to infections such as listeriosis, malaria, and human immunodeficiency virus (HIV) infections [47]. However, pregnancy is not considered an immunosuppressed state.

3.4. *Mother-Fetus Interactions: the Balancing Act of Maintaining Integrity.* A mother, an immunologically competent living system with a well-developed MC that functions as a strong barrier against the environment, will primarily rely on the innate mechanisms of her MC for appropriate implantation and placentation during the first trimester of pregnancy. The highly glycosylated uterine environment may facilitate the resetting processes of adaptation to the presence of the conceptus. The MC will regulate those innate interactions/disturbances to remain below the threshold of activation of the SC's conventional/adaptive effectors. Fetal trophoblast uses only innate mechanisms of molecular resetting/adaptation to continue growing and invading the decidual layer, the associated remodeling process facilitated by mother's NK cells and macrophages. Such a setting is unlikely to elicit immune interactions that would damage either side.

At the beginning of the second trimester, fetus and mother are individual living systems whose SCs come into close contact—separated only by the fetal STB. Fetus is in the process of developing its own SC's repertoire of T/B cells using its self-template in the selection process in thymus [10]. Its self-template rapidly changes due to endogenous physiologic processes of intense growth and differentiation of fetal organs and tissues. Sequestered/undisturbed from outside, the fetal repertoire selection will produce a self-mirroring repertoire needed for regulation of innate reactions triggered by various disturbances, which will work toward maintenance of fetus' integrity. The STB may information (various mediators, exosomes, immunoglobulins etc.) received from mother's blood "translate" into an instructive element in the process of fetal adaptation to the post-natal life. On the other hand, information from the fetal side toward mother is propagated into a large, quiescent arena of the mother's SC. Unless it contains alarming signals capable of inducing strong innate (and possibly adaptive) reactions, there is little unknown about the fetus that mother would detect as a significant disturbance requiring engagement of her adaptive effectors.

Although mother's strong MC shields the STB and fetus from exposures to the environment, the lack of a more complex/mucosa-like barrier on the fetal side makes the fetus vulnerable. Fetal SC may be exposed to exogenous/environmental disturbances otherwise innocuous for the mother (toxins, chemicals, allergens, and microbial antigens). Those could reach fetal circulation and trigger fetal systemic-level resetting processes. That may alter not only the fetal developmental processes (which, depending on the time of exposure, could cause major structural and functional alterations) but also its self-template and thus the selection of fetal T/B cell repertoire. Outcomes of those fetal systemic-level intrusions could range from the postpartum phenotypically undetectable to significant functional and immunologic alterations in early childhood/adolescence/adulthood. An extreme example of such processes is fetal inflammatory response syndrome (FIRS): mother's mild inflammatory reaction to viral infection (where infection itself does not spread to the placenta/fetus and mother's inflammatory reaction does not terminate the pregnancy) associates with increased risk for diagnosis of autism, schizophrenia, neurosensorial deficits, and psychosis later in life [48]. In that situation, despite the absence of placental transmission of infection, the sole exposure of the fetal immune system to molecular-level disturbances associated with infection may adversely affect fetal development and result in major health problems later in life. In this context, it may be necessary to rethink immunization of women during pregnancy [49].

4. Conclusions

This paper further develops the CDR's notion that adaptive arm of immune responses is activated primarily to regulate innate reactions and maintain integrity of a particular living system. It proposes that not only the already recognized adaptive repertoire selection and maintenance but also its function are all self-centered, i.e., dependent and focused on the state of self. Interpretation of regulatory processes and tolerance in allotransplantation suggests that adaptive

effectors can exert their regulatory function only in a living system whose molecular patterns of self and its MHC "code" have originally served as a template for development and maintenance of that particular system's adaptive repertoire/specificities. Therefore, congruent/matching MHC-coded communications between innate and adaptive effectors provide regulation of immune responses, which are focused on that particular living system. Consistent with such a view of MHC-restricted adaptive immunity, immunosuppression-free operational tolerance in allotransplantation is more likely in patients with stable mixed chimerism, where both donor's and recipient's adaptive effectors maintain integrity of their respective MHC-matching tissues. The coexistence of MHC-disparate entities in such a living system also confirms that immunity is about adaptation and not elimination of a foreign: immunity is focused primarily on finding a sustainable equilibrium in a system to maintain its integrity, even in an allogeneic setting.

Pregnancy is an example of coexistence of MHC-disparate entities solely due to innate-level adaptation/molecular-level resettings to foreign molecular patterns. Adaptive immunity does not regulate those interactions: semiallogeneic or entirely allogeneic living systems during pregnancy are in close contact, but innate mechanisms suffice to maintain equilibrium states of involved living systems. The fact that in pregnancy cells are interchanged between MHC-disparate living systems and are detectable in mothers and their children long after birth further supports the notion that immunity is a matter of adaptation.

Conflicts of Interest

The author declares that there is no conflict of interest regarding the publication of this paper.

References

[1] S. Balzar, "Continuous dual resetting of the immune repertoire as a basic principle of the immune system function," *Journal of Immunology Research*, vol. 2017, Article ID 3760238, 13 pages, 2017.

[2] M. Cohn, "Analysis of Paris meeting redefining the "self" of the immune system," *Immunologic Research*, vol. 62, no. 1, pp. 106–124, 2015.

[3] J. Leventhal, M. Abecassis, J. Miller et al., "Chimerism and tolerance without GVHD or engraftment syndrome in HLA-mismatched combined kidney and hematopoietic stem cell transplantation," *Science Translational Medicine*, vol. 4, no. 124, 2012.

[4] J. D. Scandling, S. Busque, J. A. Shizuru et al., "Chimerism, graft survival, and withdrawal of immunosuppressive drugs in HLA matched and mismatched patients after living donor kidney and hematopoietic cell transplantation," *American Journal of Transplantation*, vol. 15, no. 3, pp. 695–704, 2015.

[5] S. Strober, "Stable mixed chimerism and tolerance to human organ transplants," *Chimerism*, vol. 6, no. 1-2, pp. 27–32, 2015.

[6] J. Zuber, S. Rosen, B. Shonts et al., "Macrochimerism in intestinal transplantation: association with lower rejection rates and multivisceral transplants, without GVHD," *American Journal of Transplantation*, vol. 15, no. 10, pp. 2691–2703, 2015.

[7] T. Oura, A. B. Cosimi, and T. Kawai, "Chimerism-based tolerance in organ transplantation: preclinical and clinical studies," *Clinical and Experimental Immunology*, vol. 189, no. 2, pp. 190–196, 2017.

[8] J. Zuber and M. Sykes, "Mechanisms of mixed chimerism-based transplant tolerance," *Trends in Immunology*, vol. 38, no. 11, pp. 829–843, 2017.

[9] N. Abrol, C. C. Jadlowiec, and T. Taner, "Revisiting the liver's role in transplant alloimmunity," *World Journal of Gastroenterology*, vol. 25, no. 25, pp. 3123–3135, 2019.

[10] K. A. Hogquist and S. C. Jameson, "The self-obsession of T cells: how TCR signaling thresholds affect fate 'decisions' and effector function," *Nature Immunology*, vol. 15, no. 9, pp. 815–823, 2014.

[11] K. A. Newell, A. Asare, A. D. Kirk et al., "Identification of a B cell signature associated with renal transplant tolerance in humans," *The Journal of Clinical Investigation*, vol. 120, no. 6, pp. 1836–1847, 2010.

[12] K. A. Newel, A. B. Adams, and L. A. Turka, "Biomarkers of operational tolerance following kidney transplantation - the immune tolerance network studies of spontaneously tolerant kidney transplant recipients," *Human Immunology*, vol. 79, no. 5, pp. 380–387, 2018.

[13] F. A. M. Kinsella, J. Zuo, C. F. Inman et al., "Mixed chimerism established by hematopoietic stem cell transplantation is maintained by host and donor T regulatory cells," *Blood Advances*, vol. 3, no. 5, pp. 734–743, 2019.

[14] D. E. Speiser, E. Roosnek, M. Jeannet, and R. M. Zinkernagel, "T-cell immunoincompetence in allogeneic chimerism," *The New England Journal of Medicine*, vol. 326, no. 15, pp. 1028-1029, 1992.

[15] T. Kawai, D. H. Sachs, B. Sprangers et al., "Long-term results in recipients of combined HLA-mismatched kidney and bone marrow transplantation without maintenance immunosuppression," *American Journal of Transplantation*, vol. 14, no. 7, pp. 1599–1611, 2014.

[16] J. S. Young, M. D. Daniels, M. L. Miller et al., "Erosion of transplantation tolerance after infection," *American Journal of Transplantation*, vol. 17, no. 1, pp. 81–90, 2017.

[17] A. Massart, L. Ghisdal, M. Abramowicz, and D. Abramowicz, "Operational tolerance in kidney transplantation and associated biomarkers," *Clinical and Experimental Immunology*, vol. 189, no. 2, pp. 138–157, 2017.

[18] H. Waldmann, "Transplantation tolerance: the big picture. Where do we stand, where should we go?," *Clinical and Experimental Immunology*, vol. 189, no. 2, pp. 135–137, 2017.

[19] A. Wadhera, E. Maverakis, N. Mitsiades, P. N. Lara, M. A. Fung, and P. J. Lynch, "Thymoma-associated multiorgan autoimmunity: a graft-versus-host-like disease," *Journal of the American Academy of Dermatology*, vol. 57, no. 4, pp. 683–689, 2007.

[20] N. E. Gilhus, S. Tzartos, A. Evoli, J. Palace, T. M. Burns, and J. J. G. M. Verschuuren, "Myasthenia gravis," *Nature reviews: disease primers*, vol. 5, no. 1, p. 30, 2019.

[21] F. Solimani, R. Maglie, R. Pollmann et al., "Thymoma-associated paraneoplastic autoimmune multiorgan syndrome-from pemphigus to lichenoid dermatitis," *Frontiers in Immunology*, vol. 10, p. 1413, 2019.

[22] J. W. Leiding, "Neutrophil evolution and their diseases in humans," *Frontiers in Immunology*, vol. 8, p. 1009, 2017.

[23] R. L. Gieseck 3rd, M. S. Wilson, and T. A. Wynn, "Type 2 immunity in tissue repair and fibrosis," *Nature Reviews. Immunology*, vol. 18, no. 1, pp. 62–76, 2018.

[24] L. F. Lu, E. F. Lind, D. C. Gondek et al., "Mast cells are essential intermediaries in regulatory T-cell tolerance," *Nature*, vol. 442, no. 7106, pp. 997–1002, 2006.

[25] S. Balzar, M. L. Fajt, S. A. Comhair et al., "Mast cell phenotype, location, and activation in severe asthma," *American Journal of Respiratory and Critical Care Medicine*, vol. 183, no. 3, pp. 299–309, 2011.

[26] S. Balzar, H. W. Chu, M. Strand, and S. Wenzel, "Relationship of small airway chymase-positive mast cells and lung function in severe asthma," *American Journal of Respiratory and Critical Care Medicine*, vol. 171, no. 5, pp. 431–439, 2005.

[27] G. J. Burton, A. L. Watson, J. Hempstock, J. N. Skepper, and E. Jauniaux, "Uterine glands provide histiotrophic nutrition for the human fetus during the first trimester of pregnancy," *The Journal of Clinical Endocrinology and Metabolism*, vol. 87, no. 6, pp. 2954–2959, 2002.

[28] A. Erlebacher, "Immunology of the maternal-fetal interface," *Annual Review of Immunology*, vol. 31, no. 1, pp. 387–411, 2013.

[29] A. Moffett and F. Colucci, "Uterine NK cells: active regulators at the maternal-fetal interface," *The Journal of Clinical Investigation*, vol. 124, no. 5, pp. 1872–1879, 2014.

[30] K. Ohtsubo and J. D. Marth, "Glycosylation in cellular mechanisms of health and disease," *Cell*, vol. 126, no. 5, pp. 855–867, 2006.

[31] P. M. Rudd, T. Elliott, P. Cresswell, I. A. Wilson, and R. A. Dwek, "Glycosylation and the immune system," *Science*, vol. 291, no. 5512, pp. 2370–2376, 2001.

[32] G. F. Clark, "Functional glycosylation in the human and mammalian uterus," *Fertility research and practice*, vol. 1, no. 1, p. 17, 2015.

[33] S. Borowski, I. Tirado-Gonzalez, N. Freitag, M. G. Garcia, G. Barrientos, and S. M. Blois, "Altered glycosylation contributes to placental dysfunction upon early disruption of the NK cell-DC dynamics," *Frontiers in Immunology*, vol. 11, p. 1316, 2020.

[34] N. G. Than, R. Romero, C. J. Kim, M. R. McGowen, Z. Papp, and D. E. Wildman, "Galectins: guardians of eutherian pregnancy at the maternal-fetal interface," *Trends in Endocrinology and Metabolism*, vol. 23, no. 1, pp. 23–31, 2012.

[35] S. M. Blois, G. Dveksler, G. R. Vasta, N. Freitag, V. Blanchard, and G. Barrientos, "Pregnancy galectinology: insights into a complex network of glycan binding proteins," *Frontiers in Immunology*, vol. 10, p. 1166, 2019.

[36] L. Woods, V. Perez-Garcia, J. Kieckbusch et al., "Decidualisation and placentation defects are a major cause of age-related reproductive decline," *Nature Communications*, vol. 8, no. 1, p. 352, 2017.

[37] D. Tannetta, G. Collett, M. Vatish, C. Redman, and I. Sargent, "Syncytiotrophoblast extracellular vesicles - circulating biopsies reflecting placental health," *Placenta*, vol. 52, pp. 134–138, 2017.

[38] L. Czernek and M. Düchler, "Exosomes as messengers between mother and fetus in pregnancy," *International Journal of Molecular Sciences*, vol. 21, no. 12, p. 4264, 2020.

[39] D. W. Bianchi, G. K. Zickwolf, G. J. Weil, S. Sylvester, and M. A. DeMaria, "Male fetal progenitor cells persist in maternal blood for as long as 27 years postpartum," *Proceedings of the National Academy of Sciences of the United States of America*, vol. 93, no. 2, pp. 705–708, 1996.

[40] S. Maloney, A. Smith, D. E. Furst et al., "Microchimerism of maternal origin persists into adult life," *The Journal of Clinical Investigation*, vol. 104, no. 1, pp. 41–47, 1999.

[41] B. F. Haynes, M. E. Martin, H. H. Kay, and J. Kurtzberg, "Early events in human T cell ontogeny. Phenotypic characterization and immunohistologic localization of T cell precursors in early human fetal tissues," *The Journal of experimental medicine*, vol. 168, no. 3, pp. 1061–1080, 1988, Erratum in: *J Exp Med* 1989; 169(2): 603.

[42] J. E. Mold, S. Venkatasubrahmanyam, T. D. Burt et al., "Fetal and adult hematopoietic stem cells give rise to distinct T cell lineages in humans," *Science*, vol. 330, no. 6011, pp. 1695–1699, 2010, Erratum in: Science. 2011; 331 (6017): 534.

[43] D. Vermijlen and I. Prinz, "Ontogeny of innate T lymphocytes-some innate lymphocytes are more innate than others," *Frontiers in immunology*, vol. 5, 2014Erratum in: Front Immunol. 2015; 6: 624.

[44] E. R. Krow-Lucal and J. M. McCune, "Distinct functional programs in fetal T and myeloid lineages," *Frontiers in Immunology*, vol. 5, p. 314, 2014.

[45] N. M. Shah, P. F. Lai, N. Imami, and M. R. Johnson, "Progesterone-related immune modulation of pregnancy and labor," *Frontiers in Endocrinology*, vol. 10, p. 198, 2019.

[46] T. G. Wegmann, H. Lin, L. Guilbert, and T. R. Mosmann, "Bidirectional cytokine interactions in the maternal-fetal relationship: is successful pregnancy a $T_H 2$ phenomenon?," *Immunology Today*, vol. 14, no. 7, pp. 353–356, 1993.

[47] A. P. Kourtis, J. S. Read, and D. J. Jamieson, "Pregnancy and infection," *The New England Journal of Medicine*, vol. 370, no. 23, pp. 2211–2218, 2014.

[48] K. Racicot, J. Y. Kwon, P. Aldo, M. Silasi, and G. Mor, "Understanding the complexity of the immune system during pregnancy," *American Journal of Reproductive Immunology*, vol. 72, no. 2, pp. 107–116, 2014.

[49] ACOG Committee Opinion No, "Maternal immunization," *Obstetrics and Gynecology*, vol. 131, no. 6, pp. e214–e217, 2018.

Review Article

Prognostic Role of TIGIT Expression in Patients with Solid Tumors: A Meta-Analysis

Kunmin Xiao [1,2] **Kunlin Xiao** [3] **Kexin Li** [2] **Peng Xue** [1] and **Shijie Zhu** [1]

[1]*Department of Oncology, Wangjing Hospital, China Academy of Chinese Medical Sciences, Beijing, China*
[2]*Graduate School, Beijing University of Chinese Medicine, Beijing, China*
[3]*School of Nursing, Xinjiang Medical University, Urumqi, China*

Correspondence should be addressed to Peng Xue; xuepeng6399@163.com and Shijie Zhu; 20180941234@bucm.edu.cn

Background. T cell immunoglobulin and ITIM domain (TIGIT) is a recently identified immunosuppressive receptor. The expression levels of TIGIT affect the prognosis of patients with solid tumors. To fully comprehend the role of TIGIT on the prognosis of patients with solid tumors, we conducted a meta-analysis. *Methods.* We performed an online search of PubMed, Embase, Web of Science (WOS), and MEDLINE databases for literature published till March 31, 2021. The Newcastle-Ottawa Scale (NOS) was used to evaluate the quality of the literature, and Stata 16.0 and Engauge Digitizer 4.1 software were used for data analysis. *Results.* Our literature search identified eight papers comprising 1426 patients with solid tumors. Increased expression of TIGIT was associated with poor prognosis. High expression of TIGIT was a risk factor for overall survival (OS) {hazard ratio (HR) = 1.66, 95% confidence interval (CI) [1.26, 2.20], $P < 0.001$} and progression-free survival (PFS) (HR = 1.44, 95% CI [1.15, 1.81], $P = 0.01$). We performed subgroup analysis to explore the source of heterogeneity, colorectal cancer (HR = 2.07, 95% CI [0.23, 18.82], $P = 0.518$), lung cancer (HR = 1.29, 95% CI [0.96, 1.72], $P = 0.094$), esophageal cancer (HR = 1.70, 95% CI [1.20, 2.40], $P = 0.003$), and other cancers (HR = 1.83, 95% CI [1.25, 2.68], $P = 0.002$). In addition to cancer type, expression location, sample size, and different statistical analysis methods are also considered the possible causes of heterogeneity between studies. Funnel plots suggested no publication bias for OS ($P = 0.902$), and Egger's test supported this conclusion ($P = 0.537$). *Conclusion.* TIGIT expression was associated with OS and PFS in patients with solid tumors. Patients with elevated TIGIT expression have a shorter OS and PFS, and TIGIT expression could be a novel biomarker for prognosis prediction and a valuable therapeutic target for solid tumors.

1. Introduction

The global burden of cancer morbidity and mortality is rapidly increasing. By 2020, there are estimated to be 19.29 million new cancer cases and 9.96 million deaths worldwide. It is expected that by 2040, the global burden of cancer will reach 28.4 million cases, an increase of 47% compared with that in 2020 [1]. In recent years, with deepening of the understanding of tumor molecular mechanisms, many tumor markers have been identified, which can be used for tumor diagnosis and prognosis judgement. Identification of new biomarkers with the potential to predict the progress and prognosis of cancer has brought new hope for cancer patients.

T cell immunoglobulin and ITIM domain (TIGIT), also known as WUCAM, Vstm3, and VSIG9, is a newly discovered coinhibitory receptor belonging to the poliovirus receptor/nectin family. TIGIT is primarily expressed in T cells and natural killer cells. Yu's group was the first to determine the unique structure of TIGIT and explore its function [2]. TIGIT is expressed in various levels in various T cell subsets. Abnormally expressed TIGIT suppresses immune cells in multiple steps of the tumor immune cycle and promotes tumor immune escape to a great extent [2–4]. Similar to the classical immune checkpoint of programmed cell death protein 1/programmed cell death ligand 1 (PD-1/PD-L1), cytotoxic T-lymphocyte-associated antigen 4 (CTLA-4)/B7.1/2 and CD226/TIGIT-CD155/CD112 are

considered emerging pathways that precisely regulate T cell activation [5].

TIGIT is overexpressed in many solid tumors, including in liver cancer [6, 7], colorectal cancer (CRC) [8–10], breast cancer [11, 12], thyroid cancer [13], lung cancer [14–16], gastric cancer (GC) [17, 18], esophageal squamous cell carcinoma (ESCC) [19], and melanoma [20, 21]. Liang et al. discovered that TIGIT expression level in tumor tissue was correlated with CRC recurrence and survival [10]. TIGIT expression was considerably higher in advanced CRC than in early CRC. TIGIT expression is an independent prognostic factor for CRC and leads to a poor prognosis. However, other studies have shown that TIGIT expression is downregulated in the peripheral blood in advanced CRC, and there is no strong relationship between TIGIT expression and the overall survival (OS) rate of CRC [8, 9]. The prognosis prediction value of TIGIT for various cancers remains controversial. Therefore, we performed a meta-analysis to gain a better understanding of the impact of TIGIT on the prognosis of patients with solid cancer.

2. Methods

2.1. Search Strategies. We followed the Preferred Reporting Items for Systematic Reviews and Meta-Analyses (PRISMA) criteria. We searched PubMed, EMBASE, Web of Science (WOS), and MEDLINE databases for articles on the correlation between TIGIT expression and the prognosis of malignant tumors from the date of establishment of the database to March 31, 2021. The keywords used were "TIGIT," "T-cell Ig and ITIM domain," "WUCAM," "Vstm3," "VSIG9," "carcinoma," "tumor," "neoplasia," "neoplasm," "cancer," "malignancy," "malignant neoplasm," "prognostic," "survival," "prognosis," "recurrence," "outcome," and "mortality." Based on the characteristics of different databases, we conducted a comprehensive search of medical subject words (MeSH) combined with text words. The language of the restricted search was English.

2.2. Criteria for Inclusion and Exclusion. The inclusion criteria were as follows: (1) patients with solid tumors who underwent pathological testing to verify their diagnosis; (2) prospective or historical cohort studies; (3) immunohistochemistry (IHC) staining was used to determine TIGIT expression; (4) the cut-off value of TIGIT was reported; (5) correlation of TIGIT with survival indexes, such as OS, progression-free survival (PFS), disease-free survival (DFS), and relapse-free survival (RFS) was described; and (6) the hazard ratio (HR) and its 95% confidence interval (CI).

Exclusion criteria were as follows: (1) abstracts, reviews, case reports, letters, or nonclinical studies; (2) insufficient data for HR and 95% CI; (3) there were no studies published in English; and (4) duplicate data or analysis was identified in the studies.

2.3. Data Extraction and Quality Evaluation. Two independent authors (KMX and KLX) evaluated and extracted all candidate papers. In case of a dispute, the two authors consulted with a third author (KXL). The following details

were extracted from the studies: first author, publication year, patient source, sample size, TIGIT positive rate, cancer type, detection method, expression location, cut-off value, statistical method, results, HR estimation method (univariate and multivariate analysis), and HR ratio. The required data were directly extracted or obtained from the survival curve using Engauge Digitizer 4.1 software to calculate the HR and 95% CI. Two independent authors (KMX and KLX) used Newcastle-Ottawa Scale (NOS) to determine the quality of the studies involved [22]. When the score was ≥6, the included literature was considered to be of high quality.

2.4. Statistical Methods. HR and 95% CI were pooled using Stata 16.0, to evaluate the impact of high and low TIGIT expression on the prognosis of patients with solid tumors. I^2 is a quantitative statistic that reflects the percentage of interstudy variation in the overall variation [23]. According to the rule of thumb, for interpreting I^2 statistics provided by the Cochrane Handbook [24], $I^2 \geq 50\%$ indicates substantial heterogeneity. The random-effects model was used when significant heterogeneity was observed; otherwise, a fixed-effects model was used. Subgroup and sensitivity analyses were used to investigate the origins of heterogeneity; Begg's and Egger's tests were used to determine publication bias. A 2-sided $P < 0.05$ was considered statistically significant.

3. Results

3.1. Study Selection. A total of 862 papers were initially identified. After removing duplicate literature and reading the title, abstract, and full text, according to the study's inclusion and exclusion requirements, eight papers were included [9, 10, 15–17, 19, 21, 25]. The process and results of the literature screening are presented in Figure 1.

3.2. Study Characteristics. Table 1 shows the basic characteristics of the studies involved in this meta-analysis. Eight articles included in this meta-analysis were published from 2018 to 2021, involving 1426 patients. All studies used IHC to detect TIGIT expression levels, but the cut-off values were not identical. The study subjects were from China ($n = 7$) and South Korea ($n = 1$). Cancer types included melanoma, lung adenocarcinoma (LUAD), GC, small cell lung cancer (SCLC), ESCC, primary small cell carcinoma of the esophagus (PSCCE), and CRC. Five studies explicitly documented reported HRs and 95% CIs, while the other three studies calculated HR and 95% CI from the survival curves. All studies evaluated the correlation between TIGIT expression and OS in patients with solid tumors [9, 10, 15–17, 19, 21, 25], and three studies evaluated the relationship between TIGIT expression and PFS in patients with solid tumors [16, 21, 25]. Zhou et al. [9] and Liang et al. [10] reported the relationship between TIGIT expression and DFS and RFS, respectively. The NOS scores of all included articles were ≥6, and the scoring details are presented in Table S1.

3.3. Overall Survival. Eight studies provided sufficient data to investigate the connection between TIGIT expression and OS. The pooled results of the meta-analysis indicated that
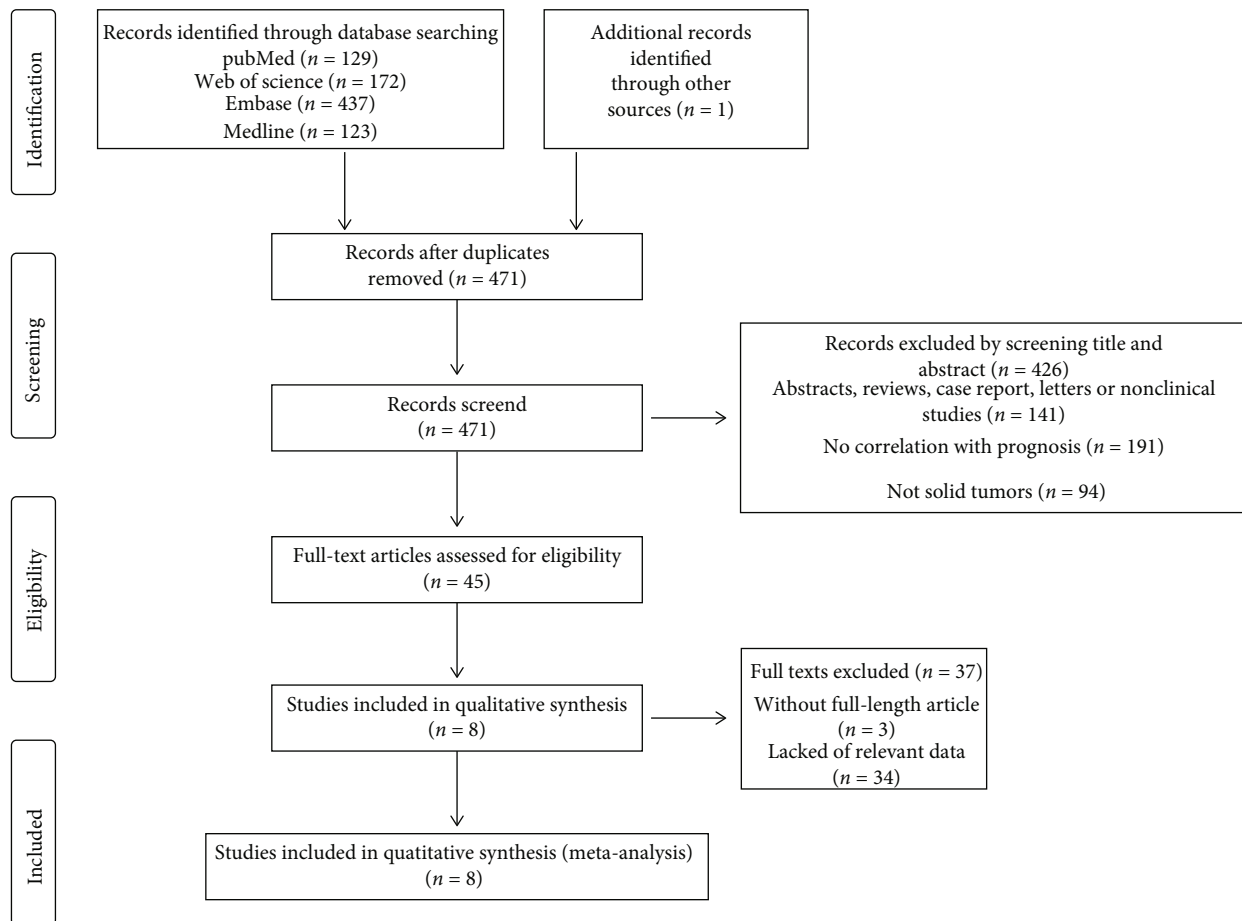
Figure 1: Literature screening process and results.

Table 1: Basic characteristics of included studies.

Author	Year	Patient source	Sample size	TIGIT +	Cancer type	Method	Expression location	Cut-off value	Outcome	M/U	HR ratio	NOS
Zhao JJ	2018	Chinese	154	76 (49.4%)	ESCC	IHC	TIL	Median level	OS	M	Reported	8
Tang W	2019	Chinese	441	343 (77.8%)	GC	IHC	Tumor cell	>5% positivity cell	OS	M	Reported	8
Xu Y	2019	Chinese	60	21 (35%)	SCLC	IHC	Tumor cell	Median level	OS	U	Survival curve	6
Lee WJ	2020	Korea	124	52 (41.9%)	Melanoma	IHC	Tumor cell	≥20% positivity cell	OS/PFS	U	Survival curve	7
Sun Y	2020	Chinese	334	204 (61.1%)	LUAD	IHC	TIL	≥5% positivity cell	OS/PFS	M	Reported/ survival curve	7
Zhao K	2020	Chinese	114	74 (64.9%)	PSCCE	IHC	Tumor cell	≥5% positivity cell	OS/PFS	M	Reported/ survival curve	8
Zhou X	2020	Chinese	60	21 (35%)	CRC	IHC	Tumor cell	Score ≥ 1	OS/DFS	M	Reported	8
Liang R	2021	Chinese	139	40 (28.8%)	CRC	IHC	Tumor cell	Median level	OS/RFS	U	Survival curve	6

OS: overall survival; PFS: progress-free survival; DFS: disease-free survival; RFS: recurrence-free survival; U: univariate; M: multivariate; TIL: tumor infiltrating lymphocyte; IHC: immunohistochemistry; LUAD: lung adenocarcinoma; GC: gastric cancer; SCLC: small cell lung cancer; ESCC: esophageal squamous cell carcinoma; PSCCE: primary small cell carcinoma of the esophagus; CRC: colorectal cancer.
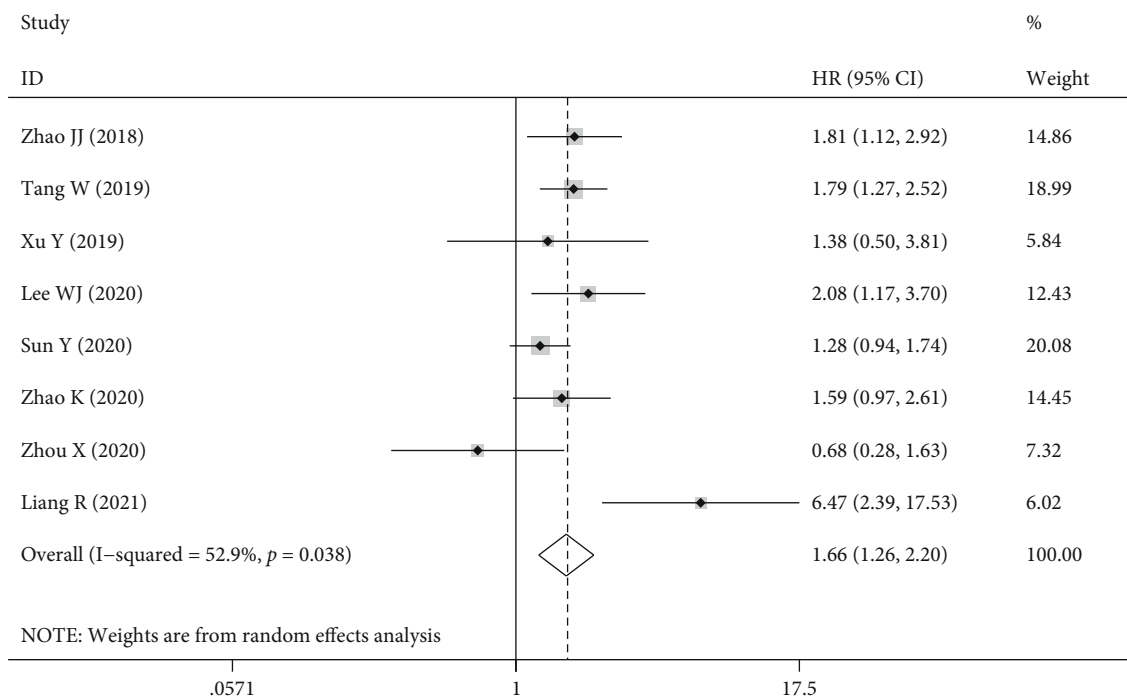
Figure 2: Forest plot for OS.

upregulation of TIGIT expression was correlated with worsening OS in patients with solid cancer (HR = 1.66, 95% CI [1.26, 2.20], $P < 0.001$). Heterogeneity across studies was $I^2 = 52.9\%$, $P = 0.038$; therefore, a random-effects model was used for analysis (as shown in Figure 2). Subgroup analysis was used to investigate the origin of heterogeneity. The heterogeneity of CRC (HR = 2.07, 95% CI [0.23, 18.82], $P = 0.518$) was as high as $I^2 = 91\%$, while lung cancer (HR = 1.29, 95% CI [0.96, 1.72], $P = 0.094$), esophageal cancer (HR = 1.70, 95% CI [1.20, 2.40], $P = 0.003$), and other cancers (HR = 1.83, 95% CI [1.25, 2.68], $P = 0.002$) did not show heterogeneity. The expression of TIGIT and TILs on tumor cells was significantly correlated with poor OS (tumor cells HR = 1.78, 95% CI [1.19–2.65], $P = 0.005$); tumor infiltrating lymphocytes (TILs) (HR = 1.41, 95% CI [1.09, 1.83], $P = 0.009$). Studies with sample sizes ≥100 showed a tendency to increase the risk of short OS (HR = 1.80, 95% CI [1.36, 2.39], $P \leq 0.001$). Studies with sample sizes >100 showed the opposite trend (HR = 0.92, 95% CI [0.47, 1.78], $P = 0.802$); however, significant differences were not observed. In terms of methods for estimating HR, univariate analysis had a greater effect on prognosis than multivariate analysis (HR = 2.57, 95% CI [1.17, 5.67], $P = 0.019$ vs. HR = 1.49, 95% CI [1.24, 1.80], $P \leq 0.001$) (Table 2).

3.4. Progression-Free Survival. Three studies involving 572 patients reported an association between TIGIT expression and PFS in patients with solid tumors, and Lee WJ analysis showed that patients with high TIGIT expression had considerably worse PFS than patients with low TIGIT expression (59.0 months vs. 32.0 months, $P = 0.01$); however, HR values and Kaplan-Meier curves were not provided; therefore, a meta-analysis could not be conducted. The

fixed-effects model was used in this analysis because there was no significant heterogeneity between the studies ($I^2 = 0.0\%$, $P = 0.583$). The results showed that high expression of TIGIT was a risk factor for poor PFS (HR = 1.44, 95% CI [1.15, 1.81], $P = 0.01$). As DFS and RFS were documented in only one related article, they were not sufficient for a meta-analysis (Figure 3).

3.5. Sensitivity Analysis. Sensitivity analysis eliminated each study individually, and then, a combined analysis was conducted for the remaining studies. The results showed that the combined effect value before and after the elimination of any study had no significant change, suggesting that the results of this study were stable (as shown in Figure 4).

3.6. Publication Bias. Begg's and Egger's methods were used to assess the publication bias. The funnel plot revealed no major asymmetry ($P = 0.902$; Figure 5(a)). Furthermore, Egger's test supported this conclusion ($P = 0.537$; Figure 5(b)). Therefore, our meta-analysis did not reveal any publication bias.

4. Discussion

TIGIT is a fairly new immunosuppressive receptor, discovered 11 years ago. In recent years, TIGIT expression has been shown to have prognostic significance in patients with solid tumors in a variety of trials, but its role has been inconsistent and unclear. Therefore, we reviewed published studies and performed a meta-analysis. Our present meta-analysis may be the only study to date evaluating the association between TIGIT expression and OS in patients with solid tumors.

TABLE 2: Subgroup analysis results.

Analysis	N	Random-effects model		Fixed-effects model		Heterogeneity	
		HR (95% CI)	P	HR (95% CI)	P	I^2	pH
Cancer type							
Colorectal cancer	2	2.07 (0.23, 18.82)	0.518	1.81 (0.94, 3.50)	0.076	91.0%	0.001
Lung cancer	2	1.29 (0.96, 1.72)	0.094	1.29 (0.96, 1.72)	0.094	0.0%	0.886
Esophagus cancer	2	1.70 (1.20, 2.40)	0.030	1.70 (1.20, 2.40)	0.003	0.0%	0.715
Others	2	1.86 (1.39, 2.50)	0.001	1.86 (1.39, 2.50)	0.001	0.0%	0.662
Expression position							
Tumor cells	6	1.78 (1.19, 2.65)	0.005	1.77 (1.40, 2.22)	0.001	57.7%	0.037
TILs	2	1.44 (1.04, 2.00)	0.027	1.41 (1.09, 1.83)	0.009	30.2%	0.231
Sample size							
<100	2	0.92 (0.46, 1.83)	0.817	0.92 (0.47, 1.78)	0.802	6.5%	0.301
≥100	6	1.80 (1.36, 2.39)	0.001	1.67 (1.40, 1.99)	0.001	54.1%	0.054
Method to estimate HR							
Multivariate analysis	5	1.49 (1.17, 1.88)	0.001	1.49 (1.24, 1.80)	0.001	31.9%	0.209
Univariate analysis	3	2.57 (1.17, 5.67)	0.019	2.42 (1.54, 3.78)	0.001	61.4%	0.075
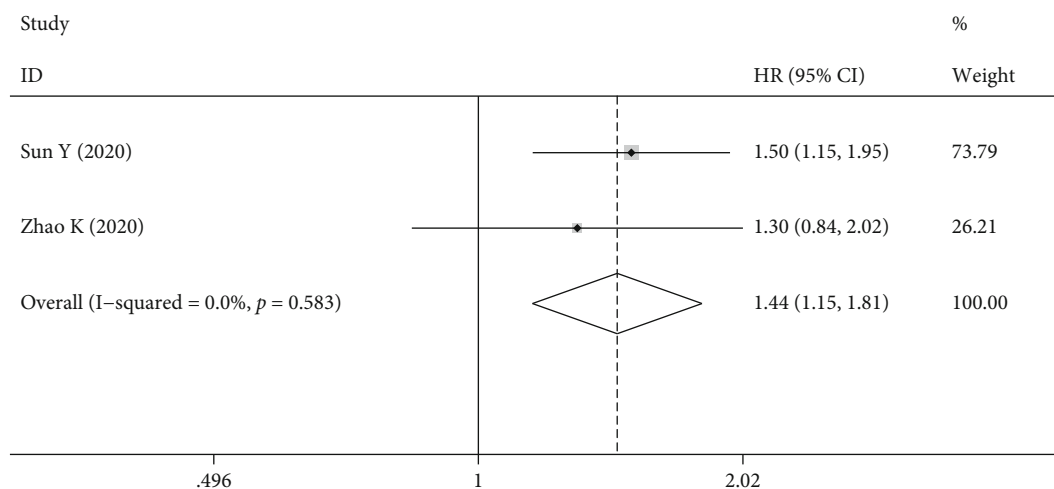
FIGURE 3: Forest plot for PFS.

Our meta-analysis included 1430 patients with solid tumors from eight studies. The results showed that increased expression of TIGIT was associated with a poor prognosis. High expression of TIGIT was a risk factor for OS (HR = 1.66, 95% CI [1.26, 2.20], $P < 0.001$) and PFS (HR = 1.44, 95% CI [1.15, 1.81], $P = 0.01$). In addition, we found that the cancer type, expression location, sample sizes, and different statistical analysis methods are possible reasons for the heterogeneity between studies. Our results emphasize the prognostic value of TIGIT expression in patients with solid tumors.

The immune checkpoint is one of the main causes of immune tolerance. Immunotherapy targeting the classical immune checkpoints of PD-1/PD-L1 and CTLA-4/B7.1/2 has brought hope to patients with tumors. However, in actual clinical applications, only a part of the dominant population has an immune response, and PD-1/PD-L1 immune checkpoint inhibitors are prone to drug resistance and

severe adverse effects [26, 27]. Therefore, there is an urgent need to identify new immune checkpoints to compensate for low response rates, drug resistance, and severe adverse reactions, such as lymphocyte activation gene 3 (LAG-3) [28], T cell immunoglobulin-3 (TIM-3) [29], and TIGIT, which can negatively regulate T cell activation and function and induce T cell exhaustion; however, they each have unique signaling pathways and regulatory functions, so their clinical applications are different [30]. Compared with those on LAG-3 and TIM-3, studies on TIGIT expression provided more encouraging results [31]. TIGIT has a higher positive rate in TILs than does PD-1 [19], and TIGIT inhibitors can transduce CD155-mediated signals to CD226 activation, thus improving immunotherapy, which is advantageous [20]. In CITYSCAPE, a phase II clinical trial, 135 patients with PD-L1 positive non-small-cell lung cancer were randomized to receive the TIGIT inhibitor tiragolumab in combination with a PD-L1 inhibitor or PD-L1 inhibitor

Meta-analysis random-effects estimates (expenential form)

Study omitted
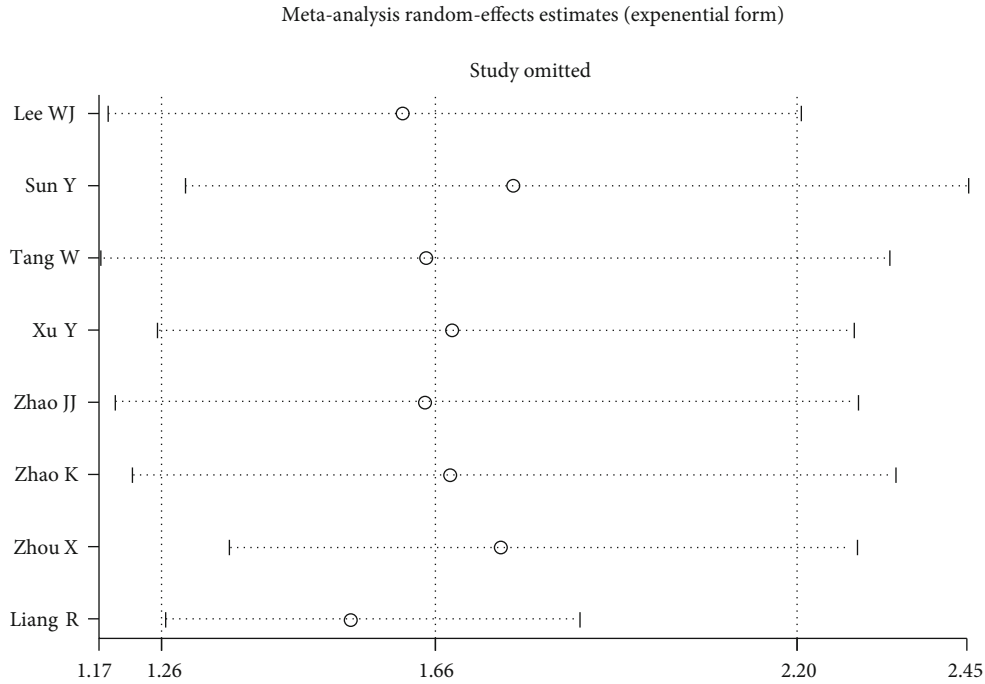
Figure 4: Consequence of sensitivity analysis.

Begg's funnel plot with pseudo 95% confidence limits

(a)

Egger's publication bias plot

(b)
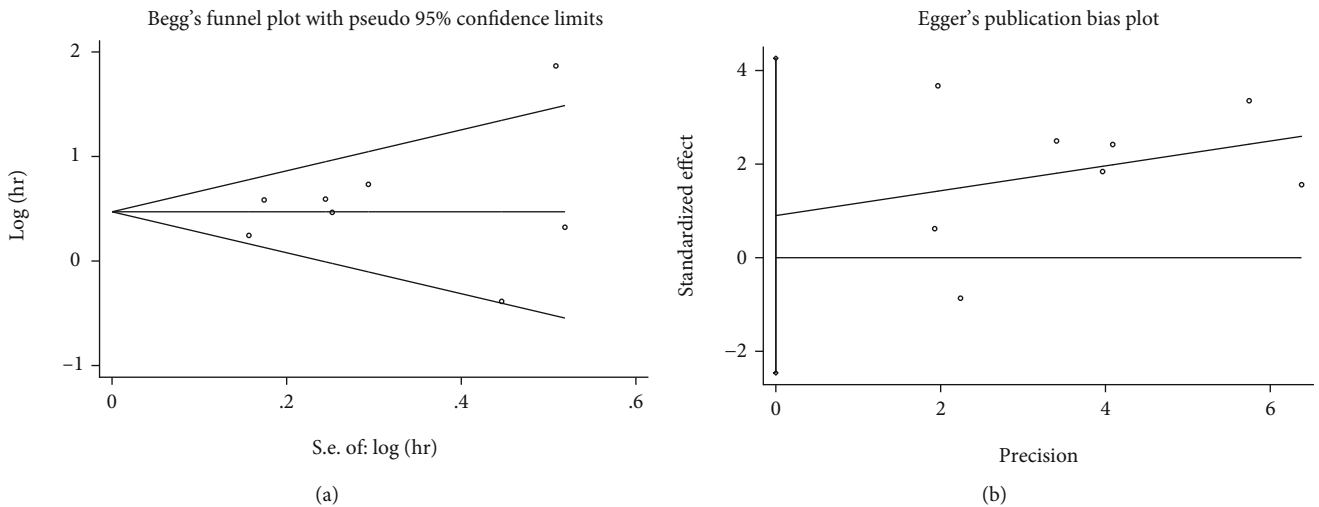
Figure 5: Result of publication bias. (a) Begg's test; (b) Egger's test.

alone. The results showed that addition of tiragolumab significantly improved patient outcomes, with the objective response rate increasing from 21% to 37% and the median PFS increasing from 3.9 months to 5.6 months without an increase in adverse events. In particular, the objective response rate of patients with high PD-L1 expression (>50%) increased from 24% to 66% after the addition of tiragolumab [32]. In addition to the combination of PD-1/PD-L1 inhibitors, the combination of TIGIT antibody and other immune checkpoint inhibitors can also produce synergistic effects and improve the efficacy of immunotherapy [33].

TIGIT affects the prognosis of cancer patients by inhibiting the function of immune cells through a variety of mechanisms [34]. These are as follows: (1) TIGIT binds to CD155 and causes T cells to send a direct inhibition signal, inducing immune tolerance [35]; (2) TIGIT stimulates the immune response indirectly by activating CD155 on DCs, increasing IL-10 secretion while decreasing IL-12 secretion [2]; (3) TIGIT not only competes with the CD226 ligand but also binds directly to CD226 and disrupts its homodimerization, thereby disrupting its costimulatory effect and preventing CD226-mediated T cell activation [4]; (4) TIGIT signaling in regulatory T cells (Tregs) affects the secretion of cytokines

and suppresses proinflammatory Th1 and Th17 T cell responses [36], which enhances the immunosuppressive function and stability of Tregs.

We showed an association between TIGIT expression and the prognosis of patients with solid tumors, but the prognostic effects of TIGIT on different tumors were inconsistent, which may be due to different characteristics and different expression sites of different tumors. Significant heterogeneity was observed in the two CRC studies, which could be explained by study's methodological design and confounders of clinical covariates. PFS, DFS, and RFS can all predict and reflect clinical benefits, but there are few relevant studies reported at present, and it is impossible to measure the combined HR. Many studies are needed to evaluate the prognostic value of TIGIT.

Although we tried our best to conduct a comprehensive analysis, our meta-analysis has certain limitations. Despite the use of subgroup and sensitivity analyses, the origin of the heterogeneity could not be completely traced. Second, all the studies were retrospective, with all subjects being Asian, which does not represent the whole population. Third, the scale of the included studies was small. Some studies include only one kind of cancer, and studies with a larger sample size are required to fully understand the connection between TIGIT and the survival index. Third, although IHC was used in all the studies, the antibodies used were no identical, and the thresholds were not consistent. We should further explore the establishment of a unified threshold. Fourth, the number of studies included in this article was very limited. When the number of included articles is less than 10, the efficiency of Begg's test and Egger's test detection tend to reduce, and as this study included English language articles, publication bias cannot be ruled out. We hope that this meta-analysis not only represents the end point of the study but also begins to pay attention to the value of TIGIT in solid tumors and to look forward to more high-quality studies.

5. Conclusion

Taken together, our findings indicate a significantly increased risk of OS and PFS associated with elevated TIGIT expression. TIGIT appears to be a promising therapeutic target for solid tumors as well as a prognostic predictor, which deserves the attention of researchers and clinicians. Due to the limitations of the number and quality of the included literature, our results need to be interpreted carefully. Further studies are necessary to evaluate the molecular mechanism of TIGIT in patients with solid tumors.

Data Availability

No new data generated.

Ethical Approval

Ethics approval was received by each involved study in this meta-analysis.

Conflicts of Interest

The authors declare that they have no conflict of interest.

Authors' Contributions

KMX and KLX shared first authors, performed the experiments, and analyzed the data. PX and SJZ contributed equally and conceived and designed the experiments. KMX wrote the manuscript. KXL contributed analysis tools. All authors read and approved the final manuscript prior to submission. KMX and KLX contributed equally to this work, and PX and SJZ shared corresponding authors.

Acknowledgments

Supplementary Materials

Table S1: Newcastle-Ottawa Scale for assessing the quality of studies in meta-analysis. (*Supplementary Materials*)

References

[1] H. Sung, J. Ferlay, R. L. Siegel et al., "Global cancer statistics 2020: GLOBOCAN estimates of incidence and mortality worldwide for 36 cancers in 185 countries," *CA: a Cancer Journal for Clinicians*, vol. 71, no. 3, pp. 209–249, 2021.

[2] X. Yu, K. Harden, L. C Gonzalez et al., "The surface protein TIGIT suppresses T cell activation by promoting the generation of mature immunoregulatory dendritic cells," *Nature Immunology*, vol. 10, no. 1, pp. 48–57, 2009.

[3] R. J. Johnston, L. Comps-Agrar, J. Hackney et al., "The immunoreceptor TIGIT regulates antitumor and antiviral CD8$^+$ T cell effector function," *Cancer Cell*, vol. 26, no. 6, pp. 923–937, 2014.

[4] E. Lozano, M. Dominguez-Villar, V. Kuchroo, and D. A. Hafler, "The TIGIT/CD226 axis regulates human T cell function," *Journal of Immunology*, vol. 188, no. 8, pp. 3869–3875, 2012.

[5] S. Tahara-Hanaoka, K. Shibuya, Y. Onoda et al., "Functional characterization of DNAM-1 (CD226) interaction with its ligands PVR (CD155) and nectin-2 (PRR-2/CD112)," *International Immunology*, vol. 16, no. 4, pp. 533–538, 2004.

[6] X. Duan, J. Liu, J. Cui et al., "Expression of TIGIT/CD155 and correlations with clinical pathological features in human hepatocellular carcinoma," *Molecular Medicine Reports*, vol. 20, no. 4, pp. 3773–3781, 2019.

[7] X. Liu, M. Li, X. Wang et al., "PD-1$^+$ TIGIT$^+$ CD8$^+$ T cells are associated with pathogenesis and progression of patients with hepatitis B virus-related hepatocellular carcinoma," *Cancer Immunology, Immunotherapy*, vol. 68, no. 12, pp. 2041–2054, 2019.

[8] B. Ma, X. Duan, Q. Zhou et al., "Use of aspirin in the prevention of colorectal cancer through TIGIT-CD155 pathway," *Journal of Cellular and Molecular Medicine*, vol. 23, no. 7, pp. 4514–4522, 2019.

[9] X. Zhou, X. Ding, H. Li et al., "Upregulation of TIGIT and PD-1 in colorectal cancer with mismatch-repair deficiency," *Immunological Investigations*, vol. 50, no. 4, pp. 338–355, 2021.

[10] R. Liang, X. Zhu, T. Lan et al., "TIGIT promotes CD8$^+$ T cells exhaustion and predicts poor prognosis of colorectal cancer," *Cancer Immunology, Immunotherapy*, vol. 70, no. 10, pp. 2781–2793, 2021.

[11] J. Fang, F. Chen, D. Liu, F. Gu, Z. Chen, and Y. Wang, "Prognostic value of immune checkpoint molecules in breast cancer," *Bioscience Reports*, vol. 40, no. 7, 2020.

[12] X. Xie, J. Zhang, Z. Shi et al., "The expression pattern and clinical significance of the immune checkpoint regulator VISTA in human breast cancer," *Frontiers in Immunology*, vol. 11, article 563044, 2020.

[13] X. Shi, C. W. Li, L. C. Tan et al., "Immune co-inhibitory receptors PD-1, CTLA-4, TIM-3, LAG-3, and TIGIT in medullary thyroid cancers: a large cohort study," *The Journal of Clinical Endocrinology and Metabolism*, vol. 106, no. 1, pp. 120–132, 2021.

[14] F. Hu, W. Wang, C. Fang, and C. Bai, "TIGIT presents earlier expression dynamic than PD-1 in activated CD8$^+$ T cells and is upregulated in non-small cell lung cancer patients," *Experimental Cell Research*, vol. 396, no. 1, article 112260, 2020.

[15] Y. Xu, G. Cui, Z. Jiang, N. Li, and X. Zhang, "Survival analysis with regard to PD-L1 and CD155 expression in human small cell lung cancer and a comparison with associated receptors," *Oncology Letters*, vol. 17, no. 3, pp. 2960–2968, 2019.

[16] Y. Sun, J. Luo, Y. Chen et al., "Combined evaluation of the expression status of CD155 and TIGIT plays an important role in the prognosis of LUAD (lung adenocarcinoma)," *International Immunopharmacology*, vol. 80, article 106198, 2020.

[17] W. Tang, X. Pan, D. Han et al., "Clinical significance of CD8$^+$ T cell immunoreceptor with Ig and ITIM domains$^+$ in locally advanced gastric cancer treated with SOX regimen after D2 gastrectomy," *Oncoimmunology*, vol. 8, no. 6, article e1593807, 2019.

[18] W. He, H. Zhang, F. Han et al., "CD155T/TIGIT signaling regulates CD8+ T-cell metabolism and promotes tumor progression in human gastric cancer," *Cancer Research*, vol. 77, no. 22, pp. 6375–6388, 2017.

[19] J. J. Zhao, Z. Q. Zhou, P. Wang et al., "Orchestration of immune checkpoints in tumor immune contexture and their prognostic significance in esophageal squamous cell carcinoma," *Cancer Management and Research*, vol. 10, pp. 6457–6468, 2018.

[20] J. M. Chauvin, O. Pagliano, J. Fourcade et al., "TIGIT and PD-1 impair tumor antigen-specific CD8$^+$ T cells in melanoma patients," *The Journal of Clinical Investigation*, vol. 125, no. 5, pp. 2046–2058, 2015.

[21] W. J. Lee, Y. J. Lee, M. E. Choi et al., "Expression of lymphocyte-activating gene 3 and T-cell immunoreceptor with immunoglobulin and ITIM domains in cutaneous melanoma and their correlation with programmed cell death 1 expression in tumor-infiltrating lymphocytes," *Journal of the American Academy of Dermatology*, vol. 81, no. 1, pp. 219–227, 2019.

[22] A. Stang, "Critical evaluation of the Newcastle-Ottawa scale for the assessment of the quality of nonrandomized studies in meta-analyses," *European Journal of Epidemiology*, vol. 25, no. 9, pp. 603–605, 2010.

[23] J. P. Higgins and S. G. Thompson, "Quantifying heterogeneity in a meta-analysis," *Statistics in Medicine*, vol. 21, no. 11, pp. 1539–1558, 2002.

[24] J. P. Higgins, J. Thomas, J. Chandler et al., *Cochrane Handbook for Systematic Reviews of Interventions Version 6.2 (Updated February 2021)*, John Wiley & Sons, 2021.

[25] K. Zhao, L. Ma, L. Feng, Z. Huang, X. Meng, and J. Yu, "CD155 overexpression correlates with poor prognosis in primary small cell carcinoma of the esophagus," *Frontiers in Molecular Biosciences*, vol. 7, article 608404, 2021.

[26] B. El Osta, F. Hu, R. Sadek, R. Chintalapally, and S. C. Tang, "Not all immune-checkpoint inhibitors are created equal: meta-analysis and systematic review of immune-related adverse events in cancer trials," *Critical Reviews in Oncology/Hematology*, vol. 119, pp. 1–12, 2017.

[27] M. A. Postow, R. Sidlow, and M. D. Hellmann, "Immune-related adverse events associated with immune checkpoint blockade," *The New England Journal of Medicine*, vol. 378, no. 2, pp. 158–168, 2018.

[28] E. Ruffo, R. C. Wu, T. C. Bruno, C. J. Workman, and D. A. A. Vignali, "Lymphocyte-activation gene 3 (LAG3): the next immune checkpoint receptor," *Seminars in Immunology*, vol. 42, article 101305, 2019.

[29] C. Solinas, P. De Silva, D. Bron, K. Willard-Gallo, and D. Sangiolo, "Significance of TIM3 expression in cancer: from biology to the clinic," *Seminars in Oncology*, vol. 46, no. 4-5, pp. 372–379, 2019.

[30] A. C. Anderson, N. Joller, and V. K. Kuchroo, "Lag-3, Tim-3, and TIGIT: co-inhibitory receptors with specialized functions in immune regulation," *Immunity*, vol. 44, no. 5, pp. 989–1004, 2016.

[31] Z. Ge, M. P. Peppelenbosch, D. Sprengers, and J. Kwekkeboom, "TIGIT, the next step towards successful combination immune checkpoint therapy in cancer," *Frontiers in Immunology*, vol. 12, article 699895, 2021.

[32] D. Rodriguez-Abreu, M. L. Johnson, M. A. Hussein et al., "Primary analysis of a randomized, double-blind, phase II study of the anti-TIGIT antibody tiragolumab (tira) plus atezolizumab (atezo) versus placebo plus atezo as first-line (1L) treatment in patients with PD-L1-selected NSCLC (CITYSCAPE)," *Journal of Clinical Oncology*, vol. 38, 15 supplement, p. 9503, 2020.

[33] S. Kurtulus, K. Sakuishi, S. F. Ngiow et al., "TIGIT predominantly regulates the immune response via regulatory T cells," *The Journal of Clinical Investigation*, vol. 125, no. 11, pp. 4053–4062, 2015.

[34] J. M. Chauvin and H. M. Zarour, "TIGIT in cancer immunotherapy," *Journal for Immunotherapy of Cancer*, vol. 8, no. 2, p. e000957, 2020.

[35] S. D. Levin, D. W. Taft, C. S. Brandt et al., "Vstm3 is a member of the CD28 family and an important modulator of T-cell function," *European Journal of Immunology*, vol. 41, no. 4, pp. 902–915, 2011.

[36] N. Joller, E. Lozano, P. R. Burkett et al., "Treg cells expressing the coinhibitory molecule TIGIT selectively inhibit proinflammatory Th1 and Th17 cell responses," *Immunity*, vol. 40, no. 4, pp. 569–581, 2014.

Research Article

Protective Effect of Uric Acid on ox-LDL-Induced HUVECs Injury via Keap1-Nrf2-ARE Pathway

Yajuan Lin, Yunpeng Xie ⑩, Zhujing Hao, Hailian Bi, Yang Liu, Xiaolei Yang ⑩, and Yunlong Xia ⑩

Department of Cardiology, First Affiliated Hospital of Dalian Medical University, Dalian, Liaoning, China

Correspondence should be addressed to Xiaolei Yang; yangxl1012@yeah.net and Yunlong Xia; dlmu_xiayunlong@163.com

Uric acid is an effective antioxidant. Oxidized low-density lipoprotein (ox-LDL) is derived from circulating LDL and promotes atherosclerosis. The Keap1-Nrf2-ARE pathway is a key body pathway involved in protection against internal and external oxidative damages. The role of uric acid on vascular endothelial function damaged by ox-LDL, and its effect on the Keap1-Nrf2-ARE pathway has not been fully explored. HUVECs were treated with different concentrations of uric acid and ox-LDL to explore the effect of uric acid in vitro. Cell phenotype was determined by cytometry and Western blot. Nuclear translocation of Nrf2 was determined by immunofluorescence. Coimmunoprecipitation was used to determine the level of Nrf2 ubiquitination. A microfluidic device was used to mimic the vascular environment in the body, and the level of mRNA levels of inflammatory factors was determined by RT-PCR. The findings of this study show that suitable uric acid can significantly reduce endothelial damage caused by ox-LDL, such as oxidative stress, inflammation, and increased adhesion. In addition, uric acid reduced Nrf2 ubiquitination and increased nuclear translocation of Nrf2 protein, thus activating the Keap1-Nrf2-ARE pathway and playing a protective role. Interestingly, the effects of UA were significantly inhibited by administration of Brusatol, an inhibitor of Nrf2. In summary, suitable concentrations of uric acid can alleviate the oxidative stress level of endothelial cells through Nrf2 nuclear translocation and further protect cells from damage.

1. Introduction

Oxidized low-density lipoprotein (ox-LDL) promotes atherosclerosis (AS). Oxidized LDL level increases during the occurrence of AS, which can lead to damage vascular endothelial cells [1]. Several studies report that vascular endothelial cell damage and functional changes are initial manifestations of the occurrence and development of AS [2]. ox-LDL deposited in the vascular wall induces vascular endothelial cell apoptosis. ox-LDL-induced oxidative stress is a major cause of endothelial cell injury [3]. ox-LDL causes apoptosis of endothelial cells by inducing intracellular oxidative stress and endoplasmic reticulum stress [2, 4]. Therefore, inhibiting ox-LDL-mediated endothelial injury is a potential strategy for preventing or slowing progression of AS.

Uric acid (UA) is the final metabolite of purine catabolism in humans. Studies report that hyperuricemia can induce endothelial dysfunction and lead to the occurrence and development of a variety of cardiovascular diseases [5–11]. However, in an in vitro study, it was demonstrated that the antioxidant effect of UA is equal to that of ascorbate, a significant antioxidant in plasma [12]. Human plasma urate levels are significantly greater than ascorbate levels. As a result, UA is estimated to be responsible for neutralizing more than half of the free radicals in human blood [13]. UA effectively removes reactive oxygen free radicals, hydroxyl free radicals, and peroxides in the body. In addition, it blocks the nitrification reaction and chelates metal ions such as iron ions, thus reducing oxidative stress reaction in the body and maintaining immune defense ability of the body [14–16]. A previous study reports that the appropriate concentration of UA ($300\,\mu$M) can significantly increase the activity of neurons and reduce the production of reactive oxygen species [17]. In addition, significantly low

levels of uric acid are associated with Alzheimer's disease, cardiovascular disease, diabetes, and other neurological diseases. Therefore, we hypothesized that appropriate uric acid concentration can be effectively alleviated of ox-LDL-mediated endothelial injury.

The Kelch-like ECH-associated protein 1-nuclear factor erythroid 2-related factor 2-antioxidant response elements (Keap1-Nrf2-ARE) pathway is one of the most important defense mechanisms against oxidative stress [18] and is associated with a number of oxidative stress-related diseases, including cancer, neurodegenerative diseases, cardiovascular diseases, and aging [19]. Nrf2 signaling pathway activation can modulate expression of genes implicated in detoxification and antioxidant defense functions, such as NAD (P) H: quinone oxidoreductase 1, superoxide dismutase, heme oxygenase-1 (HO-1) and catalase, thioredoxin reductase [20]. In the physiological environment, Nrf2 is located in the cytoplasm and it binds to Keap1 which controls Nrf2 activity. Oxidative or electrophilic stress induces a conformational change of Keap1 or directly promotes phosphorylation of Nrf2. Therefore, Nrf2 is segregated from Keap1 and translocated to the nucleus to effectively combine with antioxidant reaction components (ARE). As a result, it upregulates transcription of antioxidant and detoxifying genes [21]. Studies report that Nrf2 activation can protect endothelial cells from oxidative damage [22] and inflammatory response [23].

In this study, it was hypothesized that suitable concentrations of UA can minimize endothelial cell damage caused by ox-LDL. Therefore, the mechanism of action of uric acid in alleviating ox-LDL-induced damage and its effect on the Nrf2 pathway in human umbilical vein endothelial cells (HUVECs) were explored.

2. Materials and Methods

2.1. Materials. UA was obtained from Sigma-Aldrich (St. Louis, MO, USA). ox-LDL (UBC-ox-LDL5) was obtained from Yiyuanbiotech (Guangzhou, China) with a 2.1-2.5 mg/mL concentration. Brusatol (BT, a Nrf2 inhibitor) was purchased from MCE (Burlington, NJ, USA) and was dissolved in dimethyl sulfoxide (DMSO, the final concentration < 0.1%). An antibody against ICAM-1 was obtained from Cell Signaling Technology (Danvers, MA, USA). Dihydroethidine (DHE) was obtained from Sigma-Aldrich (St. Louis, MO, USA). Endothelial Cell Medium (ECM) was obtained from ScienCell (San Diego, CA, USA). Antibodies against histone H3 (17168-1-AP), HO-1 (10701-1-AP), NQO1 (11451-1-AP), and α-tubulin (66031-1-Ig) were purchased from Proteintech (Wuhan, Hubei, China). Antibodies against Keap1 (ab139729) and Nrf2 (ab137550) were purchased from Abcam (Cambridge, MA, USA).

2.2. Cell Culture. HUVECs and THP-1 cell were donated by Yang et al. [24]. HUVECs were incubated in ECM contained with 5% fetal bovine serum (FBS), containing 1% penicillin/-streptomycin (P/S) and 1% endothelial cell growth factor at 5% CO_2 and 37°C. THP-1 cells were incubated in RPMI1640

containing 10% FBS and 1% P/S. After achieving ~70% confluence, cells were divided into the five groups. The groups included a control group, in which cells were grown in ECM; an UA group, in which cells were grown for 24 h in different concentrations of UA (1, 2, 3, 5, 6, 9, 12, 15, and 18 mg/dL); an ox-LDL group, in which cells were grown for 24 h in different concentrations of ox-LDL (10, 20, 50, 100, and 200 μg/mL); an ox-LDL+UA group, in which cells were grown in different concentrations of UA and ox-LDL (100 μg/mL) for 24 h; and an ox-LDL+UA+brusatol group, in which cells were pretreated with brusatol (300 nM) for 2 h before incubation with UA (5 mg/dL)+ox-LDL (100 μg/mL) for 24 h.

2.3. Cell Viability Assay. Cell Counting Kit-8 (CCK-8) (Key-GEN Biotech, Jiangsu, Nanjing, China) was used to explore cell viability of HUVECs following the manufacturer's instructions. In summary, HUVECs were incubated in a 96-well plate and were treated with CCK-8 diluted in culture medium (1 : 10) for 4 hours. Cell viability, using a microplate reader (M1000 PRO, Tecan, USA), was then determined at 450 nm. A total of 5 replicates were used.

2.4. MDA, ET-1, and NO Levels. MDA level was measured using a Nanjing Jiancheng assay kit to determine lipid peroxidation. Level of MDA was measured using the assay kit following the manufacturer's instructions. Human plasma endothelin-1 level (ET-1) was determined using CUSABIO BIOTECH human ET-1 enzyme-linked immunosorbent assay (ELISA) kit (Wuhan, China). The NO level was determined by the Classic Griess Reagent method using a NO production assay kit.

2.5. Nrf2 Nuclear Translocation. HUVECs were fixed with 4% paraformaldehyde for 15 minutes and blocked with 10% goat serum for 60 minutes and with 2‰ Triton X-100 for 15 minutes at room temperature. Cells were then grown overnight at 4°C with anti-Nrf2 rabbit polyclonal antibody (1 : 500 dilution) and then probed for 1 h with goat anti-rabbit secondary antibody Alexa Fluor ® 488 (1 : 500) at room temperature under dark conditions. Nuclear staining was performed using DAPI (100 ng/mL) for 5 minutes and then observed under a microscope (Nikon).

2.6. Western Blot Analysis. HUVECs were added to ice-cold RIPA buffer containing inhibitors and PMSF (100 mM; Solarbio, Beijing, CHN) and sonicated. The BCA method was used to determine protein concentration. Proteins were transferred to SDS-PAGE gel and separated by electrophoresis; then, they were blotted onto the PVDF membrane (Millipore, Billerica, MA, USA). Nrf2 (1 : 500), NQO1 (1 : 1000), Keap1 (1 : 500), HO-1 (1 : 1000), α-Tubulin (1 : 2500), and Histone-3 (1: 500) antibodies were used. The blots were generated using enhanced chemiluminescent system (ECL Plus, Thermo Fisher, Waltham, MA, USA), and FluorChem M system (ProteinSimple, San Jose, CA, USA) was used for signal acquisition. ImageJ software was used for quantitative analysis of protein, which were then standardized using the concentration of endogenous α-tubulin and histone-3.

2.7. Realtime PCR. Total RNA was extracted from HUVECs using TRIzol reagent and reverse transcribed using a reverse transcription kit to synthesize first-strand cDNA (RR047A; Takara, Tokyo, JPN). qPCR amplification was conducted using SYBR Green on an Applied Bio Systems 7500 Real-Time PCR system (Applied Bio systems/Thermos Fisher Scientific, Foster City, CA, USA). cDNA was amplified using a primer pair specific to human TGFβ IL-1β, IL-6, NOX 4, TNFα, and GADPH. Relative levels of mRNA were standardized to endogenous control (GAPDH) levels. Primer sequences are presented in Table 1.

2.8. Immunofluorescence Staining. HUVECs were fixed on coverslips for 15 minutes at room temperature with 4% paraformaldehyde. After blocking cells in 10% goat serum for 1 h and 1‰ Triton-X 100 for 15 minutes, ICAM-1 antibody diluted at 1 : 100 was added and the mixture was incubated overnight at 4°C. After washing three times with PBS, the second Alexa Fluor ® 555 antibody at a concentration of 1 μg/mL was added and the mixture incubated for 1 h at room temperature. Nuclei were stained with 100 ng/mL DAPI for 5 min. 1 : 200 dilutions of dihydroethidine (DHE) were added for 1 hour at room temperature. Covers were then sealed, and cells were observed under fluorescence microscopy with an antifade mounting medium (magnification, ×20).

2.9. Immunoprecipitation. Immunoprecipitation was used to determine the level of Nrf2 ubiquitination as described previously [25]. In summary, cell extracts were treated with a primary antibody (4 μg) and incubated overnight at 4°C. Cells were then centrifuged at 3000 rpm at 4°C. Bound proteins were eluted in 4x sample buffer by boiling beads. Precipitated proteins were separated by SDS-PAGE using 6 percent gels followed by Western blot analysis. ImageJ was used for analysis and quantification of immunoblot data.

2.10. Cell Adhesion Assay. Cells were added into 6-well plates, and the adhesion assay was performed to determine the effect of uric acid and ox-LDL on THP-1 cell adhesion to HUVECs. HUVECs stimulated with UA or ox-LDL were dyed with green fluorescence (Mito-Tracker Green, Solarbio, Beijing, China) and incubated on the lower Transwell chamber (8.0 μm diameter pore, Corning) at 5% CO$_2$ at 37°C for 24 h. After 24 h in the upper chamber DiI (red fluorescence), prestained THP-1 cells were cocultured with HUVECs for 4 h. After washing, the adhesion rate of THP-1 cells was determined by observation under a fluorescence microscope (Olympus BX50).

2.11. Development of Microfluidic Devices. As previously described [26], microdevices were designed using standard microfabrication techniques. PDMS prepolymer (10 : 1 = base: curing agent) was degassed and filled in equipped masters before sealing it irreversibly with a clean glass substrate. The unit used for cell culture had one entry, one outlet, and four chambers measuring 200 μm in height, 1 mm in width, and 2 cm in length.

2.12. Statistical Analysis. The GraphPad Prism-7.0 application was used to do all statistical calculations. The mean ± standard deviation was used to express all of the data. To identify differences among various groups, one-way or two-way ANOVA was used, followed by a Tukey post hoc test for pairwise comparison. $P < 0.05$ was used to determine statistical differences.

3. Results and Discussion

3.1. Effect of Uric Acid and ox-LDL on HUVECs. The CCK-8 assay was used to investigate the effect of varying ox-LDL concentrations on HUVEC viability. Cell viability gradually decreased with an increase in ox-LDL concentration (Figures 1(a) and 1(b)). MDA and DHE staining were used for determination of ROS levels in HUVECs after treatment different concentrations of ox-LDL. Increased ox-LDL concentration resulted in a considerable increase in MDA levels (Figure 1(c)). The intensity of DHE staining increased as the concentration of ox-LDL increased, according to the findings (Figures 1(d) and 1(e)). ICAM-1 staining was used to detect occurrence of inflammatory response after treatment with different concentrations of ox-LDL. Similarly, as the concentration of ox-LDL increased, the fluorescence intensity of ICAM-1 increased considerably (Figures 1(f)–1(g)). Treatment with different high concentrations of uric acid (6 to 18 mg/dL) showed strong ($P < 0.05$) cytotoxicity towards HUVECs.

Treatment with concentration of UA ≥ 6 mg/dL significantly decreased cell viability (Figures 2(a) and 2(b)). In addition, a significant increase in fluorescence intensity of DHE and ICAM-1 was observed (Figures 2(c)–2(f)). However, treatment with 1-5 mg/dL uric acid had no effect on cell viability.

Treatment of HUVECs with UA and ox-LDL showed strongest cell viability at 5 mg/dL UA concentration compared with treatment with ox-LDL (100 μg/mL) alone (Figures 3(a) and 3(b)). Pretreatment with 5 mg/dL uric acid significantly decreased MDA level by 53% ($P < 0.05$; Figure 3(c)). Similarly, the fluorescence intensity of DHE and ICAM1 were weakest after treatment with 5 mg/dL UA (Figures 3(d)–3(g)). These findings show the stable dose range for uric acid against HUVECs cell line for subsequent studies and show that the adverse effect of ox-LDL can be attenuated by uric acid. Subsequent experiments were performed using 5 mg/dL uric acid.

3.2. Uric Acid Attenuated HUVEC Injury Induced by ox-LDL. Further, the effect of uric acid protected HUVECs against ox-LDL-induced inflammation and oxidative stress. Fluorescence intensity of DHE staining and ICAM-1 staining in the ox-LDL group increased by 386% and 484%, respectively ($P < 0.05$ vs. the control group; Figures 4(a)–4(c)). Notably, uric acid (5 mg/dL)+ox-LDL (100 μg/mL) treatment reduced fluorescence intensity of DHE staining and ICAM-1 staining by 61.6% and 50.2%, respectively ($P < 0.05$ vs. the ox-LDL group; Figures 4(a)–4(c)). The control group and uric acid group showed no significant difference in fluorescence staining ($P > 0.05$). Furthermore,

TABLE 1: Primers used for quantitative real-time PCR analysis.

Gene	Forward Primer	Reverse primer
TGFβ	5′-CGCCGAGCCCTGGACACCAACTA-3′	5′-GACAGCTGCTCCACCTTGGGCTT-3′
NOX4	5′- CCGAACACTCTTGGCTTACCTCC-3′	5′- AGCAGCCCTCCTGAAACATGCAA-3′
TNFα	5′- CACGCTCTTCTGCCTGCTGCACT-3′	5′- GGTACAGGCCCTCTGATGGCACCAC-3′
IL-1β	5′-TCCAGCTACGAATCTCCGACCAC-3′	5′-TGGGCAGACTCAAATTCCAGCTT-3′
IL-6	5′- AGCCACTCACCTCTTCAGAACGA-3′	5′- ACTTTTGTACTCATCTGCACAGCTC-3′
GAPDH	5'-CACCATCTTCCAGGAGCGAGATCCC-3'	5'-CCATCACGCCACAGTTTCCCGGAGG-3'

TGFβ, transforming growth factor-β; Nox4, nicotinamide adenine dinucleotide phosphatase oxidase 4; IL-1β, Interleukin-1β; IL-6, Interleukin-6; TNF-α, Tumor necrosis factor; GAPDH, Glyceraldehyde 3-phosphate dehydrogenase.

treatment with UA (5 mg/dL) significantly reduced ox-LDL-induced inflammatory responses in HUVECs, as shown by a significant decrease in monocyte adhesive capacity ($P < 0.05$ vs. the ox-LDL group; Figures 4(d)–4(f)). Levels of NO and ET-1 in the culture medium were determined to explore the effect of UA treatment on endothelial function in ox-LDL-induced HUVECs damage. ET-1 levels were slightly higher whereas NO production levels were decreased in the ox-LDL group ($P < 0.05$ vs. the control group; Figures 4(g) and 4(h)). In addition, the uric acid (5 mg/dL)+ox-LDL (100 μg/mL) group showed significantly lower ET-1 levels and higher NO production levels compared with the levels in the ox-LDL group ($P < 0.05$; Figures 4(g) and 4(h)).

3.3. Activation of Nrf2 Is Consistent with the Protective Effect of Uric Acid against ox-LDL-Induced HUVEC Injury.

To explore the correlation between the protective effect of uric acid on ox-LDL-induced HUVEC injury and Nrf2 activation, cytosolic and nuclear compartments of HUVEC cells were fractionated and immunoblotted. Treatment with uric acid (5 mg/dL)+ox-LDL (100 μg/mL) resulted in 2.33-fold and 3.44-fold increase in cytoplasmic Nrf2 protein levels and resulted in 1.62-fold and 4.14-fold increase in nuclear Nrf2 protein levels compared with the levels in the control and ox-LDL groups ($P < 0.05$; Figures 5(a)–5(c)). Additionally, determination of protein level of keap1 showed that uric acid and ox-LDL did not affect the expression of Keap1 (Figure 5(d)). To further verify that uric acid protects HUVECs injured by ox-LDL through the Nrf2 pathway, cells were cotreated with brusatol. Expression levels of total Nrf2, HO-1, and NQO1 were determined through Western blotting (Figure 5(e)). On the contrary to treatment with ox-LDL alone, uric acid pretreatment increased expression levels of total Nrf2, HO-1, and NQO1 by 60%, 63.5%, and 106.5%, respectively ($P < 0.05$; Figures 5(f)–5(h)). Also, ET-1 levels were significantly reduced compared with the levels in the ox-LDL group whereas levels of NO production were significantly increased in the UA+ox-LDL group ($P < 0.05$, Figures 5(i) and 5(j)). However, these changes were reversed by administration with brusatol. Further, immunofluorescence staining was performed to explore the subcellular distribution of Nrf2. Analysis showed that expression levels of Nrf2 in the control group were significantly higher in the

cytoplasm, whereas lower expression levels were observed in the nucleus. On the contrary in the UA+ox-LDL group, Nrf2 was mainly localized in the nucleus. Treatment with the inhibitor showed reduction in Nrf2 levels in the nucleus compared with the levels in the UA+ox-LDL group (Figure 5(l)).

3.4. Uric Acid Suppressed Nrf2 Ubiquitination and Degradation.

Nrf2 is a main regulator of the transcription of several antioxidant genes that protect cells against oxidative stress. In this study, treatment with 5 mg/dL uric acid significantly increased Nrf2 protein levels in nucleus and cytoplasm. Therefore, ubiquitin protein level and its interaction with Nrf2 were determined through immunoprecipitation. Notably, addition of proteasome inhibitor MG132 showed significant decrease in levels of ubiquitin protein in Nrf2 immunoprecipitation from uric acid treated cells. However, the protein expression level of Nrf2 showed a significant increase (Figures 5(m) and 5(k)).

3.5. Effects of Uric Acid on Inflammation and Oxidative Stress Caused by ox-LDL in Microfluidic Devices.

The vascular microfluidic model was used to verify the stable and appropriate concentration of uric acid for establishing a mouse model in vivo (Figures 6(a)–6(c)). HUVECs were incubated with ox-LDL (100 μg/mL) with or without uric acid (5 mg/dL) for 24 h under low shear stress (5 μL/min) in a microfluidic sdevice (Figure 6(b)). THP-1 cells and HUVECs were cocultured in a microfluidic system for 4 hours under low shear pressure (Figures 6(c) and 6(d)). Analysis showed that HUVECs treated with UA attenuated THP-1 cell adhesion compared with those treated with ox-LDL alone. qPCR analysis was used to determine mRNA expression level of TGFβ, IL-1β Nox4, IL-6, and TNF α to further explore the anti-inflammatory and antioxidant effect of uric acid in ox-LDL-treated HUVECs. Treatment with ox-LDL significantly increased expression levels of above genes ($P < 0.05$ vs. the control; Figure 6(e)). Notably, pretreatment with uric acid (5 mg/dL) resulted in 53.9%, 59.6%, 93.8%, 32.3%, and 74.2% decrease in mRNA expression level of TGFβ, IL-1β, Nox4, IL-6, and TNFα, respectively ($P = 0.05$ vs. the ox-LDL group; Figure 6(e)).
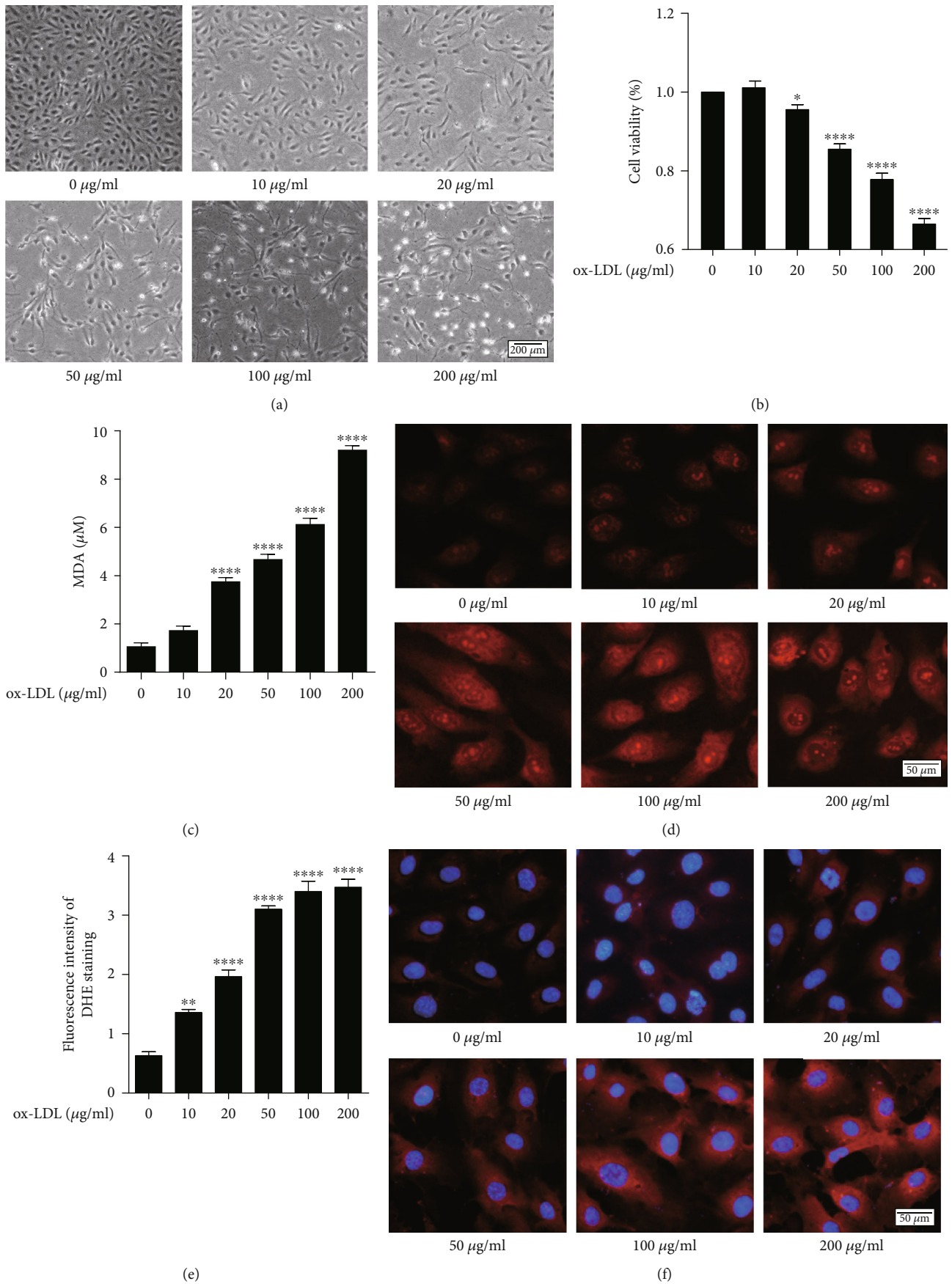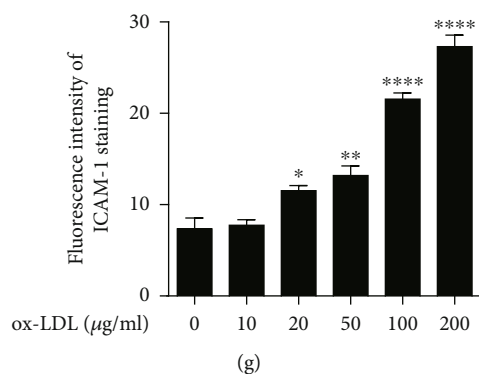
(a)

(b)

(c)

(d)

(e)

(f)

FIGURE 1: Continued.

(g)

FIGURE 1: HUVEC injury caused by ox-LDL stimulation at different concentrations HUVECs were stimulated with 0, 10, 20, 50, 100, and 200 μg/mL ox-LDL for 24 h. Changes in (a) cell morphology in different groups. (b) Cell survival rate in different groups by CCK-8 assay. Scale bar = 200 μm. (c) Changes in MDA levels. (d, e) DHE immunofluorescence image and densitometry analysis of immunofluorescent intensity of DHE. Scale bar = 50 μm. (f, g) ICAM1 immunofluorescence image and densitometry analysis of immunofluorescent intensity of ICAM1. Scale bar = 50 μm. DHE: dihydroethidium; HUVECs: human umbilical vein endothelial cells; ox-LDL: oxidized low-density lipoprotein; MDA: malondialdehyde. The statistical analyses were done using GraphPad Prism V-7.0 software. Data are expressed as the mean ± standard deviation ($n = 3$). One-way ANOVA was used in statistical analyses ($n = 3$/group). $^*P < 0.05$, $^{**}P < 0.01$, $^{***}P < 0.001$, and $^{****}P < 0.0001$ versus the control.
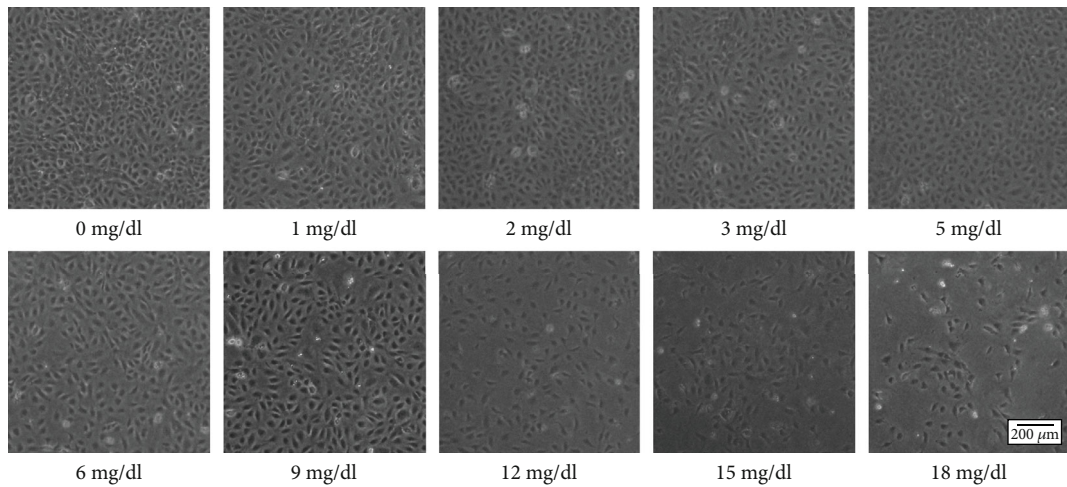
4. Discussion

Uric acid is considered a neuroprotective agent for Parkinson's disease. And uric acid has direct and indirect neuroprotective effects [27, 28]. However, the mechanisms that underlie the protection of uric acid in cardiovascular remains poorly understood. In this study, we evaluated the effect of uric acid on ox-LDL-induced HUVECs damage. We found that ox-LDL (100 μg/mL) reduced cell viability and increased the level of MDA, while the effect of uric acid (5 mg/dL) for 24 h reversed this effect. The findings of this study showed that UA was effectively inhibited ox-LDL-induced HUVEC damage in vitro. The protective effect was mediated through (1) inhibition of ROS production, (2) suppression of inflammation, and (3) inhibition of Nrf2 ubiquitination, induction of Nrf2 nuclear translocation, and induction of HO-1 and NQO1 gene expression as shown in Figure 7. Notably, protective effects caused by UA were reversed by treatment with brusatol. These findings showed that UA protected HUVECs from ox-LDL damage through induction of Keap1-Nrf2-ARE pathway activation.

Several essential mechanisms, including oxidative stress [29], vascular endothelial damage [30], and the release of inflammatory mediators [31], can initiate and exacerbate atherosclerosis, which is a contributing factor in many cardiac and cerebral vascular disorders. ox-LDL is implicated in the initiation and progression of atherosclerosis, through endothelial damage, adhesion molecule expression, and leukocyte recruitment and retention [32]. Accumulation of ox-LDL in the blood vessel wall can cause early vascular dysfunction, significantly decreasing NO production and increasing ROS [33]. These changes affect vascular endothelial function and promote atherosclerosis-related pathogenic processes. In previous studies, they demonstrated that ox-LDL (100-150 μg/mL) exposure reduced cell viability [34, 35]. Consistent with the previous studies, the findings of the current study showed that high ox-LDL concentration

(20-200 μg/mL) induced cytotoxic effects, directly up-regulated production of ROS, significantly increased MDA level, and enhanced expression of ICAM1 in HUVECs (Figure 1). Therefore, we used ox-LDL as a drug to induce endothelial injury of HUVECs as an in vitro model to study the protective effect of uric acid on HUVECs.

Endothelial cells play a key role in maintaining the physiological functions of the cardiovascular system by regulating blood circulation, coagulation, angiogenesis, and inflammation [36]. The present study shows that uric acid can inhibit ROS production, and suppress inflammation responses of HUVECs exposed to ox-LDL (Figure 4), which is in accordance with a clinical trial study that reported using intravenous uric acid injections in healthy and diabetes volunteers can restore endothelial function in diabetes patients who are regular smokers [37]. Previous studies also reported that short-term administration can enhance the physiological effects of uric acid to avoid oxidative and free-radical driven tissue damage, such as sepsis. Early use of combination of uric acid and antioxidants results in a significant increase in cardiovascular hemodynamic [38]. Furthermore, administration of uric acid and vitamin C to healthy volunteers showed a significant enhancement in serum free-radical scavenging capacity from baseline, with no adverse effects observed after administration of 1,000 mg uric acid [39]. However, our results are also contradictory to previous reports on the effect of uric acid on cardiovascular disease. For example, epidemiological studies have also shown that serum uric acid levels are related to hypertension, dyslipidemias, diabetes, chronic kidney disease, atrial fibrillation, and cardiovascular events [5–11]. Basic experimental researches have shown that uric acid leads to endothelial dysfunction by activating NADPH oxidase, activating the RAAS system, and increasing oxidative stress and inflammation [24, 40]. In the current study, we observed that 0-5 mg/dL uric acid did not induce HUVEC damage (Figure 2), and 5 mg/dL uric acid can significantly reduce endothelial damage caused by

0 mg/dl 1 mg/dl 2 mg/dl 3 mg/dl 5 mg/dl

6 mg/dl 9 mg/dl 12 mg/dl 15 mg/dl 18 mg/dl

(a)

(b)

0 mg/dl 1 mg/dl 2 mg/dl 3 mg/dl 5 mg/dl

6 mg/dl 9 mg/dl 12 mg/dl 15 mg/dl 18 mg/dl
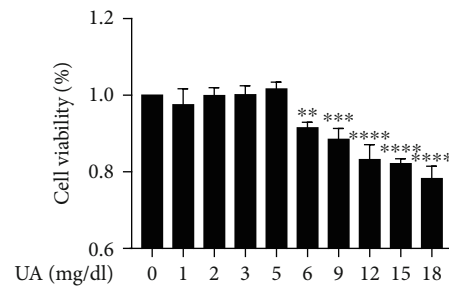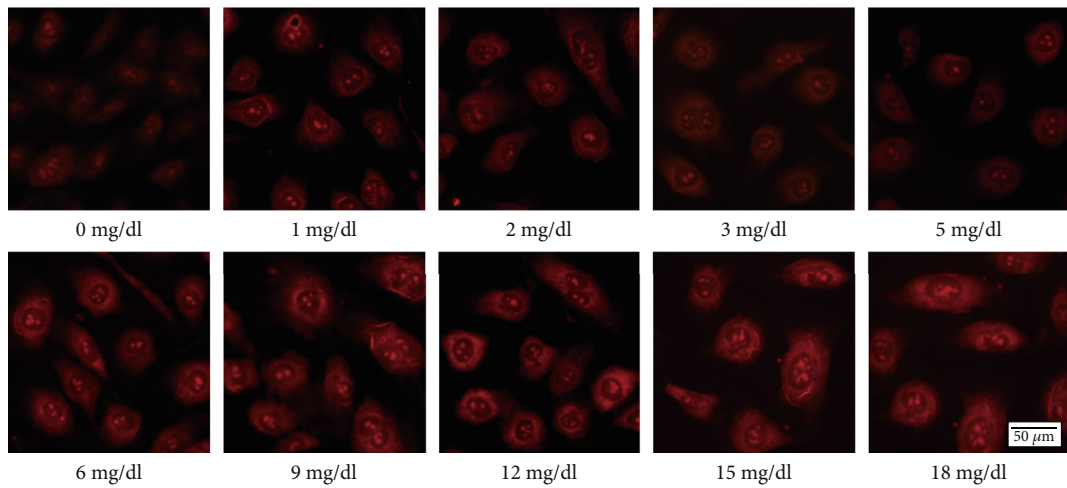
(c)

(d)

Figure 2: Continued.

(e)

(f)
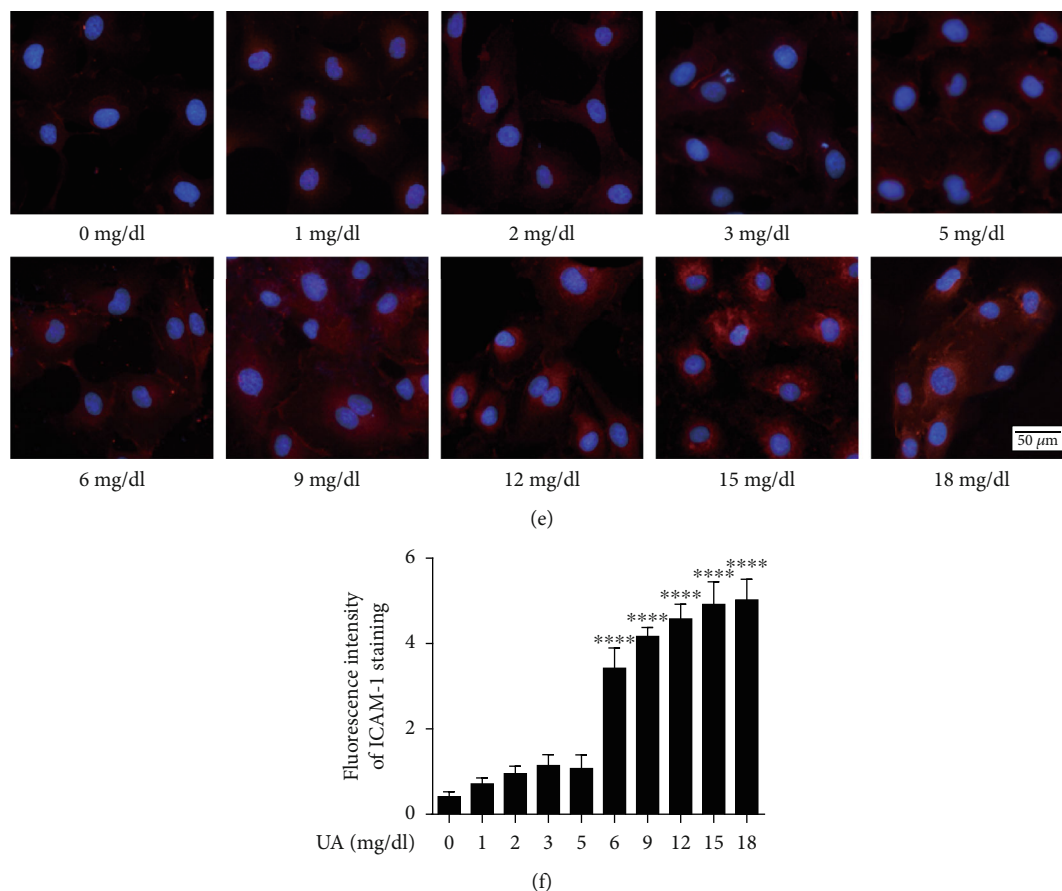
FIGURE 2: Changes of HUVECs under the stimulation of different concentrations of uric acid HUVECs were stimulated with 0, 1, 2, 3, 5, 6, 9, 12, 15, and 18 mg/dL uric acid for 24 h. Changes in (a) cell morphology in different groups. Scale bar = 200 μm. (b) Cell survival rate in different groups by CCK-8 assay. (c, d) DHE immunofluorescence image and densitometry analysis of immunofluorescent intensity of DHE. Scale bar = 50 μm. (e, f) ICAM1 immunofluorescence image and densitometry analysis of immunofluorescent intensity of ICAM1. Scale bar = 50 μm. DHE: dihydroethidium; HUVECs: human umbilical vein endothelial cells. The statistical analyses were done using GraphPad Prism V-7.0 software. Data are expressed as the mean ± standard deviation ($n = 3$). One-way ANOVA was used in statistical analyses ($n = 3$/group). $^{*}P < 0.05$, $^{**}P < 0.01$, $^{***}P < 0.001$, and $^{****}P < 0.0001$ versus the control.

ox-LDL (Figure 4). However uric acid (>5 mg/dL) had adverse effects on HUVEC (Figure 2) and >5 mg/dL uric acid had a synergistic effect on endothelial cell damage with ox-LDL (Figure 3). This phenomenon is because different concentrations of uric acid will produce different effects. As we all know, the physiological role of uric acid is a powerf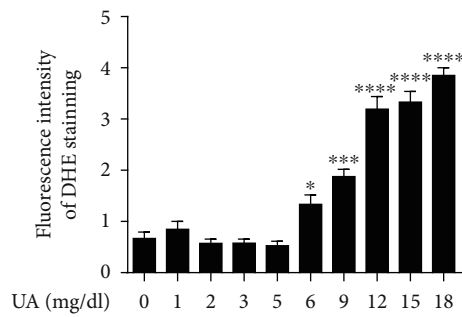ul antioxidant [12]. As the level of uric acid in the body increases, the absorption of uric acid into endothelial cells through uric acid transporters increases, leading to inflammation, oxidative stress, eNOS dephosphorylation, and endothelial dysfunction by reducing the bioavailability of NO [41].

This study showed that uric acid activated the Nrf2 antioxidant pathway and had a protective effect on endothelial damage induced by ox-LDL (Figure 5). Previous studies report that Nrf2 plays a key role in promoting cell redox homeostasis, thus maintaining cardiovascular health [42, 43]. Several experimental studies have determined the role of Nrf2 on expression of oxidative stress defense genes and protection of vascular health [43], and overexpression of Nrf2 in endothelial cells can reduce expression levels ofinter-

leukin1β (IL-1β), tumur necrosis factor (TNF), and protein 1 vascular cell adhesion (VCAM1) and protein 1 monocyte chemoattractant (MCP-1) [43]. However, low Nrf2 activity promotes to overexpression of proinflammatory chemokines and adhesion molecules in endothelial cells [44]. Our results showed that ox-LDL promoted oxidative stress, reduced Nrf2 protein expression, and Nrf2 nuclear translocation (Figure 5), which is inconsistent with previous reports [34, 45]. This contradiction may be because ox-LDL can induce endothelial cell senescence [46], and endothelial cell senescence is caused by transcriptional inhibition of Nrf2 expression [35, 47]. In previous studies, UA reduced the ubiquitination and degradation of Nrf2, promoted its nuclear translocation, and promoted the transcription and translation of antioxidant genes targeted by Nrf2, thereby providing neuroprotection to dopaminergic cells against 6-OHDA toxicity [48]. Therefore, the activation of Nrf2 may be an important mechanism of uric acid against atherosclerosis, but it has not been reported in the literature. In our study, UA stimulation increased the protein expression of Nrf2 in the nucleus and cytoplasm, suggesting that UA

ox-LDL 100 μg/ml · UA 1mg/dl+ox-LDL 100 μg/ml · UA 2mg/dl+ox-LDL 100 μg/ml · UA 3mg/dl+ox-LDL 100 μg/ml · UA 5mg/dl+ox-LDL 100 μg/ml

UA 6mg/dl+ox-LDL 100 μg/ml · UA 9mg/dl+ox-LDL 100 μg/ml · UA 12mg/dl+ox-LDL 100 μg/ml · UA 15mg/dl+ox-LDL 100 μg/ml · UA 18mg/dl+ox-LDL 100 μg/ml

200 μm

(a)

(b)

(c)

ox-LDL 100 μg/ml · UA 1mg/dl+ox-LDL 100 μg/ml · UA 2mg/dl+ox-LDL 100 μg/ml · UA 3mg/dl+ox-LDL 100 μg/ml · UA 5mg/dl+ox-LDL 100 μg/ml

UA 6mg/dl+ox-LDL 100 μg/ml · UA 9mg/dl+ox-LDL 100 μg/ml · UA 12mg/dl+ox-LDL 100 μg/ml · UA 15mg/dl+ox-LDL 100 μg/ml · UA 18mg/dl+ox-LDL 100 μg/ml

50 μm

(d)

FIGURE 3: Continued.

(e)

(f)

(g)

FIGURE 3: Changes of HUVECs under the stimulation of different concentrations of uric acid and fixed concentration ox-LDL. HUVECs were pretreated with 0, 1, 2, 3, 5, 6, 9, 12, 15, and 18 mg/dL uric acid 2 h before 100ug/mL ox-LDL stimulated. Changes in (a) cell morphology in different groups. Scale bar = 200 μm. (b) Cell survival rate in different groups by CCK-8 assay. (c) MDA level in different groups. (d, e) DHE immunofluorescence image and densitometry analysis of immunofluorescent intensity of DHE. Scale bar = 50 μm. (f, g) ICAM1 immunofluorescence image and densitometry analysis of immunofluorescent intensity of ICAM1. Scale bar = 50 μm. DHE: dihydroethidium; HUVECs: human umbilical vein endothelial cells; ox-LDL: oxidized low-density lipoprotein; MDA: malondialdehyde. The statistical analyses were done using GraphPad Prism V-7.0 software. Data are expressed as the mean ± standard deviation ($n = 3$). One-way ANOVA was used in statistical analyses ($n = 3$/group). $^{*}P < 0.05$, $^{**}P < 0.01$, $^{***}P < 0.001$, and $^{****}P < 0.0001$ versus the control.
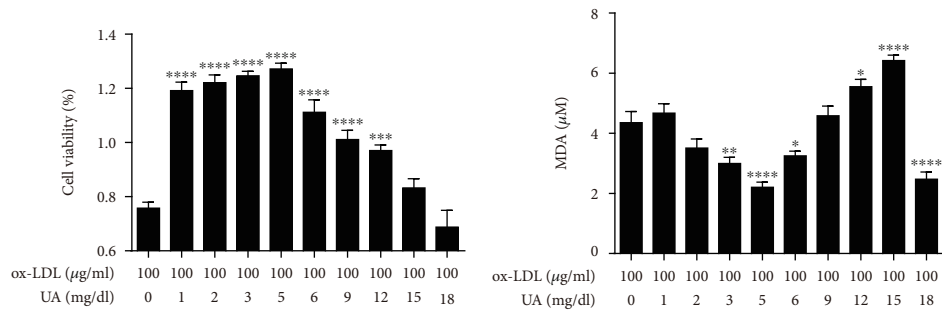
treatment can promote the translocation of Nrf2 into the nucleus and reduce Nrf2 ubiquitination (Figure 5). But it did not affect the expression of Keap1 protein, suggesting that uric acid can enhance the stability of Nrf2 at the protein level. It is generally believed that the chemical activation of Nrf2 is due to the separation of Nrf2 from Keap1, allowing Nrf2 to escape from Keap1-mediated proteasome degradation. This structure-activity relationship may be one of the mechanisms by which uric acid activates Nrf2. Structurally, UA assumes the form of a ketoenol tautomer, which can react with the cysteine residue of Keap1, so that the Nrf2 bound by Keap1 cannot be reached by ubiquitin ligase [49]. This mechanism is consistent with the recently reported 5,6-dihydrocyclopenta-1,2-dithio-3-thione (CPDT) and sulforaphane to activate Nrf2 and urate in 6-hydroxydopamine (6-OHDA) to activate Nrf2.
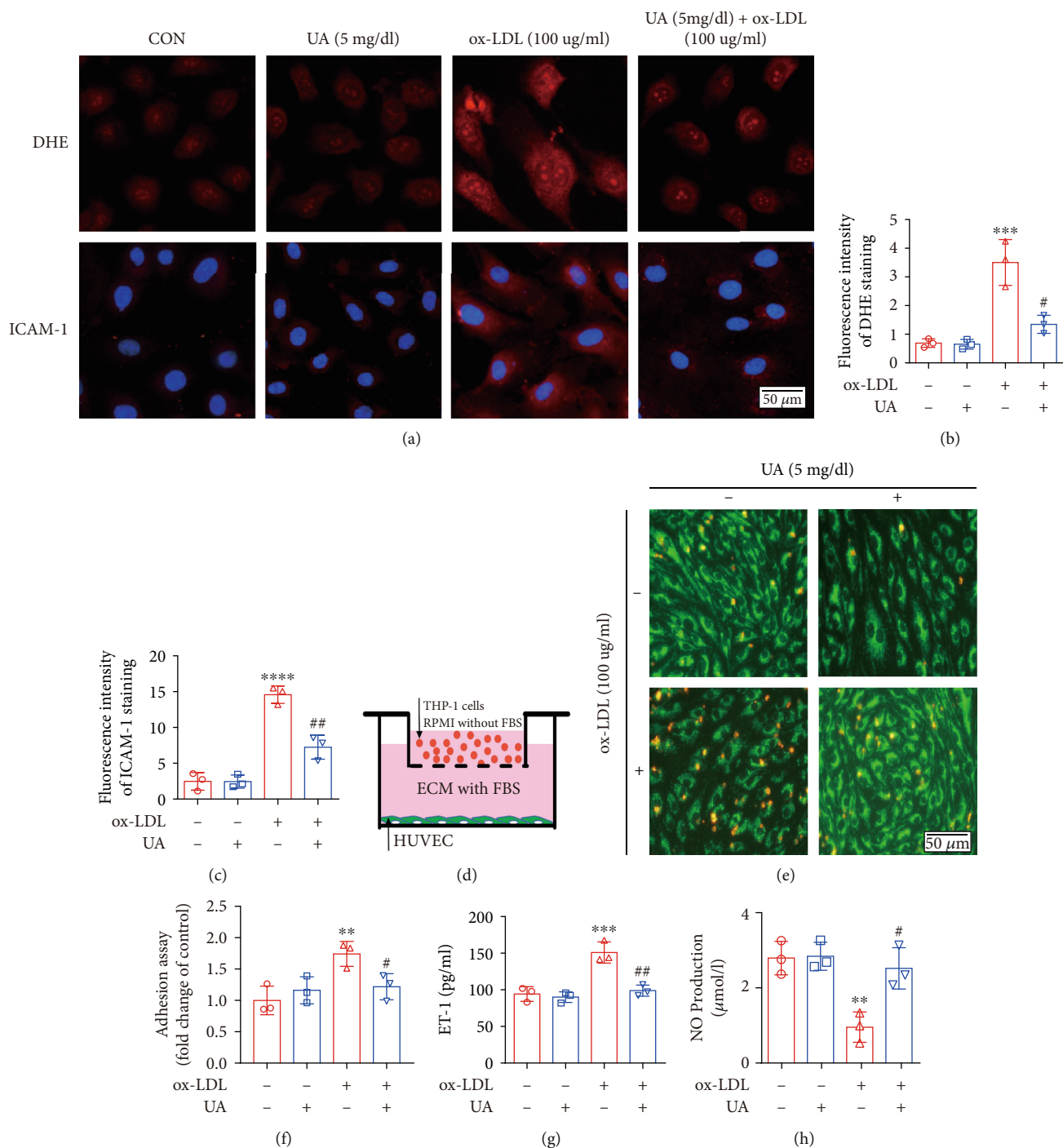
FIGURE 4: Appropriate concentration uric acid attenuated ox-LDL-induced injured in HUVECs. HUVECs were incubated with ox-LDL (100 μg/mL) for 24 h, with or without uric acid (5 mg/dL) preincubated for 2 h. Or HUVECs were incubated with uric acid (5 mg/dL) alone for 24 h. (a) Representative immunofluorescence image of DHE and ICAM1. Scale bar = 50 μm. (b) Densitometry analysis of immunofluorescent intensity of DHE in the HUVECs in different groups. (c) Densitometry analysis of immunofluorescent intensity of ICAM1 in the HUVECs in different groups. (d–f) Representative images showed adhesive monocytes to HUVECs under uric acid (5 mg/dL) treatment or ox-LDL (100ug/mL) treatment or uric acid (5 mg/dL)+ ox-LDL (100 μg/mL). HUVECs were stained by Mito-Green, determined by green fluorescence, while THP-1 cells were stained by Dil, determined by yellow fluorescence. Quantitation of adhesive monocytes in different groups was presented in (f). (g) The effect of uric acid and ox-LDL on ET-1 expression in HUVECs. ET-1 released into the supernatant was measured by ELISA. (h) The effect of uric acid and ox-LDL on NO production in HUVECs. The results were independently repeated at least three times. DHE: dihydroethidium; HUVECs: human umbilical vein endothelial cells. The statistical analyses were done using GraphPad Prism V-7.0 software. Data are expressed as the mean ± standard deviation ($n = 3$). One-way ANOVA and unpaired t-test was used in statistical analyses ($n = 3$/group). $^{*}P < 0.05$, $^{**}P < 0.01$, $^{***}P < 0.001$, and $^{****}P < 0.0001$ versus the control. $^{\#}P < 0.05$, $^{\#\#}P < 0.01$, $^{\#\#\#}P < 0.001$, $^{\#\#\#\#}P < 0.0001$ versus the ox-LDL group.

(a)

(b)

(c)

(d)

(e)

(f)

(g)

(h)

(i)

(j)

(k)
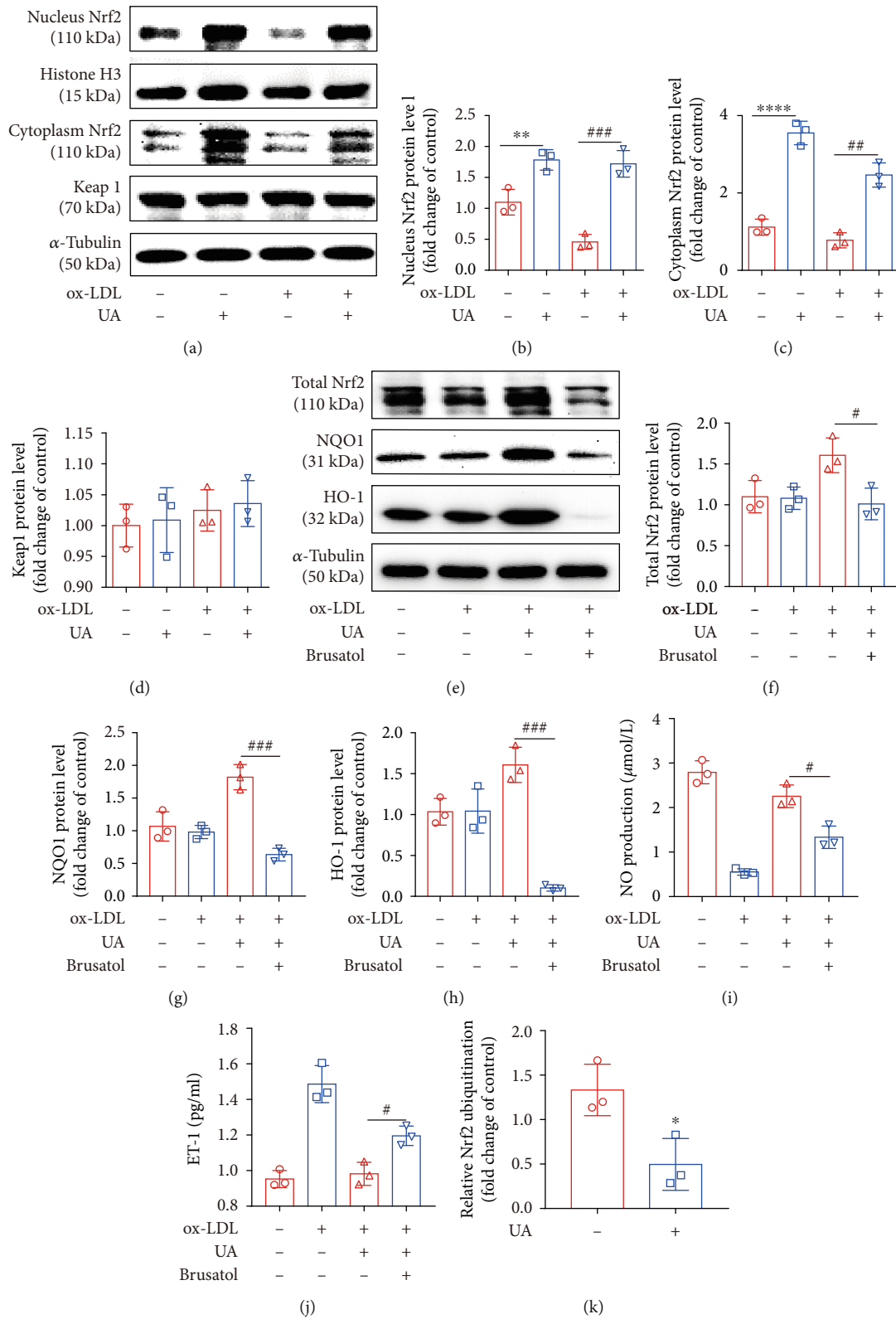
Figure 5: Continued.

(l)

(m)
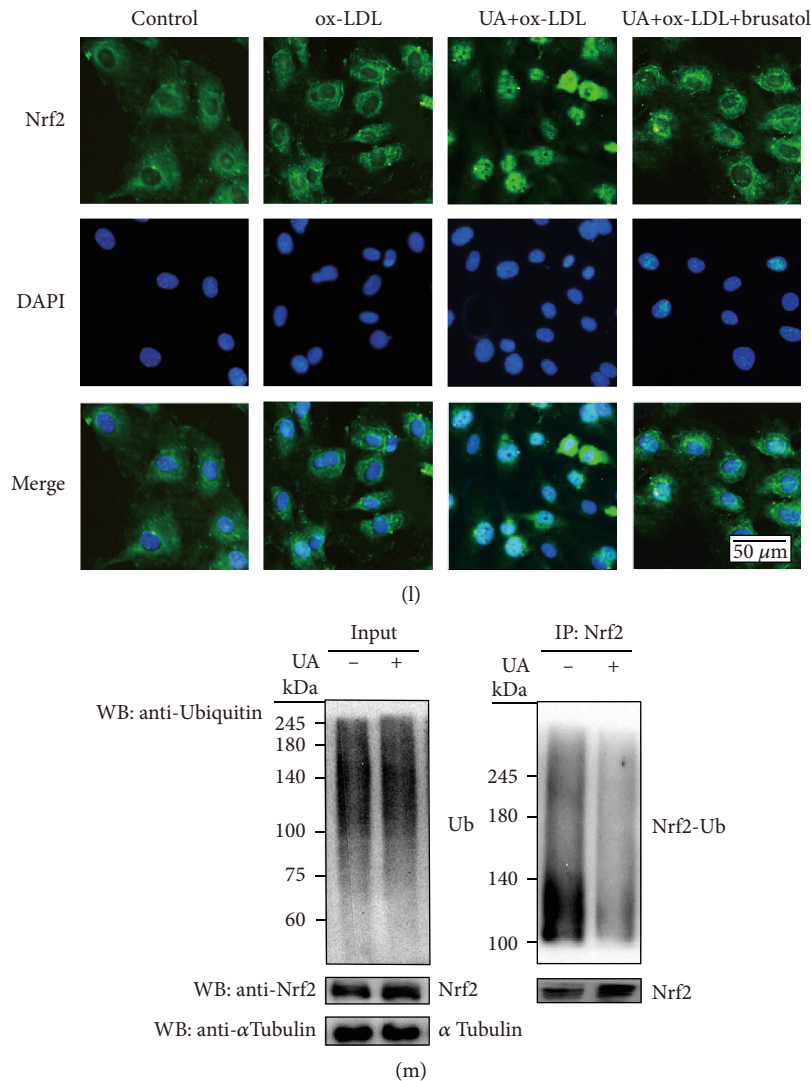
FIGURE 5: Nrf2 activation is associated with protective effect of uric acid-mediated on ox-LDL induced HUVECs injury. HUVECs were incubated with ox-LDL (100 μg/mL) for 24 h, with or without uric acid (5 mg/dL) preincubated for 2 h. HUVECs were preincubated with brusatol (300 nM) for 2 h before incubated with UA (5 mg/dL)+ox-LDL (100 μg/mL) for 24 h. (a–d) The cytosolic and nuclear compartments of HUVEC cells were fractionated, cell lysates were analyzed by Western blotting with primary antibodies against Nrf2 and Keap1. Protein levels were quantified by densitometry. α-Tubulin and histone H3 were used as internal controls. (e–h) Cell lysates were analyzed by Western blotting with primary antibodies against Nrf2, NQO1, and HO-1. Protein levels were quantified by densitometry. α-Tubulin was used as internal controls. (i) The effect of brusatol, uric acid, and ox-LDL on ET-1 expression in HUVECs. ET-1 released into the supernatant was measured by ELISA. (j) The effect of brusatol, uric acid, and ox-LDL on NO production in HUVECs. (k–m) Uric acid inhibited Nrf2 ubiquitination. Cells were treated with or without uric acid (5 mg/dL) for 6 h in the presence of MG132 (25 mM). For detecting ubiquitinated Nrf2, samples were subjected to IP with anti-Nrf2, followed by IB with an anti-Ub antibody. Nrf2 ubiquitination protein levels were quantified by densitometry. (l) Representative pictures showing the subcellular distribution of Nrf2 (FITC/green) in HUVECs. Nuclei were stained with DAPI (blue). Scale bar = 50 μm. The statistical analyses were done using GraphPad Prism V-7.0 software. Data are expressed as the mean ± standard deviation ($n = 3$). One-way ANOVA was used in statistical analyses ($n = 3$/group). $^{*}P < 0.05, ^{**}P < 0.01, ^{***}P < 0.001$, and $^{****}P < 0.0001$ versus the control. $^{#}P < 0.05, ^{##}P < 0.01, ^{###}P < 0.001$, and $^{####}P < 0.0001$ versus the ox-LDL+UA group.

At the same time, consistent with previous studies [49, 50], we found that UA promoted the protein expression of HO-1 and NQO1 (Figure 5). HO-1 and NQO1 are regulated by Nrf2, which directly affects the body's antioxidant balance [20]. Importantly, after the preadministration of brusatol, the ability of UA to promote the protein expression of Nrf2/HO-1/NQO1 protein and nuclear translocation of Nrf2 was significantly hindered, suggesting that

UA may regulate the expression of ARE-related genes by promoting the activation of Nrf2 and exerting an antioxidant effect. Brusatol treatment could inhibit the protective effect of UA on HUVECs damaged by ox-LDL. These data strongly proved the antioxidant effect and endothelial cell protection effect of UA activating the Nrf2 signaling pathway. However, this requires further research to evaluate this mechanism.

Endothelial cell

(a)

Microfluidic device

Microchamber

1000 μm

(b)

HUVEC

THP-1

(c)
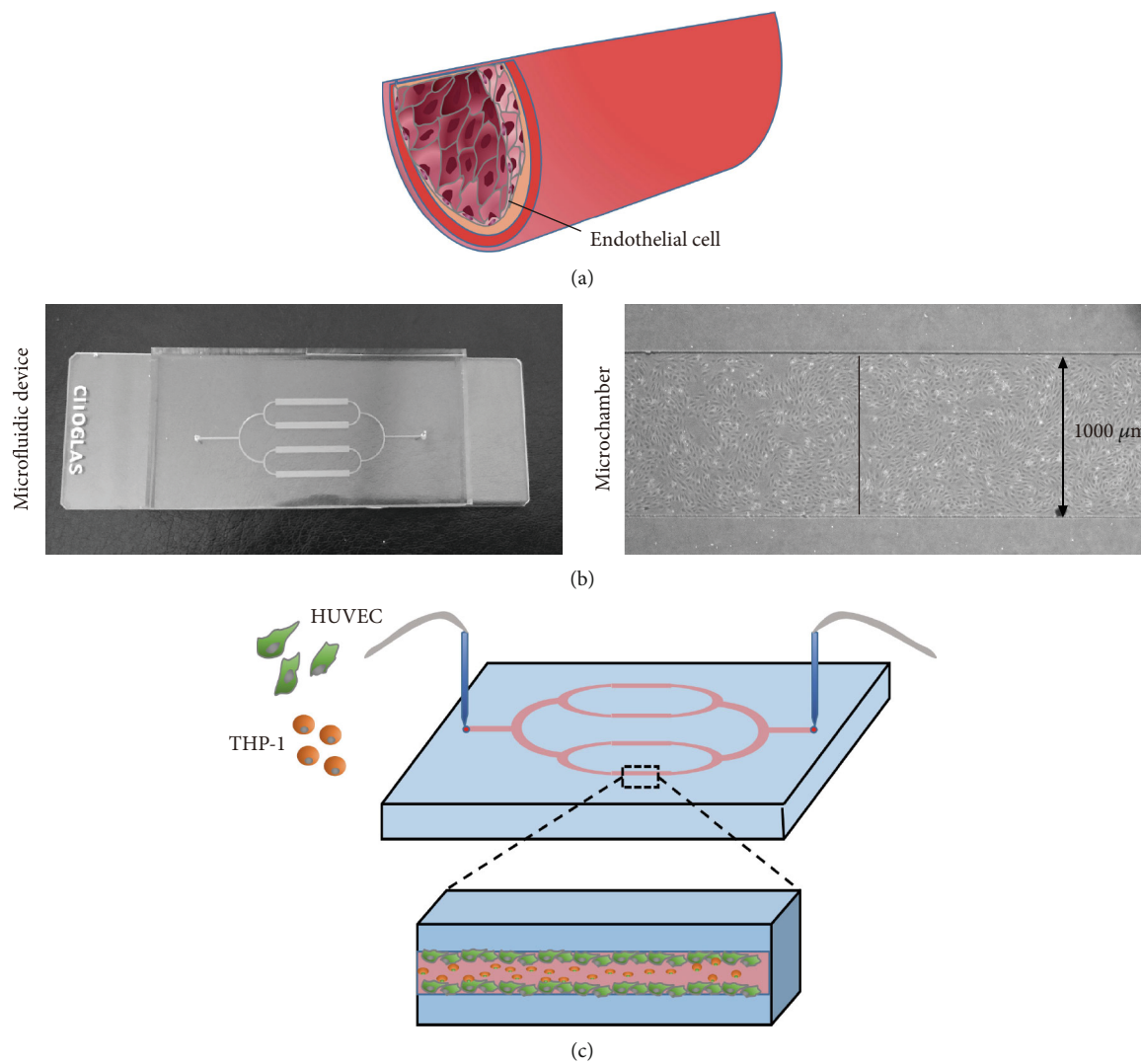
FIGURE 6: Continued.

(d)

Figure 6: Continued.

(e)
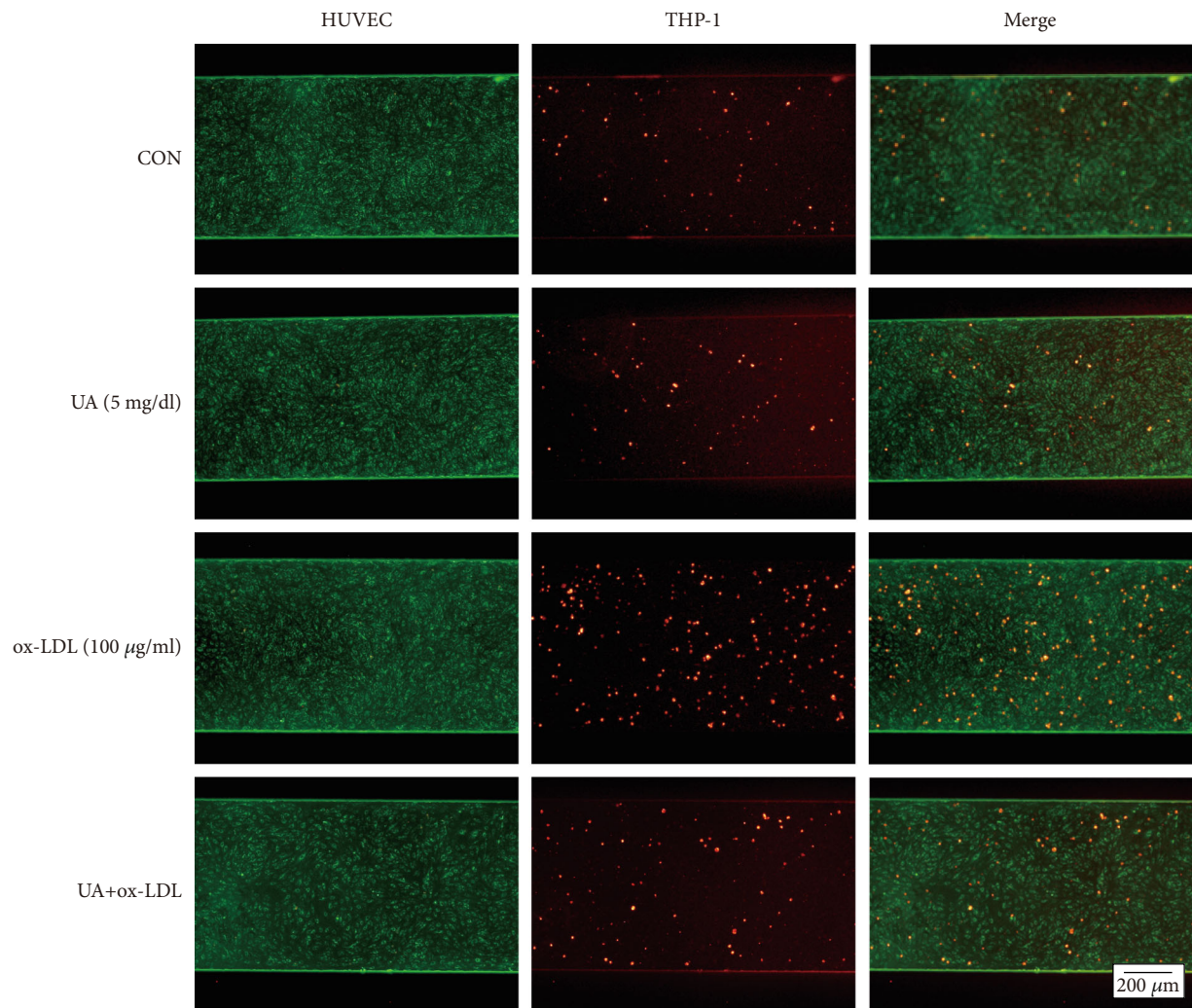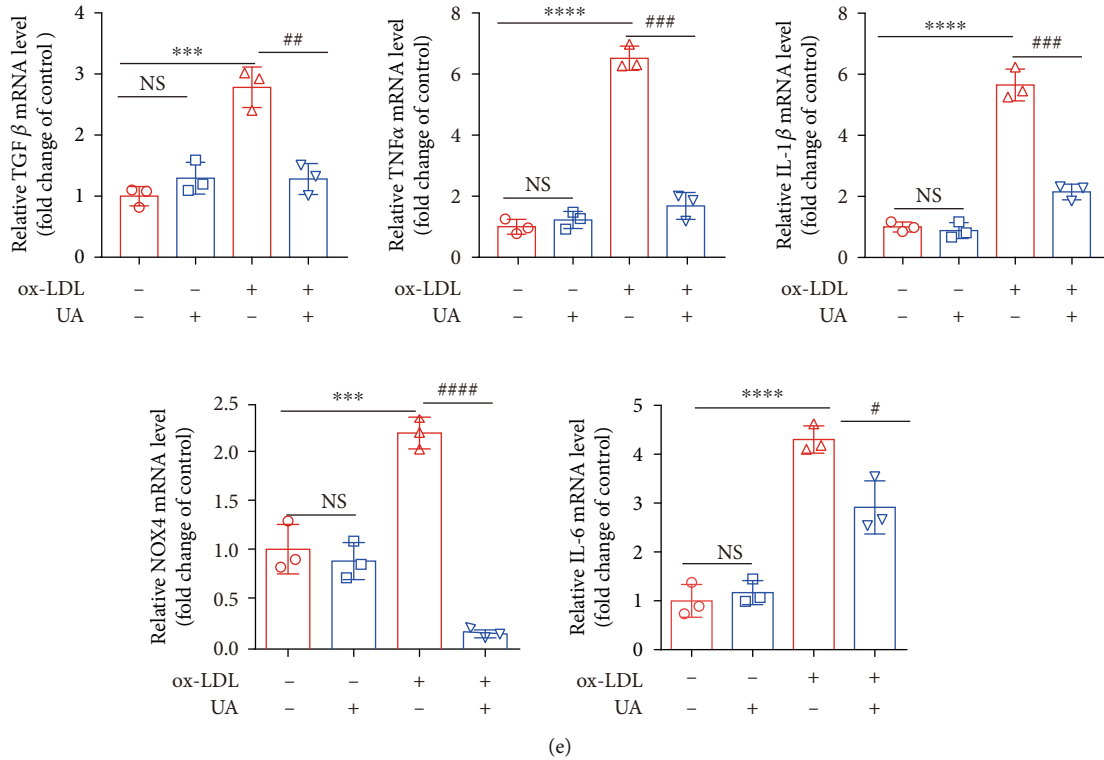
FIGURE 6: Effects of uric acid in microfluidic devices on inflammation and oxidative stress caused by ox-LDL in HUVECs. (a) Schematic diagram of vascular endothelial cells. (b) Photograph of a prototype. (c) A schematic diagram of cells in the micro chambers. (d) The microfluidic chambers were perfused with medium containing red THP-1 cells at velocity of 5 μL/min. HUVECs were stained by Mito-Green, determined by green fluorescence. Scale bar = 200 μm. (e) The mRNA levels of TGFβ, TNFα, IL-1β, IL-6, and Nox4 were assessed by reserve transcription PCR. GAPDH served as loading controls. Group data were obtained by normalizing to GAPDH and expressed as fold of control values. The statistical analyses were done using GraphPad Prism V-7.0 software. Data are expressed as the mean $\pm$ standard deviation ($n = 3$). One-way ANOVA was used in statistical analyses ($n = 3$/group). $^{*}P < 0.05$, $^{**}P < 0.01$, $^{***}P < 0.001$, and $^{****}P < 0.0001$ versus the control. $^{\#}P < 0.05$, $^{\#\#}P < 0.01$, $^{\#\#\#}P < 0.001$, and $^{\#\#\#\#}P < 0.0001$ versus the ox-LDL group.
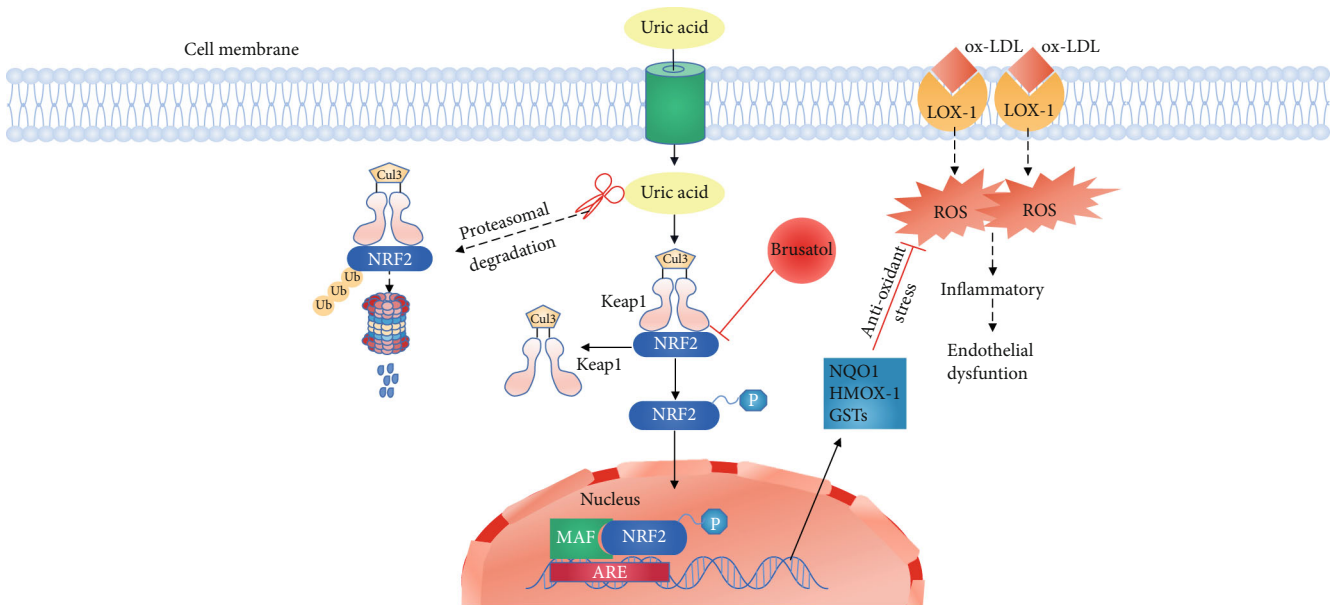
FIGURE 7: The potential protective mechanisms of UA on ox-LDL-induced HUVEC injury via the Keap1-Nrf2-Are pathway.

Currently, it is challenging to establish a stable uric acid concentration model in mice. Therefore, a microfluidic chip was used to further verify that an appropriate concentration of uric acid can reduce vascular damage caused by ox-LDL. The development of microfluidic organ models is a major field in bioanalytical chemistry, which is used in biological research, mainly in drug development. In addition to major organs including the lungs and liver, blood vessels are significant targets for biological examination [51]. Under static conditions, two dimensionally cultured experimental animals or cells are used to study blood vessels and related diseases. However, the results obtained from animal experiments are not always applicable to humans, and cells cultured *in vitro* are not a good model for vascular disease due to size differences and lack of blood flow. Three-dimensional (3D) primary cultures of human cells have been developed to imitate the human body in recent organ-on-chip studies. These *in vitro* models can be used to cultivate cells in extracellular (ECM) gels to imitate the organ micro-environment. In the microfluidic chip model, normal blood vessels, ox-LDL stimulated blood vessels, uric acid-stimulated blood vessels, and uric acid+ox-LDL costimulated blood vessels were simulated. Immunofluorescence results showed that ox-LDL significantly increased the expression of adhesion molecules on HUVECs, but 5 mg/dL uric acid reversed this phenomenon. The microfluidic chip also showed that uric acid suppressed inflammatory response and oxidative stress, as evidenced by decreased mRNA expression of TGFβ, TNFα, IL-1b, IL-6, and Nox4 in HUVEC cells (Figure 6). Previous studies have demonstrated that HUVECs injured by ox-LDL secreted and expressed multiple proinflammatory cytokines, including IL-6, TNFα, IL-1β, and MCP-1 [34, 52], which is consistent with our *in vitro* results. These data indicated that the microfluidic model is feasible to mimic the in vivo environment. Further exploration is needed in the future.

5. Conclusions

Overall, the results showed that suitable concentration UA can attenuate oxidative stress and inflammatory response caused by ox-LDL in HUVECs through the Keap1-Nrf2-ARE pathway (Figure 7). The different concentrations of uric acid still have important guiding significance for clinical work. Therefore, although there is need to pay attention to hyperuricemia, the physiological effect of uric acid should be considered.

Data Availability

The corresponding author will provide the data used in this study upon request. Owing to privacy concerns, the data is not publicly accessible.

Conflicts of Interest

There are no conflicts of interest reported by the authors in relation to the study, authorship, or publication of this paper.

Authors' Contributions

Yajuan Lin and Yunpeng Xie contributed equally to this work.

References

[1] I. Tabas, K. J. Williams, and J. Boren, "Subendothelial lipoprotein retention as the initiating process in atherosclerosis: update and therapeutic implications," *Circulation*, vol. 116, no. 16, pp. 1832–1844, 2007.

[2] L. Cao, Z. Zhang, Y. Li, P. Zhao, and Y. Chen, "LncRNA H19/miR-let-7 axis participates in the regulation of ox-LDL-induced endothelial cell injury _via_ targeting periostin," *International Immunopharmacology*, vol. 72, pp. 496–503, 2019.

[3] H. Itabe, "Oxidized low-density lipoprotein as a biomarker of in vivo oxidative stress: from atherosclerosis to periodontitis," *Journal of Clinical Biochemistry and Nutrition*, vol. 51, no. 1, pp. 1–8, 2012.

[4] W. Yuan, H. Chang, X. Liu, S. Wang, H. Liu, and H. Xuan, "Brazilian green propolis inhibits ox-LDL-stimulated oxidative stress in human umbilical vein endothelial cells partly through PI3K/Akt/mTOR-mediated Nrf2/HO-1 pathway," *Evidence-based Complementary and Alternative Medicine*, vol. 2019, Article ID 5789574, 12 pages, 2019.

[5] M. Kuwabara, K. Niwa, S. Nishihara et al., "Hyperuricemia is an independent competing risk factor for atrial fibrillation," *International Journal of Cardiology*, vol. 231, pp. 137–142, 2017.

[6] D. Cheng, R. Du, X. Y. Wu et al., "Serum uric acid is associated with the predicted risk of prevalent cardiovascular disease in a community-dwelling population without diabetes," *Biomedical and Environmental Sciences*, vol. 31, no. 2, pp. 106–114, 2018.

[7] L. Qin, Z. Yang, H. Gu et al., "Association between serum uric acid levels and cardiovascular disease in middle-aged and elderly Chinese individuals," *BMC Cardiovascular Disorders*, vol. 14, no. 1, p. 26, 2014.

[8] G. Ndrepepa, "Uric acid and cardiovascular disease," *Clinica Chimica Acta*, vol. 484, pp. 150–163, 2018.

[9] T. Y. Yang, C. Y. Fang, J. S. Chen et al., "Association of serum uric acid with cardiovascular disease in Taiwanese patients with primary hypertension," *Acta Cardiologica Sinica*, vol. 31, no. 1, pp. 42–51, 2015.

[10] S. K. Zalawadiya, V. Veeranna, S. Mallikethi-Reddy et al., "Uric acid and cardiovascular disease risk reclassification:

findings from NHANES III," *European Journal of Preventive Cardiology*, vol. 22, no. 4, pp. 513–518, 2015.

[11] W. Zhang, H. Iso, Y. Murakami et al., "Serum uric acid and mortality form cardiovascular disease: EPOCH-JAPAN study," *Journal of Atherosclerosis and Thrombosis*, vol. 23, no. 6, pp. 692–703, 2016.

[12] B. N. Ames, R. Cathcart, E. Schwiers, and P. Hochstein, "Uric acid provides an antioxidant defense in humans against oxidant- and radical-caused aging and cancer: a hypothesis," *Proceedings of the National Academy of Sciences of the United States of America*, vol. 78, no. 11, pp. 6858–6862, 1981.

[13] G. K. Glantzounis, E. C. Tsimoyiannis, A. M. Kappas, and D. A. Galaris, "Uric acid and oxidative stress," *Current Pharmaceutical Design*, vol. 11, no. 32, pp. 4145–4151, 2005.

[14] G. L. Squadrito, R. Cueto, B. Dellinger, and W. A. Pryor, "Quinoid redox cycling as a mechanism for sustained free radical generation by inhaled airborne particulate matter," *Free Radical Biology & Medicine*, vol. 31, no. 9, pp. 1132–1138, 2001.

[15] F. Regoli and G. W. Winston, "Quantification of total oxidant scavenging capacity of antioxidants for peroxynitrite, peroxyl radicals, and hydroxyl radicals," *Toxicology and Applied Pharmacology*, vol. 156, no. 2, pp. 96–105, 1999.

[16] M. Whiteman, U. Ketsawatsakul, and B. Halliwell, "A reassessment of the peroxynitrite scavenging activity of uric acid," *Annals of the New York Academy of Sciences*, vol. 962, no. 1, pp. 242–259, 2002.

[17] B. Zhang, N. Yang, S. P. Lin, and F. Zhang, "Suitable concentrations of uric acid can reduce cell death in models of OGD and cerebral ischemia-reperfusion injury," *Cellular and Molecular Neurobiology*, vol. 37, no. 5, pp. 931–939, 2017.

[18] W. Tu, H. Wang, S. Li, Q. Liu, and H. Sha, "The anti-inflammatory and anti-oxidant mechanisms of the Keap1/Nrf2/ARE signaling pathway in chronic diseases," *Aging and Disease*, vol. 10, no. 3, pp. 637–651, 2019.

[19] M. C. Lu, J. A. Ji, Z. Y. Jiang, and Q. D. You, "The Keap1-Nrf2-ARE pathway as a potential preventive and therapeutic target: an update," *Medicinal Research Reviews*, vol. 36, no. 5, pp. 924–963, 2016.

[20] S. Dhakshinamoorthy, D. Long, and A. K. Jaiswal, "Antioxidant regulation of genes encoding enzymes that detoxify xenobiotics and carcinogens," *Current Topics in Cellular Regulation*, vol. 36, pp. 201–216, 2001.

[21] S. K. Niture, R. Khatri, and A. K. Jaiswal, "Regulation of Nrf2–an update," *Free Radical Biology & Medicine*, vol. 66, pp. 36–44, 2014.

[22] Y. Ding, B. Zhang, K. Zhou et al., "Dietary ellagic acid improves oxidant-induced endothelial dysfunction and atherosclerosis: role of Nrf2 activation," *International Journal of Cardiology*, vol. 175, no. 3, pp. 508–514, 2014.

[23] X. L. Chen, G. Dodd, S. Thomas et al., "Activation of Nrf2/ARE pathway protects endothelial cells from oxidant injury and inhibits inflammatory gene expression," *American Journal of Physiology. Heart and Circulatory Physiology*, vol. 290, no. 5, pp. H1862–H1870, 2006.

[24] X. Yang, J. Gu, H. Lv et al., "Uric acid induced inflammatory responses in endothelial cells via up- regulating(pro)renin receptor," *Biomedicine & Pharmacotherapy*, vol. 109, pp. 1163–1170, 2019.

[25] H. L. Bi, X. L. Zhang, Y. L. Zhang et al., "The deubiquitinase UCHL1 regulates cardiac hypertrophy by stabilizing epidermal growth factor receptor," *Science Advances*, vol. 6, no. 16, article eaax4826, 2020.

[26] E. W. Young and C. A. Simmons, "Macro- and microscale fluid flow systems for endothelial cell biology," *Lab on a Chip*, vol. 10, no. 2, pp. 143–160, 2010.

[27] X. Liu, M. Liu, M. Chen, Q. M. Ge, and S. M. Pan, "Serum uric acid is neuroprotective in Chinese patients with acute ischemic stroke treated with intravenous recombinant tissue plasminogen activator," *Journal of Stroke and Cerebrovascular Diseases*, vol. 24, no. 5, pp. 1080–1086, 2015.

[28] R. Li, C. Huang, J. Chen, Y. Guo, and S. Tan, "The role of uric acid as a potential neuroprotectant in acute ischemic stroke: a review of literature," *Neurological Sciences*, vol. 36, no. 7, pp. 1097–1103, 2015.

[29] A. J. Kattoor, N. V. K. Pothineni, D. Palagiri, and J. L. Mehta, "Oxidative stress in atherosclerosis," *Current Atherosclerosis Reports*, vol. 19, no. 11, p. 42, 2017.

[30] E. Mannarino and M. Pirro, "Endothelial injury and repair: a novel theory for atherosclerosis," *Angiology*, vol. 59, 2_suppl, pp. 69S–72S, 2008.

[31] J. K. Lang and T. R. Cimato, "Cholesterol and hematopoietic stem cells: inflammatory mediators of atherosclerosis," *Stem Cells Translational Medicine*, vol. 3, no. 5, pp. 549–552, 2014.

[32] J. A. Berliner and J. W. Heinecke, "The role of oxidized lipoproteins in atherogenesis," *Free Radical Biology & Medicine*, vol. 20, no. 5, pp. 707–727, 1996.

[33] Y. Yao, Y. Wang, Y. Zhang, and C. Liu, "Klotho ameliorates oxidized low density lipoprotein (ox-LDL)-induced oxidative stress via regulating LOX-1 and PI3K/Akt/eNOS pathways," *Lipids in Health and Disease*, vol. 16, no. 1, p. 77, 2017.

[34] H. Mao, T. Tao, X. Wang et al., "Zedoarondiol attenuates endothelial cells injury induced by oxidized low-density lipoprotein via Nrf2 activation," *Cellular Physiology and Biochemistry*, vol. 48, no. 4, pp. 1468–1479, 2018.

[35] Z. Zhu, J. Li, and X. Zhang, "Astragaloside IV protects against oxidized low-density lipoprotein (ox-LDL)-induced endothelial cell injury by reducing oxidative stress and inflammation," *Medical Science Monitor*, vol. 25, pp. 2132–2140, 2019.

[36] Y. Wang, X. Wei, X. Xiao et al., "Arachidonic acid epoxygenase metabolites stimulate endothelial cell growth and angiogenesis via mitogen-activated protein kinase and phosphatidylinositol 3-kinase/Akt signaling pathways," *The Journal of Pharmacology and Experimental Therapeutics*, vol. 314, no. 2, pp. 522–532, 2005.

[37] W. S. Waring, J. A. McKnight, D. J. Webb, and S. R. Maxwell, "Uric acid restores endothelial function in patients with type 1 diabetes and regular smokers," *Diabetes*, vol. 55, no. 11, pp. 3127–3132, 2006.

[38] H. F. Galley, P. D. Howdle, B. E. Walker, and N. R. Webster, "The effects of intravenous antioxidants in patients with septic shock," *Free Radical Biology & Medicine*, vol. 23, no. 5, pp. 768–774, 1997.

[39] S. W. Waring, D. J. Webb, and S. R. J. Maxwell, "Systemic uric acid administration increases serum antioxidant capacity in healthy volunteers," *Journal of Cardiovascular Pharmacology*, vol. 38, no. 3, pp. 365–371, 2001.

[40] Y. Y. Sautin, T. Nakagawa, S. Zharikov, and R. J. Johnson, "Adverse effects of the classic antioxidant uric acid in adipocytes: NADPH oxidase-mediated oxidative/nitrosative stress," *American Journal of Physiology. Cell Physiology*, vol. 293, no. 2, pp. C584–C596, 2007.

[41] T. Maruhashi, I. Hisatome, Y. Kihara, and Y. Higashi, "Hyperuricemia and endothelial function: from molecular background to clinical perspectives," *Atherosclerosis*, vol. 278, pp. 226–231, 2018.

[42] A. Alfieri, S. Srivastava, R. C. Siow, M. Modo, P. A. Fraser, and G. E. Mann, "Targeting the Nrf2-Keap1 antioxidant defence pathway for neurovascular protection in stroke," *The Journal of Physiology*, vol. 589, no. 17, pp. 4125–4136, 2011.

[43] T. Cui, Y. Lai, J. S. Janicki, and X. Wang, "Nuclear factor erythroid-2 related factor 2 (Nrf2)-mediated protein quality control in cardiomyocytes," *Frontiers in Bioscience*, vol. 21, pp. 192–202, 2016.

[44] W. Takabe, E. Warabi, and N. Noguchi, "Anti-atherogenic effect of laminar shear stress via Nrf2 activation," *Antioxidants & Redox Signaling*, vol. 15, no. 5, pp. 1415–1426, 2011.

[45] L. Ma, X. Liu, Y. Zhao, B. Chen, X. Li, and R. Qi, "Ginkgolide B reduces LOX-1 expression by inhibiting Akt phosphorylation and increasing Sirt1 expression in oxidized LDL-stimulated human umbilical vein endothelial cells," *PLoS One*, vol. 8, no. 9, article e74769, 2013.

[46] G. F. Ming, Y. J. Tang, K. Hu, Y. Chen, W. H. Huang, and J. Xiao, "Visfatin attenuates the ox-LDL-induced senescence of endothelial progenitor cells by upregulating SIRT1 expression through the PI3K/Akt/ERK pathway," *International Journal of Molecular Medicine*, vol. 38, no. 2, pp. 643–649, 2016.

[47] H. W. Yang, H. L. Hong, W. W. Luo et al., "mTORC2 facilitates endothelial cell senescence by suppressing Nrf2 expression via the Akt/GSK-3β/C/EBPα signaling pathway," *Acta Pharmacologica Sinica*, vol. 39, no. 12, pp. 1837–1846, 2018.

[48] N. Zhang, H. Y. Shu, T. Huang et al., "Nrf2 signaling contributes to the neuroprotective effects of urate against 6-OHDA toxicity," *PLoS One*, vol. 9, no. 6, article e100286, 2014.

[49] B. L. Ya, Q. Liu, H. F. Li et al., "Uric acid protects against focal cerebral ischemia/reperfusion-induced oxidative stress via activating Nrf2 and regulating neurotrophic factor expression," *Oxidative Medicine and Cellular Longevity*, vol. 2018, Article ID 6069150, 10 pages, 2018.

[50] R. Bakshi, H. Zhang, R. Logan et al., "Neuroprotective effects of urate are mediated by augmenting astrocytic glutathione synthesis and release," *Neurobiology of Disease*, vol. 82, pp. 574–579, 2015.

[51] K. Sato and K. Sato, "Recent progress in the development of microfluidic vascular models," *Analytical Sciences*, vol. 34, no. 7, pp. 755–764, 2018.

[52] Y. Wu and H. Huang, "Synergistic enhancement of matrix metalloproteinase-9 expression and pro-inflammatory cytokines by influenza virus infection and oxidized-LDL treatment in human endothelial cells," *Experimental and Therapeutic Medicine*, vol. 14, no. 5, pp. 4579–4585, 2017.

Research Article

COVID-19 and Cancer: Discovery of Difference in Clinical Immune Indexes

Xiaojiao Zeng, Xianghu Jiang, Liu Yang, Yunbao Pan [ID], and Yirong Li [ID]

Department of Laboratory Medicine, Zhongnan Hospital of Wuhan University, Wuhan University, Wuhan, China

Correspondence should be addressed to Yunbao Pan; panyunbao@outlook.com and Yirong Li; liyirong2021@126.com

Objective. This study explored the consistency and differences in the immune cells and cytokines between patients with COVID-19 or cancer. We further analyzed the correlations between the acute inflammation and cancer-related immune disorder. *Methods*. This retrospective study involved 167 COVID-19 patients and 218 cancer patients. COVID-19 and cancer were each further divided into two subgroups. Quantitative and qualitative variables were measured by one-way ANOVA and chi-square test, respectively. Herein, we carried out a correlation analysis between immune cells and cytokines and used receiver operating characteristic (ROC) curves to discover the optimal diagnostic index. *Results*. COVID-19 and cancers were associated with lymphopenia and high levels of monocytes, neutrophils, IL-6, and IL-10. IL-2 was the optimal indicator to differentiate the two diseases. Compared with respiratory cancer patients, COVID-19 patients had lower levels of IL-2 and higher levels of $CD3^+CD4^+$ T cells and $CD19^+$ B cells. In the subgroup analysis, IL-6 was the optimal differential diagnostic parameter that had the ability to identify if COVID-19 patients would be severely affected, and severe COVID-19 patients had lower levels of lymphocyte subsets ($CD3^+$ T cells, $CD3^+CD4^+$ T cells, $CD3^+CD8^+$T cells, and $CD19^+$ B cells) and $CD16^+CD56^+$ NK cells and higher level of neutrophils. There were significant differences in the levels of $CD3^+CD4^+$ T cells and $CD19^+$ B cells between T_{1-2} and T_{3-4} stages as well as IL-2 and $CD19^+$ B cells between N_{0-1} and N_{2-3} stages while no significant differences between the metastatic and nonmetastatic cancer patients. Additionally, there were higher correlations between IL-2 and IL-4, TNF-α and IL-2, TNF-α and IL-4, TNF-α and IFN-γ, and $CD16^+CD56^+$NK cells and various subsets of T cells in COVID-19 patients. There was a higher correlation between $CD3^+CD4^+$ T cells and $CD19^+$ B cells in cancer patients. *Conclusion*. Inflammation associated with COVID-19 or cancer had effects on patients' outcomes. Accompanied by changes in immune cells and cytokines, there were consistencies, differences, and satisfactory correlations between patients with COVID-19 and those with cancers.

1. Introduction

A new coronavirus appeared in 2019 after two major infectious disease pandemics caused by the severe acute respiratory syndrome coronavirus (SARS-CoV) and the Middle East respiratory syndrome coronavirus (MERS-CoV) in 2002 and 2012, respectively. The virus was named SARS-CoV-2 by the Coronaviridae Study Group (CSG) of the International Committee on Taxonomy of Viruses [1]. Coronavirus disease 2019 (COVID-19) caused by SARS-CoV-2 has a wider and deeper impact and has been declared a Public Health Emergency of International Concern (PHEIC) by the World Health Organization (WHO). There

were more than 50 million confirmed cases and more than 1 million deaths by November 2020, and the virus remains a threat to human health [2]. After SARS-CoV-2 infection, the body activates innate and adaptive immunity to implement an immune response, which results in distinct heterogeneity of COVID-19 by involving a series of physiological and pathological mechanisms, such as mild respiratory symptoms and severe respiratory diseases. Acute inflammation is critical for the regulation of tissue repair, regeneration, and homeostasis. In patients with severe COVID-19, activated immune cells produce various cytokines, and then, cytokines act on immune cells and create an amplified inflammatory cascade. Lung injury and death are mainly

induced by an excessive inflammatory response [3]. Lymphocyte and macrophage infiltration into the lung parenchyma often occurs in COVID-19 patients [4].

Cancer, the enemy of mankind, is always harmful to human health. The incidence and mortality of cancer are rapidly increasing around the world. According to the GLO-BOCAN 2020 report by the International Agency for Research on Cancer, it was estimated that there were approximately 19.3 million new cancer cases and nearly 10 million cancer deaths worldwide in 2020 [5]. In past decades, there was interest in studying the immune-inflammatory response that occurs in cancer. Infectious (Helicobacter pylori, human papillomavirus, and hepatitis B virus) and noninfectious stimulation (obesity, smoking, and alcohol consumption) can lead to the proliferation and activation of immune cells and cytokines and the formation of an inflammatory microenvironment. The stimulation of chronic inflammation easily promotes the occurrence, progression, and metastasis of cancer and cancer-related immune disorder persists and forms the tumor microenvironment [6–8].

Numerous studies have shown that there are significant changes in immune cells and cytokines during the occurrence and development of COVID-19 and cancer. Tan and Yang [9] revealed that SARS-CoV-2 can activate various immune cells (T cells, B cells, macrophages, and natural killer (NK) cells) and cytokines (interleukin- (IL-) 2, IL-4, IL-6, interferon- (IFN-) γ, and tumor necrosis factor- (TNF-) α), which can lead to excessive inflammation and pulmonary immunopathology. Dranoff's study in 2004 found that there were complex immune cells and cytokines in the tumor microenvironment, and the interaction between them played a decisive role in the antitumor immune response [10].

In this study, we analyzed the immune cells and cytokines between COVID-19 and cancer patients to explore the consistency, difference, and differential diagnostic efficiency of these indexes between the acute inflammation and cancer-related immune disorder. In addition, COVID-19 and cancer patients were each divided into two groups according to the condition of severity and metastasis. We analyzed the immune cells and cytokines of the four subgroups to discover the correlations, influencing factors, and the optimal diagnostic indexes among COVID-19 and cancer patients.

2. Materials and Methods

2.1. Patients. We retrospectively recruited 167 and 218 patients who were diagnosed with COVID-19 or cancer at the Zhongnan Hospital of Wuhan University from December 2018 to October 2020, respectively. There were 86 male and 81 female patients with COVID-19, with a median age of 58 (range 17-93 years). According to the clinical classification standard of the 7th edition of Guidelines for the Diagnosis and Treatment of COVID-19, those with severe or critical disease were classified as the severe group, while mild and ordinary types were classified as nonsevere groups. There were 51 severe and 116 nonsevere patients. There

were 152 males and 66 females with a median age of 57 (range 9-85 years) who had respiratory and nonrespiratory cancers. There were 96 nonmetastatic and 29 metastatic cancer patients, and the status of 93 cancer patients was unknown.

2.2. Inclusion Criteria and Enrollment. The inclusion criteria in this study were (1) patients with definite diagnosis of COVID-19 and solid cancers and (2) patients with complete records of immune cells and cytokines. Exclusion criteria were as follows: (1) patients with both COVID-19 and cancers, (2) patients with hematological malignancy, and (3) patients with incomplete medical records.

2.3. Physical Examination and Hematological Data. Peripheral blood cells, such as neutrophils, lymphocytes, and monocytes, were analyzed with a Beckman Coulter DxH 800 automated blood analyzer according to the manufacturer's instructions (Beckman, California, USA). Serum cytokines, including IL-2, IL-4, IL-6, IL-10, TNF-α, and IFN-γ, were analyzed by BD FACSCalibur flow cytometry according to the manufacturer's instructions. Peripheral absolute cell counts of $CD3^+$ T cells, $CD3^+CD4^+$ T cells, $CD3^+CD8^+$ T cells, $CD19^+$ B cells, and $CD16^+CD56^+$ natural killer (NK) cells were obtained by flow cytometry according to the manufacturer's instructions.

2.4. Statistical Analysis. The statistical analyses were conducted by IBM SPSS version 22.0 software (SPSS, Chicago, IL). Quantitative and qualitative variables were measured by one-way ANOVA and chi-square test, respectively. Pairwise comparisons and correlation analyses between groups were plotted by GraphPad Prism v7.0 software. The receiver operating characteristic (ROC) curve was applied to assess the diagnostic efficiency of various immune indicators. A p value < 0.05 was considered statistically significant.

3. Results

3.1. Baseline Characteristics between COVID-19 and Cancer Patients. The patients recruited in our study consisted of those with COVID-19 or cancer of various types. The general parameters of the patients were shown in Table 1. Cancer was common in men and younger patients, with respiratory cancers being the most common. There were significant differences between metastatic and nonmetastatic cancer patients as well as between severe and nonsevere COVID-19 patients. Moreover, most cytokines and immune cells were significantly different, including IL-6, IL-10, $CD3^+$ T cells, $CD3^+CD4^+$ T cells, 4/8 ratio, and $CD19^+$ B cells.

3.2. Variance Analysis of Immune Cells and Cytokines in Different Groups. COVID-19 and cancer patients were each further divided into two subgroups, for a total of four subgroups, and the logarithmic levels of immune cells and cytokines were displayed in Figure S1. There were 96 nonmetastatic and 29 metastatic cancer patients, and 116 nonsevere and 51 severe COVID-19 patients, respectively (Table 1). Immune cells and cytokines of COVID-19 and cancer patients were analyzed by one-way ANOVA

TABLE 1: Baseline parameters between COVID-19 and cancer patients.

Variables	n	p
Sex		≤0.001
Cancer		
Male	152	
Female	66	
COVID-19		
Male	86	
Female	81	
Age		0.646
Cancer		
<60	120	
≥60	98	
COVID-19		
<60	88	
≥60	79	
COVID-19		≤0.001
Nonsevere	116	
Severe	51	
Cancer type		0.104
Respiratory system	121	
Nonrespiratory system	97	
Cancer distant metastasis		≤0.001
M0	96	
M1	29	
Unknown	93	
IL-2		0.906
Cancer		
Normal	195	
High	23	
COVID-19		
Normal	150	
High	17	
IL-4		0.156
Cancer		
Normal	198	
High	20	
COVID-19		
Normal	144	
High	23	
IL-6		≤0.001
Cancer		
Normal	48	
High	170	
COVID-19		
Normal	83	
High	84	
IL-10		≤0.001

TABLE 1: Continued.

Variables	n	p
Cancer		
Normal	188	
High	30	
COVID-19		
Normal	118	
High	49	
IFN-γ		0.105
Cancer		
Normal	218	
High	0	
COVID-19		
Normal	165	
High	2	
TNF-α		0.850
Cancer		
Normal	217	
High	1	
COVID-19		
Normal	166	
High	1	
CD3$^+$Abs Cnt		0.028
Cancer		
Normal	102	
Low	116	
COVID-19		
Normal	97	
Low	70	
CD3$^+$CD4$^+$Abs Cnt		0.003
Cancer		
Normal	126	
Low	92	
COVID-19		
Normal	121	
Low	46	
CD3$^+$CD8$^+$Abs Cnt		0.109
Cancer		
Normal	79	
Low	139	
COVID-19		
Normal	74	
Low	93	
4/8 ratio		0.014
Cancer		
Normal	110	
High	56	
Low	52	

TABLE 1: Continued.

Variables	n	p
COVID-19		
Normal	90	
High	56	
Low	21	
CD19$^+$Abs Cnt		0.019
Cancer		
Normal	35	
Low	183	
COVID-19		
Normal	43	
Low	124	
CD16$^+$CD56$^+$Abs Cnt		0.403
Cancer		
Normal	102	
Low	116	
COVID-19		
Normal	71	
Low	96	
LYM		0.625
Cancer		
Normal	111	
High	1	
Low	106	
COVID-19		
Normal	89	
Low	78	
NEU		0.260
Cancer		
Normal	144	
High	53	
Low	21	
COVID-19		
Normal	122	
High	35	
Low	10	
MONO		0.268
Cancer		
Normal	148	
High	65	
Low	5	
COVID-19		
Normal	126	
High	38	
Low	3	

Abbreviations: M: metastasis; CD3$^+$Abs: absolute count of CD3$^+$T cells; CD3$^+$CD4$^+$Abs: absolute count of CD3$^+$CD4$^+$T cells; CD3$^+$CD8$^+$Abs: absolute count of CD3$^+$CD8$^+$T cells; CD19$^+$Abs: absolute count of CD19$^+$ B cells; CD16$^+$CD56$^+$Abs: absolute count of CD16$^+$CD56$^+$NK cells; LYM: lymphocyte; NEU: neutrophil; MONO: monocyte.

(Figure 1). The results showed that there were significant differences in the levels of IL-2, IL-10, absolute count of lymphocyte subsets (CD3$^+$ T cells, CD3$^+$CD4$^+$ T cells, CD3$^+$CD8$^+$ T cells, and CD19$^+$ B cells), CD16$^+$CD56$^+$ NK cells, and neutrophils between patents with COVID-19 and cancers. Moreover, immune cell levels were statistically different between COVID-19 subgroups, including lymphocyte subsets, NK cells, and neutrophils, whereas there was no significant difference between metastatic and nonmetastatic cancer subgroups (Figure 1). Moreover, we further analyzed immune cells and cytokines in different T stages, N stages, and differentiation of cancers (Table S1). There were significant differences in the levels of CD3$^+$CD4$^+$ T cells and CD19$^+$ B cells between T$_{1-2}$ and T$_{3-4}$ stages as well as IL-2 and CD19$^+$ B cells between N$_{0-1}$ and N$_{2-3}$ stages (Figure S2).

There were 121 patients with respiratory cancers and 97 patients with nonrespiratory cancers (Table S1). And there were significant differences in the levels of NK cells and neutrophils between squamous carcinoma and adenocarcinoma in patients with respiratory cancers as well as NK cells between patients with distant and nondistant metastatic respiratory cancers (Figure S2). A further analysis was conducted of immune cells and cytokines among patients with COVID-19 or cancer. The results suggested that there were significant differences in the levels of IL-2, IL-6, IL-10, CD3$^+$ T cells, CD3$^+$CD4$^+$T cells, and CD19$^+$ B cells (Figure 2).

3.3. Correlation Analysis of Immune Cells and Cytokines. A correlation analysis was performed on immune cells and cytokines among patients with COVID-19 or cancer (Figure 3). The results suggested that there was a satisfactory correlation among most of these inflammatory markers, and the correlation analysis was plotted (Figure 4). In the severe COVID-19 group, the correlation coefficients between IL-4 and IL-2, CD16$^+$CD56$^+$ NK cells and CD3$^+$ T cells, CD16^{+-}CD56$^+$ NK cells and CD3$^+$CD4$^+$ T cells, CD16$^+$CD56$^+$ NK cells and CD3$^+$CD8$^+$ T cells, TNF-α and IL-2, TNF-α and IL-4, and TNF-α and IFN-γ were 0.961, 0.804, 0.659, 0.848, 0.733, 0.7, and 0.629, respectively. In the nonsevere COVID-19 group, the correlation coefficients of IL-4 and IL-2, TNF-α and IL-2, TNF-α and IFN-γ, and TNF-α and IL-4 were 0.887, 0.795, 0.699, and 0.674, respectively. In the metastatic group, the correlation coefficient between IL-4 and IL-2, and CD3$^+$CD4$^+$ T cells and CD19$^+$ B cells were 0.848 and 0.655, respectively. Additionally, the correlation coefficients were 0.66 and 0.598 in the nonmetastatic group for two pairs of indexes, respectively. Moreover, the correlation coefficients for IL-4 and IL-2, IL-4 and TNF-α, and NK cells and T cells were the lowest in nonmetastatic patients, followed by metastatic and nonsevere COVID-19 patients, and were the highest in severe COVID-19 patients. The correlation coefficients for TNF-α and IL-2, and TNF-α and IFN-γ were higher in the COVID-19 group than that in the cancer group, while the correlation coefficients between CD3$^+$CD4$^+$ T cells and CD19$^+$ B cells were higher in the cancer group than that in the COVID-19 group (Figure 3).
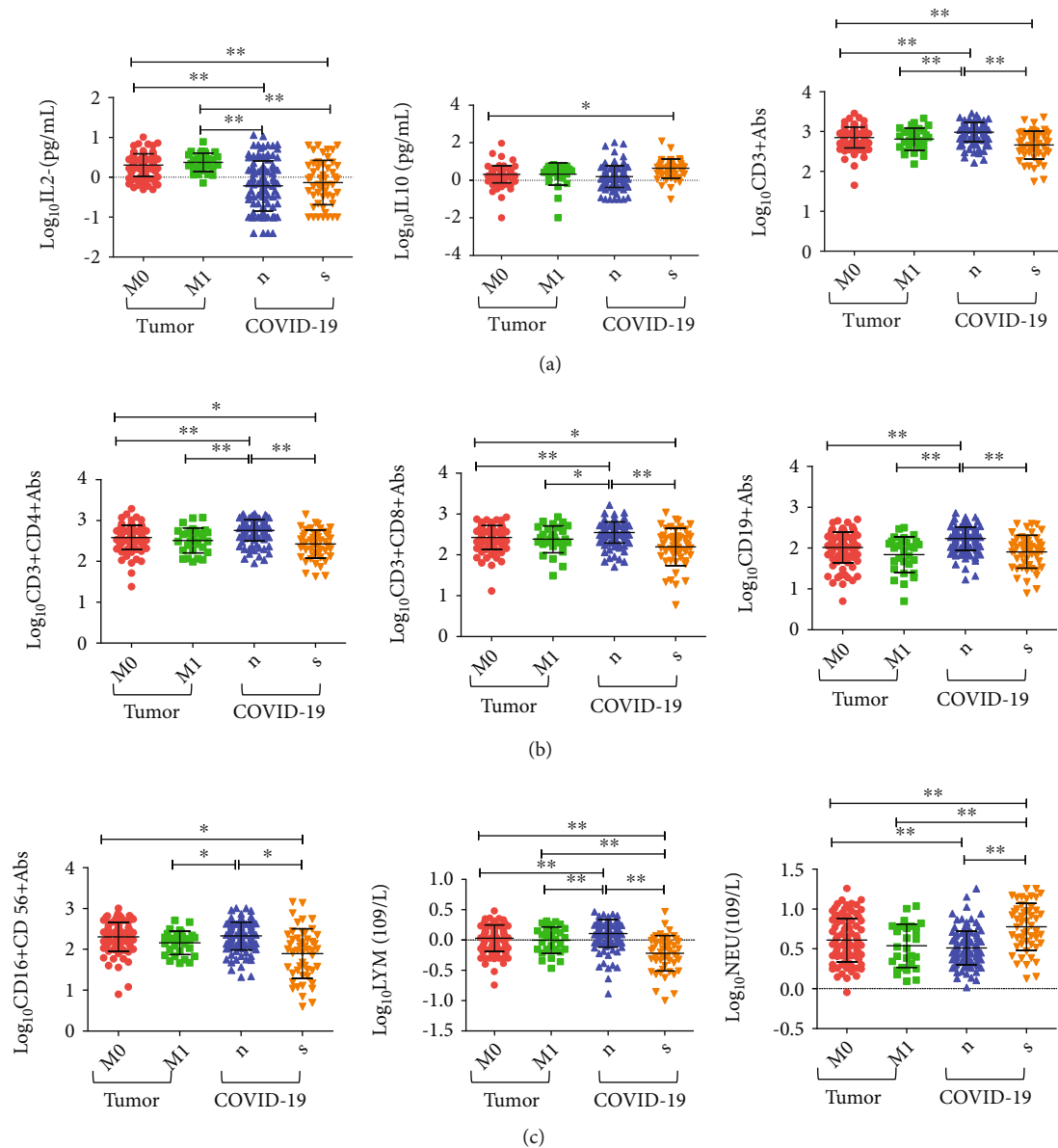
FIGURE 1: Analysis of immune cells and cytokines in the four subgroups of patients with COVID-19 or cancer. *n*: nonsevere; *s*: severe. (a) IL-2 (left), IL-10 (middle), and CD3$^+$ Abs (right). (b) CD3$^+$CD4$^+$ Abs (left), CD3$^+$CD8$^+$ Abs (middle), and CD19$^+$ Abs (right). (c) CD16$^+$CD56$^+$ Abs (left), LYM (middle), and NEU (right).

In addition, there was a significant correlation between immune cells and cytokines (Figure 5). Monocytes were negatively correlated with IL-2, IL-4, and TNF-α in the COVID-19 severe group. In the metastatic group, neutrophils were positively correlated with IL-10. In the nonmetastatic group, NK cells and lymphocytes were positively correlated with IL-2 and negatively correlated with IL-6, and T cells were positively correlated with IL-4 and TNF-α and negatively correlated with IL-6 and IL-10.

3.4. ROC Curve Analysis of Immune Cells and Cytokines. We used ROC curves to explore the ability of immune cells and cytokines to differentiate between COVID-19 and cancers (Figure 6(a)). The area under the ROC curve (AUC) for IL-2 (0.741, 0.687-0.796) was larger than that for the other

indexes, indicating that IL-2 was the most optimal differential diagnostic value between the two diseases. The AUC of the cytokines IL-4, IL-6, IL-10, IFN-γ, and TNF-α was 0.679, 0.669, 0.541, 0.647, and 0.553, respectively. The AUCs of the CD3$^+$CD4$^+$ T and CD19$^+$ B immune cells were 0.606 and 0.61, respectively. We further investigated the ability of immune indexes to differentiate between severe and nonsevere COVID-19 (Figure 6(b)). The AUCs of immune indexes such as IL-6, IL-10, neutrophils, CD3$^+$ T cells, CD3$^+$CD4$^+$ T cells, CD3$^+$CD8$^+$ T cells, CD19$^+$ B cells, CD16$^+$CD56$^+$ NK cells, and lymphocytes were 0.848, 0.743, 0.768, 0.792, 0.791, 0.76, 0.746, 0.733, and 0.839, respectively. These results suggested that there was more optimal differential diagnostic value for IL-6 and lymphocytes between the two groups of COVID-19 patients.
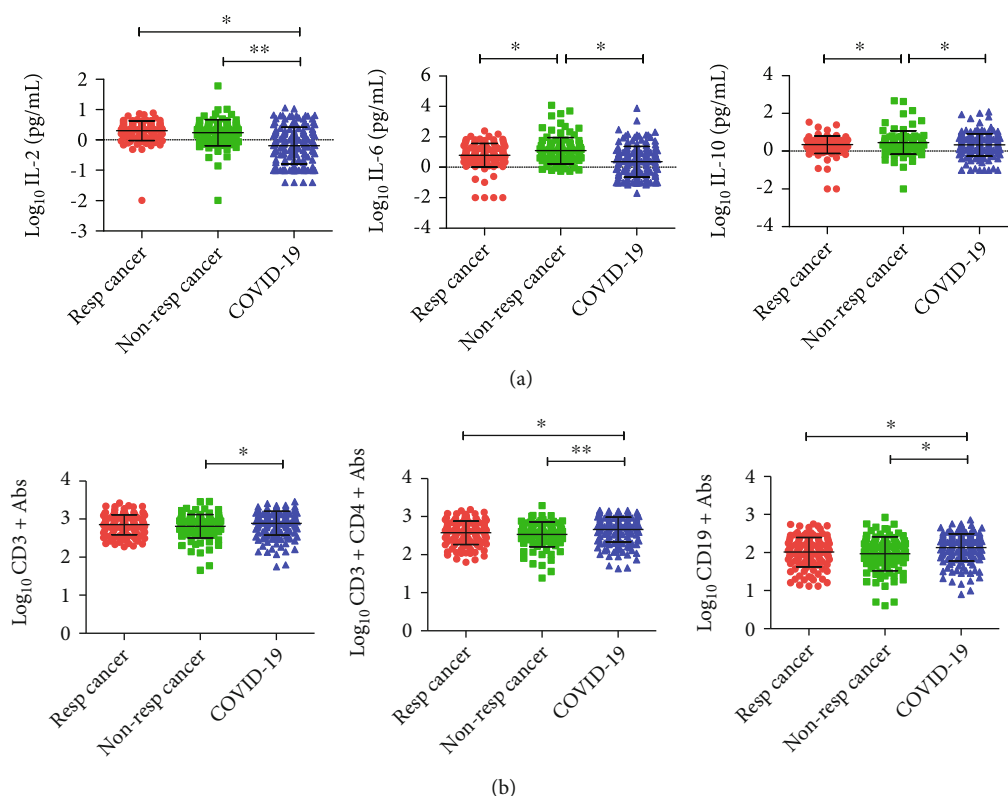
(a)

(b)

Figure 2: Analysis of immune cells and cytokines in three groups of patients with COVID-19 or cancer. Resp: respiratory cancer; Non-resp: nonrespiratory cancer. (a) IL-2 (left), IL-6 (middle), and IL-10 (right). (b) CD3^{+} Abs (left), CD3^{+}CD4^{+}Abs (middle), and CD19^{+} Abs (right).

However, they exhibited poor diagnostic efficiency in differentiating distant metastatic patients from nonmetastatic patients (Figure S3).

4. Discussion

Most studies have shown that COVID-19 is often accompanied by lymphopenia, and high levels of neutrophils and mononuclear macrophages in patients. Cytokine storms with significant increases in IL-6 and IL-10 often occur in patients with severe COVID-19 and may play an important role in the development of lymphopenia, high neutrophils, and high mononuclear macrophages [11–13]. Giamarellos-Bourboulis et al. [14] reported that immune dysregulation in cases of severe COVID-19 was mainly characterized by low expression of IL-6-mediated human leukocyte antigen D-related (HLA-DR) and a decrease in lymphocytes and NK cells. Jamilloux et al. [15] found that the type I IFN response was prolonged or decreased in COVID-19 patients, the innate and adaptive immune responses were suppressed, and both NK cells and lymphocyte subsets were reduced, which indicates that SARS-CoV-2 is not subject to immune control.

An excessive inflammatory response is significantly correlated with poor prognosis in COVID-19 patients. Moreover, Li et al. [16] showed that IL-2, IL-4, IFN-γ, and TNF-α levels were not significantly different between deceased patients and survivors of COVID-19, and the absolute counts of CD3^{+} T cells, CD3^{+} CD4^{+} T cells, and CD3[+-]CD8^{+} T cells in the deceased group were always at a low

level. Wu et al. [17] showed that there were no significant differences in IL-6, IFN-γ, TNF-α, or lymphocyte levels between patients with mild and moderate COVID-19, while the IL-10 level was significantly increased, and the neutrophil level was significantly decreased in the moderate group.

In this study, there were no significant differences in cytokines between the severe and nonsevere COVID-19 groups. In accordance with the conclusion of previous studies, the neutrophils were significantly elevated, and the absolute counts of CD3^{+} T cells, CD3^{+}CD4^{+} T cells, CD3^{+}CD8^{+} T cells, CD19^{+} B cells, and NK cells were significantly decreased in patients with severe COVID-19. Moreover, ROC curve analysis suggested that IL-6 was the optimal diagnostic index to distinguish severe and nonsevere COVID-19 in patients.

Currently, many studies have proved the relationship between chronic inflammation and the occurrence and development of cancers. Our previous studies also reported the relationship between immune cells and prognosis of cancer [18]. Neutrophils and monocytes can induce immune tolerance, distant metastasis, chemotherapy resistance, and cancer progression by forming tumor-associated neutrophils (TAN) and tumor-associated macrophages (TAM). The effective immunity of cancer mainly depends on the function of NK cells and CD3^{+}CD8^{+} T cells, as cytotoxic lymphocytes of the innate and adaptive immune system, respectively [19–21]. Toyoshima et al. [22] reported that high levels of IL-6 can interfere with type-I IFN signals in the immune system and is accompanied by low expression
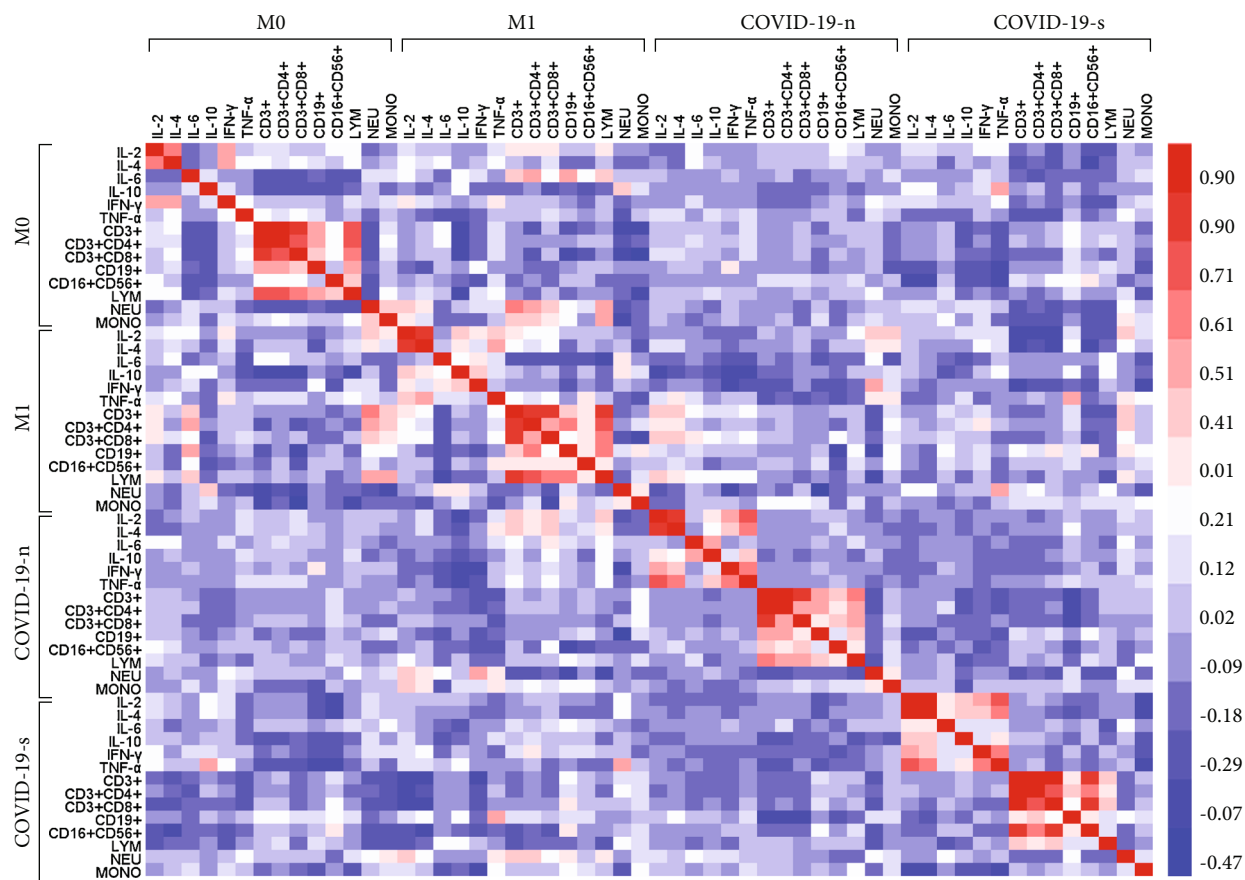
FIGURE 3: Heat maps for correlation coefficients of patients with COVID-19 or cancer. M0: nonmetastatic cancer patients; M1: metastatic cancer patients; COVID-19-n nonsevere COVID-19 patients; COVID-19-s: severe COVID-19 patients.

of major histocompatibility complex class I (MHC I) molecules, which can then weaken the antitumor effect of CD3^{+-}CD8$^+$ T cells and promote tumor growth, development, and distant colonization. IL-10, an anti-inflammatory cytokine, protects the body from damage caused by immune overreaction, while IL-10 in cancer has two opposite effects. A high level of IL-10 has an immunosuppressive effect that facilitates the immune escape of cancer cells, but IL-10 also has an antitumor effect by increasing the infiltration of CD3+CD8+ T cells and the production of IFN-γ in tissues, which may be related to the fact that IL-10 targets different cells (myeloid and T cells) in different cancers or that T cells respond differently to IL-10 at different effective stages [23].

These studies showed that both COVID-19 and cancer have the phenomenon of interference in the type-I IFN response, immunosuppression, and high levels of cytokines, such as IL-6 and IL-10. Our results were consistent with these conclusions. When we analyzed the immune cells and cytokines between COVID-19 and cancer patients, we discovered that there were similar changes in these biomarkers, such as low lymphocytes, high monocytes, high neutrophils, high IL-6, and high IL-10. The ROC curve suggested that IL-2 was the optimal diagnostic index for both diseases. We further compared the immune cells and cyto-

kines in patients with COVID-19 or respiratory cancers. The results showed that there was no significant difference in IL-6 and IL-10 between the two groups, while COVID-19 patients had lower levels of IL-2 and higher levels of CD3$^+$CD4$^+$ T cells and CD19$^+$ B cells. Moreover, the interaction between cancer and inflammation is regulated through a complex network. The inflammatory response may be varied at different stages of cancer development. Our study suggested that cancer patients in T$_{3-4}$ stages had lower levels of CD3$^+$CD4$^+$ T cells and CD19$^+$ B cells, and patients in N$_{2-3}$ stages had lower levels of CD19$^+$ B cells and higher levels of IL-2. In addition, we conducted a correlation analysis of these inflammatory indexes in COVID-19 and cancers, and the results suggested that there was a higher correlation between IL-2 and IL-4, NK cells and T cells in COVID-19 patients, and a higher correlation between CD3^{+-}CD4$^+$ T cells and CD19$^+$ B cells in cancer patients.

Luo et al. [24] revealed that multiple elevated cytokines were associated with poor prognosis of severe COVID-19 patients, including IL-2, IL-4, IL-6, IL-10, IFN-γ, and TNF-α. With the same cytokine receptor γ chain, IL-2 and IL-4 together regulate cell differentiation, promote the formation of immune cells, improve the killing activity of cytotoxic T lymphocyte (CTL) and NK cells, and play an important role in inflammation and cancers [25]. Our study showed that
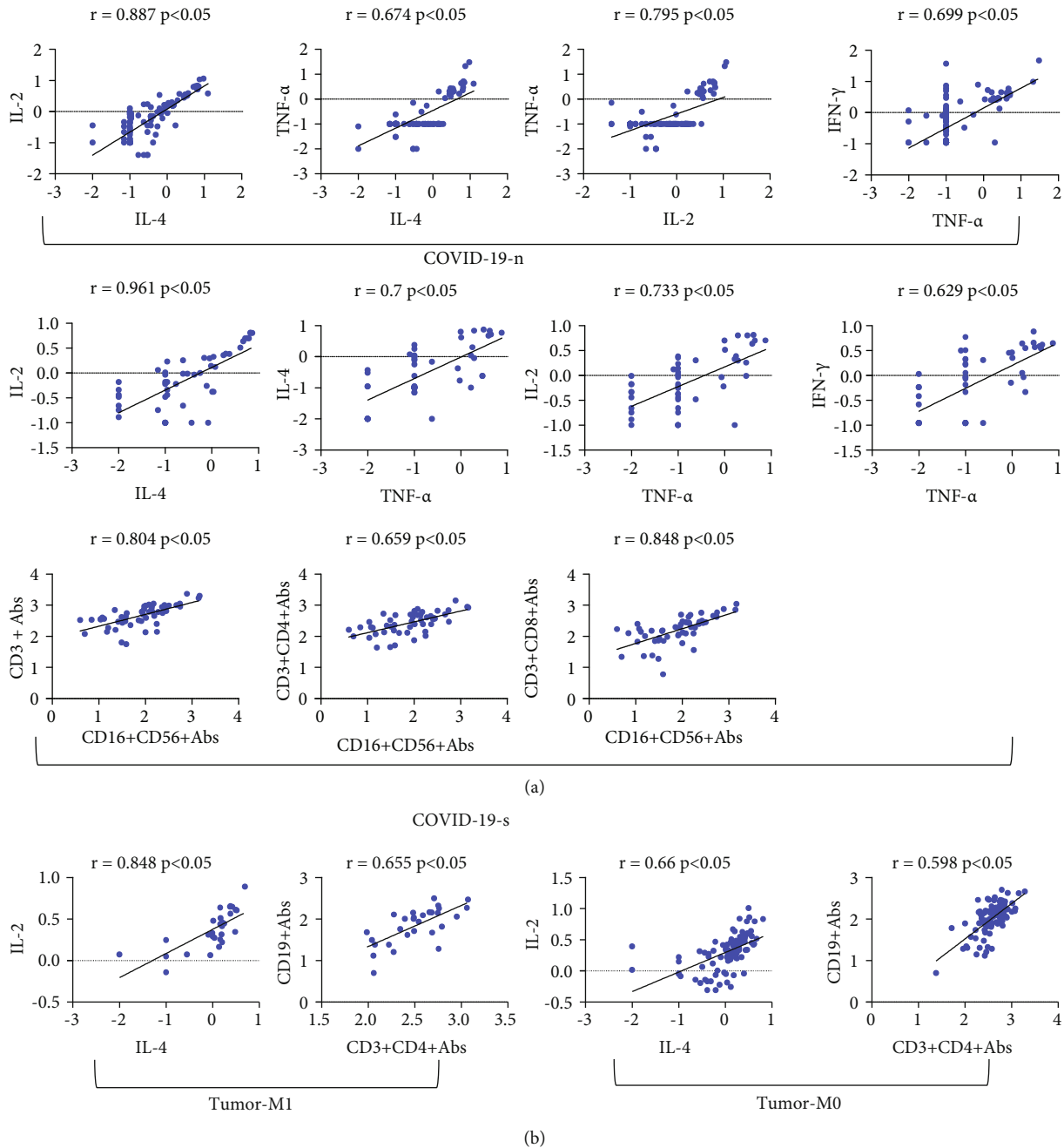
FIGURE 4: The correlation analysis of the four subgroups of patients with COVID-19 or cancer. (a) COVID-19 patients. (b) Cancer patients.

there was a good correlation between IL-2 and IL-4 in patients with COVID-19 or cancers.

TNF-α can guide circulating monocytes to the site of injury so that they can differentiate into mature macrophages [6]. Cytokines secreted by macrophages can activate NK cells, and IFN-γ produced by NK cells acts on alveolar macrophages to amplify the inflammatory response [26]. Karki et al. [27] reported that the synergistic effects of TNF-α and IFN-γ in COVID-19 patients can induce various types of cell death and tissue damage and result in a poor prognosis. In patients with severe COVID-19, we found that TNF-α was satisfactorily correlated with IL-2, IL-4, and

IFN-γ, and monocytes were negatively correlated with IL-2, IL-4, and TNF-α. In nonmetastatic cancer patients, T cells were negatively correlated with IL-6 and IL-10 and were positively correlated with IL-4 and TNF-α.

Although we conducted an analysis of different immune cells and cytokines between COVID-19 and cancers, there were some deficiencies in our study. The examination of cytokines was carried out in 2018, and there was incomplete case information for many cancer patients. Thus, only 29 metastatic patients were recruited, and they were accompanied by 93 cases with unknown metastatic status in this study. In addition, this was a single-center retrospective
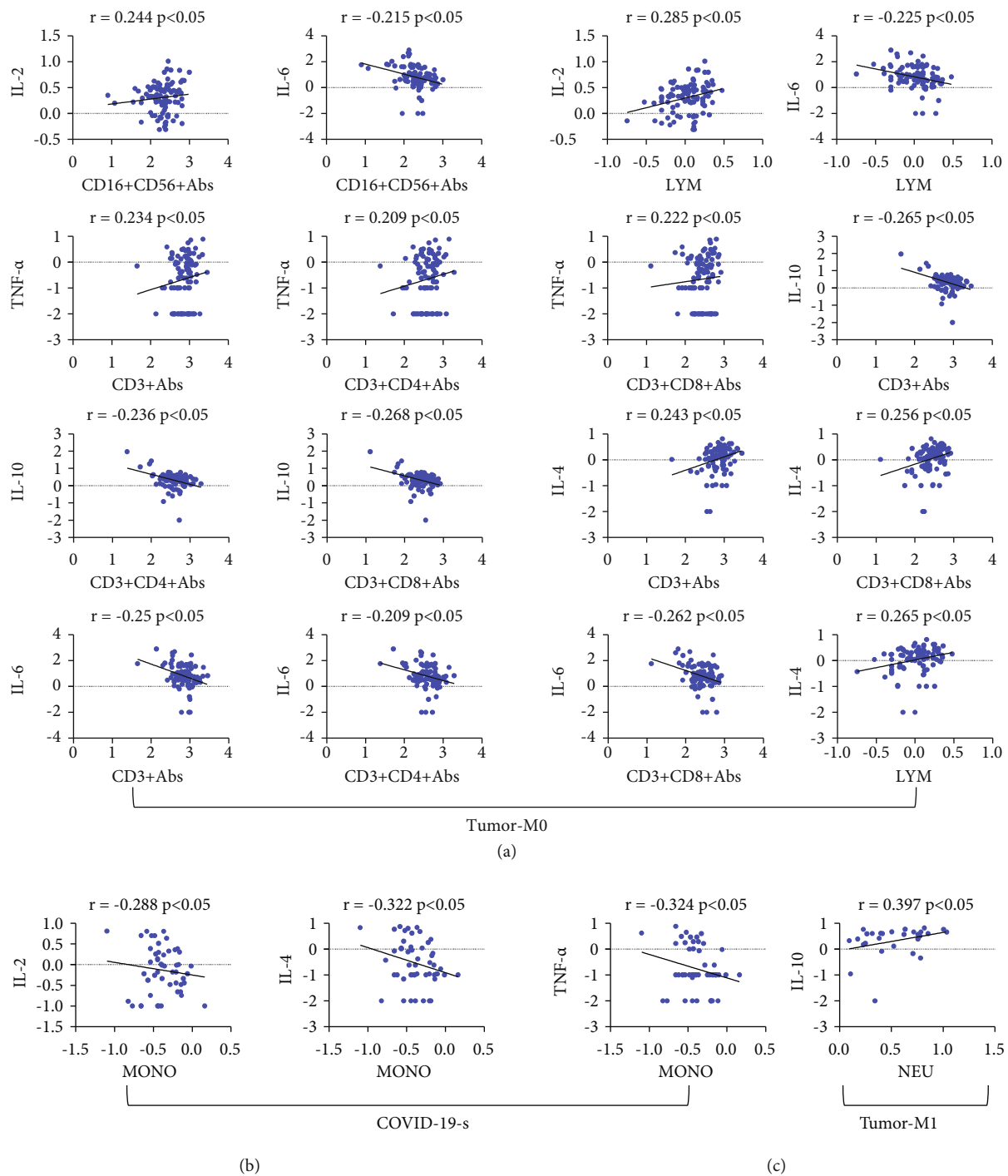
FIGURE 5: The correlation analysis between immune cells and cytokines of patients with COVID-19 or cancer. (a) Nonmetastatic cancer patients. (b) Severe COVID-19 patients. (c) Metastatic cancer patients.

study. We require data from a larger and multicenter cohort to better assess the changes in immune response after acute infection and cancer-related immune disorder.

In conclusion, both COVID-19 and cancers were associated with lymphopenia and high levels of monocytes, neutrophils, IL-6, and IL-10. IL-2 was the optimal indicator to differentiate between the COVID-19 and cancer-related immune disorder. In comparing patients with respiratory cancers, COVID-19 patients had lower levels of IL-2 and higher levels of CD3$^+$CD4$^+$ T cells and CD19$^+$ B cells, and no difference in levels of IL-6 and IL-10. In addition, there were higher correlations between IL-2 and IL-4, TNF-α and IL-2, TNF-α and IL-4, TNF-α and IFN-γ, and NK cells and T cells in COVID-19 patients, and there was a higher correlation between CD3$^+$CD4$^+$ T cells and CD19 + T cells in cancer patients.

(a)

(b)
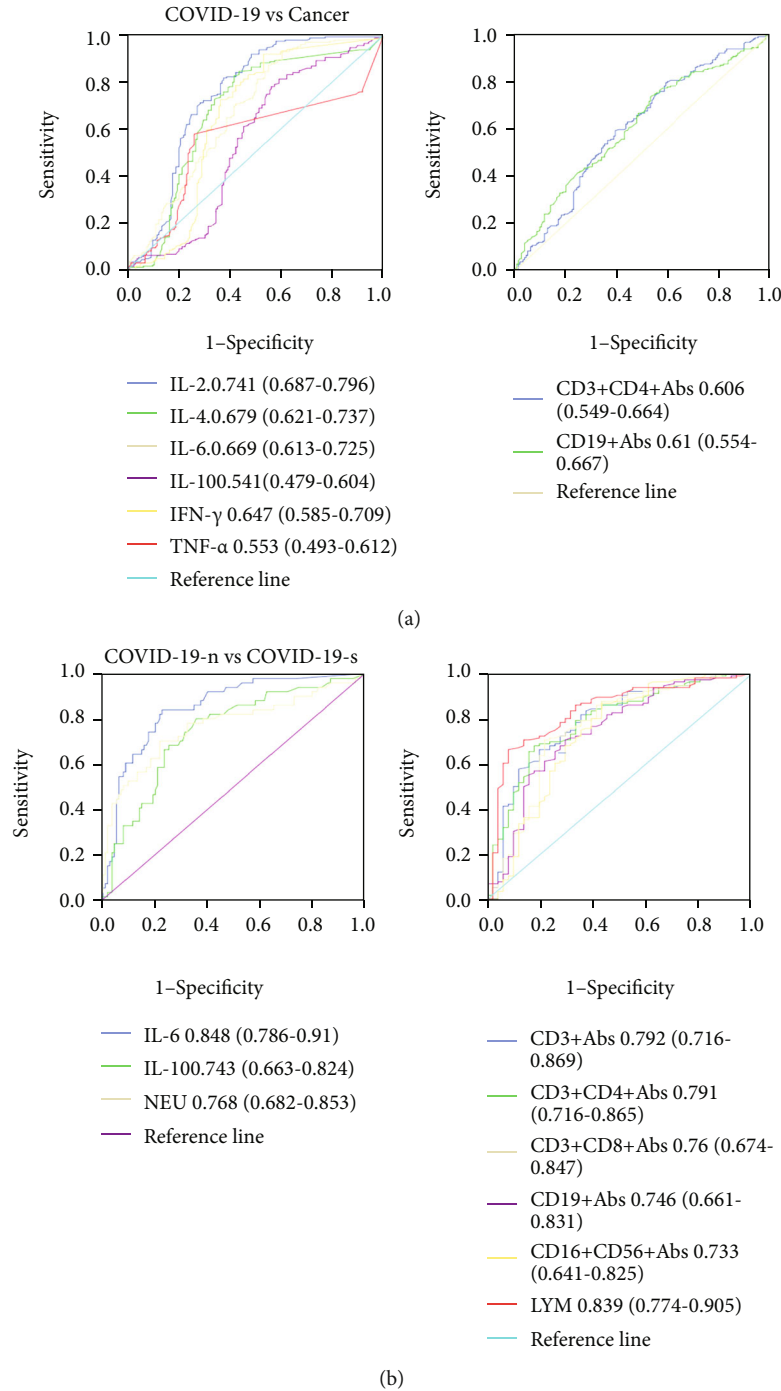
Figure 6: ROC curve analysis of immune cells and cytokines. (a) Between COVID-19 and cancer patients and (b) between severe and nonsevere COVID-19 patients.

Moreover, there were lower levels of lymphocyte subsets (CD3$^+$ T cells, CD3$^+$CD4$^+$ T cells, CD3$^+$CD8$^+$ T cells, and CD19$^+$ B cells) and NK cells and higher level of neutrophils in severe COVID-19 patients, and IL-6 exhibited the most optimal ability for differential diagnosis between severe and nonsevere COVID-19 patients. As for cancer patients, there were no significant differences in immune cells and cytokines between the metastatic and the nonmetastatic group.

Data Availability

The original contributions presented in the study are included in the article material. Further inquiries can be directed to the corresponding authors.

Conflicts of Interest

The authors declare that they have no conflicts of interest.

Authors' Contributions

Conceptualization was done by YP. Methodology was done by XZ and XJ. Formal analysis was done by XZ and LY. Investigation was done by YP and YL. Writing—original draft was done by XZ. Writing—review and editing was done by YP. Supervision was done by YP and YL. Xiaojiao Zeng and Xianghu Jiang contributed equally to this work and should be considered as co-first authors.

Acknowledgments

Supplementary Materials

Supplementary 1. Figure S1: heat maps for levels of various immune cells and cytokines in patients with COVID-19 or cancer.

Supplementary 2. Figure S2: analysis of immune cells and cytokines in different stages and differentiations of cancers. (a) Between T_{1-2} and T_{3-4} and (b) between N_{0-1} and N_{2-3} and (c) between squamous carcinoma and adenocarcinoma of respiratory cancers and (d) between M0 and M1 of respiratory and nonrespiratory cancers. (a) $CD3^+CD4^+$ Abs (left), $CD19^+$ Abs (middle), LYM (right). (b) IL-2 (left), $CD19^+$ Abs (right). (c) $CD16^+CD56^+$ Abs (left), NEU (right). (d) IL-6 (left), TNF-α (middle), $CD16^+CD56^+$ Abs (right). (e) Sex variables in different TNM stages of cancer patients.

Supplementary 3. Figure S3: ROC curve analysis of immune cells and cytokines between metastatic and nonmetastatic patients.

Supplementary 4. Table S1: stages and differentiation types of cancers.

References

[1] Coronaviridae Study Group of the International Committee on Taxonomy of Viruses, "The species _severe acute respiratory syndrome-related coronavirus_ : classifying 2019-nCoV and naming it SARS-CoV-2," *Nature Microbiology*, vol. 5, no. 4, pp. 536–544, 2020.

[2] N. Taleghani and F. Taghipour, "Diagnosis of COVID-19 for controlling the pandemic: a review of the state-of- the-art," *Biosensors & Bioelectronics*, vol. 174, p. 112830, 2021.

[3] J. Stebbing, A. Phelan, I. Griffin et al., "COVID-19: combining antiviral and anti-inflammatory treatments," *The Lancet Infectious Diseases*, vol. 20, no. 4, pp. 400–402, 2020.

[4] J. N. Gustine and D. Jones, "Immunopathology of hyperinflammation in COVID-19," *The American Journal of Pathology*, vol. 191, no. 1, pp. 4–17, 2021.

[5] H. Sung, J. Ferlay, R. L. Siegel et al., "Global cancer statistics 2020: GLOBOCAN estimates of incidence and mortality worldwide for 36 cancers in 185 countries," *CA: a cancer journal for clinicians*, vol. 71, no. 3, pp. 209–249, 2021.

[6] N. M. Iyengar, A. Gucalp, A. J. Dannenberg, and C. A. Hudis, "Obesity and cancer mechanisms: tumor microenvironment and inflammation," *Journal of Clinical Oncology*, vol. 34, no. 35, pp. 4270–4276, 2016.

[7] B. Ritter and F. R. Greten, "Modulating inflammation for cancer therapy," *The Journal of Experimental Medicine*, vol. 216, no. 6, pp. 1234–1243, 2019.

[8] F. R. Greten and S. I. Grivennikov, "Inflammation and cancer: triggers, mechanisms, and consequences," *Immunity*, vol. 51, no. 1, pp. 27–41, 2019.

[9] Y. Tan and F. Tang, "SARS-CoV-2-mediated immune system activation and potential application in immunotherapy," *Medicinal Research Reviews*, vol. 41, no. 2, pp. 1167–1194, 2021.

[10] G. Dranoff, "Cytokines in cancer pathogenesis and cancer therapy," *Nature Reviews. Cancer*, vol. 4, no. 1, pp. 11–22, 2004.

[11] E. Terpos, I. Ntanasis-Stathopoulos, I. Elalamy et al., "Hematological findings and complications ofCOVID-19," *American Journal of Hematology*, vol. 95, no. 7, pp. 834–847, 2020.

[12] Y. Tang, J. Liu, D. Zhang, Z. Xu, J. Ji, and C. Wen, "Cytokine storm in COVID-19: the current evidence and treatment strategies," *Frontiers in Immunology*, vol. 11, p. 1708, 2020.

[13] B. M. Henry, S. W. Benoit, J. Vikse et al., "The anti-inflammatory cytokine response characterized by elevated interleukin-10 is a stronger predictor of severe disease and poor outcomes than the pro-inflammatory cytokine response in coronavirus disease 2019 (COVID-19)," *Clinical Chemistry and Laboratory Medicine*, vol. 59, no. 3, pp. 599–607, 2021.

[14] E. J. Giamarellos-Bourboulis, M. G. Netea, N. Rovina et al., "Complex immune dysregulation in COVID-19 patients with severe respiratory failure," *Cell Host & Microbe*, vol. 27, no. 6, pp. 992–1000.e3, 2020.

[15] Y. Jamilloux, T. Henry, A. Belot et al., "Should we stimulate or suppress immune responses in COVID-19? Cytokine and anti-cytokine interventions," *Autoimmunity Reviews*, vol. 19, no. 7, p. 102567, 2020.

[16] Q. Li, W. Xu, W. X. Li, C. L. Huang, and L. Chen, "Dynamics of cytokines and lymphocyte subsets associated with the poor prognosis of severe COVID-19," *European Review for Medical and Pharmacological Sciences*, vol. 24, no. 23, pp. 12536–12544, 2020.

[17] H. Wu, H. Zhu, C. Yuan et al., "Clinical and immune features of hospitalized pediatric patients with coronavirus disease 2019 (COVID-19) in Wuhan China," *JAMA Network Open*, vol. 3, no. 6, article e2010895, 2020.

[18] X. Zeng, G. Liu, Y. Pan, and Y. Li, "Development and validation of immune inflammation-based index for predicting the clinical outcome in patients with nasopharyngeal carcinoma," *Journal of Cellular and Molecular Medicine*, vol. 24, no. 15, pp. 8326–8349, 2020.

[19] M. E. Shaul and Z. G. Fridlender, "Tumour-associated neutrophils in patients with cancer," *Nature Reviews. Clinical Oncology*, vol. 16, no. 10, pp. 601–620, 2019.

[20] H. Cho, Y. Seo, K. M. Loke et al., "Cancer-stimulated CAFs enhance monocyte differentiation and protumoral TAM activation via IL6 and GM-CSF secretion," *Clinical Cancer Research*, vol. 24, no. 21, pp. 5407–5421, 2018.

[21] J. A. Myers and J. S. Miller, "Exploring the NK cell platform for cancer immunotherapy," *Nature Reviews. Clinical Oncology*, vol. 18, no. 2, pp. 85–100, 2021.

[22] Y. Toyoshima, H. Kitamura, H. Xiang et al., "IL6 modulates the immune status of the tumor microenvironment to facilitate metastatic colonization of colorectal cancer cells," *Cancer Immunology Research*, vol. 7, no. 12, pp. 1944–1957, 2019.

[23] M. Saraiva, P. Vieira, and A. O'Garra, "Biology and therapeutic potential of interleukin-10," *The Journal of Experimental Medicine*, vol. 217, no. 1, 2020.

[24] W. Luo, Y. X. Li, L. J. Jiang, Q. Chen, T. Wang, and D. W. Ye, "Targeting JAK-STAT signaling to control cytokine release syndrome in COVID-19," *Trends in Pharmacological Sciences*, vol. 41, no. 8, pp. 531–543, 2020.

[25] W. J. Leonard, J. X. Lin, and J. J. O'Shea, "The γ_c family of cytokines: basic biology to therapeutic ramifications," *Immunity*, vol. 50, no. 4, pp. 832–850, 2019.

[26] C. Melenotte, A. Silvin, A. G. Goubet et al., "Immune responses during COVID-19 infection," *Oncoimmunology*, vol. 9, no. 1, p. 1807836, 2020.

[27] R. Karki, B. R. Sharma, S. Tuladhar et al., "Synergism of TNF-α and IFN-γ triggers inflammatory cell death, tissue damage, and mortality in SARS-CoV-2 infection and cytokine shock syndromes," *Cell*, vol. 184, no. 1, pp. 149–168.e17, 2021.

Research Article

Probiotics Alleviated Nonalcoholic Fatty Liver Disease in High-Fat Diet-Fed Rats via Gut Microbiota/FXR/FGF15 Signaling Pathway

Minmin Luo ⑩,[1] **Junbin Yan** ⑩,[1] **Liyan Wu** ⑩,[2] **Jinting Wu** ⑩,[1] **Zheng Chen** ⑩,[1] **Jianping Jiang** ⑩,[3,4] **Zhiyun Chen** ⑩,[1] **and Beihui He** ⑩[1]

[1]*Key Laboratory of Integrative Chinese and Western Medicine for the Diagnosis and Treatment of Circulatory Diseases of Zhejiang Province, The First Affiliated Hospital of Zhejiang Chinese Medical University, Hangzhou, 310006 Zhejiang, China*
[2]*Department of Gastroenterology, Tongde Hospital of Zhejiang Province, Hangzhou, 310012 Zhejiang, China*
[3]*Department of Pharmacy, School of Medicine, Zhejiang University City College, Hangzhou, 310015 Zhejiang, China*
[4]*Zhejiang You-du Biotech Limited Company, Quzhou, 324000 Zhejiang, China*

Correspondence should be addressed to Beihui He; graf303@sina.com

Minmin Luo and Junbin Yan contributed equally to this work.

Gut microbiota (GM) dysbiosis and bile acid (BA) metabolism disorder play an important role in the pathogenesis of nonalcoholic fatty liver disease (NAFLD). Probiotics had a beneficial effect on NAFLD, but further study is needed to explore probiotics as a potential therapeutic agent to NAFLD. The aim of this study was to investigate the regulatory effect of probiotics on gut microbiota in NAFLD rats and to explore the possible mechanism of probiotics regulating the bile acid receptor farnesoid X receptor/growth factor 15 (FXR/FGF15) signaling pathway in rats. We established a rat model of NAFLD fed with a high-fat diet (HFD) for 14 weeks, which was given different interventions (312 mg/kg/day probiotics or 10 mg/kg/day atorvastatin) from the 7th week. Serum lipids and total bile acids (TBA) were biochemically determined; hepatic steatosis and lipid accumulation were evaluated with HE staining. The expression levels of FXR, FGF15 mRNA, and protein in rat liver were detected. 16S rDNA was used to detect the changes of gut microbiota in rats. Compared with the HFD group, probiotics and atorvastatin significantly reduced serum lipids and TBA levels. And probiotics increased dramatically the expression of FXR, FGF15 mRNA, and protein in the liver. But there were no significant changes in the atorvastatin group. Probiotics and atorvastatin can upregulate the diversity of gut microbiota and downregulate the abundance of pathogenic bacteria in NAFLD model rats. In summary, probiotics alleviated NAFLD in HFD rats via the gut microbiota/FXR/FGF15 signaling pathway.

1. Introduction

Nonalcoholic liver disease (NAFLD) is the most common cause of chronic liver disease worldwide, which is predicted to become the most frequent indication for liver transplantation in the next decade [1]. NAFLD is confined to liver-related morbidity and mortality, but now, more and more evidence shows that NAFLD is a multifactorial disease. It is strongly associated with dyslipidemia, obesity, hypertension, and diabetes [2, 3]. However, the pathogenesis of NAFLD is not totally clear, and it lacks effective pharmacological treatments.

Recently, bile acid metabolism plays an essential role in regulating the absorption of food lipids and cholesterol metabolism and also participates in the balance of glucose and lipid metabolism, mainly by regulating farnesoid X receptor (FXR) and then inducing the expression of fibroblast growth factor 15 (FGF15) [4, 5]. Many studies have revealed the role of gut microbiota in the pathophysiology of NAFLD, including the dysbiosis of gut microbiota composition and abundance, which leads to the destruction of intestinal endothelial barrier function and can further induce bacterial translocation and liver inflammation [6, 7]. Therefore, gut microbiota

and bile acids play a key role in NAFLD and may be potential therapeutic targets.

Probiotics are live microorganisms present in cultured dairy products, which play a fundamentally important role in health and disease [8–10]. A study has shown that probiotics can reduce liver injury and improve liver function in patients with NAFLD [11]. Probiotics can regulate gut microbiota, enhance intestinal barrier function, regulate the immune system [12, 13], and improve liver lipid metabolism by modulating short-chain fatty acid and bile acid metabolism [14], all of which contribute to the amelioration of NAFLD.

Therefore, it is crucial to study the role of FXR and its signaling pathway in liver bile acid metabolism for exploring the pathogenesis of NAFLD and finding effective therapeutic targets. This study is aimed at studying NAFLD bile acid metabolism changes and FXR signaling pathway, exploring the effect of probiotics on the pathway, and seeking new therapy for NAFLD to provide a theoretical and experimental basis.

2. Materials and Methods

2.1. Animals. 24 male Sprague-Dawley rats (160-180 g) were purchased from Shanghai Sino-British SIPPR/BK Laboratory Animal Co. Ltd. (Shanghai, China). All rats were housed in specific pathogen-free conditions (22°C, a 12 h light/dark cycle) with ad libitum access to standard laboratory chow. All animal experiments were approved by the ethics committee of Zhejiang Chinese Medical University (no. ZSLL-2018-048), and the study was conducted following the guidelines of the NIH *Guide for the Care and Use of Laboratory Animals*.

2.2. Animal Experimental Procedures. 24 male SD rats were randomly divided into four groups ($n = 6$): a normal diet control (NC) group, a high-fat diet-fed (HFD) group, a high-fat diet-fed+probiotic treatment (HFD-P) group, and a high-fat diet-fed+atorvastatin (HFD-A) treatment. Atorvastatin has been proven to improve dyslipidemia in patients with NAFLD and improve NAFLD effectively. Thus, the atorvastatin treatment group was increased and compared with the probiotic treatment group to clearly show the effect of gut microbiota in NAFLD treatment. The rats were fed either a normal diet (10% kcal% fat LAD0011) or HFD (45 kcal% fat TP23000) (Trophic Animal Feed High-tech Co., Ltd, Nantong, China). After 6 weeks, rats in the NC and HFD groups were given normal saline. The HFD+P group rats were given 312 mg/kg/d probiotics by gavage once a day for 8 weeks (Compound Eosinophil-Lactobacillus Tablets, Tonghua Golden-Horse Pharmaceutical Industry Co., Ltd, Jilin, China; 10^7 Eosinophil-Lactobacillus per gram). Rats in the HFD+A were given 10 mg/kg/d atorvastatin by gavage once a day (Lipitor, Pfizer, Dalian, China) for 8 weeks. The clinical dosage of Compound Eosinophil-Lactobacillus Tablets is two tablets at a time for adults (0.5 g each), three times a day. After conversion, the clinical dosage of adults is 50 mg/kg/d (the adult weight is considered 60 kg). The equivalent dose for rats is 6.25 times that of adults. Therefore, each rat is best given 312 mg/kg/d probiotics. In the same way, the dose of atorvastatin in rats is calculated to be 10 mg/kg/d. The rats were sacrificed at the end of 14 weeks,

blood was taken from the abdominal vein under fasting anesthesia, and liver samples were taken.

2.3. Biochemical Analysis. Serological tests were used to detect the serum content of triglyceride (TG), cholesterol (CHOL), alanine aminotransferase (ALT), aspartate aminotransferase (AST), high-density lipoprotein (HDL), low-density lipoprotein (LDL), and total bile acid (TBA) (Nanjing Jiancheng Bioengineering Institute, Nanjing, China). The instrument is an automatic biochemistry analyzer (HITACHI, Japan).

2.4. Liver Histological Examination. The liver tissue of rats was fixed in 4% neutral-buffered formaldehyde for 24 hours, and then, hematoxylin-eosin (HE) staining was used to observe the presence of fat droplets in the liver under the microscope (Zeiss, Axio Scan Z1, Germany). The NAFLD activity score is regarded as a semiquantitative assessment of the degree of liver inflammation. NAS is calculated from the weighted sum of hepatocyte steatosis (0 to 3), lobular inflammation (0 to 3), and ballooning (0 to 2). According to the NAS, NAFLD is divided into "non-NASH" (NAS < 3), "edge NASH" (NASH = 3-4), and "definite NASH" (NAS = 5-8).

2.5. Detection and Analysis of Gut Microbiota. DNA from different faecal samples was extracted using a E.Z.N.A.® Stool DNA Kit (OMEGA Bio-Tek Inc., GA, USA) according to the manufacturer's instructions. The total DNA was eluted in 50 μL of elution buffer and stored at -80°C until measurement in the PCR. The V3-V4 hypervariable region of the 16S rDNA gene uses primers 341F (5′-CCTACGGG NGGCWGCAG-3′) and 805R (5′-GACTACHVGGGTAT CTAATCC-3′). The amplification was carried out as follows: initial denaturation at 98°C for 30 s, followed by 30 cycles of denaturation at 98°C for 10 s, annealing at 54°C for 30 s, elongation at 72°C for 45 s, and finally 72°C for 10 min. For each faecal sample, sequencing and bioinformatics were carried out by LC-Bio Technology Co., Ltd (Hangzhou, China) on the NovaSeq PE250 platform.

2.6. Real-Time qRT-PCR Analysis. Total RNA was isolated from the liver using the TaKaRa MiniBEST Universal RNA Extraction Kit (TaKaRa, Japan; cat. no. 9767) according to the manufacturer's instructions. Real-time PCR was performed using the TB Green™ Premix Ex Taq™ Kit (TaKaRa, Japan; Cat. no. RR820A) and a CFX384 Real-Time PCR system (Bio-Rad, USA). The PCR program included 1 cycle of 95°C for 3 min and 40 cycles of 95°C for 5 s and 60°C for 45 s. The specific primers used for amplification are shown in Table 1. The results were expressed by calculating the $2^{-\Delta\Delta CT}$ values, and the housekeeping gene is β-actin.

2.7. Western Blotting Analysis. The sample preparation and extraction were carried out according to the standard scheme. Total proteins were extracted from liver tissues of rats using a total protein extraction kit (KeyGENBioTECH, KGP2100, Jiangsu, China). The protein content was determined by the BCA protein assay kit (MultiSciences, 70-PQ0011, Hangzhou, China). Then, we use SDS-PAGE gel (10%) isolate proteins, and they were transferred to PVDF membranes (Bio-Rad, USA). They were blocked with 5%

TABLE 1: The specific primers used for amplification.

Name		Primers (5′ ⟶ 3′)	NCBI gene ID
β-Actin	Sense	TGCTGTCACCTTCACCGTTC	81822
	Antisense	GTCCACCGCAAATGCTTCTA	
FXR	Sense	CTCCCTGCATGACTTTGTTGTC	60351
	Antisense	AAGAGATGGGAATGTTGGCTG	
FGF15	Sense	AAGTGGAGTGGGCGTATTGT	170582
	Antisense	AGTGGACCTTCATCCGACAC	

skim milk in TBS-Tween 20 (TBST) for 1 h. The membranes were then incubated with primary antibodies overnight at 4°C. The primary antibodies are FXR monoclonal antibody, 1 : 1000 dilution (abs122163, Abisin); FGF15 monoclonal antibody, 1 : 1000 dilution (sc-398338, Santa Cruz); and β-actin monoclonal antibody, 1 : 5000 dilution (Multi Science Biotech, Cat. no. ab008). Then, the blots were incubated with the secondary antibodies HRP-conjugated goat anti-rabbit IgG (1 : 5000) dilution (Multi Science Biotech, Cat. no. GAR0072) or HRP-conjugated goat anti-mouse IgG (1 : 5000) dilution (Multi Science Biotech, Cat. no. GAM0072) for 1 h. Finally, protein expressions were detected with the enhanced chemiluminescence (ECL) method, and signals were captured with the Odyssey Fc (LI-COR, USA).

2.8. Statistical Analysis. The SPSS 26.0 software was used for statistical analysis. All quantitative data are presented as the means ± standard deviation. The significant differences between and within the different groups were examined using one-way ANOVAs, followed by Dunnett's test. Microbiome-related analysis figures were created by R software. $P < 0.05$ was considered statistically significant.

3. Results

3.1. Body Weight. In the 6th week, compared with the NC group (378.7 ± 23.1, mean ± SD), the weight of the rats fed a high-fat diet increased, but the difference was not statistically significant ($P > 0.05$) (HFD: 405.5 ± 25.0, HFD-P: 386.7 ± 16.8, HFD-A: 398.7 ± 27.6, mean ± SD). At the end of the 10th week and 14th week, compared with the HFD group, the weight of the HFD-P group and HFD-A group decreased, but the difference was not statistically significant ($P > 0.05$) (Figure 1) (NC: 444.5 ± 33.7, HFD: 456.2 ± 27.1, HFD-P: 409.6 ± 23.9, HFD-A: 428 ± 22.9, 10th week; NC: 467.8 ± 44.1, HFD: 475.2 ± 29.3, HFD-P: 422.3 ± 31.1, HFD-A: 444.7 ± 31.3, 14th week, mean ± SD).

3.2. Histology Results. HE staining showed that in the NC group, the structure of hepatic lobules was clear and complete, without lipid infiltration. In the HFD group, there were evident steatosis, fatty vacuoles, disorganized structure of hepatic cord, and infiltration of inflammatory cells. However, the liver's fatty degeneration and inflammatory cell infiltration in the HFD-P and HFD-A groups were significantly reduced. The results of NAS also showed that the hepatic inflammation in the HFD group was significantly worse than
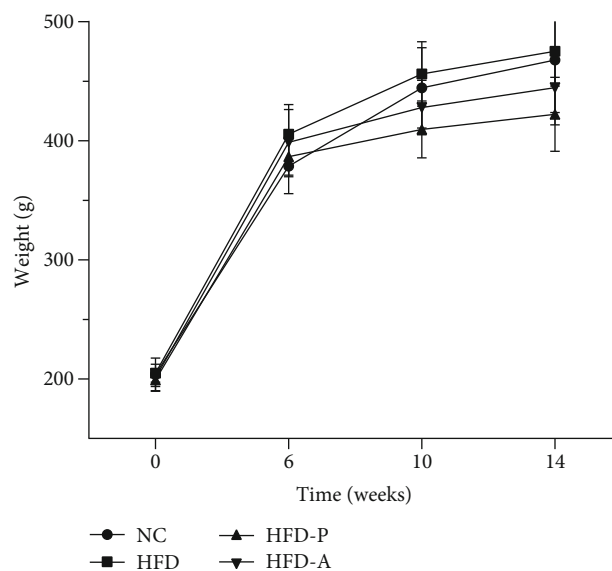
FIGURE 1: Changes in body weight.

that in the NC group. In addition, hepatic inflammation was greatly improved after treatment with probiotics (HFD-P group) and atorvastatin (HFD-A group) (Figure 2).

3.3. Biochemical Indexes. Compared with the NC group, the levels of ALT, AST, TG, CHOL, LDL, and TBA in the HFD group increased significantly ($P < 0.01$), while the level of HDL decreased, but there was no statistical difference ($P > 0.05$); compared with the HFD group, the levels of ALT, AST, TG, and TBA in the HFD-P group and HFD-A group decreased ($P < 0.05$ or $P < 0.01$), and the level of CHOL in the HFD-P group decreased ($P < 0.01$) (Table 2, Figure 3).

3.4. Probiotics Improve Gut Microbiota in HFD-Induced NAFLD. Compared with the NC group, the alpha diversity index (Shannon and Simpson) of the HFD group decreased significantly ($P < 0.01, P < 0.05$). The HFD-P group and the HFD-A group were upregulated considerably, and the bacterial diversity was increased ($P < 0.05$) (Figure 4(a)). The differences of gut microbiota among the four groups of rats can be classified by Principal Component Analysis (PCA) and Principal Coordinate Analysis (PCoA) (Figure 4(b)). The four groups can cluster on the PCoA map, and there is no overlap, indicating that there are differences in beta diversity

(a)   (b)

FIGURE 2: Effect of probiotics on the histology of liver tissue induced by HFD in NAFLD rats. (a) HE staining results: (A) NC group; (B) HFD group; (C) HFD-P group; (D) HFD-A group (×200 magnification). (b) NAFLD activity score results. $^{##}P < 0.01$ versus the NC group; $^{**}P < 0.01$ versus the HFD group.

TABLE 2: Biochemical indexes in all groups.

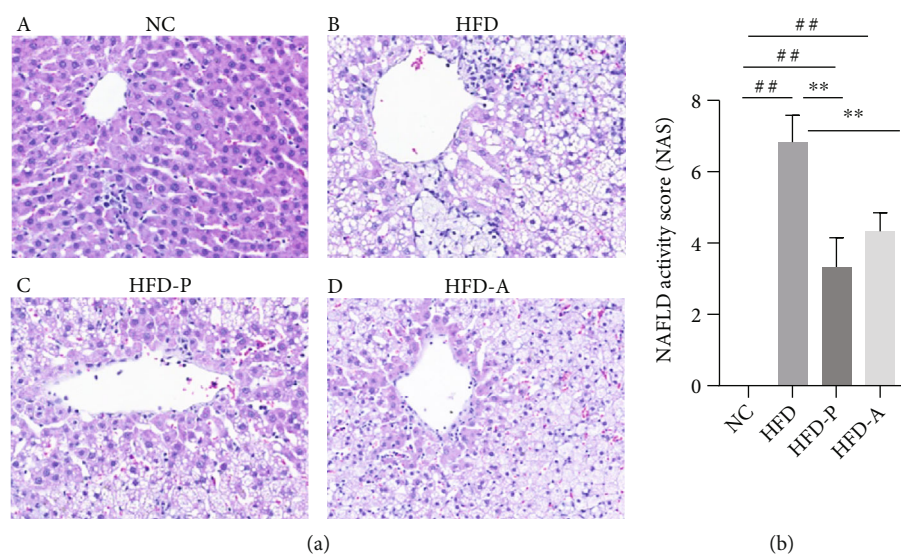|	NC	HFD	HFD-P	HFD-A
ALT (U/L)	50.4 ± 4.2	$221.6 \pm 60.8^{##}$	$161.8 \pm 40.5^{*}$	$167.0 \pm 48.1^{*}$
AST (U/L)	133.4 ± 20.7	$362.8 \pm 75.4^{##}$	$288.6 \pm 42.0^{*}$	$267.8 \pm 57.4^{**}$
HDL (mmol/L)	0.45 ± 0.07	0.42 ± 0.08	0.47 ± 0.10	0.43 ± 0.05
LDL (mmol/L)	0.16 ± 0.02	$0.42 \pm 0.12^{##}$	0.34 ± 0.09	0.44 ± 0.08
CHOL (mmol/L)	1.32 ± 0.19	$2.27 \pm 0.47^{##}$	$1.98 \pm 0.44^{**}$	2.18 ± 0.17
TG (mmol/L)	0.35 ± 0.06	$0.53 \pm 0.13^{##}$	$0.33 \pm 0.07^{**}$	$0.31 \pm 0.08^{**}$
TBA (μmol/L)	21.85 ± 10.07	$66.28 \pm 19.9^{##}$	$31.42 \pm 6.04^{**}$	$42.67 \pm 9.88^{*}$

$^{##}P < 0.01$ and $^{#}P < 0.05$ versus NC; $^{**}P < 0.01$ and $^{*}P < 0.05$ versus HFD. $n = 6$ in each group.

of gut microbiota among the four groups of rats. The separation between the four groups was far, which represents that the extent of similarity between different microbial communities is low. The HFD-P group was close to the NC group after the intervention, which stated that probiotic intervention had a certain effect on the diversity of gut microbiota in NAFLD model rats. Compared with the NC group, *Bacteroidia* was increased and *Clostridia* was decreased in the HFD group at the class level. After the intervention, *Bacteroidia* was decreased in the HFD-P group and *Clostridia* was increased in the HFD-A group. At the family level, *Porphyromonadaceae* was decreased in the HFD group, the HFD-P group, and the HFD-A group, while *Desulfovibrionaceae was* increased in the HFD-P group and the HFD-A groups (Figure 4(c)). These results indicate that probiotics and atorvastatin can upregulate the diversity of gut microbiota and downregulate the abundance of pathogenic bacteria in NAFLD model rats, improving the imbalance of gut microbiota.

3.5. Effects of Probiotics on the Expression of FXR/FGF15 in the Liver of NAFLD Rats. The expression of FXR and FGF15 mRNA in liver tissue of the HFD group was signifi-

cantly lower than that of the NC group ($P < 0.01$), and after probiotic intervention, the expression of FXR and FGF15 mRNA was increased dramatically than the HFD group ($P < 0.05$). There was no significant difference between the HFD-A group and the HFD group after atorvastatin intervention ($P > 0.05$). The protein expression of FXR and FGF15 in liver tissue of the HFD group was significantly lower than that of the NC group ($P < 0.05, P < 0.01$). After probiotic intervention, FGF15 was markedly higher than that of the HFD group ($P < 0.01$), and there was no significant difference in FXR ($P > 0.05$). There was no significant difference between the HFD-A group and the HFD group ($P > 0.05$) (Figure 5).

4. Discussion

Emerging evidence has suggested that bile acid metabolism is closely associated with NAFLD [15, 16]. Bile acids are important signaling molecules that participate in glycolipid metabolism and energy metabolism and modulate inflammation in enterohepatic circulation and peripheral organs [17, 18].
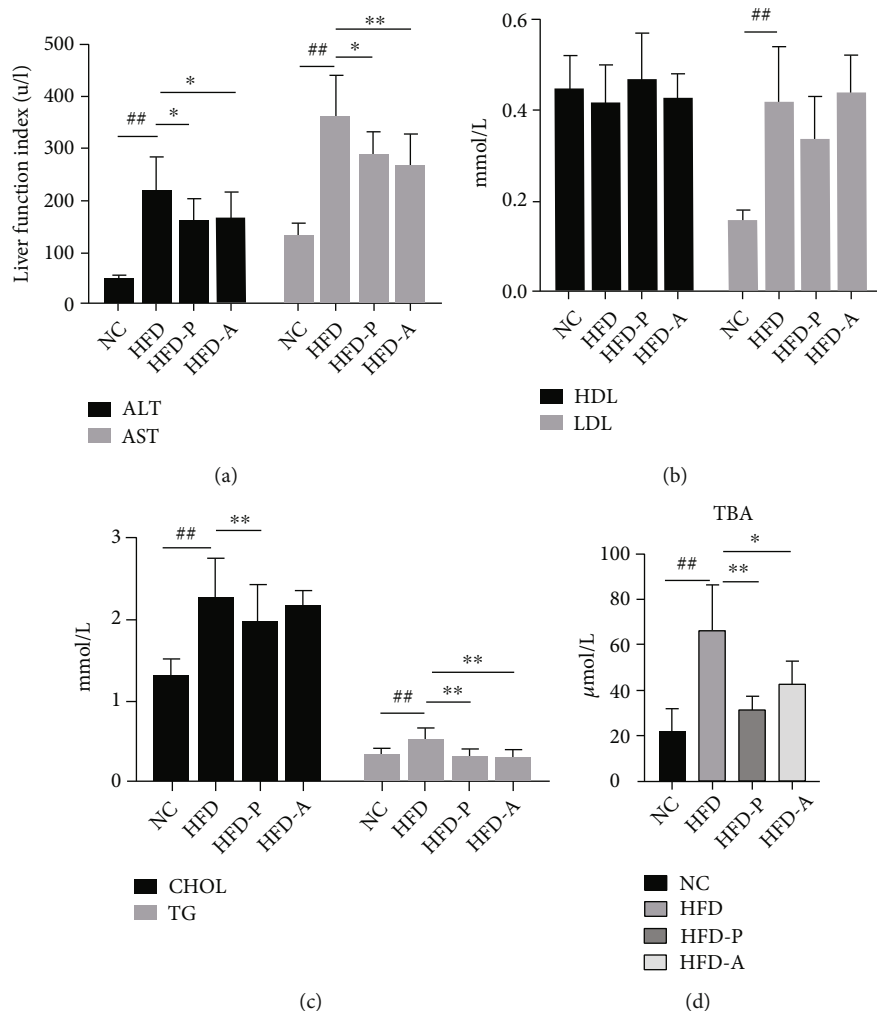
(a)

(b)

(c)

(d)

FIGURE 3: Biochemical index changes in all groups: (a) the levels of ALT and AST; (b) the levels of HDL and LDL; (c) the levels of CHOL and TG; (d) the level of TBA. $^{#}P < 0.05$ and $^{##}P < 0.01$ versus the NC group; $^{*}P < 0.05$ and $^{**}P < 0.01$ versus the HFD group.

Some studies have shown that high-fat diet (HFD) can change the composition of gut microbiota resulting in loss of commensal bacteria, leading to low-grade inflammation (LGI) and NAFLD [19, 20]. The composition of the bile acid (BA) pool is modified by gut microbiota. Perturbations of gut microbiota shape the BA composition, which, in turn, may alter essential BA signaling and affect host metabolism [21]. Bile acids are endogenous ligands, which can activate nuclear receptors, such as farnesoid X receptor (FXR). In the liver, FXR regulates cholesterol metabolism by regulating the expression of cholesterol 7α-hydroxylase (CYP7A1). In intestinal epithelial cells, activated FXR can induce the synthesis of fibroblast growth factor 15/19 (rat/human), which inhibits the expression of CYP7A1 to limit the synthesis of bile acids [22].

Clinical and animal experiments have proved that probiotics can improve the imbalance of gut microbiota and intestinal inflammation [23, 24]. Many types of probiotics were studied for NAFLD treatment; the most common include *Lactobacillus* and *Bifidobacteria*. The mechanism mainly includes improving transaminase, liver steatosis, reducing liver inflammation, and regulating gut microbiota

[25]. This study is aimed at targeting probiotic (Eosinophil-Lactobacillus) intervention to regulate the gut microbiota-FXR-FGF15 axis and improve HFD-induced NAFLD in rat. This work will provide experimental basis for probiotic monotherapy or combination therapy in the treatment of NAFLD.

In this study, a NAFLD rat model was established by feeding rats with high-fat diet for 6 weeks. Compared with the NC group, the serum levels of ALT, AST, TG, CHOL, and LDL were increased, and HDL in the HFD group was decreased. The content of TBA in serum increased significantly. Meanwhile, HE staining has shown that the structure of hepatic lobules was clear and complete, without lipid infiltration in the NC group. In the HFD group, there were obvious steatosis, fatty vacuoles, disorganized structure of hepatic cord, and infiltration of inflammatory cells. These findings indicated that the lipid metabolism and bile acid metabolism were disordered, and the NAFLD model was successfully established. Compared with the HFD group, the levels of ALT, AST, TG, CHOL, and TBA in the HFD-P group and HFD-A group were lower. The levels of LDL were lower, and the levels of HDL were higher. However, there was no

Venn diagram of HF_A_vs_HF_P_vs_HF_vs_control
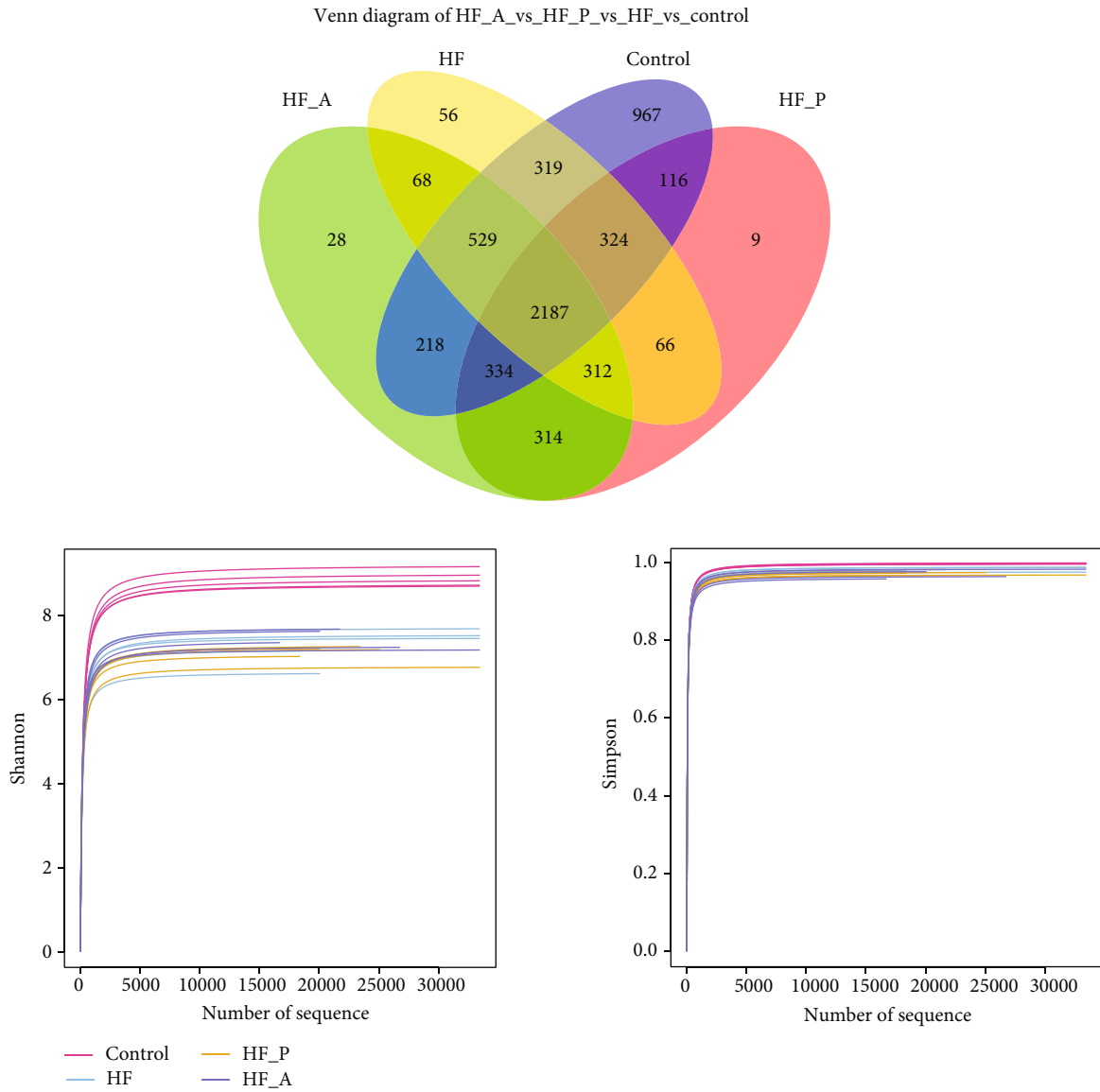
(a)

Figure 4: Continued.
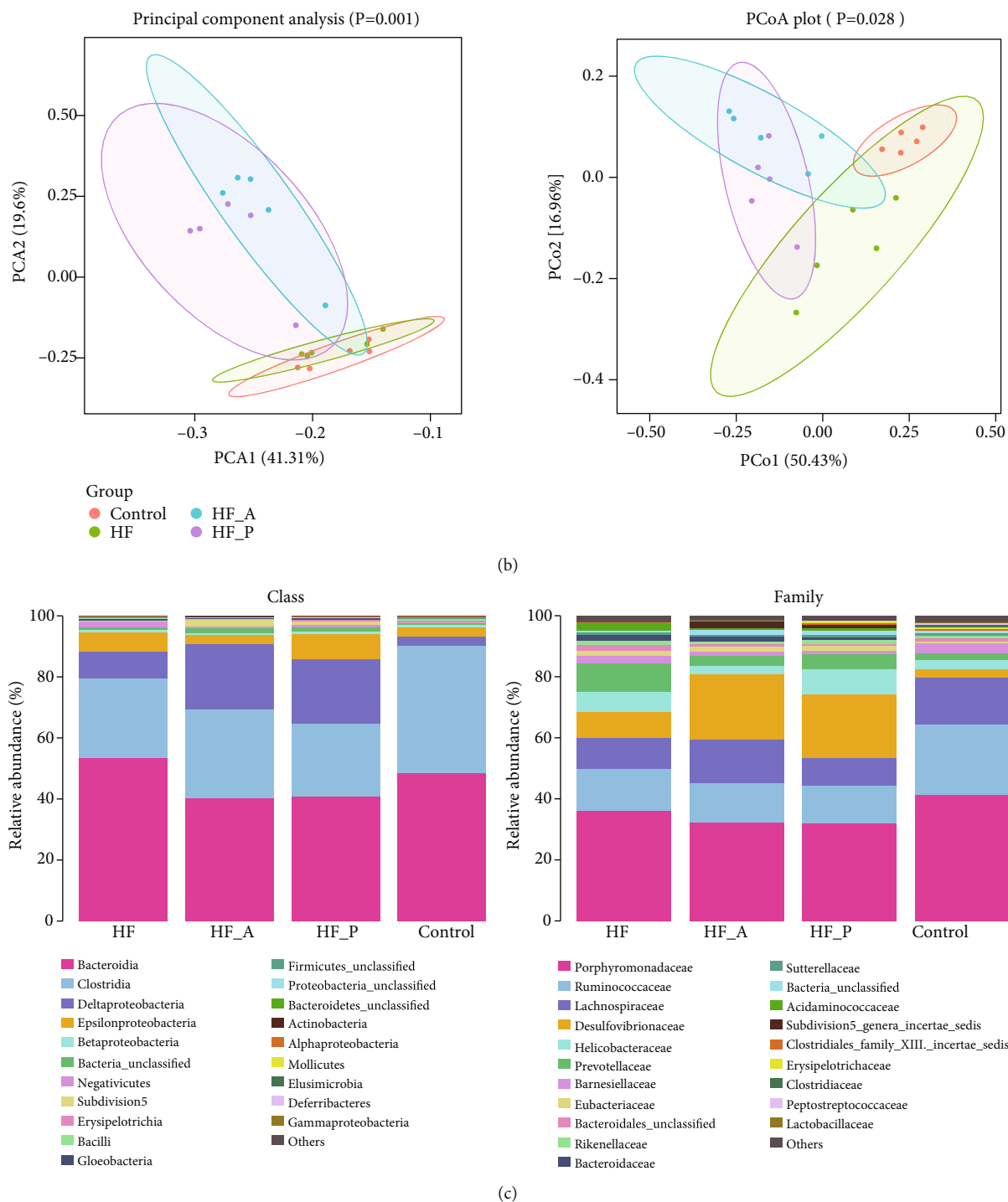
FIGURE 4: Probiotics improve gut microbiota in HFD-induced NAFLD: (a) Venn diagram, Shannon, and Simpson; (b) PCA and PCoA; (c) relative abundance of four groups in class and family level.

statistical difference, suggesting that probiotics and statins have a particular role in protecting the liver and regulating lipid and bile acid metabolism.

Gut microbiota is closely related to bile acid metabolism. The main pathway to regulate bile acid metabolism is hydrolysis combined with bile acid, which makes free bile acid dehydroxylation and complete modification [26]. In this study, we analyzed the changes of gut microbiota in four

groups. At the phylum level, Bacteroidia was increased, and Clostridia was decreased in the HFD group. The phylum of Bacteroidia was reduced in the HFD-P group and raised in the HFD-A group after intervention. At the family level, Porphyromonadaceae was decreased in the HFD group, the HFD-P group, and the HFD-A group, while Desulfovibrionaceae was increased in the HFD-P group and the HFD-A group. These results indicate that probiotics and atorvastatin

(a)

(b)
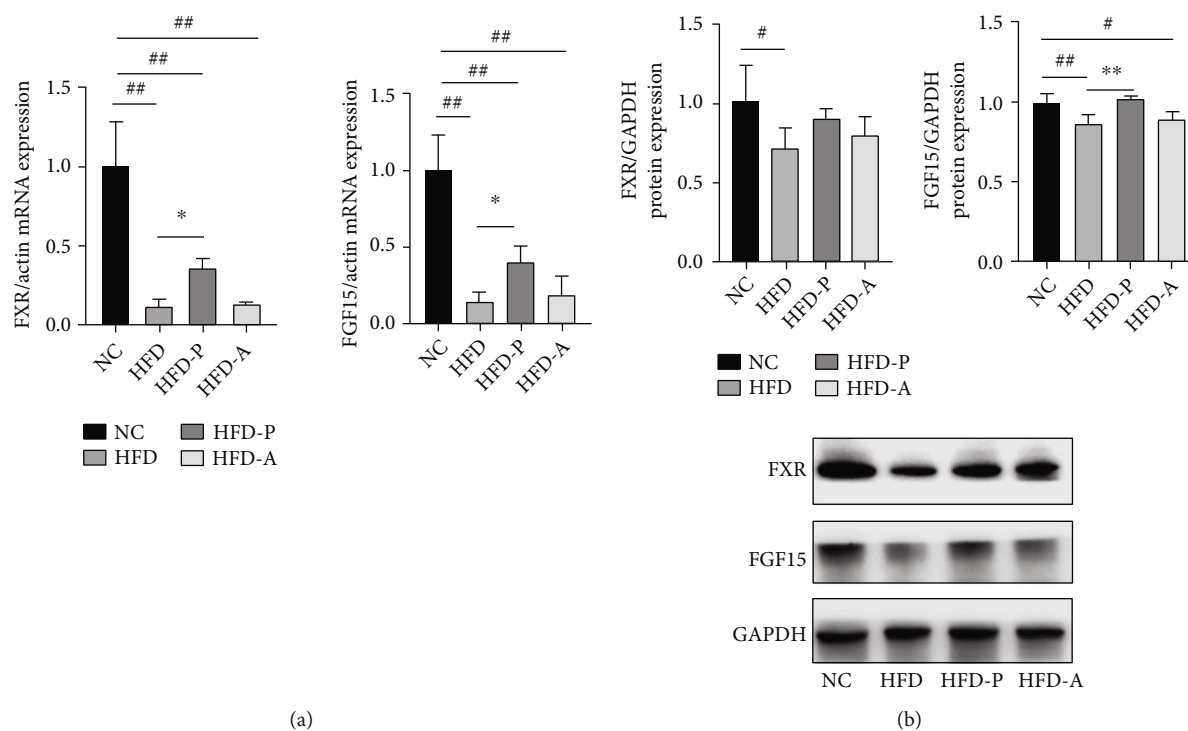
Figure 5: Effects of probiotics on the expression of FXR/FGF15 in the liver of NAFLD rats: (a) the expression of FXR and FGF15 in the liver of NAFLD rats; (b) Western blot for FXR and FGF15 in the liver of NAFLD rats. $^#P < 0.05$ and $^{##}P < 0.011$ versus the NC group; $^*P < 0.05$ and $^{**}P < 0.01$ versus the HFD group.

can upregulate gut microbiota diversity and downregulate the abundance of pathogenic bacteria in NAFLD model rats, improving gut microbiota dysbiosis.

FXR/FGF-15 is an adverse feedback regulation pathway of bile acid synthesis; FXR agonist regulated faecal bile acid levels in probiotic-treated mice [27]. In our report, the mRNA and protein expressions of FXR and FGF15 in liver tissues in the HFD model group were significantly lower than those in the NC group. After probiotic treatment, the mRNA and/or protein expressions of FXR and FGF15 were substantially higher than those in the HFD group, indicating that probiotics may affect bile acid metabolism by upregulating the expression of the FXR/FGF15 pathway. The improvement effect of atorvastatin was not noticeable.

5. Conclusion

In conclusion, our study demonstrated that probiotics had a protective effect against NAFLD in a rat model; its treatment significantly ameliorated the liver pathology injuries and serum lipid profiles and alleviated hepatic steatosis in HFD diet-fed rats; probiotics may affect bile acid metabolism by upregulating the expression of the FXR/FGF15 pathway and improving the gut microbiota dysbiosis. In addition, these protective mechanisms of probiotics on NAFLD may be related to a reduction in blood lipids, improved liver pathology, and increased bile acid receptor expression via the gut microbiota/FXR/FGF15 signaling pathway.

Abbreviations

ALT: Alanine aminotransferase
AST: Aspartate aminotransferase
CHOL: Cholesterol
CYP7A1:   Cholesterol 7α-hydroxylase
FGF15:   Fibroblast growth factor 15
FXR: Farnesoid X receptor
HDL: High-density lipoprotein
HE: Hematoxylin-eosin
HFD: High-fat diet
LDL: Low-density lipoprotein
LGI: Low-grade inflammation
NAFLD: Nonalcoholic fatty liver disease
TBA: Total bile acid
TG: Triglyceride
PCA: Principal Component Analysis
PCoA: Principal Coordinate Analysis.

Data Availability

The data in this study is available from the corresponding author upon reasonable request.

Conflicts of Interest

The authors declare that there is no conflict of interest regarding the publication of this article.

Authors' Contributions

He BH and Chen ZY designed the study and contributed to the writing of the manuscript; Luo MM, Yan JB, Wu JT, and Chen Z performed the experiment and revised the manuscript; and Wu LY and Jiang JP analyzed the data. All authors read and approved the final manuscript. Minmin Luo and Junbin Yan are co-first author. Minmin Luo and Junbin Yan contributed equally to this work.

Acknowledgments

References

[1] S. L. Attia, S. Softic, and M. Mouzaki, "Evolving role for pharmacotherapy in NAFLD/NASH," *Clinical and Translational Science*, vol. 14, no. 1, pp. 11–19, 2021.

[2] M. A. Konerman, J. C. Jones, and S. A. Harrison, "Pharmacotherapy for NASH: current and emerging," *Journal of Hepatology*, vol. 68, no. 2, pp. 362–375, 2018.

[3] P. Kasper, A. Martin, S. Lang et al., "NAFLD and cardiovascular diseases: a clinical review," *Clinical research in cardiology : official journal of the German Cardiac Society*, vol. 110, no. 7, pp. 921–937, 2021.

[4] J. D. Schumacher and G. L. Guo, "Pharmacologic modulation of bile acid-FXR-FGF15/FGF19 pathway for the treatment of nonalcoholic steatohepatitis," *Handbook of Experimental Pharmacology*, vol. 256, pp. 325–357, 2019.

[5] J. Schmitt, B. Kong, B. Stieger et al., "Protective effects of farnesoid X receptor (FXR) on hepatic lipid accumulation are mediated by hepatic FXR and independent of intestinal FGF15 signal," *Liver International : official journal of the International Association for the Study of the Liver*, vol. 35, no. 4, pp. 1133–1144, 2015.

[6] J. Mouries, P. Brescia, A. Silvestri et al., "Microbiota-driven gut vascular barrier disruption is a prerequisite for non- alcoholic steatohepatitis development," *Journal of Hepatology*, vol. 71, no. 6, pp. 1216–1228, 2019.

[7] Z. Safari and P. Gérard, "The links between the gut microbiome and non-alcoholic fatty liver disease (NAFLD)," *Cellular and Molecular Life Sciences : CMLS*, vol. 76, no. 8, pp. 1541–1558, 2019.

[8] E. S. Lee, E. J. Song, Y. D. Nam, and S. Y. Lee, "Probiotics in human health and disease: from nutribiotics to pharmabiotics," *Journal of microbiology (Seoul, Korea)*, vol. 56, no. 11, pp. 773–782, 2018.

[9] S. K. Kim, R. B. Guevarra, Y. T. Kim et al., "Role of probiotics in human gut microbiome-associated diseases," *Journal of Microbiology and Biotechnology*, vol. 29, no. 9, pp. 1335–1340, 2019.

[10] Z. Zhou, X. Chen, H. Sheng et al., "Engineering probiotics as living diagnostics and therapeutics for improving human health," *Microbial Cell Factories*, vol. 19, no. 1, p. 56, 2020.

[11] C. Loguercio, A. Federico, C. Tuccillo et al., "Beneficial effects of a probiotic VSL#3 on parameters of liver dysfunction in chronic liver diseases," *Journal of Clinical Gastroenterology*, vol. 39, no. 6, pp. 540–543, 2005.

[12] P. A. Bron, M. Kleerebezem, R. J. Brummer et al., "Can probiotics modulate human disease by impacting intestinal barrier function?," *The British Journal of Nutrition*, vol. 117, no. 1, pp. 93–107, 2017.

[13] A. Raheem, L. Liang, G. Zhang, and S. Cui, "Modulatory effects of probiotics during pathogenic infections with emphasis on immune regulation," *Frontiers in Immunology*, vol. 12, article 616713, 2021.

[14] J. M. Natividad, B. Lamas, H. P. Pham et al., "Bilophila wadsworthia aggravates high fat diet induced metabolic dysfunctions in mice," *Nature Communications*, vol. 9, no. 1, p. 2802, 2018.

[15] N. Jiao, S. S. Baker, A. Chapa-Rodriguez et al., "Suppressed hepatic bile acid signalling despite elevated production of primary and secondary bile acids in NAFLD," *Gut*, vol. 67, no. 10, pp. 1881–1891, 2018.

[16] O. Chávez-Talavera, A. Tailleux, P. Lefebvre, and B. Staels, "Bile acid control of metabolism and inflammation in obesity, type 2 diabetes, dyslipidemia, and nonalcoholic fatty liver disease," *Gastroenterology*, vol. 152, no. 7, pp. 1679–1694.e3, 2017.

[17] F. J. Gonzalez, C. Jiang, and A. D. Patterson, "An intestinal microbiota-farnesoid X receptor axis modulates metabolic disease," *Gastroenterology*, vol. 151, no. 5, pp. 845–859, 2016.

[18] S. Carbajo-Pescador, D. Porras, M. V. García-Mediavilla et al., "Beneficial effects of exercise on gut microbiota functionality and barrier integrity, and gut-liver axis crosstalk in anin vivomodel of early obesity and NAFLD," *Disease Models & Mechanisms*, vol. 12, no. 5, 2019.

[19] C. Leung, L. Rivera, J. B. Furness, and P. W. Angus, "The role of the gut microbiota in NAFLD," *Nature Reviews Gastroenterology & Hepatology*, vol. 13, no. 7, pp. 412–425, 2016.

[20] J. Chen and L. Vitetta, "Gut microbiota metabolites in NAFLD pathogenesis and therapeutic implications," *International Journal of Molecular Sciences*, vol. 21, no. 15, p. 5214, 2020.

[21] M. Wei, F. Huang, L. Zhao et al., "A dysregulated bile acid-gut microbiota axis contributes to obesity susceptibility," *EBioMedicine*, vol. 55, article 102766, 2020.

[22] Y. Duan, F. Zhang, W. Yuan et al., "Hepatic cholesterol accumulation ascribed to the activation of ileum Fxr-Fgf15 pathway inhibiting hepatic Cyp7a1 in high-fat diet-induced obesity rats," *Life Sciences*, vol. 232, article 116638, 2019.

[23] N. Kobyliak, L. Abenavoli, G. Mykhalchyshyn et al., "A multistrain probiotic reduces the fatty liver index, cytokines and aminotransferase levels in NAFLD patients: evidence from a randomized clinical trial," *Journal of Gastrointestinal and Liver Diseases*, vol. 27, no. 1, pp. 41–49, 2019.

[24] N. Kobyliak, L. Abenavoli, T. Falalyyeyeva, and T. Beregova, "Efficacy of probiotics and smectite in rats with non-alcoholic fatty liver disease," *Annals of Hepatology*, vol. 17, no. 1, pp. 153–161, 2018.

[25] G. Paolella, C. Mandato, L. Pierri, M. Poeta, M. di Stasi, and P. Vajro, "Gut-liver axis and probiotics: their role in non-

alcoholic fatty liver disease," *World Journal of Gastroenterology*, vol. 20, no. 42, pp. 15518–15531, 2014.

[26] O. Ramírez-Pérez, V. Cruz-Ramón, P. Chinchilla-López, and N. Méndez-Sánchez, "The role of bile acids in glucose metabolism and their relation with diabetes," *Annals of Hepatology*, vol. 16, Suppl. 1: s3-105., pp. s15–s20, 2017.

[27] C. Degirolamo, S. Rainaldi, F. Bovenga, S. Murzilli, and A. Moschetta, "Microbiota modification with probiotics induces hepatic bile acid synthesis via downregulation of the Fxr-Fgf15 axis in mice," *Cell Reports*, vol. 7, no. 1, pp. 12–18, 2014.

Research Article

Neuroprotective Effect of Taurine against Cell Death, Glial Changes, and Neuronal Loss in the Cerebellum of Rats Exposed to Chronic-Recurrent Neuroinflammation Induced by LPS

Samara P. Silva,[1] **Adriana M. Zago** [iD](,[1] **Fabiano B. Carvalho** [iD](,[1] **Lucas Germann** [iD](,[1]
Gabriela de M. Colombo,[1] **Francine L. Rahmeier** [iD](,[1] **Jessié M. Gutierres** [iD](,[1]
Cristina R. Reschke [iD](,[2,3] **Margarete D. Bagatini** [iD](,[4] **Charles E. Assmann** [iD](,[5]
and Marilda da C. Fernandes [iD][1]

[1]*Pathology Research Laboratory, Federal University of Health Sciences of Porto Alegre, Sarmento Leite 245, CEP 90050-170 Porto Alegre, RS, Brazil*
[2]*School of Pharmacy and Biomolecular Sciences, RCSI University of Medicine and Health Sciences, Dublin, D02 YN77, Ireland*
[3]*FutureNeuro, The Science Foundation Ireland Research Centre for Chronic and Rare Neurological Diseases, RCSI University of Medicine and Health Sciences, Dublin, D02 YN77, Ireland*
[4]*Graduate Program in Medical Sciences, Federal University of Fronteira Sul, Chapecó, SC, Brazil*
[5]*Postgraduate Program in Biological Sciences: Toxicological Biochemistry, Federal University of Santa Maria, Santa Maria, RS, Brazil*

Correspondence should be addressed to Fabiano B. Carvalho; carvalhofb.bio@gmail.com
and Marilda da C. Fernandes; marneuro@ufcspa.edu.br

The present study investigated the neuroprotective effect of taurine against the deleterious effects of chronic-recurrent neuroinflammation induced by LPS in the cerebellum of rats. Adult male *Wistar* rats were treated with taurine for 28 days. Taurine was administered at a dose of 30 or 100 mg/kg, by gavage. On days 7, 14, 21, and 28, the animals received LPS (250 μg/kg) intraperitoneally. The vehicle used was saline. The animals were divided into six groups: vehicle, taurine 30 mg/kg, taurine 100 mg/kg, LPS, LPS *plus* taurine 30 mg/kg, and LPS *plus* taurine 100 mg/kg. On day 29, the animals were euthanized, and the cerebellum was removed and prepared for immunofluorescence analysis using antibodies of GFAP, NeuN, CD11b, and cleaved caspase-3. LPS group showed a reduction in the immunoreactivity of GFAP in the *arbor vitae* and medullary center and of NeuN in the granular layer of the cerebellar cortex. LPS increased the immunoreactivity of CD11b in the *arbor vitae* and in the medullary center. Taurine protected against these effects induced by LPS in immunoreactivity of GFAP, NeuN, and CD11b, with the 100 mg/kg dose being the most effective. LPS induced an increase in the number of positive cleaved caspase-3 cells in the Purkinje cell layers, granular layer, *arbor vitae*, and medullary center. Taurine showed its antiapoptotic activity by reducing the cleaved caspase-3 cells in relation to the LPS group. Here, a potential neuroprotective role of taurine can be seen since this amino acid was effective in protecting the cerebellum of rats against cell death and changes in glial and neuronal cells in the face of chronic-recurrent neuroinflammation.

1. Introduction

Neurological and neurodegenerative diseases are devastating conditions that can affect different brain structures, including the cerebellum [1]. The cerebellum is a central brain structure deeply integrated into major loops with the cerebral cortex, brainstem, and spinal cord and is essential for the performance of smooth and accurate goal-directed movements, making postural adjustments to maintain balance and also learning new motor skills [2–4]. New evidence points to the

role of the cerebellum in almost all neurological functions, including cognitive, emotional-social-psychological process, and lesions of its different parts affect each of these domains [5–7].

Neuroinflammation is considered a hallmark of brain diseases [8]. It is characterized by an increase of proinflammatory mediators and in the quantity of apoptotic neurons [9, 10] and often accompanies and/or precedes the development of pathologies such as ataxia, Parkinson's and Alzheimer's diseases [11], and epilepsy [12]. An important tool to mimic neuroinflammation *in vivo* is the administration of lipopolysaccharide (LPS), a molecule present in the outer membrane of Gram-negative bacteria. LPS causes an immediate systemic inflammatory response mainly by activating the toll-like receptor (TLR) 4, although there is also evidence of its interaction with transient *receptor* potential- (TRP-) like channels [13, 14]. Generally, LPS is used in order to stimulate glial cells, mainly microglia. However, astrocytes and some populations of neurons also express TLR4 receptors, becoming a target of this toxin, either by direct or indirect mechanisms [15–19]. Notably, microglial cells and macrophages may increase their activity mediated by cytokines and chemokines, such as tumor necrosis factor alpha (TNF-α), interleukin- (IL-) 1β, and nuclear factor-kappa B (NF-$\kappa\beta$) [9, 20–22].

The use of nutraceuticals has gained predominance in recent years. For decades, nutritional errors have been attributed to the onset of chronic diseases, and an adequate diet or replacement of nutrients may be the key to a good quality of life. Taurine (2-aminoethanesulfonic acid) is a free amino acid commonly found in human tissues [23–26], which can be synthesized in the body from the amino acids methionine and cysteine [27, 28]. Another source of taurine is diet since this amino acid is absorbed from foods that include meat, nuts, seafood, beans, milk, and their derivatives [26]. Taurine acts as Anti-inflammatory agent suppressing inducible nitric oxide synthase (iNOS), cyclo-oxygenase 2 (COX-2), and prostaglandin E2 expression and has inhibitory effects against the NF-$\kappa\beta$ p65 and NF-κB DNA-binding activity on exposed macrophages to the LPS [29]. In the CNS, it regulates ion channels significantly influencing neuronal activity [23–26]. It has been suggested that taurine supplementation to antiseizure drugs may be a promising approach [30].

In the CNS, the upregulation of taurine gene 1 attenuates inflammation via targeting NF-κB1/p50 in a model to multiple sclerosis [31]. Taurine has the ability to neutralize the deleterious effects caused by reactive species and regular pathways of apoptosis in neurons and astrocytes, protecting them from cell death [32–34]. Furthermore, taurine effectively maintains neurogenesis in subgranular zone (SGZ) and attenuates the increase in hippocampal microgliosis and peripheral proinflammatory cytokines induced by LPS [35].

Based on this evidence, we designed a study to assess whether supplementation with taurine attenuates glial activation, neuronal death, and apoptosis in the cerebellum of rats exposed to LPS-induced chronic-recurrent neuroinflammation.

2. Materials and Methods

2.1. Chemicals. Lipopolysaccharides from *Escherichia coli* (055:B5) and taurine (TAU, ≥99%, T0625-500G) were obtained from Sigma-Aldrich Chemical Co. (St. Louis, MO, USA). All other reagents used in the experiments were of analytical grade and of highest purity.

2.2. Animals. Male adult *Wistar* rats ($n = 48$) weighing 300 g on average, from the local breeding colony of Universidade Federal de Ciências da Saúde de Porto Alegre (UFCSPA, Brazil), were used. All procedures were approved by the Ethics Committee of UFCSPA (Protocol 192/16, Identification code: 488/16). The animals were maintained in the Central Animal House of the UFCSPA in colony cages at an ambient temperature of $23 \pm 2°C$ and relative humidity of 45–55% with 12 h light/dark cycles. The animals had free access to a standard rodent pellet diet and water *ad libitum*.

2.3. Experimental Protocol

2.3.1. Treatments. Rats were treated by gavage (1 ml/kg) with taurine in the doses of 30 and 100 mg/kg body weight, previously dissolved in saline during 28 days (at 9 : 00 am). The doses were chosen based on a previous study by our research group [34]. LPS was dissolved in saline, and the selected dose was 250 μg/kg as previously described [9, 36], and this toxin was administered intraperitoneally (i.p.) on days 7, 14, 21, and 28 (mimicking a chronic-recurrent neuroinflammation; [37]). A total of 4 administrations were performed. The control groups received only the vehicle (1 ml/kg of saline, i.p.). Rats were randomly distributed into six groups: vehicle, taurine 30 mg/kg (TAU30), taurine 100 mg/kg (TAU100), LPS, LPS *plus* taurine 30 mg/kg (LPS30), and LPS *plus* taurine 100 mg/kg (LPS100). Further information can be viewed in the experimental design (Figure 1(a)).

2.4. Preparation of Samples for Immunofluorescence Analysis. On day 29, the animals were deeply anesthetized with an i.p. injection of ketamine (80 mg/kg; Syntech) and xylazine (5 mg/kg; Syntech 2%) and transcardially perfused with saline 0.9% (during 10 min) and 4% paraformaldehyde (PFA, during 30 min) in 1% phosphate-buffered saline (PBS at pH 7.4). The cerebellums were postfixed in 4% PFA (24 hours), transferred to a solution of 30% sucrose in PBS-1% until total submersion [38]. Then, the frozen fixed cerebellums were sectioned (5 and 16 μm coronal sections) using a cryostat Leica CM3050S (Leica Microsystem, German). Next, the sections were mounted on slides coated with 2% gelatin plus 0.08% chromalin (chromium and potassium sulfate, from Sigma-Aldrich, Brazil) and finally allowed to dry at room temperature during 24 hours. At last, all sections were stored at -20°C until use.

2.5. Immunofluorescence. Firstly, the cryosections were immersed in cold acetone (4°C, PA) for 10 minutes. After, the sections were washed in PBS twice (10 min) then blocked/permeabilized with 5% bovine serum albumin (BSA) and PBS plus 0.1% Triton X-100 for 2 hours at room temperature (RT). Sections were incubated with primary antibodies
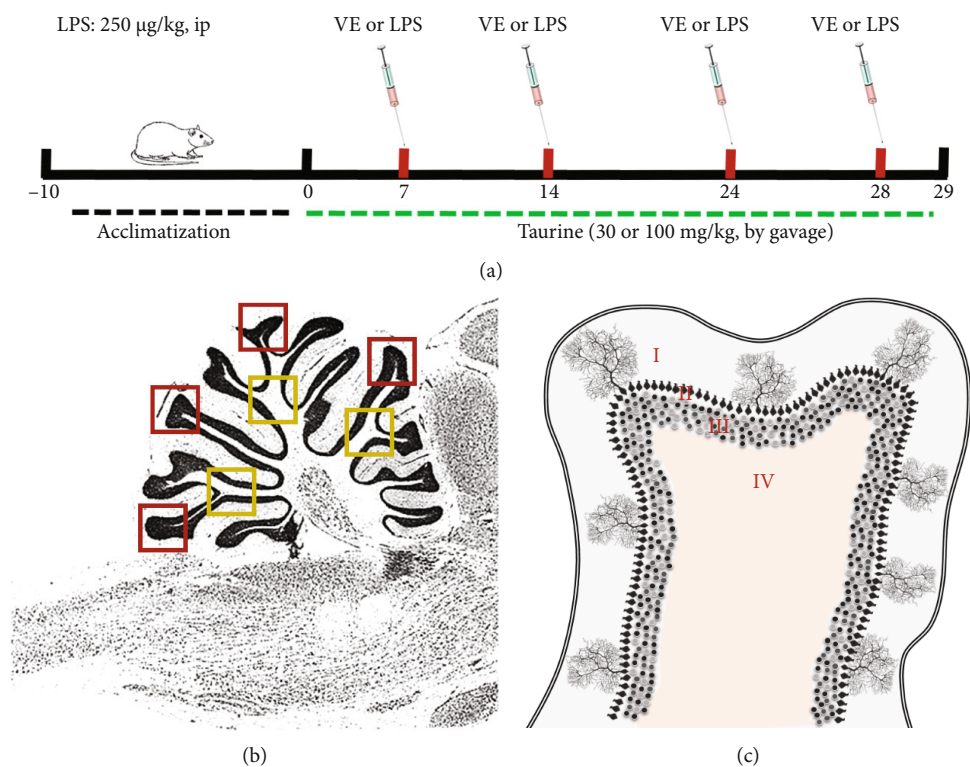
FIGURE 1: (a) Schematic illustration of experimental protocol for the taurine (TAU) at doses of 30 or 100 mg/kg and chronically exposed to lipopolysaccharide (LPS) toxin (250 μg/kg, intraperitoneally) treatments of rats. First, the rats were acclimatized for 10 days. Then, the treatment with TAU occurred once a day through an intragastric tube (gavage) during days 0 until 28. The LPS toxin was administered on days 7, 14, 21, and 28. On day 29, the animals were euthanized for cerebellar acquisition. (b) Representation of the fields chosen for the acquisition of the images of the tissue sections. A total of 5 sections were used for each rat. The red squares point to the cerebellar cortex of the cerebellar leaflets. The yellow squares show the regions chosen for the *arbor vitae*. The blue squares show the areas where images of the medullary center of the cerebellum were obtained. The images were acquired in a magnification of 200x, objective lens 20x, and field area of 200,500.10 μm^2. (c) Representation of the layers of the cerebellar leaflets: I, molecular layer; II, Purkinje cell layer; III, granular layer; and IV, white matter.

diluted in 5% BSA solution: (a) Mouse anti-CD11B (sections of 16 μm, microglia marker) 1 : 500, overnight at 4°C, Abcam followed by secondary antibody (goat anti-mouse alexa fluor 488, 1 : 500, 2 hr, RT in the dark; Thermo Fischer); (b) Rabbit anti-GFAP (sections of 16 μm, astrocyte marker) 1 : 800, overnight at 4°C, DAKO followed by secondary antibody (goat anti-rabbit alexa fluor 555, 1 : 1,000, 2 hr, RT in the dark; Thermo Fischer); (c) Mouse anti-NeuN (sections of 5 μm, mature neuronal marker) 1 : 6,000, overnight at 4°C, MilliPore followed by secondary antibody (goat anti-mouse alexa fluor 488, 1 : 500, 2 hr, RT in the dark, Thermo Fischer); and (d) Rabbit anticleaved caspase-3 (sections of 16 μm, apoptosis marker) 1 : 200, overnight at 4°C, Cell Signaling followed by secondary antibody (goat anti-rabbit alexa 555, 1 : 1,000, 2 hr RT in the dark, ThermoFischer). The 4′,6-diamidino-2-phenylindole (DAPI) solution (1 μg/ml) was prepared in PBS-Tx, and an incubation was carried out for 10 minutes in the dark. Then, the sections were washed 4 times with PBS-Tx for 5 minutes each. Vecta-Shield was added over the sections which were then overlaid with a coverslip.

The images were acquired using a Leica DM6-B microscope, Leica DFC 7000-T camera, and Leica Las X software. A total of 5 sections were used for each rat (see Figure 1(b)). For each section, 4 images were acquired on the cerebellar leaflets (cerebellar cortex in the red squares and *arbor vitae* in the yellow ones) and 3 images on the medullary center (blue squares, see Figure 1(b)). The images were acquired in a magnification of 200x, objective lens 20x, and field area of 200.500,10 μm^2.

The quantification of GFAP immunoreactivity occurred in the center of the *arbor vitae* and the cerebellar leaflet. The quantification of NeuN immunoreactivity occurred in the granular layer located in the center of the cerebellar leaflets and at the edge of the medullary center. Quantification of CD11b occurred in the middle of both the *arbor vita*e and the medullary center. The positive cleaved caspase-3 cells were counted in the molecular layer of the cerebellar leaflets, in the Purkinje cells layer, in the granular layer of the cerebellar leaflets, in the white substance of *arbor vitae*, and in the medullary center. Optical density was performed using the Image Pro-Plus®.

2.6. Statistical Analysis. The normality analysis of the samples was performed by Kolmogorov Smirnov test. Afterwards, parametric data were analyzed using two-way analysis of variance (ANOVA) followed by the Bonferroni test when appropriate. Results were expressed as the mean ± standard

Arbor *vitae*

Center of leaflet

(a)

(b)

Representative   Arbor *vitae*   Center of leaflet
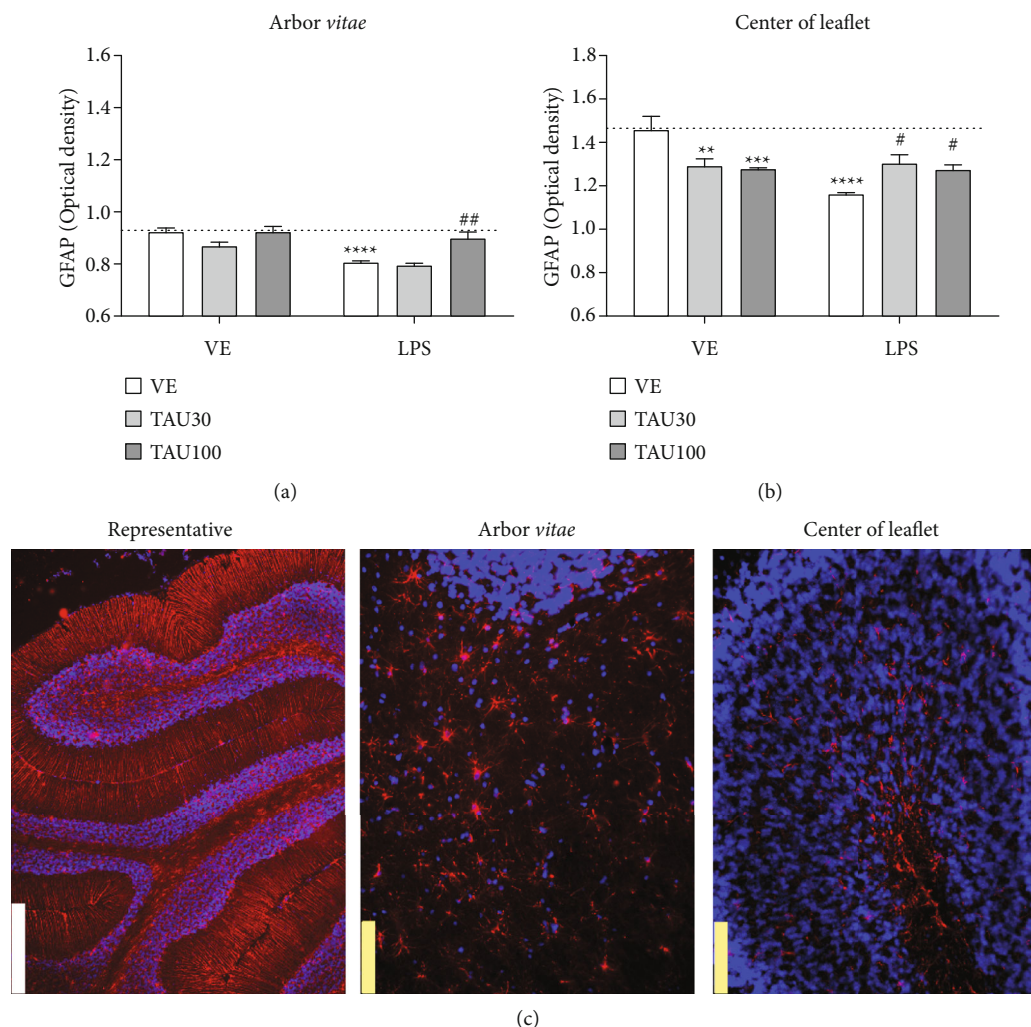
(c)

FIGURE 2: Neuroprotective effect of taurine (TAU, 30-100 mg/kg by gavage; vehicle saline) on the reduction of glial fibrillary acid protein (GFAP) in the *arbor vitae* (a) and in the center of leaflet (b) regions of rats exposed to chronic-recurrent neuroinflammation induced by the LPS toxin (250 μg/kg, intraperitoneally; vehicle saline). (c) Representative image of the immunostaining obtained through the fluorescence of the selected fields (white bar: 500 μm; yellow bar: 100 μm). $P < 0.05$ was considered to represent a significant difference. * denotes a significant difference compared to the vehicle group (VE). # denotes a significant difference compared to the LPS group. Two-way ANOVA followed by Bonferroni's post hoc. * or # denotes a difference of $P < 0.05$; ** or ## denotes a difference of $P < 0.01$; *** or ### denotes a difference of $P < 0.001$. Data are expressed as mean ± standard error of the mean (SEM), $n = 5$-6 per group.

error (SE). P values less than 0.05 ($P < 0.05$) were considered as indicative of significance.

3. Results and Discussion

3.1. Taurine Restores Immunoreactivity of GFAP in the Cerebellum of Rats Subjected to Chronic-Recurrent Neuroinflammation. Figure 2 shows the immunoreactivity of the GFAP protein in the *arbor vitae* and medullary center in the cerebellum of rats submitted to chronic-recurrent neuroinflammation induced by LPS and treated with different doses of taurine. Figure 2(a) shows a significant interaction between taurine versus LPS treatments ($F_{(2.28)} = 3{,}912$, $P < 0.05$) for the GFAP in the arbor vitae. LPS reduced the GFAP immunoreactivity in relation to the vehicle group ($F_{(1.28)} = 24.37$, $P < 0.001$; Figure 2(a)). Taurine 100 mg/kg

protected against reduction of GFAP immunoreactivity induced by LPS ($P < 0.01$; Figure 2(a)); however, similar results were not met by taurine 30 mg/kg. In the medullary center, we verified that LPS also reduced immunoreactivity of GFAP in relation to the vehicle group ($F_{(1.26)} = 6.678$, $P < 0.05$; Figure 2(b)). Taurine reduced immunoreactivity of GFAP *per se* at doses of 30 ($P < 0.01$) and 100 mg/kg ($P < 0.001$). A significant interaction between taurine versus LPS treatments was also seen, showing that taurine protected against the reduction of GFAP induced by LPS at doses of 30 and 100 mg/kg ($F_{(2.26)} = 8.102$, $P < 0.05$, Figure 2(b)).

Astrocytes, microglia, and neurons may be affected by LPS via TLR-4 expressed on their membranes or by the pro-inflammatory cascade mediated by this toxin. Thus, studying these cell populations against an inflammatory condition is extremely relevant. The glial fibrillary acidic protein (GFAP)

(a)

(b)

Representative
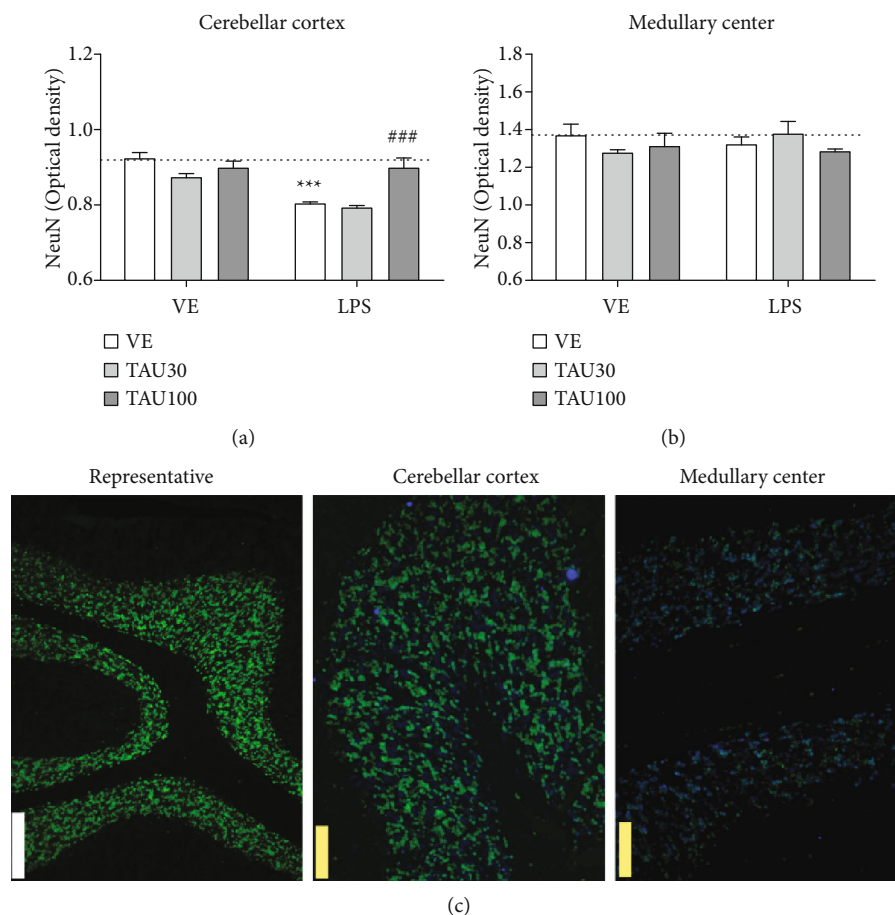
Cerebellar cortex

Medullary center

(c)

FIGURE 3: Neuroprotective effect of taurine (TAU, 30-100 mg/kg, by gavage; vehicle saline) on the reduction of immunoreactivity for the NeuN protein in the cerebellar cortex (a) and edges of the medullary center (b) regions of rats exposed to chronic-recurrent neuroinflammation induced by the LPS toxin (250 μg/kg, intraperitoneally; vehicle saline). (c) Representative image of the immunostaining obtained through the fluorescence of the selected fields (white bar: 500 μm; yellow bar: 100 μm). $P < 0.05$ was considered to represent a significant difference. * denotes a significant difference compared to the vehicle group (VE). # denotes a significant difference compared to the LPS group. Two-way ANOVA followed by Bonferroni's post hoc. *** or ### denotes a difference of $P < 0.001$. Data are expressed as mean ± standard error of the mean (SEM), $n = 5\text{-}6$ per group.

is an intermediate filament protein present in astrocytes, and its quantification is widely used to verify astrogliosis. Astrocytes have a range of control and homeostatic functions in health and disease and assume a reactive phenotype in acute central nervous system (CNS) traumas, ischemia, and in neurodegenerative diseases [39]. In acute conditions, LPS stimulates the expression of GFAP, protecting neuronal activity during inflammatory challenges [40]. On the other hand, microglia comprise between 5 and 20% of the total glial cell population, are more frequent in the grey matter, and found throughout the normal mammalian CNS [41]. The microglia are the only immune cells present in the CNS parenchyma and are thus the first responders to environmental change. Under conditions of tissue damage such as that associated with bacterial or viral infections of the CNS, microglia play a critical role in clearing debris and restoring homeostasis in the CNS [42].

Fu et al. [43] verified astrogliosis in rats exposed to LPS (2 mg/kg) over 30 days. Through this time-curve, after a single i.p. injection, there is an increase in immunoreactivity of GFAP between days 1 and 7 [43]. Acute exposures to LPS

are capable of inducing astrogliosis by elevating GFAP content and immunoreactivity in the nervous system, highlighting the hippocampus [44] and cerebellum [45]. As reported by Perez-Dominguez et al. [37], until seven days after the systemic LPS challenge, astrocytes present mild cell body hypertrophy, extended cell processes, and an increased GFAP immunoreactivity in the hippocampus. However, a repeated LPS exposure did not elicit an evident astrocytic reaction suggesting a lack of persistent astrocytic response after a repeated inflammatory challenge [37]. The same effect was observed by Fu et al. [43], who reported a gradual increase in the expression of GFAP, IL-1β, and TNF-α in the hippocampus up to seven days after the administration of 2 mg/kg of LPS. After the seventh day, there were no significant differences in the GFAP expression [43]. We observed the same effect of LPS on GFAP in both regions studied, but only in the central medullary region the dose of taurine 30 mg/kg showed a protective effect. Although LPS-induced neuroinflammation has been pivotally associated with microglia activation, astrocytes play an important role in maintaining brain homeostasis
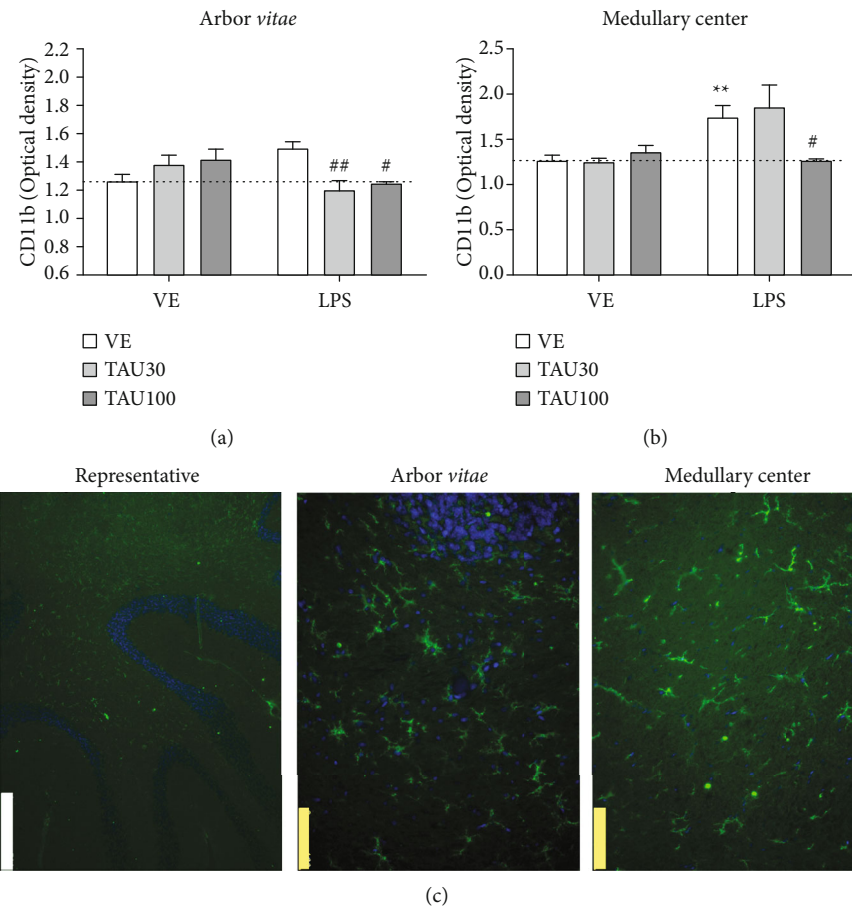
FIGURE 4: Neuroprotective effect of taurine (TAU, 30-100 mg/kg by gavage; vehicle saline) on the increase in CD11b protein in the *arbor vitae* (a) and medullary center (b) regions of rats exposed to chronic-recurrent neuroinflammation induced by the LPS toxin (250μg/kg, intraperitoneally; vehicle saline). (c) Representative image of the immunostaining obtained through the fluorescence of the selected fields (white bar: 500μm; yellow bar: 100μm). $P < 0.05$ was considered to represent a significant difference. * denotes a significant difference compared to the vehicle group (VE). # denotes a significant difference compared to the LPS group. Two-way ANOVA followed by Bonferroni's post hoc. * or # denotes a difference of $P < 0.05$; ** or ## denotes a difference of $P < 0.01$. Data are expressed as mean ± standard error of the mean (SEM), $n = 5$-6 per group.

and protecting surrounding neurons from damage like infective agents [46].

3.2. Taurine Prevents LPS-Induced Neuronal Death in the Rat Cerebellum. Figure 3 shows the immunoreactivity for the NeuN protein in the regions of the cerebellar cortex and at the edges of the medullary center of the cerebellum of rats subjected to chronic-recurrent neuroinflammation induced by LPS and treated with different doses of taurine. Figure 3(a) shows a significant interaction between taurine versus LPS treatments ($F_{(2.26)} = 7,539$, $P < 0.01$) for the NeuN protein in the cerebellar cortex. LPS reduced the immunoreactivity of the NeuN protein in relation to the vehicle group ($F_{(1.26)} = 26.26$, $P < 0.001$; Figure 3(a)). Again, taurine 100 mg/kg, but not 30 mg/kg, protected against the reduction in immunoreactivity for NeuN induced by LPS ($P < 0.001$; Figure 3(a)). In the granular layer present at the edge of the medullary center, no significant differences were observed between treatments for the immunoreactivity of the NeuN protein ($F_{(2.26)} = 0.2621$, $P > 0.05$; Figure 3(b)).

Neuronal nuclei (NeuN) is a well-recognized marker that is exclusively detected in postmitotic neurons. NeuN is distributed in the nuclei of mature neurons and has been considered a reliable marker of mature neurons in certain diseases and specific physiological states [47].

Pinato and colleagues [48] reported that intracerebroventricular LPS triggers a reduction in immunoreactivity for NeuN in the cerebral cortex, in the dentate gyrus of the hippocampus, and in the granular layer of the cerebellum of rats. The same effect is reproduced in cerebellar cell culture. In addition, the authors described that this reduction was also accompanied by an increase in positive fluoro-jade cells, which indicate a death of adult neurons by neuroinflammation [48]. Although inflammation is implicated in the progressive nature of neurodegenerative conditions, such as Alzheimer's and Parkinson's diseases [49], and also in seizure recurrence in epilepsy [19], the mechanisms are yet poorly understood. Systemic LPS administration results in rapid brain TNF-α increase by activating brain microglia to produce chronically elevated proinflammatory factors and
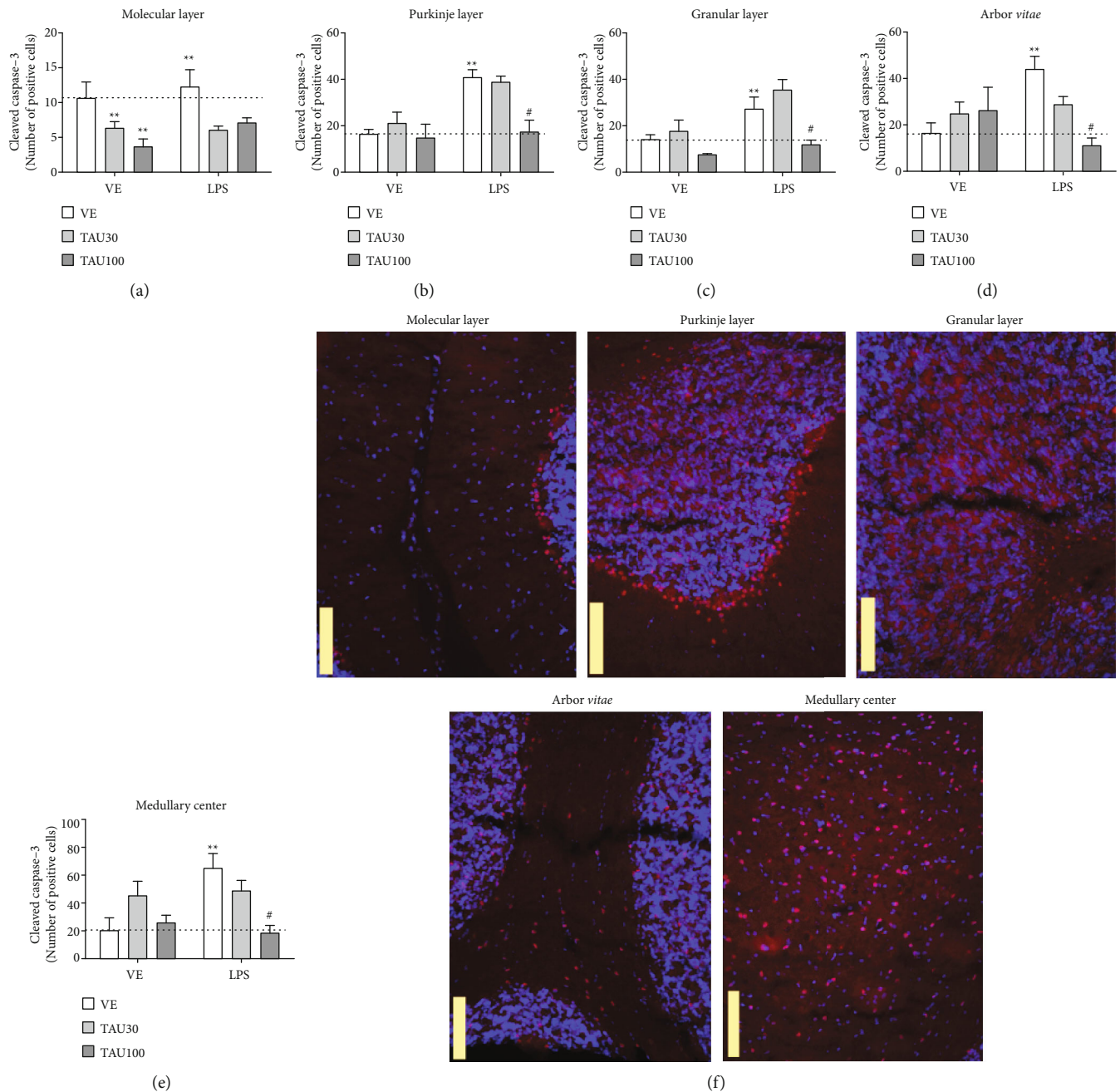
FIGURE 5: Neuroprotective effect of taurine (TAU, 30-100 mg/kg by gavage; vehicle saline) on cell apoptosis by the number of cleaved caspase-3 positive cells in the regions: (a) molecular layer, (b) Purkinje cell layer, (c) granular layer, (d) *arbor vitae*, and (e) medullary center in cerebellum of rats exposed to chronic-recurrent neuroinflammation induced by the LPS toxin (250 μg/kg, intraperitoneally; vehicle saline). (f) Representative image of the immunostaining obtained through the fluorescence of the selected fields (yellow bar: 100 μm). $P < 0.05$ was considered to represent a significant difference. * denotes a significant difference compared to the vehicle group (VE). # denotes a significant difference compared to the LPS group. Two-way ANOVA followed by Bonferroni's post hoc. * or # denotes a difference of $P < 0.05$; ** or ## denotes a difference of $P < 0.01$. Data are expressed as mean ± standard error of the mean (SEM), $n = 4$-5 per group.

culminating in delayed and progressive loss of neurons in the nervous system [50, 51].

3.3. Taurine Suppresses Microglial Immunoreactivity in the Cerebellum of Rats Submitted to Chronic-Recurrent Neuroinflammation Induced by LPS.

Figure 4 shows the immunoreactivity of the CD11b protein in the *arbor vitae* and medullary center of the cerebellum of rats submitted to chronic-recurrent neuroinflammation induced by LPS and treated with different doses of taurine. Figure 4(a) shows a significant interaction between taurine versus LPS treatments ($F_{(2,32)} = 6.428$, $P < 0.01$) for the CD11b protein in the *arbor vitae*. LPS increased the immunoreactivity of the CD11b in relation to the vehicle group ($F_{(1,32)} = 26.26$, $P < 0.001$;

Figure 4(a)). Treatment with either taurine 30 or 100 mg/kg prevented the expected LPS-induced microglial activation (TAU 30 mg/kg, $P < 0.01$; TAU 100 mg/kg, $P < 0.05$, Figure 4(a)). In the medullary center, only the 100 mg/kg dose was able to protect against the increased immunoreactivity of CD11b induced by LPS ($F_{(2,24)} = 3.777$, $P < 0.05$; Figure 4(b)). Microglia, which are the resident macrophages in the brain, play an important role in the occurrence and development of neuroinflammation. Under physiological conditions, microglia mainly eliminate metabolic products and toxic materials. However, if stimulated, microglia migrate to the lesion and remove cellular debris. While microglia activation is necessary and critical for host defense, excessive or prolonged activation of microglia leads to neuronal death and an increase in proinflammatory cytokines and oxidative stress [4, 9]. LPS dose-dependently increases microglial CD11b expression and is an important marker of neuroinflammation [52]. Indeed, we verified a reduction in astrogliosis and in the population of mature neurons in the cerebellum of rats, as well as an increase in microglial immunoreactivity in the LPS group. Next, we determined whether these events can be associated with apoptotic cell death in different layers and regions of the cerebellum.

3.4. Taurine Reduces Cell Apoptosis in Different Layers of the Cerebellum of Rats Exposed to LPS-Induced Chronic-Recurrent Neuroinflammation. Figure 5 shows the immunoreactivity for the cleaved caspase-3 protein in the molecular layer, granular layer, layer of Purkinje cells and white substance of the *arbor vitae*, and medullary center in the cerebellum of rats subjected to chronic-recurrent neuroinflammation induced by LPS and treated with different doses of taurine. Figure 5(a) shows that treatment with LPS did not change the number of positive cleaved caspase-3 cells in the cerebellar molecular layer ($P > 0.05$) compared to the vehicle group. Taurine 30 and 100 mg/kg were able to reduce the number of cleaved caspase-3 cells in relation to the vehicle group ($F_{(2,20)} = 8.21$; $P = 0.025$; Figure 5(a)). There were no significant interactions between treatments ($F_{(2,20)} = 0.6446$; $P = 0.5354$; Figure 5(a)).

In the Purkinje cell layer, it was observed that LPS increased the number of positive cleaved caspase-3 cells in relation to the vehicle group ($F_{(1,20)} = 12.21$; $P = 12.21$; Figure 5(b)). The treatment with TAU 100 mg/kg, but not 30 mg/kg, protected against the increase in the number of cells in apoptosis induced by LPS ($F_{(2,20)} = 4.985$; $P = 0.0189$; Figure 5(b)). LPS also increased the number of cleaved caspase-3 cells in the granular cell layer ($F_{(1,20)} = 12.54$; $P = 0.0019$; Figure 5(c)), and treatment with TAU 100 mg/kg prevented this effect ($F_{(2,20)} = 9.121$; $P = 0.0014$; Figure 5(c)). A similar result was observed in the *arbor vitae* region where LPS triggered an increase in the number of apoptotic cells ($F_{(1,20)} = 4.980$; $P = 0.023$; Figure 5(d)), which was again prevented by TAU 100 mg/kg supplementation ($F_{(2,20)} = 5.516$; $P = 0.0116$; Figure 5(d)). Finally, apoptosis was also triggered in the medullary center of the animals in the LPS group in relation to the vehicle

group ($F_{(1,20)} = 4.099$; $P = 0.029$; Figure 5(e)), which was consistently prevented by TAU 100 mg/kg treatment ($F_{(2,20)} = 3.998$; $P = 0.0398$; Figure 5(e)). Liu and colleagues showed that concentrations above 1 ng/ml of LPS induce apoptosis in microglial cell culture by analyzing TUNEL positive cells, DNA fragmentation, nuclear morphology, and quantification of cleaved caspase-3 [53]. Furthermore, intraperitoneal LPS has been shown to be able to increase not only the activity and expression of iNOS but also the number of apoptotic brain and Bax-positive cells, as well as decrease the amount of Bcl-2-positive cells [54].

It is evident that this inflammation orchestrated by the stimulation of TL4R triggered by LPS resulted in an increase in apoptosis in different regions of the cerebellum, but with no effect on the molecular layer. This chronic-recurrent process reduced the number of mature neurons and astrocytes while induced microglia activation. Several evidences have pointed out the anti-inflammatory role of taurine supplementation, and its ability has already been described to protect macrophages [55], BV2 microglial [56], and liver cells [57]. Notably, the majority of the studies focus on taurine's neuroprotective effects on the hippocampus [35, 58], and thus far, little is known about the cerebellum and its layers and regions. Further studies should be done to understand the complexity of the effects caused by chronic-recurrent inflammation on the populations that constitute the nervous system and the action mechanism of taurine as a neuroprotective agent. Here, we have verified the antiapoptotic activity of this nutraceutical agent and the ability to protect neurons and glial cells against systemic chronic-recurrent inflammation in the cerebellum.

4. Conclusion

Finally, taurine supplementation not only protects the cerebellum against neuronal death but also reduces microglial activation induced by the recurrent administration of LPS in the cerebellum of rats. Taurine also showed an interesting antiapoptotic activity by reducing the increase in caspase-3 cells cleaved in the molecular layer, granular layer, layer of Purkinje cells and white substance of the *arbor vitae*, and medullary center in the cerebellum. Understanding the role of taurine in the cerebellum and its regulation in several brain regions should facilitate studies on its neuroprotective mechanisms. In this regard, considering taurine as an emerging adjuvant or alternative drug for neuroprotection, further study is necessary to understand its real potential human health benefits.

Data Availability

All results are included in the manuscript.

Ethical Approval

The study was approved by the Ethics Committee of UFC-SPA (Protocol number 192/16, Identification code: 488/16).

Conflicts of Interest

The authors declare that they have no competing interests.

Acknowledgments

References

[1] H. Amani, H. Kazerooni, H. Hassanpoor, A. Akbarzadeh, and H. Pazoki-Toroudi, "Tailoring synthetic polymeric biomaterials towards nerve tissue engineering: a review," *Artificial Cells, Nanomedicine, and Biotechnology*, vol. 47, no. 1, pp. 3524–3539, 2019.

[2] N. L. Cerminara, E. J. Lang, R. V. Sillitoe, and R. Apps, "Redefining the cerebellar cortex as an assembly of non-uniform Purkinje cell microcircuits," *Nature Reviews. Neuroscience*, vol. 16, no. 2, pp. 79–93, 2015.

[3] E. D'Angelo, "Physiology of the cerebellum," *Handbook of Clinical Neurology*, vol. 154, pp. 85–108, 2018.

[4] J. Zhao, W. Bi, S. Xiao et al., "Neuroinflammation induced by lipopolysaccharide causes cognitive impairment in mice," *Scientific Reports*, vol. 9, no. 1, article 5790, 2019.

[5] J. D. Schmahmann, X. Guell, C. J. Stoodley, and M. A. Halko, "The theory and neuroscience of cerebellar cognition," *Annual Review of Neuroscience*, vol. 42, no. 1, pp. 337–364, 2019.

[6] A. Sathyanesan, J. Zhou, J. Scafidi, D. H. Heck, R. V. Sillitoe, and V. Gallo, "Emerging connections between cerebellar development, behaviour and complex brain disorders," *Nature Reviews. Neuroscience*, vol. 20, no. 5, pp. 298–313, 2019.

[7] M. L. Streng and E. Krook-Magnuson, "The cerebellum and epilepsy," *Epilepsy & Behavior*, no. article 106909, 2020.

[8] S. M. Lucas, N. J. Rothwell, and R. M. Gibson, "The role of inflammation in CNS injury and disease," *British Journal of Pharmacology*, vol. 147, Supplement 1, pp. S232–S240, 2006.

[9] F. B. Carvalho, J. M. Gutierres, A. Bueno et al., "Anthocyanins control neuroinflammation and consequent memory dysfunction in mice exposed to lipopolysaccharide," *Molecular Neurobiology*, vol. 54, no. 5, pp. 3350–3367, 2017.

[10] O. Lykhmus, N. Mishra, L. Koval et al., "Molecular mechanisms regulating LPS-induced inflammation in the brain," *Frontiers in Molecular Neuroscience*, vol. 9, p. 19, 2016.

[11] M. T. Heneka, M. J. Carson, J. El Khoury et al., "Neuroinflammation in Alzheimer's disease," *The Lancet Neurology*, vol. 14, no. 4, pp. 388–405, 2015.

[12] A. Vezzani, "Brain inflammation and seizures: evolving concepts and new findings in the last 2 decades," *Epilepsy Currents*, vol. 20, Supplement 6, pp. 40S–43S, 2020.

[13] V. Meseguer, Y. A. Alpizar, E. Luis et al., "TRPA1 channels mediate acute neurogenic inflammation and pain produced by bacterial endotoxins," *Nature Communications*, vol. 5, no. 1, p. 3125, 2014.

[14] Y. A. Alpizar, B. Boonen, A. Sanchez et al., "TRPV4 activation triggers protective responses to bacterial lipopolysaccharides

in airway epithelial cells," *Nature Communications*, vol. 8, no. 1, article ???, 2017.

[15] R. Gorina, M. Font-Nieves, L. Marquez-Kisinousky, T. Santalucia, and A. M. Planas, "Astrocyte TLR4 activation induces a proinflammatory environment through the interplay between MyD88-dependent NFκB signaling, MAPK, and Jak1/Stat1 pathways," *Glia*, vol. 59, no. 2, pp. 242–255, 2011.

[16] Y. Shen, H. Qin, J. Chen et al., "Postnatal activation of TLR4 in astrocytes promotes excitatory synaptogenesis in hippocampal neurons," *The Journal of Cell Biology*, vol. 215, no. 5, pp. 719–734, 2016.

[17] C. Acosta and A. Davies, "Bacterial lipopolysaccharide regulates nociceptin expression in sensory neurons," *Journal of Neuroscience Research*, vol. 86, no. 5, pp. 1077–1086, 2008.

[18] S. Leow-Dyke, C. Allen, A. Denes et al., "Neuronal Toll-like receptor 4 signaling induces brain endothelial activation and neutrophil transmigration in vitro," *Journal of Neuroinflammation*, vol. 9, p. 230, 2012.

[19] M. Maroso, S. Balosso, T. Ravizza et al., "Toll-like receptor 4 and high-mobility group box-1 are involved in ictogenesis and can be targeted to reduce seizures," *Nature Medicine*, vol. 16, no. 4, pp. 413–419, 2010.

[20] S. M. Pacheco, J. H. Azambuja, T. R. de Carvalho et al., "Glioprotective effects of lingonberry extract against altered cellular viability, acetylcholinesterase activity, and oxidative stress in lipopolysaccharide-treated astrocytes," *Cellular and Molecular Neurobiology*, vol. 38, no. 5, pp. 1107–1121, 2018.

[21] R. F. Zanin, E. Braganhol, L. S. Bergamin et al., "Differential macrophage activation alters the expression profile of NTPDase and ecto-5'-nucleotidase," *PLoS One*, vol. 7, no. 2, article e31205, 2012.

[22] A. Vezzani and T. Z. Baram, "New roles for interleukin-1 Beta in the mechanisms of epilepsy," *Epilepsy Currents*, vol. 7, no. 2, pp. 45–50, 2007.

[23] S. S. Oja and P. Saransaari, "Pharmacology of taurine," *Proceedings of the Western Pharmacology Society*, vol. 50, pp. 8–15, 2007.

[24] C. De la Puerta, F. J. Arrieta, J. A. Balsa, J. I. Botella-Carretero, I. Zamarron, and C. Vazquez, "Taurine and glucose metabolism: a review," *Nutrición Hospitalaria*, vol. 25, no. 6, pp. 910–919, 2010.

[25] M. C. Shivaraj, G. Marcy, G. Low et al., "Taurine induces proliferation of neural stem cells and synapse development in the developing mouse brain," *PLoS One*, vol. 7, no. 8, article e42935, 2012.

[26] A. De Luca, S. Pierno, and D. C. Camerino, "Taurine: the appeal of a safe amino acid for skeletal muscle disorders," *Journal of Translational Medicine*, vol. 13, no. 1, p. 243, 2015.

[27] V. Vitvitsky, S. K. Garg, and R. Banerjee, "Taurine biosynthesis by neurons and astrocytes," *The Journal of Biological Chemistry*, vol. 286, no. 37, pp. 32002–32010, 2011.

[28] J. Menzie, H. Prentice, and J. Y. Wu, "Neuroprotective mechanisms of taurine against ischemic stroke," *Brain Sciences*, vol. 3, no. 4, pp. 877–907, 2013.

[29] H. Lee, D. S. Lee, K. J. Chang, S. H. Kim, and S. H. Cheong, "Ribose-taurine suppresses inflammation through NF-κB regulation in activated RAW 264.7 macrophages," *Advances in Experimental Medicine and Biology*, vol. 1155, pp. 1057–1067, 2019.

[30] S. Kumar and R. Goel, "Taurine supplementation to antiseizure drugs as the promising approach to treat

pharmacoresistant epilepsy: a pre-clinical study," *International Journal of Epilepsy*, vol. 4, no. 2, pp. 119–124, 2017.

[31] P. Yue, L. Jing, X. Zhao, H. Zhu, and J. Teng, "Down-regulation of taurine-up-regulated gene 1 attenuates inflammation by sponging miR-9-5p via targeting NF-κB1/p50 in multiple sclerosis," *Life Sciences*, vol. 233, p. 116731, 2019.

[32] K. Szymanski and K. Winiarska, "Taurine and its potential therapeutic application," *Postepy Higieny i Medycyny Doswiadczalne*, vol. 62, pp. 75–86, 2008.

[33] S. W. Schaffer, J. Azuma, and M. Mozaffari, "Role of antioxidant activity of taurine in diabetes," *Canadian Journal of Physiology and Pharmacology*, vol. 87, no. 2, pp. 91–99, 2009.

[34] F. L. Rahmeier, L. S. Zavalhia, L. S. Tortorelli et al., "The effect of taurine and enriched environment on behaviour, memory and hippocampus of diabetic rats," *Neuroscience Letters*, vol. 630, pp. 84–92, 2016.

[35] G. Wu, T. Matsuwaki, Y. Tanaka, K. Yamanouchi, J. Hu, and M. Nishihara, "Taurine counteracts the suppressive effect of lipopolysaccharide on neurogenesis in the hippocampus of rats," *Advances in Experimental Medicine and Biology*, vol. 775, pp. 111–119, 2013.

[36] L. S. Tortorelli, D. S. Engelke, P. Lunardi, E. S. T. Mello, J. G. Santos-Junior, and C. A. Goncalves, "Cocaine counteracts LPS-induced hypolocomotion and triggers locomotor sensitization expression," *Behavioural Brain Research*, vol. 287, pp. 226–229, 2015.

[37] M. Perez-Dominguez, E. Avila-Munoz, E. Dominguez-Rivas, and A. Zepeda, "The detrimental effects of lipopolysaccharide-induced neuroinflammation on adult hippocampal neurogenesis depend on the duration of the pro-inflammatory response," *Neural Regeneration Research*, vol. 14, no. 5, pp. 817–825, 2019.

[38] P. M. Canas, L. O. Porciuncula, G. M. Cunha et al., "Adenosine A2A receptor blockade prevents synaptotoxicity and memory dysfunction caused by beta-amyloid peptides via p38 mitogen-activated protein kinase pathway," *The Journal of Neuroscience*, vol. 29, no. 47, pp. 14741–14751, 2009.

[39] E. M. Hol and M. Pekny, "Glial fibrillary acidic protein (GFAP) and the astrocyte intermediate filament system in diseases of the central nervous system," *Current Opinion in Cell Biology*, vol. 32, pp. 121–130, 2015.

[40] B. C. Borges, R. Rorato, J. Antunes-Rodrigues, and L. L. Elias, "Glial cell activity is maintained during prolonged inflammatory challenge in rats," *Brazilian Journal of Medical and Biological Research*, vol. 45, no. 8, pp. 784–791, 2012.

[41] C. Sousa, K. Biber, and A. Michelucci, "Cellular and molecular characterization of microglia: a unique immune cell population," *Frontiers in Immunology*, vol. 8, p. 198, 2017.

[42] A. Waisman, F. Ginhoux, M. Greter, and J. Bruttger, "Homeostasis of microglia in the adult brain: review of novel microglia depletion systems," *Trends in Immunology*, vol. 36, no. 10, pp. 625–636, 2015.

[43] H. Q. Fu, T. Yang, W. Xiao et al., "Prolonged neuroinflammation after lipopolysaccharide exposure in aged rats," *PLoS One*, vol. 9, no. 8, article e106331, 2014.

[44] C. Da Re, J. M. Souza, F. Froes et al., "Neuroinflammation induced by lipopolysaccharide leads to memory impairment and alterations in hippocampal leptin signaling," *Behavioural Brain Research*, vol. 379, article 112360, 2020.

[45] V. S. Andrade, D. B. Rojas, R. B. de Andrade et al., "A possible anti-inflammatory effect of proline in the brain cortex and cerebellum of rats," *Molecular Neurobiology*, vol. 55, no. 5, pp. 4068–4077, 2018.

[46] A. Volterra and J. Meldolesi, "Astrocytes, from brain glue to communication elements: the revolution continues," *Nature Reviews. Neuroscience*, vol. 6, no. 8, pp. 626–640, 2005.

[47] W. Duan, Y. P. Zhang, Z. Hou et al., "Novel insights into NeuN: from neuronal marker to splicing regulator," *Molecular Neurobiology*, vol. 53, no. 3, pp. 1637–1647, 2016.

[48] L. Pinato, S. da Silveira Cruz-Machado, D. G. Franco et al., "Selective protection of the cerebellum against intracerebroventricular LPS is mediated by local melatonin synthesis," *Brain Structure & Function*, vol. 220, no. 2, pp. 827–840, 2015.

[49] A. De Virgilio, A. Greco, G. Fabbrini et al., "Corrigendum to "Parkinson's disease: autoimmunity and neuroinflammation" [Autoimmun Rev 15 (10) (2016) 1005-1011]," *Autoimmunity Reviews*, vol. 15, no. 12, p. 1210, 2016, Autoimmun Rev 15 (10) (2016) 1005-1011.

[50] L. Qin, X. Wu, M. L. Block et al., "Systemic LPS causes chronic neuroinflammation and progressive neurodegeneration," *Glia*, vol. 55, no. 5, pp. 453–462, 2007.

[51] H. M. Gao and J. S. Hong, "Why neurodegenerative diseases are progressive: uncontrolled inflammation drives disease progression," *Trends in Immunology*, vol. 29, no. 8, pp. 357–365, 2008.

[52] M. Kellom, M. Basselin, V. L. Keleshian, M. Chen, S. I. Rapoport, and J. S. Rao, "Dose-dependent changes in neuroinflammatory and arachidonic acid cascade markers with synaptic marker loss in rat lipopolysaccharide infusion model of neuroinflammation," *BMC Neuroscience*, vol. 13, p. 50, 2012.

[53] B. Liu, K. Wang, H. M. Gao, B. Mandavilli, J. Y. Wang, and J. S. Hong, "Molecular consequences of activated microglia in the brain: overactivation induces apoptosis," *Journal of Neurochemistry*, vol. 77, no. 1, pp. 182–189, 2001.

[54] A. Semmler, T. Okulla, M. Sastre, L. Dumitrescu-Ozimek, and M. T. Heneka, "Systemic inflammation induces apoptosis with variable vulnerability of different brain regions," *Journal of Chemical Neuroanatomy*, vol. 30, no. 2-3, pp. 144–157, 2005.

[55] H. Lee, D. S. Lee, K. J. Chang, S. H. Kim, and S. H. Cheong, "Anti-inflammatory action of glucose-taurine reduced by inhibiting NF-κB activation in LPS-activated RAW264.7 macrophages," *Advances in Experimental Medicine and Biology*, vol. 1155, pp. 989–999, 2019.

[56] H. Lee, D. S. Lee, K. J. Chang, S. H. Kim, and S. H. Cheong, "Glucose-taurine reduced exerts neuroinflammatory responses by inhibition of NF-κB activation in LPS-induced BV2 microglia," *Advances in Experimental Medicine and Biology*, vol. 1155, pp. 857–867, 2019.

[57] Y. Huang, M. Sun, X. Yang, A. Ma, Y. Ma, and A. Zhao, "Baicalin relieves inflammation stimulated by lipopolysaccharide via upregulating TUG1 in liver cells," *Journal of Physiology and Biochemistry*, vol. 75, no. 4, pp. 463–473, 2019.

[58] X. Wu, C. Liu, L. Chen et al., "Protective effects of tauroursodeoxycholic acid on lipopolysaccharide-induced cognitive impairment and neurotoxicity in mice," *International Immunopharmacology*, vol. 72, pp. 166–175, 2019.

Research Article

Crosstalk between RNA-Binding Proteins and Immune Microenvironment Revealed Two RBP Regulatory Patterns with Distinct Immunophenotypes in Periodontitis

Lu Xing,[1] Guanqun Meng,[2] Tian Chen,[3] Xiaoqi Zhang,[1] Ding Bai,[3] and Hui Xu [3]

[1]*State Key Laboratory of Oral Diseases & National Clinical Research Center for Oral Diseases, Sichuan University, Chengdu, China*
[2]*Department of Population and Quantitative Health Sciences, School of Medicine, Case Western Reserve University, Cleveland, OH 44106, USA*
[3]*State Key Laboratory of Oral Diseases & National Clinical Research Center for Oral Diseases; Department of Orthodontics, West China Hospital of Stomatology, Sichuan University, Chengdu, China*

Correspondence should be addressed to Hui Xu; zybbda@126.com

Periodontitis is an inflammatory disease whose pathogenesis is closely related with immunology. RNA-binding proteins (RBPs) were found to play crucial roles in immunity. Therefore, we aimed to investigate the potential impact of RBPs in the immune microenvironment in periodontitis. The differential expressions of RBPs in periodontitis and healthy samples were determined and were used to construct an RBP-based classifier for periodontitis using logistic regression. The correlations between RBPs and immune characteristics were investigated by the Spearman correlation. Unsupervised clustering was conducted to identify the RBP regulatory patterns. RBP-related genes were identified by WGCNA, while biological distinctions were revealed by GSVA and GO. 24 dysregulated RBPs were identified, from which a 12-RBP classifier was established to distinguish periodontitis with AUC of 0.942. Close protein-protein interactions and expression correlations were observed especially between SPATS2 and ISG20. ISG20 and ESRP1 were found to be highly correlated with immunocyte infiltration, immune signaling activation, and HLA expressions in periodontitis. Two distinct RBP regulatory patterns were identified with different immune and other biological characteristics in periodontitis. Our findings indicate a significant impact of RBPs in shaping the immune microenvironment in periodontitis, which might bring new insights into the understanding of immune mechanisms in the pathogenesis of periodontitis.

1. Introduction

Periodontitis is an inflammatory disease initiated by bacteria infection. It detrimentally affects periodontal supporting tissues, causing symptoms such as swelling of gingiva, periodontal pyorrhea, and tooth loosening [1]. It is reported that severe periodontitis is the sixth most prevalent health condition, affecting 10.8% of the population around the globe [2]. It brings about severe health and economic burdens, as prosthodontic cost for tooth loss caused by periodontitis is usually not a small budget [2, 3]. Over the years, periodontitis have been implicated as an etiological factor in systemic diseases such as diabetes, rheumatoid arthritis, and cardiovascu-lar diseases [4]. Unfortunately, treatment for periodontitis has thus far failed to reverse the tissue damage, which means that actually there is currently no cure for periodontitis [5].

The initiation of periodontitis can be recognized to be a cascade of immune/inflammatory responses that was triggered by periodontal pathogens. The degree of periodontal damage relies heavily on the host response, particularly on the inflammatory process and the activation patterns of immune response pathways during periodontitis [6]. Failure to resolve inflammation and attempt to restore tissue homeostasis cause neutrophil-mediated destruction in both the alveolar bone and extracellular matrix [7]. The inflammatory reaction, rather than the pathogens, causes irreversible

damage in the periodontal tissue. Thus, a promising therapy for periodontitis is to resolve inflammation and return tissue to homeostasis. Elucidation of the mechanisms of immune regulations in periodontitis is crucial to the development of novel treatment strategies.

RNA-binding proteins (RBPs) are a large group of proteins that bind to RNA either directly or as a part of a macromolecular complex. As a critical part of the posttranscriptional gene regulator, RBPs facilitate the maturation, stability, transportation, and degradation of cellular RNAs [8]. RBPs play pivotal roles in cell development and stress response, and its dysregulation could certainly cause diseases [9]. Various types of RBPs have been identified to be implicated in the maintenance of immune homeostasis [10]. For instance, conditional deletion of Elavl1 caused impediment to immune cell development [11, 12]. hnRNPC was involved in follicular B cell maintenance [13]. Based on the immunoregulatory role of RBPs and immunomicrobial pathogenesis of periodontitis, it is plausible to deduce that RBPs might play a crucial part in periodontitis. The RBP HuR was reported to modulate inflammatory responses in periodontitis by regulating IL-6 [14]. However, evidence on the regulatory role of RBPs in periodontitis is quite rare. Systematic analyses exploring the functions of RBPs and their roles in shaping the immune microenvironment in periodontitis are warranted.

Considering the unveiled role of RBPs in periodontitis and involvement of RBPs in immunoregulation, this study is aimed at portraying the overall landscape of RBPs in periodontitis and uncovering its implications with the immune microenvironment of periodontitis. The findings are expected to reveal the pathogenesis of periodontitis in the perspective of RBP-mediated immunoregulatory mechanism.

2. Results

2.1. Expression Landscape of RBPs in Periodontitis. The overall regulatory mechanisms of RBPs in the immune microenvironment in periodontitis were presented in Figure 1(a). The RBP gene list was obtained from a previous research [15]. The types of RNA which the RBPs were binding to were concluded in the pie chart (Figure 1(b)). Differential analysis revealed that 24 RBPs were significantly dysregulated between periodontally healthy and periodontitis samples (adjust p value < 0.01 and |logFC| >0.5, Figure 1(c), Table S1). Box plot and heatmap demonstrated the expression status of the 24 dysregulated RBPs (Figures 1(d) and 1(e)). To figure out the interaction relationship of these dysregulated RBPs, a protein-protein interaction network was constructed (Figure 1(f)), and their expression correlation relationship was calculated by correlation analysis. It was found that the most positively correlated pair is ZC3H12D-SIDT1 while the most negatively correlated pair is ISG20-ESRP1 (Figure 1(g)).

2.2. Differential Expression Patterns of RBPs between Periodontitis and Periodontally Healthy Samples. To further validate the distinction of RBPs expressions between periodontally healthy and periodontitis samples, logistic regression was conducted. Univariate logistic regression analysis

was performed on the 24 significantly dysregulated RBPs, and their odds ratio were presented on the forest plot with the 95% confidence interval (Figure 2(a), Table S2). It was found that they were all significantly related with periodontitis (adjust p value < 0.05). To make dimension reduction and remove unimportant features, we performed least absolute shrinkage and selection operator (LASSO) regression for feature selection and reduce overfitting of the model, and 12 RBPs were identified with the lambda of 0.0146 (Figures 2(b) and 2(c)). Multivariate logistic regression analysis was performed on the 12 RBPs to construct a 12-RBP classifier for periodontitis (Figure 2(d), Table S3), with the risk score calculated for each of the samples (Figure 2(f)). Receiver operating Characteristic (ROC) analysis revealed that the classifier had excellent discriminative ability with the area under the curve (AUC) of 0.942 (Figure 2(e)). Periodontitis samples had much higher risk scores compared with periodontally healthy ones (Figure 2(f)). PCA analysis based on the 12 RBPs suggests that periodontitis and periodontally healthy samples had distinct expression patterns of the 12 RBPs (Figure 2(g)).

2.3. Immune Microenvironment Characteristics in Periodontitis and Their Correlations with RBPs. The immune microenvironment of periodontitis was explored in 241 periodontitis and 69 periodontally healthy samples. In brief, relative enrichment score of immunocytes, relative activity of immune-related pathways, and expression of HLA were calculated, and their correlations with RBPs were investigated.

The majority of the types of immunocytes showed significantly increased infiltration in periodontitis samples compared with periodontally healthy ones ($p < 0.05$) (Figure S1A, Table S4). The most positively correlated immunocyte-RBP pair is activated B cell and ISG20, both significantly upregulated in periodontitis. The most negatively correlated immunocyte-RBP pair is activated B cell and ESRP1, with significant downregulation of ESRP1 in periodontitis (Figures 3(a)–3(c), Table S5).

Similarly, as for immune-related pathways, almost all are significantly activated in periodontitis, except for TGFb family member receptor which had a significantly lower activity (Figure S1B, Table S6). Correlation analysis demonstrated that the most positively correlated immune pathway-RBP pair is BCR signaling pathway (B cell receptor signaling pathway) and ISG20, with higher activities of both in periodontitis. The most negatively correlated pair is BCR signaling pathway and ESRP1, with a higher activity of BCR signaling pathway and a lower expression of ESRP1 in periodontitis (Figures 4(a)–4(c), Table S7). Similar results were also found in HLA expression. Almost all the HLA genes were significantly upregulated in periodontitis, except for HLA-DQB2 which showed a significantly lower expression (Figure S1C, Table S8). Correlation analysis revealed HLA-DOB and ISG20 as the most positively correlated HLA-RBP pair, with higher activities of both in periodontitis. The most negatively correlated pair is HLA-DOB and ESRP1, with a higher expression of HLA-DOB
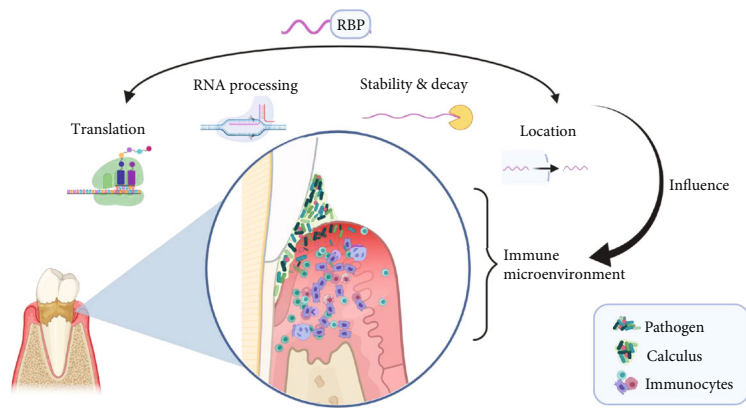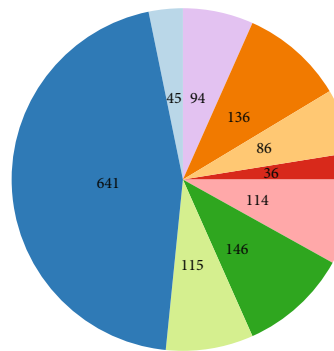
(a)

(b)

(c)
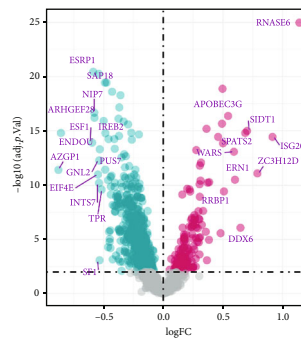
(d)

FIGURE 1: Continued.

(e)   (f)   (g)

FIGURE 1: Expression landscape of RNA binding proteins (RBPs) in periodontitis. (a) The overview of RBPs' regulatory role in periodontitis. (b) A summary of the types of RNA which the RBPs were binding to. (c) The volcano plot demonstrated the differentially expressed RBPs in periodontitis and periodontally healthy samples. RBPs with adjust p value < 0.01 and |logFC| >0.5 were considered to be significantly dysregulated, and their gene names were marked. The box plot (d)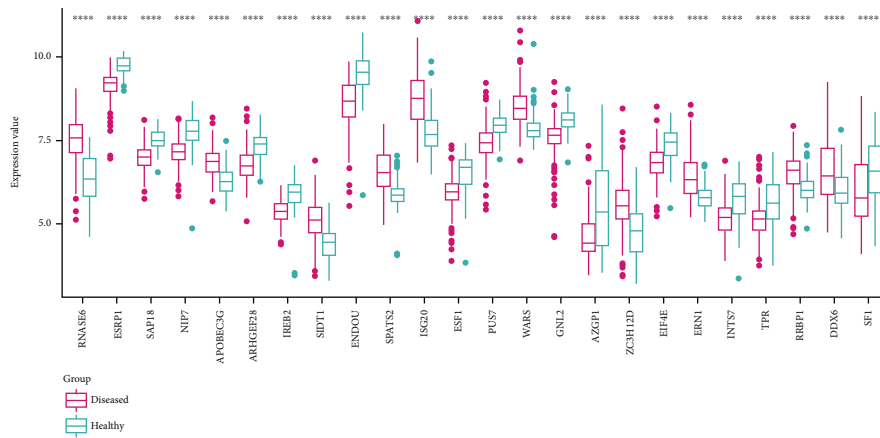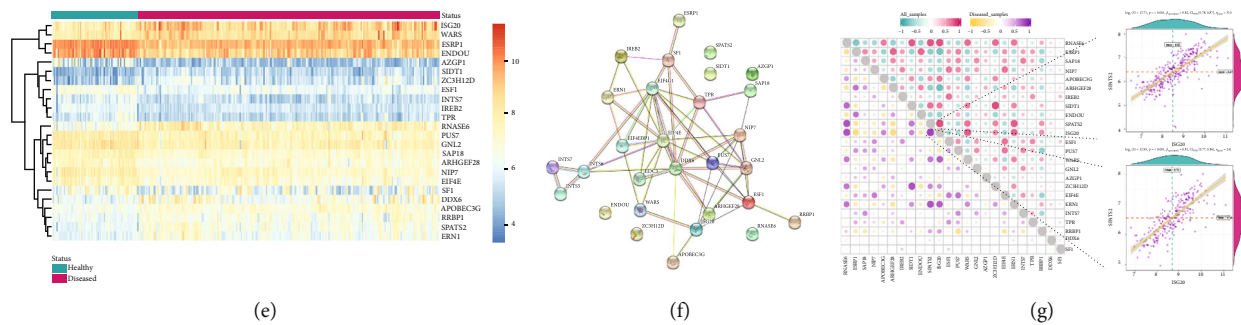 and heatmap (e) demonstrated the expression status of the 24 dysregulated RBPs between periodontally healthy and periodontitis samples. (f) The protein-protein interaction network of the 24 dysregulated RBPs. (g) The correlation among the 24 significantly dysregulated RBPs in periodontitis samples and whole samples. The most correlated RBPs in all samples and periodontitis samples were demonstrated in the dot plot.

and a lower expression of ESRP1 (Figures 5(a)–5(c), Table S9).

These findings demonstrated strong correlations of the RBPs ISG20 and ESRP1 with activated B cell infiltration, BCR signaling activation, and HLA-DOB expression, which were among the immune characteristics showing the most significant difference between periodontitis and periodontally healthy samples.

2.4. Identification of Distinct RBP Regulatory Patterns within Periodontitis Samples. Since RBPs had been linked with periodontal immune homeostasis, we clustered the samples based on its RBP expression to see if subtypes could be observed within periodontitis samples. Unsupervised consensus clustering analysis was performed on the 241 periodontitis samples based on their RBP expressions and identified two subtypes (Figures 6(a)–6(c), Table S10). PCA analysis demonstrated that the two subtypes had distinct RBP regulatory patterns (Figure 6(d)). Furthermore, we compared the clinical characteristics and found that there was a significant difference in gender between the two subtypes (Figure 6(e)). The subtype-specific RBPs were identified, showing different expression patterns between the two subtypes (adjust p value < 0.01, |logFC| >0.6, Figures 6(f) and 6(g), Table S11).

2.5. Distinct Immune Characteristics Were Observed between Two RBP Regulatory Patterns. Considering the strong correlations found between RBPs and the immune microenvironment, we looked further into the subtypes to see if different RBP regulatory patterns correspond to distinct immune characteristics. Subtype-2 demonstrated more intense immune reactions, with higher relative enrichment scores of immunocytes, higher activities of immune-related pathways, and higher HLA expressions. For instance, the aforementioned activated B cell and HLA-DOB, which fell into the most correlated immunocyte-RBP and HLA-RBP pairs, respectively, were significantly upregulated in subtype-2 compared with subtype-1. In addition, the BCR signaling pathway, which belonged to the aforementioned

most correlated immune pathway-RBP pair, had higher activity in subtype-2. These findings linked two RBP regulatory patterns to distinct immune characteristics in periodontitis (Figures 7(a)–7(c)).

2.6. Biological Distinctions between the Two RBP Regulatory Patterns. To figure out the biological reactions happening under the two RBP regulatory patterns, Gene Set Variation Analysis (GSVA) on Hallmarks and KEGG pathways was employed which revealed biological pathway differences in the two subtypes, respectively (Figure S2A and B). Then, in order to find what caused the biological differences between the two RBP regulatory patterns, we identified RBP phenotype-related genes and employed GO-BP functional enrichment analysis on them (Figure S2C). To find out if biological differences occurred specifically regarding immunity, we employed GO-BP functional enrichment analysis on RBP phenotype-related immune genes and clustered them according to the function, and those genes were mostly enriched on immune receptor related pathways such as the Fc receptor signaling pathway and immune response-regulating cell surface receptor signaling pathway (Figure S2D). Furthermore, to identify gene modules involved in the two RBP regulatory subtypes, WGCNA was employed. 22 gene modules were identified, and we performed correlation analysis of those gene modules with the two subtypes. We found that each RBP regulatory pattern had their respective matching gene modules. The modules mostly positively correlated with subtype-1 or subtype-2 were represented by blue or brown, respectively. (Figure S3A-D, Table S12).

3. Materials and Methods

3.1. Data Preprocessing. The 310 samples included in this study (69 periodontally healthy samples and 241 periodontitis samples) came from 120 patients that underwent periodontal surgery [16]. The procedure of sample procession and RNA extraction were described in the previous study [16]. The gene expression was detected by Affymetrix Human Genome U133 Plus 2.0 Array microarray according
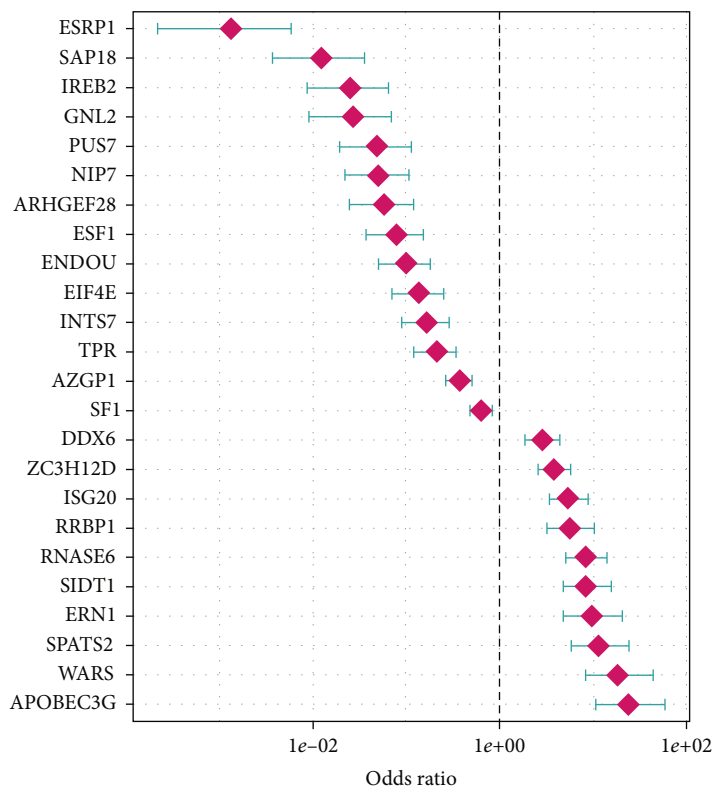
(a)
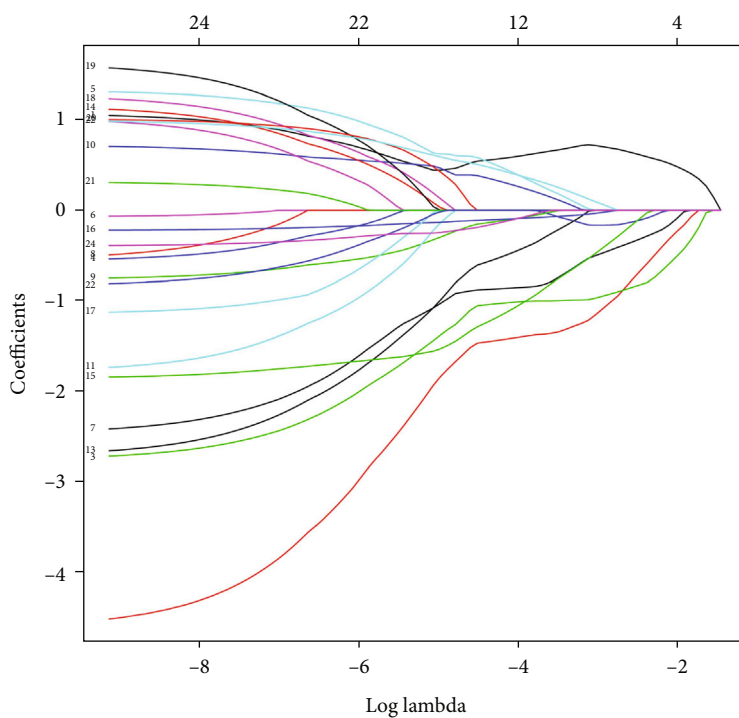
(b)

FIGURE 2: Continued.

(c)

(d)

(e)

FIGURE 2: Continued.

(f)

(g)

FIGURE 2: RBPs can well distinguish periodontally healthy and periodontitis samples. (a) Univariate logistic regression analysis was performed on 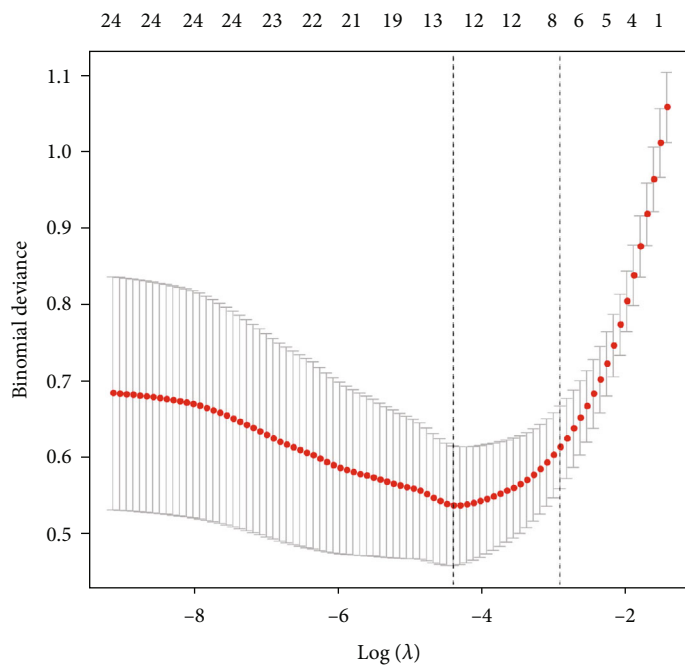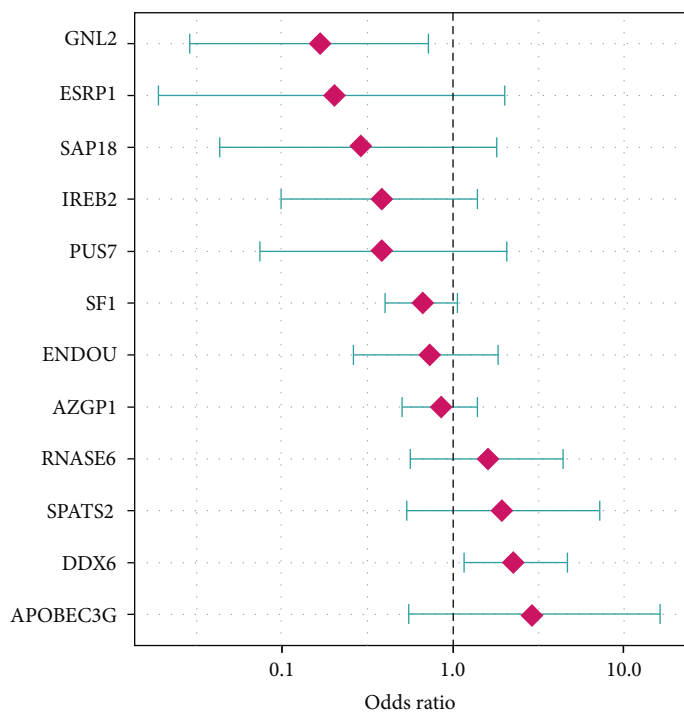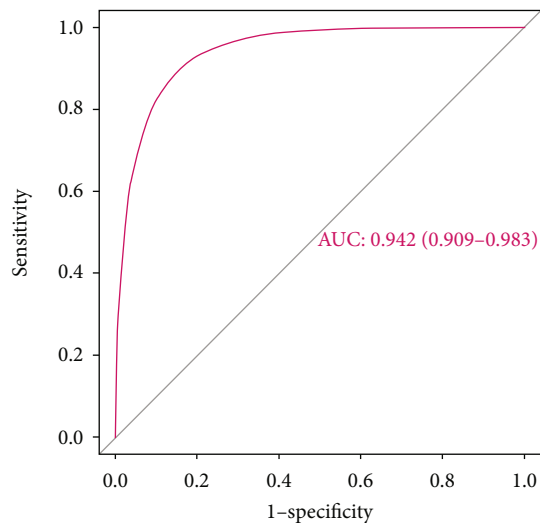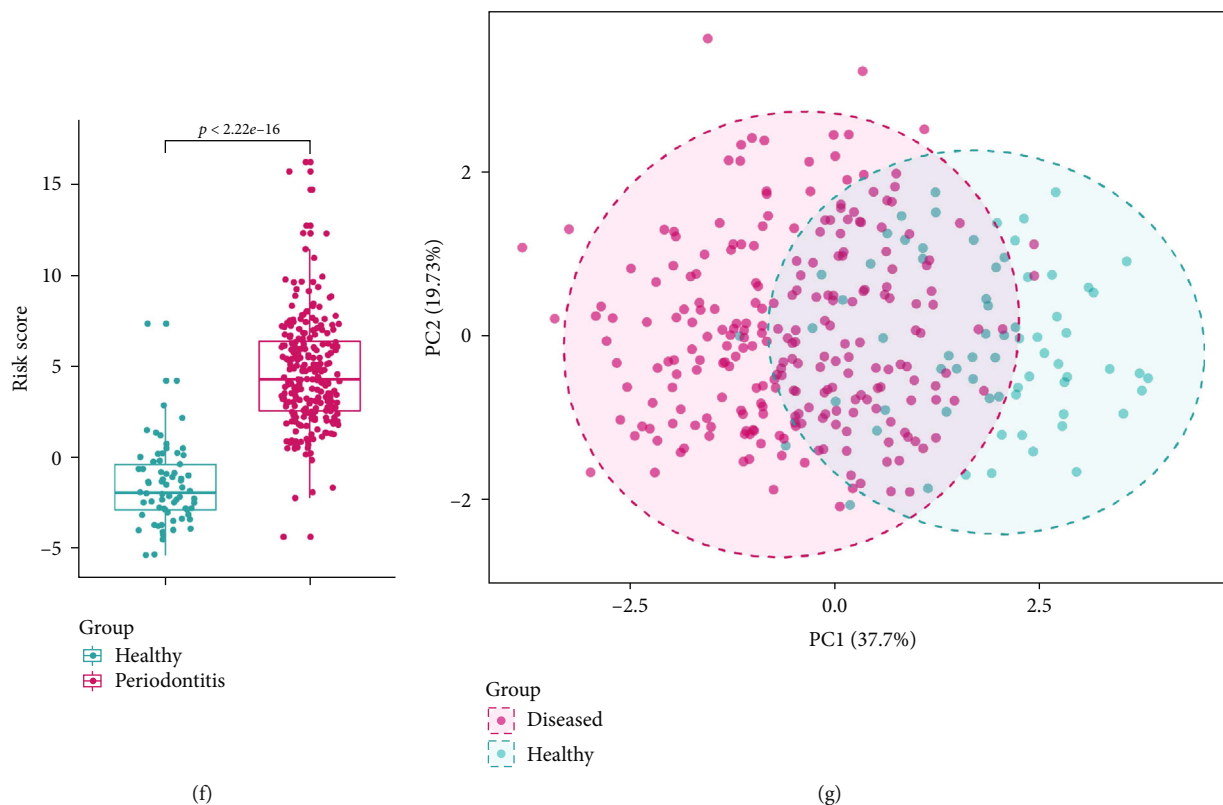the 24 dysregulated RBPs. (b) Least absolute shrinkage and selection operator (LASSO) regression coefficients of the 24 dysregulated RBPs. (c) Tenfold crossvalidation for tuning parameter selection in LASSO regression. The partial likelihood deviance is plotted against $\log(\lambda)$, where λ is the tuning parameter. Partial likelihood deviance values are shown, with error bars representing SE. The dotted vertical lines are drawn at the optimal values by minimum criteria and 1-SE criteria. (d) Multivariate logistic regression analysis was performed to establish a 12-RBP classifier. (e) Receiver operating characteristic (ROC) analysis evaluated the discrimination ability of the 12-RBP classifier. (f) Risk score distribution of periodontitis and periodontally healthy samples. (g) PCA analysis of the periodontitis and periodontally healthy samples based on the expression of the 12 RBPs.

to the manufacturer's instructions [16]. The data was reserved in the GEO database under the serial number GSE16134 (https://www.ncbi.nlm.nih.gov/geo/query/acc.cgi?acc=gse16134) and obtained by the R package "GEOquery." CEL files in the series were processed by "RMA" package in R with "justRMA" function under default parameters. Probes were annotated as gene symbols, and probes without matching gene symbols or had multiple matching gene symbols were excluded. Expressions of duplicate genes were calculated as the median value. Normalization of the gene expression was processed by "normalizeBetweenArrays" in the R package "limma." The 1542 RBP gene list used in this study was obtained from a previous research screening for human RBPs [15] R version: 3.6.1. The overall regulatory mechanisms of RBPs in the immune microenvironment of periodontitis were presented in the graphical abstract which was created with http://biorender.com/.

3.2. Identification of Dysregulated RBPs and the Construction of the RBP Classifier. Dysregulated RBPs were evaluated by the "limma" package with adjust p value < 0.01 and | logFoldChange | >0.5. The protein-protein network of the dysregulated RBPs was constructed by the online database STRING (https://string-db.org/). Correlation analyses of the

dysregulated RBPs as well as other correlation analysis in this study were conducted by the Spearman correlation analysis. Univariate logistic regression, LASSO regression, and multivariate logistic regression were used to establish the 12-RBP classifier and receiver operating characteristic (ROC) analyses were used to evaluate its classification ability.

3.3. Quantitative Evaluation of Immune Microenvironment in Periodontitis. The evaluation of the overall status of immune infiltration in periodontitis and healthy samples was conducted using the same method as we have illustrated in the previous study, and the results were consistent [17, 18]. In brief, single-sample Gene Set Enrichment Analysis (ssGSEA) was conducted to evaluate the relative enrichment score of immunocytes and the activity of immune-related pathways. The gene sets used in ssGSEA for immune-related pathway evaluation were from the online database Immport (http://www.immport.org) [19]. The comparisons of relative enrichment score of immunocytes [20], activity of immune-related pathways, and expression of HLA between periodontitis and periodontally healthy samples were conducted using Wilcox test; $p < 0.05$ was considered to be significant.
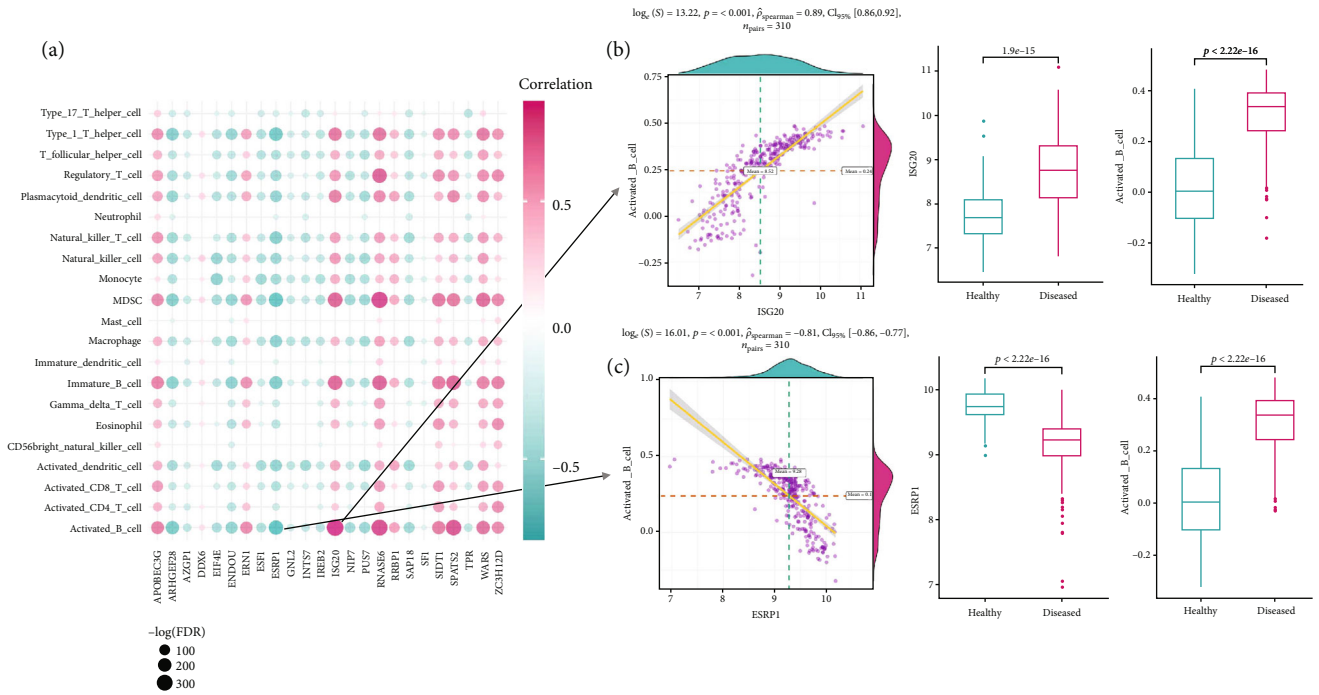
Figure 3: Immunocyte infiltration status in periodontitis and their correlation with RBPs. (a) Correlation analysis between relative enrichment score of immunocytes and RBP expression levels. (b) Dot plot and box plot reveal the relationship between the most positively correlated immunocyte-RBP pair, activated_B_cell, and ISG20, with a higher enrichment score of activated_B_cell and higher expression of ISG20 in periodontitis samples. (c) Dot plot and box plot reveal the relationship between the most negatively correlated immunocyte-RBP pair, activated_B_cell, and ESRP1. A higher enrichment score of activated_B_cell and lower expression of ESRP1 were observed in periodontitis samples.
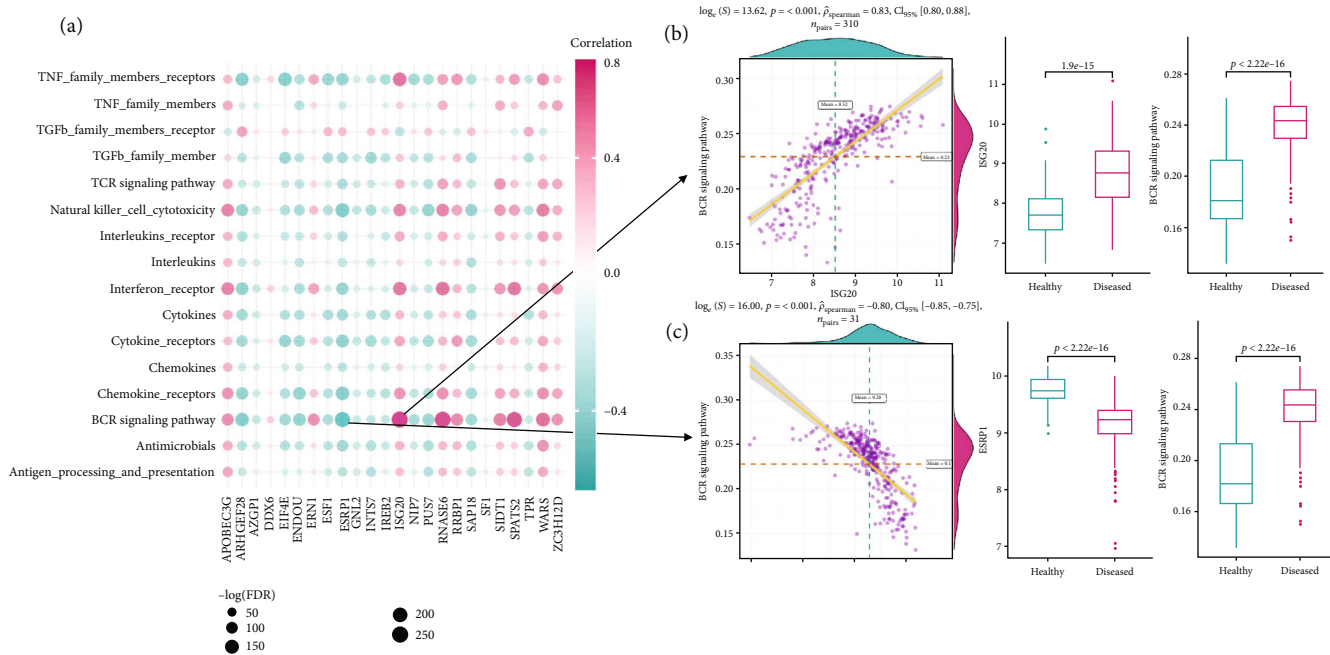
Figure 4: Immune-related pathways in periodontitis and their correlation with RBPs. (a) Correlation analysis between activities of immune pathways and RBPs expression levels. (b) Dot plot and box plot reveal the relationship between the most positively correlated immune pathway-RBP pair, BCR signaling pathway, and ISG20. A higher activity of BCR signaling pathway and higher expression of ISG20 were observed in periodontitis samples. (c) Dot plot and box plot reveal the relationship between the most negatively correlated immune pathway-RBP pair, BCR signaling pathway, and ESRP1. A higher activity of BCR signaling pathway and lower expression of ESRP1 were observed in periodontitis samples.

FIGURE 5: HLA expression status in periodontitis and their correlation with RBPs. (a) Correlation analysis between HLA and RBP expression levels. (b) Dot plot and box plot reveal the relationship between the most positively correlated HLA-RBP pair, HLA-DOB, and ISG20. Higher expressions of HLA-DOB and ISG20 were observed in periodontitis samples. (c) Dot plot and box plot reveal the relationship between the most negatively correlated HLA-RBP pair, HLA-DOB, and ESRP1. Higher expression of HLA-DOB and lower expression of ESRP1 were observed in periodontitis samples.

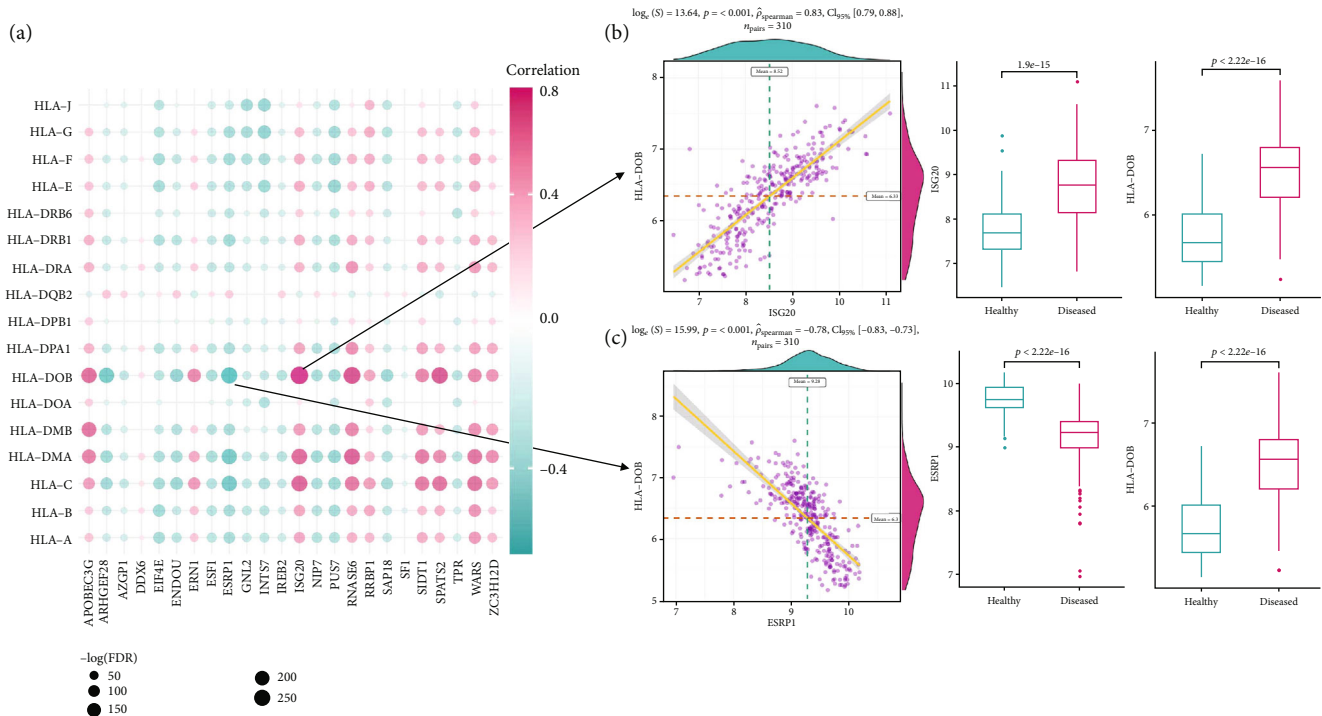*3.4. Identification of RBP Regulatory Patterns.* Based on the expressions of the 1542 RBP genes, the periodontitis samples were clustered into two subtypes using unsupervised clustering analysis. The cluster numbers and robustness were evaluated by consensus clustering algorithm [20, 21]. The R package "ConsensuClusterPlus" was used to conduct the steps described above for 1000 iterations in order to guarantee the robustness of the clustering [22]. The comparisons of relative enrichment score of immunocytes, activity of immune-related pathways, and expression of HLA between the two subtypes were conducted using the Wilcoxon test.

3.5. Biological Functions of the Two RBP Regulatory Patterns. Hallmarks and KEGG pathways were used to summarize the biological functions and distinction of the two RBP regulatory patterns. Gene Set Variation Analysis was used to evaluate enrichment levels, and the R package "limma" was used to compare between the two subtypes. Pathways with p value < 0.01 were considered to be significant. The gene sets were from "h.all.v7.0.symbols" and "c2.cp.kegg.v7.0.symbols" which were downloaded from the MSigDB database. The GO-BP enrichment analysis of the RBP phenotype-related genes and immune genes was conducted by the "clusterProfiler" package. In addition, to identify gene modules related to RBP regulatory patterns, weighted gene coexpression network analysis (WGCNA) was employed on periodontitis samples using "WGCNA" package. Correlation analysis between gene modules and subtypes was conducted with the Pearson correlation analysis.

4. Discussion

Periodontitis is a complex infectious disease, and dysregulation of innate and adaptive immunity plays a key role in the etiology [23]. With more knowledge of RBP regulatory mechanisms, more evidences show that RBPs play a significant role in the initiation and regulation of immune responses [24]. Our study identified 24 significantly dysregulated RBPs to distinguish periodontitis from periodontally healthy samples, with 12 of them selected to compose a molecular classifier for periodontitis, and revealed two RBP regulatory subtypes corresponding to distinct immunophenotypes in periodontitis, with two gene modules significantly correlated with the division of the two subtypes. It is by far the first evidence on systematic evaluation of the role of RPBs in the immune microenvironment in periodontitis.

In this study, the immune microenvironment of periodontitis was found to be characterized by increased infiltration of immunocytes, higher activities of immune-related pathways, and upregulated HLA expression, among which, activated B cells, BCR signaling pathway, and HLA-DOB were ones of those showing the most significant difference from periodontally healthy samples, as well as being significantly upregulated in the subtype of periodontitis with more
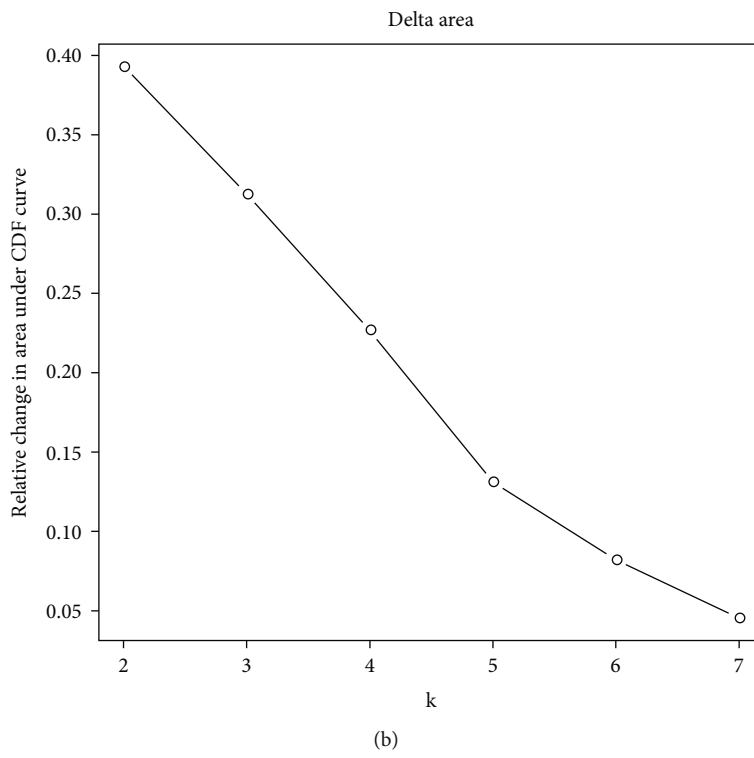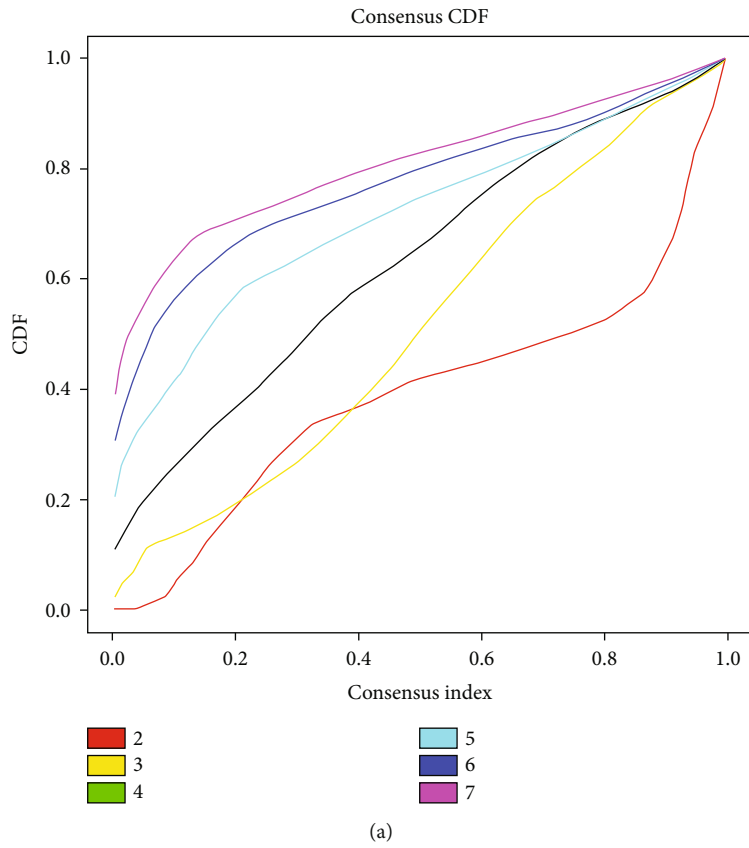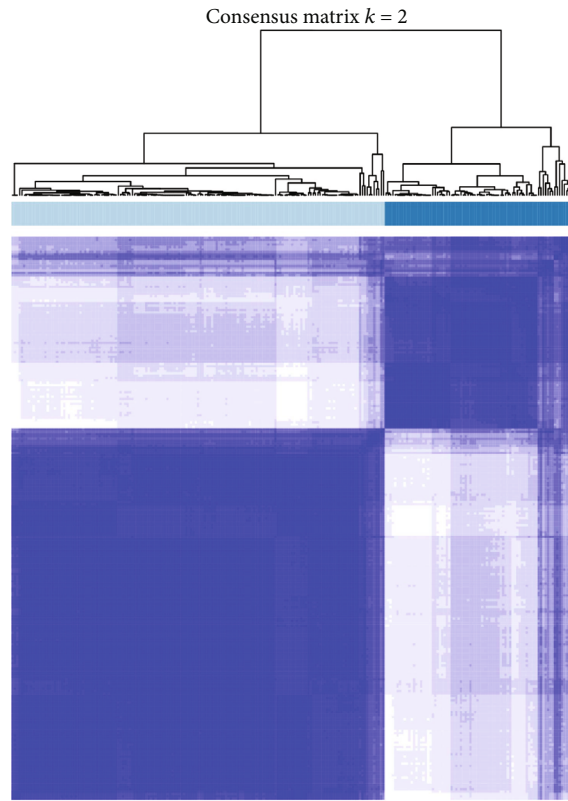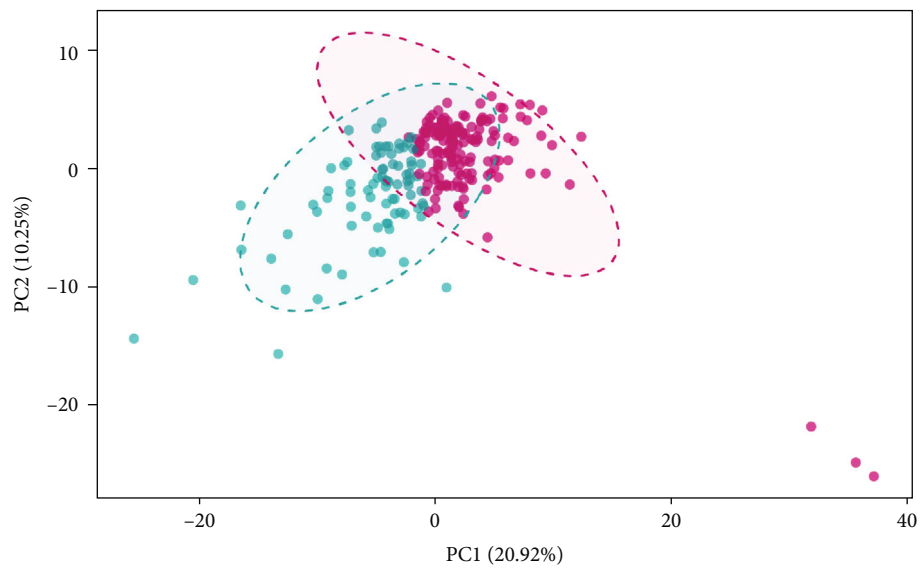
Consensus CDF

(a)

(b)

Figure 6: Continued.
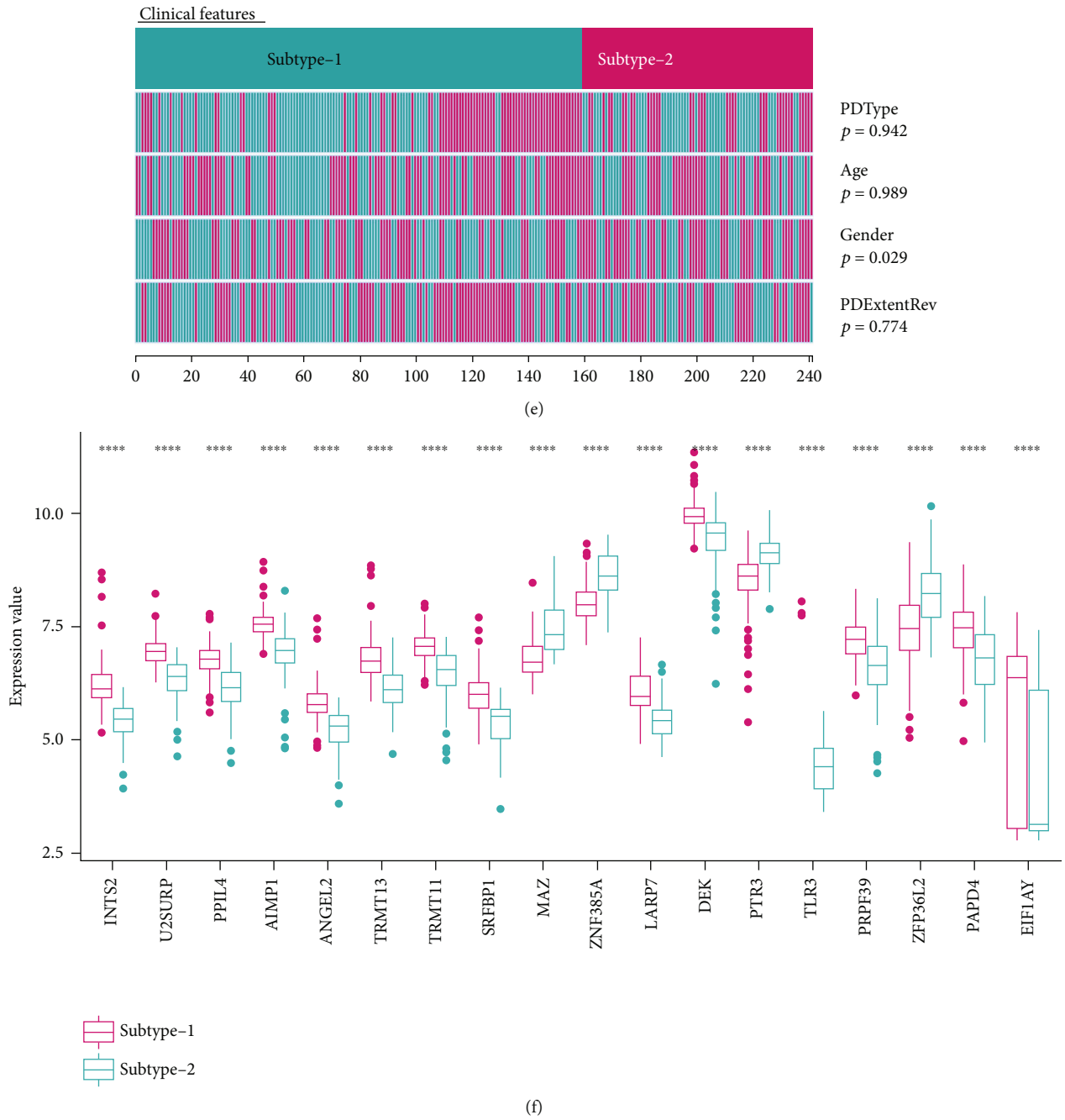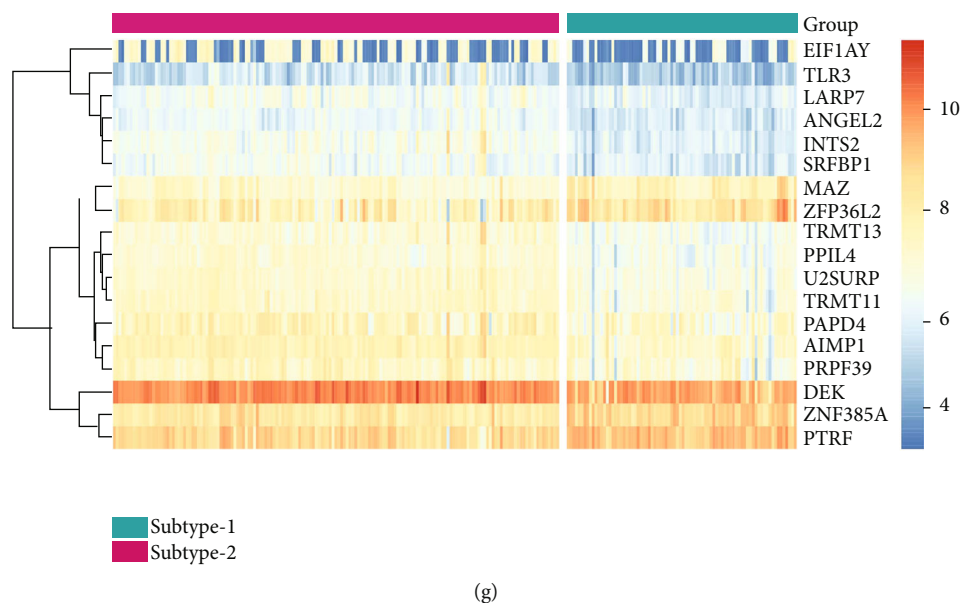
(c)

(d)

Figure 6: Continued.

(e)

(f)

Figure 6: Continued.

(g)

FIGURE 6: Unsupervised clustering of periodontitis samples based on the RBP expression. (a) Consensus clustering cumulative distribution function (CDF) for $k = 2$–7. (b) Relative change in area under the CDF curve for $k = 2$–7. (c) Heatmap of the matrix of cooccurrence proportions for periodontitis samples. (d) Principle component analysis (PCA) of the two RBP regulatory subtypes. (e) Clinical features of the two RBP regulatory subtypes. (f) Expression of subtype-specific RBPs. The subtype-specific RBPs were the differentially expressed RBPs between the two RBP regulatory subtypes (adjust p value < 0.01, $|logFC| > 0.6$). (g) Heatmap of the expression of subtype-specific RBPs.

intense immune reactions. Interestingly, those three were also the ones having the most significant correlations with RBP expressions. Paired with the immune characteristics above, the most strongly correlated RBPs were ISG20 and ESRP1, suggesting that ISG20 and ESRP1 might have potent impact on the immune microenvironment in periodontitis.

ISG20 (interferon-stimulated exonuclease gene 20) responds to interferon and exerts its antiviral abilities by binding to single-stranded RNA and acts as exonuclease to degrade viral RNAs. It mainly targets RNA viruses including hepatitis C virus (HCV), hepatitis A virus (HAV), and yellow fever virus (YFV) [25]. Higher expression of ISG20 was associated with suppressed adaptive immune responses, increased infiltration of monocyte-derived macrophages and neutrophils, higher tumor grade, and poorer clinical outcome in glioma [26]. In chronic periodontitis, researchers detected aberrantly upregulated ISG20 genes in monocytes stimulated by LPS from *Porphyromonas gingivalis* [27]. ESRP1 encodes a mRNA splicing factor that regulates the formation of epithelial cell-specific isoforms [28]. In melanoma, patients with a lower expression of ESRP1 expressed mesenchymal markers and higher level of immune cytolytic activity and experienced better survival rate [29]. In our study, ISG20 was found to be highly positively correlated with activated B cell infiltration, BCR signaling activity, and HLA-DOB expression, while ESRP1 was highly negatively correlated with the above. In periodontitis, B cells initiate immune responses by producing antibodies against periodontal pathogens, and activated B cells could serve as antigen presenting cells towards CD4+ and CD8+ T cells [30]. In individuals more susceptible to periodontitis, B cells exhibited more autoreactive properties [31]. HLA-DOB belongs to the MHC class II beta chain which forms

HLA-DO to interact with HLA-DM on B cells in the antigen presentation process [32]. The strong associations among ISG20, ESRP1 and activated B cell, BCR signaling pathway, and HLA-DOB in periodontitis were first identified in our study. Our findings might help to reveal the pathogenesis of periodontitis in the perspective of RBP-related molecular biology and to find novel immune therapeutic target for periodontitis.

Two RBP regulatory subtypes of periodontitis we have identified exhibited distinct immune profiles, with subtype-2 having increased infiltration of immunocytes, and higher activities of immune-related pathways and expressions of HLA compared with subtype-1, indicating more intense immune reactions in subtype-2. Furthermore, GSVA and functional enrichment analyses revealed other biological distinctions between the two RBP regulatory subtypes aside from the immune aspects. This RBP-based clustering method not only gave distinct division of immunophenotypes, but also sorted out different biological profiles in periodontitis. The possible associations among the RBPs, immunophenotypes, and other biological signaling are of interest for further investigations.

Since RBP regulatory subtypes have been linked with distinct periodontal immune microenvironment and biological profiles, comparing the clinical information between the subtypes is meaningful and worthwhile. However, a limitation of this study was insufficient information on clinical features (only gender, age, and PD type were recorded). Therefore, this comparison could not reflect the entire profile of clinical characteristics. We found a significant difference in gender between the two RBP regulatory subtypes, indicating that individuals of different genders might have different RBP regulatory patterns, corresponding to different periodontal
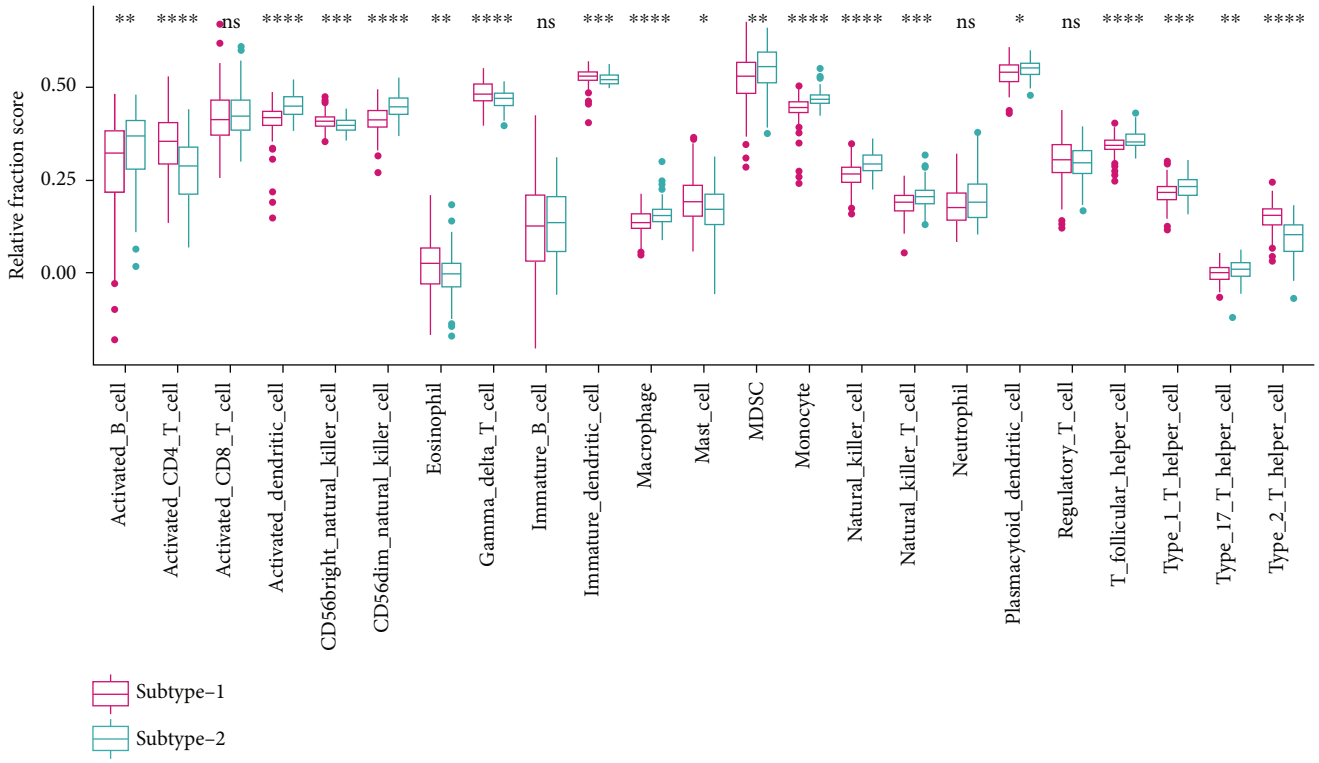
(a)
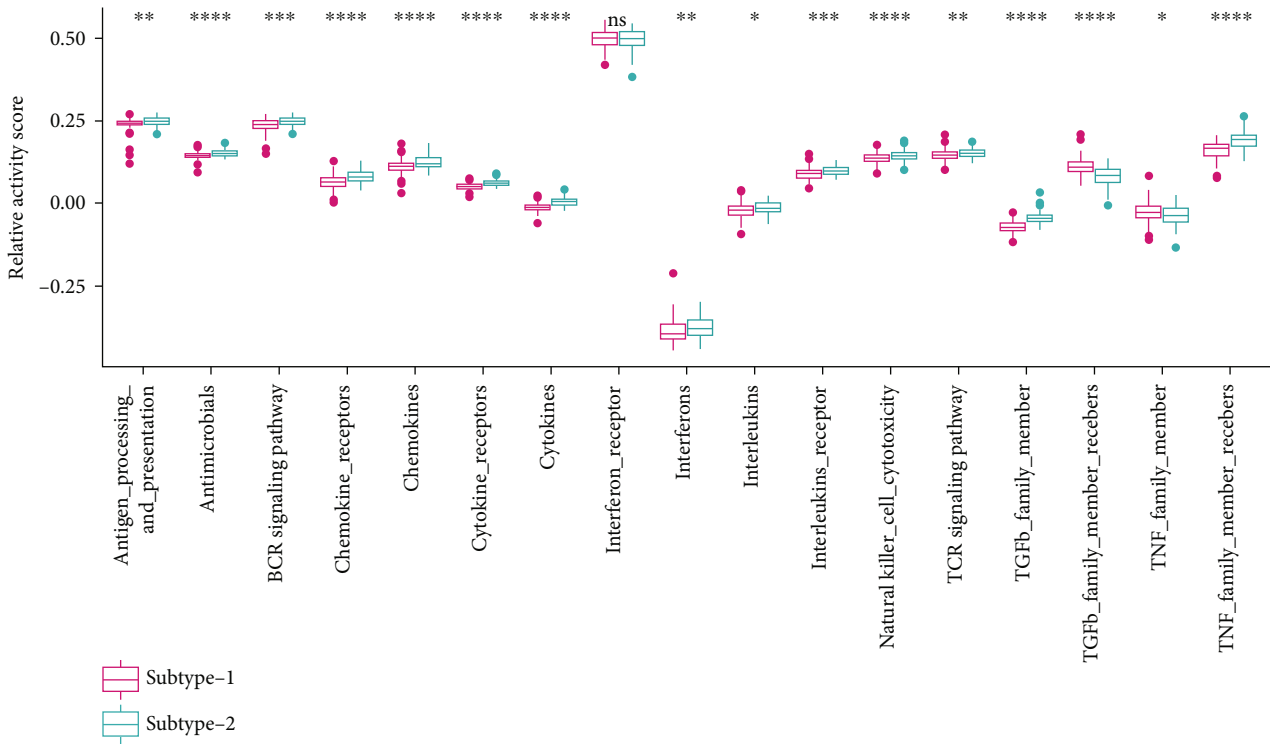
(b)

FIGURE 7: Continued.

(c)
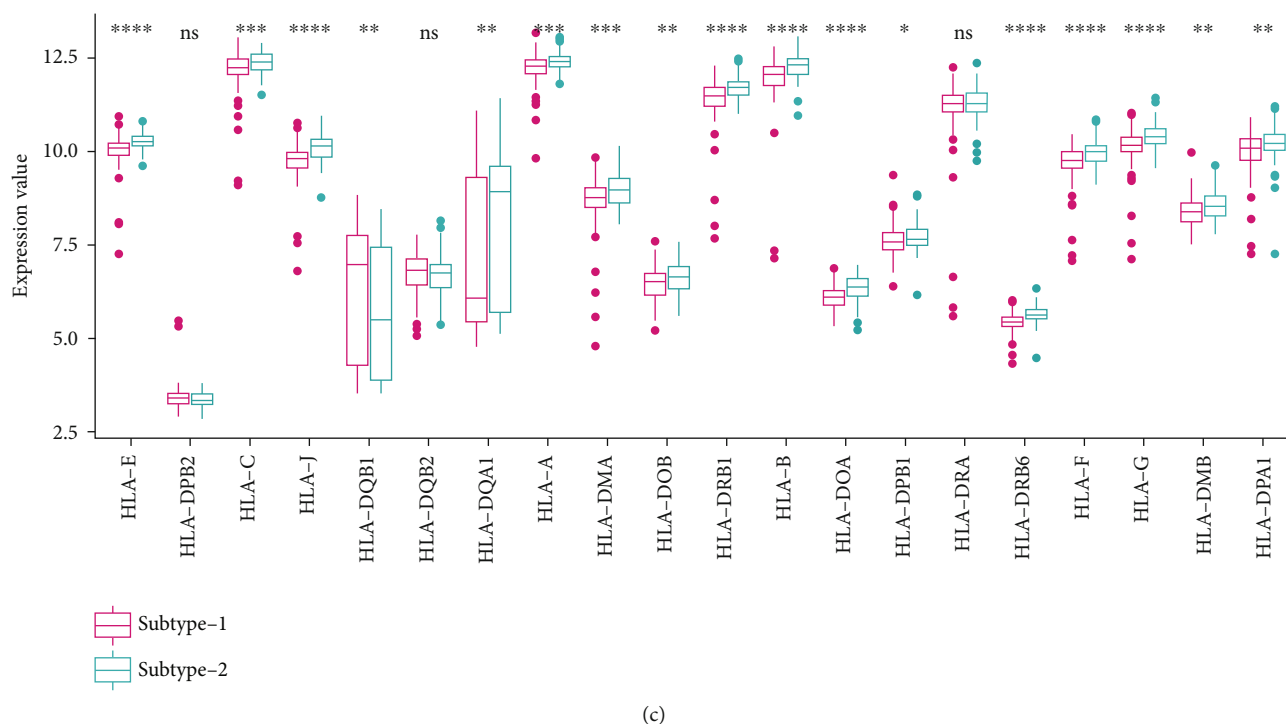
Figure 7: Immune characteristics in the two RBP regulatory subtypes. (a) Immunocyte infiltration status in the two RBP regulatory subtypes. (b) Activity of immune pathways in the two RBP regulatory subtypes. (c) HLA expression levels in the two RBP regulatory subtypes.

immune phenotypes, and possibly associated with distinct genetic susceptibility to periodontitis. More information on clinical phenotype and prognosis are expected to draw further conclusions.

5. Conclusion

Our study depicted the correlations among RBPs and immune microenvironment and biological reactions in periodontitis, with strong correlations of the RBPs ISG20 and ESRP1 with activated B cell infiltration, BCR signaling activation, and HLA-DOB expression. These findings indicated that RBP-mediated regulation of immune microenvironment as an important mechanism in the pathogenesis of periodontitis, which might inspire development of new therapeutic approaches.

Data Availability

The data that support the findings of this study are available in https://www.ncbi.nlm.nih.gov/geo/query/acc.cgi?acc=gse16134.

Conflicts of Interest

The authors declare no conflict of interest.

Authors' Contributions

Lu Xing and Hui Xu performed conceptualization. Guanqun Meng and Hui Xu curated the data. Lu Xing and Hui Xu performed the formal analysis. Ding Bai and Hui Xu acquired

Supplementary Materials

Supplementary figures (FigureS1-S3) were uploaded entitled "supplementary figures.docx." Supplementary tables (Table S1-S12) were uploaded entitled "Table S1: significantly dysregulated RBPs .txt." "Table S2: results of univariate logistic regression.txt." "Table S3: results of multivariate logistic regression.txt." "Table S4: diversity of immunocytes between healthy and periodontitis samples.txt." "Table S5: correlation analysis between immnuocytes and RBPs.txt." "Table S6: diversity of immune pathways between healthy and periodontitis samples.txt." "Table S7: Correlations between RBPs and immune pathways.txt." "Table S8: diversity of HLA expression

between healthy and periodontitis samples.txt." "Table S9: correlation between RBPs and HLA expression.txt." "Table S10: RBP regulatory subtypes.txt." "Table S11: RBP regulatory subtype related genes.txt." "Table S12: gene significance and module membership.txt," respectively, with their filename indicating the contents of the tables. *(Supplementary Materials)*

References

[1] J. Slots, "Periodontitis: facts, fallacies and the future," *Periodontol 2000*, vol. 75, no. 1, pp. 7–23, 2017.

[2] M. A. Peres, L. M. D. Macpherson, R. J. Weyant et al., "Oral diseases: a global public health challenge," *Lancet*, vol. 394, no. 10194, pp. 249–260, 2019.

[3] K. Nasseh, M. Vujicic, and M. Glick, "The relationship between periodontal interventions and healthcare costs and utilization. Evidence from an integrated dental, medical, and pharmacy commercial claims database," *Health Economics*, vol. 26, no. 4, pp. 519–527, 2017.

[4] I. L. Chapple, R. Genco, and on behalf of working group 2 of the joint EFP/AAP workshop, "Diabetes and periodontal diseases: consensus report of the joint EFP/AAP Workshop on Periodontitis and Systemic Diseases," *Journal of Periodontology*, vol. 84, no. 4-s, pp. S106–S112, 2013.

[5] N. J. Kassebaum, E. Bernabé, M. Dahiya, B. Bhandari, C. J. Murray, and W. Marcenes, "Global burden of severe periodontitis in 1990-2010: a systematic review and meta-regression," *Journal of Dental Research*, vol. 93, no. 11, pp. 1045–1053, 2014.

[6] A. Cekici, A. Kantarci, H. Hasturk, and T. E. Van Dyke, "Inflammatory and immune pathways in the pathogenesis of periodontal disease," *Periodontol 2000*, vol. 64, no. 1, pp. 57–80, 2014.

[7] T. E. Van Dyke and C. N. Serhan, "Resolution of inflammation: a new paradigm for the pathogenesis of periodontal diseases," *Journal of Dental Research*, vol. 82, no. 2, pp. 82–90, 2003.

[8] J. Konig, K. Zarnack, N. M. Luscombe, and J. Ule, "Protein-RNA interactions: new genomic technologies and perspectives," *Nature Reviews. Genetics*, vol. 13, no. 2, pp. 77–83, 2012.

[9] W. Li, L. N. Gao, P. P. Song, and C. G. You, "Development and validation of a RNA binding protein-associated prognostic model for lung adenocarcinoma," *Aging (Albany NY)*, vol. 12, no. 4, article 102828, pp. 3558–3573, 2020.

[10] M. Turner and M. D. Diaz-Munoz, "RNA-binding proteins control gene expression and cell fate in the immune system," *Nature Immunology*, vol. 19, no. 2, pp. 120–129, 2018.

[11] M. D. Diaz-Muñoz, S. E. Bell, K. Fairfax et al., "The RNA-binding protein HuR is essential for the B cell antibody response," *Nature Immunology*, vol. 16, no. 4, pp. 415–425, 2015.

[12] O. Papadaki, S. Milatos, S. Grammenoudi, N. Mukherjee, J. D. Keene, and D. L. Kontoyiannis, "Control of thymic T cell maturation, deletion and egress by the RNA-binding protein HuR," *Journal of Immunology*, vol. 182, no. 11, pp. 6779–6788, 2009.

[13] N. Sadri, J. Y. Lu, M. L. Badura, and R. J. Schneider, "AUF1 is involved in splenic follicular B cell maintenance," *BMC Immunology*, vol. 11, no. 1, p. 1, 2010.

[14] K. Ouhara, S. Munenaga, M. Kajiya et al., "The induced RNA-binding protein, HuR, targets 3'-UTR region of IL-6 mRNA

[15] S. Gerstberger, M. Hafner, and T. Tuschl, "A census of human RNA-binding proteins," *Nature Reviews. Genetics*, vol. 15, no. 12, pp. 829–845, 2014.

[16] M. Kebschull, R. T. Demmer, B. Grun, P. Guarnieri, P. Pavlidis, and P. N. Papapanou, "Gingival tissue transcriptomes identify distinct periodontitis phenotypes," *Journal of Dental Research*, vol. 93, no. 5, pp. 459–468, 2014.

[17] X. Zhang, S. Zhang, X. Yan et al., "m6A regulator-mediated RNA methylation modification patterns are involved in immune microenvironment regulation of periodontitis," *Journal of Cellular and Molecular Medicine*, vol. 25, no. 7, pp. 3634–3645, 2021.

[18] X. Zhang, Y. Jin, Q. Wang et al., "Autophagy-mediated regulation patterns contribute to the alterations of the immune microenvironment in periodontitis," *Aging (Albany NY)*, vol. 13, no. 1, article 202165, pp. 555–577, 2020.

[19] S. Bhattacharya, S. Andorf, L. Gomes et al., "ImmPort: disseminating data to the public for the future of immunology," *Immunologic Research*, vol. 58, no. 2-3, pp. 234–239, 2014.

[20] B. Zhang, Q. Wu, B. Li, D. Wang, L. Wang, and Y. L. Zhou, "m6A regulator-mediated methylation modification patterns and tumor microenvironment infiltration characterization in gastric cancer," *Molecular Cancer*, vol. 19, no. 1, article 1170, p. 53, 2020.

[21] R. C. Chai, F. Wu, Q. X. Wang et al., "m6A RNA methylation regulators contribute to malignant progression and have clinical prognostic impact in gliomas," *Aging (Albany NY)*, vol. 11, no. 4, article 101829, pp. 1204–1225, 2019.

[22] M. D. Wilkerson and D. N. Hayes, "ConsensusClusterPlus: a class discovery tool with confidence assessments and item tracking," *Bioinformatics*, vol. 26, no. 12, pp. 1572-1573, 2010.

[23] J. L. Ebersole, D. Dawson 3rd, P. Emecen-Huja et al., "The periodontal war: microbes and immunity," *Periodontol 2000*, vol. 75, no. 1, pp. 52–115, 2017.

[24] M. D. Diaz-Munoz and M. Turner, "Uncovering the role of RNA-binding proteins in gene expression in the immune system," *Frontiers in Immunology*, vol. 9, p. 1094, 2018.

[25] L. H. Nguyen, L. Espert, N. Mechti, and D. M. Wilson 3rd., "The human interferon- and estrogen-regulated ISG20/HEM45 gene product degrades single-stranded RNA and DNA in vitro," *Biochemistry*, vol. 40, no. 24, pp. 7174–7179, 2001.

[26] M. Gao, Y. Lin, X. Liu et al., "ISG20 promotes local tumor immunity and contributes to poor survival in human glioma," *Oncoimmunology*, vol. 8, no. 2, article e1534038, 2018.

[27] L. Gölz, B. C. Buerfent, A. Hofmann et al., "Genome-wide transcriptome induced by Porphyromonas gingivalis LPS supports the notion of host-derived periodontal destruction and its association with systemic diseases," *Innate Immunity*, vol. 22, no. 1, pp. 72–84, 2016.

[28] C. C. Warzecha, T. K. Sato, B. Nabet, J. B. Hogenesch, and R. P. Carstens, "ESRP1 and ESRP2 are epithelial cell-type-specific regulators of FGFR2 splicing," *Molecular Cell*, vol. 33, no. 5, pp. 591–601, 2009.

[29] J. Yao, O. L. Caballero, Y. Huang et al., "Altered expression and splicing of ESRP1 in malignant melanoma correlates with epithelial-mesenchymal status and tumor-associated immune cytolytic activity," *Cancer Immunology Research*, vol. 4, no. 6, pp. 552–561, 2016.

[30] J. R. Gonzales, "T- and B-cell subsets in periodontitis," *Periodontol 2000*, vol. 69, no. 1, pp. 181–200, 2015.

[31] T. Berglundh, B. Liljenberg, A. Tarkowski, and J. Lindhe, "The presence of local and circulating autoreactive B cells in patients with advanced periodontitis," *Journal of Clinical Periodontology*, vol. 29, no. 4, pp. 281–286, 2002.

[32] T. Yoon, H. Macmillan, S. E. Mortimer et al., "Mapping the HLA-DO/HLA-DM complex by FRET and mutagenesis," *Proceedings of the National Academy of Sciences of the United States of America*, vol. 109, no. 28, pp. 11276–11281, 2012.

Review Article

An Update on the Pathogenic Role of Macrophages in Adult-Onset Still's Disease and Its Implication in Clinical Manifestations and Novel Therapeutics

Po-Ku Chen[1,2,3] **and Der-Yuan Chen** [iD] [1,2,3,4]

[1]*Rheumatology and Immunology Center, China Medical University Hospital, Taichung, Taiwan*
[2]*College of Medicine, China Medical University, Taichung, Taiwan*
[3]*Translational Medicine Laboratory, Rheumatology and Immunology Center, Taichung, Taiwan*
[4]*Ph.D. Program in Translational Medicine and Rong Hsing Research Center for Translational Medicine, National Chung
 Hsing University, Taichung, Taiwan*

Correspondence should be addressed to Der-Yuan Chen; dychen1957@gmail.com

Increasing evidence indicates a pivotal role of macrophages in innate immunity, which contributes to the pathogenesis of adult-onset Still's disease (AOSD). Despite the available reviews that summarized the pathogenic role of proinflammatory cytokines in AOSD, a systematic approach focusing on the crucial role of macrophages in this disease is still lacking. This review summarizes the updated functions of macrophages in AOSD and their implication in clinical manifestations and therapeutics. We searched the MEDLINE database using the PubMed interface and reviewed the English-language literature as of 31 March 2021, from 1971 to 2021. We focus on the existing evidence on the pathogenic role of macrophages in AOSD and its implication in clinical characteristics and novel therapeutics. AOSD is an autoinflammatory disease mainly driven by the innate immune response. Among the innate immune responses, macrophage activation is a hallmark of AOSD pathogenesis. The pattern recognition receptors (PRRs) on macrophages recognize pathogen-associated molecular patterns and damage-associated molecular patterns and subsequently cause overproduction of proinflammatory cytokines and recruit adaptive immunity. Some biomarkers, such as ferritin and gasdermin D, reflecting macrophage activation were elevated and correlated with AOSD activity. Given that macrophage activation with the overproduction of proinflammatory cytokines plays a pathogenic role in AOSD, these inflammatory mediators would be the therapeutic targets. Accordingly, the inhibitors to interleukin- (IL-) 1, IL-6, and IL-18 have been shown to be effective in AOSD treatment. Gaining insights into the pathogenic role of macrophages in AOSD can aid in identifying disease biomarkers and therapeutic agents for this disease.

1. Introduction

Adult-onset Still's disease (AOSD) is a systemic inflammatory disorder characterized by fever, rash, arthritis, liver dysfunction, lymphadenopathy, variable multisystemic involvement, hyperferritinemia, and even life-threatening complications such as macrophage activation syndrome (MAS) [1–4]. AOSD is a rare but important cause of fever of unknown origin [5]. The reported incidence rates of AOSD were 0.16, 0.22, and 0.4 per 100,000 persons in west

France [6], Japan [7], and northern Norway [8], respectively. It is considered an autoinflammatory disease (AID) due to its characteristic phenotypes and the absence of detectable autoantibodies [9]. The innate immune system encompasses the germline-encoded pattern recognition receptors (PRRs), including Toll-like receptors (TLRs) and cytosol-expressed nucleotide-binding oligomerization- (NOD-) like receptors (NLRs) [10], which may drive autoinflammation with unknown etiology. Increasing evidence indicates a pivotal role of macrophage activation in the innate immune response

with subsequent inflammatory reactions [11], giving rise to the clinical manifestations of AOSD. Moreover, proinflammatory cytokines such as interleukin- (IL-) 1β, IL-6, IL-18, and tumor necrosis factor- (TNF-) α play a pathogenic role in AOSD [12–18], leading to an implication of new targeted therapies [19–22]. Therefore, the biologics targeting IL-1, IL-6, or IL-18 have been proven effective in the treatment of AOSD [23–28].

With increasing evidence indicating an immunopathogenesis of AOSD, which is attributable to significant advances in using therapeutic targets for AOSD, this review is aimed at summarizing the current research results regarding the pathogenic role of macrophage activation in AOSD and its clinical implication in clinical characteristics and therapeutics.

2. Materials and Methods

2.1. Literature Search. The present review focuses on the existing evidence on the pathogenic role of the macrophage activation and cytokine storm in AOSD and its clinical implication in therapeutics. We searched the MEDLINE database using the PubMed interface and reviewed the English-language literature as of 31 March 2021, from 1971 to 2021. The search keywords for this updated review included macrophage, innate immunity, immune response, inflammation, pathogenesis, trigger factors, pathogen-associated molecular patterns (PAMPs), damage-associated molecular patterns (DAMPs), TLRs, inflammasomes, proinflammatory cytokines, cytokine storm, MAS, clinical manifestations, AOSD, autoinflammatory disorders, clinical implication, disease activity, and therapeutic strategies. The relevant drugs include corticosteroids, nonsteroidal anti-inflammatory drugs (NSAIDs), conventional synthetic disease-modifying antirheumatic drugs (csDMARDs), biologic DMARDs (bDMARDs), and targeted synthetic DMARDs (tsDMARDs), mainly Janus kinase (JAK) inhibitors.

2.2. Study Selection. Two authors (PK Chen and DY Chen) independently assessed the titles and abstracts of articles identified by the literature search and retrieved the relevant full-text articles. Both authors also evaluated the full-text articles for eligibility and examined the selected articles' references for reference. We selected articles if they (1) were probably relevant to the pathogenic role of macrophages or macrophage-derived cytokines in AOSD and (2) were potentially relevant to therapeutic agents targeting macrophage-related cytokines in AOSD. Both authors extracted data from these studies electronically. Our emphasis is on the updated role of macrophages in the pathogenesis of AOSD and the clinical implication in therapeutics by targeting the mediators involved in AOSD pathogenesis.

3. Results

3.1. Roles of Macrophage Activation in the Innate Immune Responses. The innate immune system provides an early defense to protect the host from invading foreign pathogens, endogenous danger signals, and allergens [29]. The cells (monocytes, macrophages, neutrophils, natural killer cells, and dendritic cells) of innate immunity play a crucial role in maintaining immune homeostasis by recognizing and removing pathogens. These cells interact with the adaptive immune system through cytotoxic reaction or production of antigen-specific antibodies and cytokines [30]. By the real-time imaging platform, Kapellos et al. revealed that bone marrow-derived macrophage priming with Th2 cytokines such as IL-4 and IL-10 resulted in higher phagocytic function compared with M1 polarization [31]. Macrophages promote tissue homeostasis through regulatory and repair functions [32] and could be divided into classically activated macrophages, wound healing or tissue repairing macrophages, and regulatory macrophages based on three different homeostatic activities [33]. Host-derived DAMPs released from damaged tissue, dying cells, or pathogen infections can be recognized by PRRs on macrophages and subsequently initiate an immune reaction [30, 33–34]. TLRs are well known as a type of PRRs that mediate PAMP and DAMP recognition. Upon PAMP and DAMP recognition, TLRs recruit adapter molecules such as myeloid differentiation primary response 88 (MyD88), activate the downstream signal cascade through NF-κB, and drive proinflammatory cytokine expression [35]. The NLRs are a family of intracellular sensors to mediate innate immunity and inflammation. NLRP (nucleotide-binding oligomerization domain, leucine-rich repeat, and pyrin domain) can form multimeric protein complexes in response to stimuli. The assembly of NLRP inflammasomes triggers cascade-1 activation to convert pro-IL-1β and pro-IL-18 into mature IL-18 [36–37]. NLRP inflammasomes can be activated by PAMPs such as microbial toxins and whole pathogens, including bacterial, viral, and fungal [38]. They can also recognize danger molecules such as ATP, extracellular glucose, crystals of monosodium urate, and calcium oxalate crystals [39–42]. These observations suggest that the macrophages can be activated through the recognition of various PAMPs and DAMPs by different types of PRRs.

3.2. Pathogenic Role of Innate Immunity in AOSD

3.2.1. Triggering Factors of Innate Immunity in AOSD. The exact etiology of AOSD is not fully understood, although various infections, mainly viral infections, have been suggested as possible causative agents [43]. The reported infectious triggers, so-called PAMPs, include cytomegalovirus (CMV), parvovirus B19, Epstein-Barr virus, rubella virus, *Measles morbillivirus*, hepatitis virus, influenza virus, adenovirus, human immunodeficiency virus, *Mycoplasma pneumonia*, and severe acute respiratory syndrome coronavirus 2 (SARS-CoV-2) emerging in late 2019 [43–55]. We demonstrated that parvovirus B19 nonstructural protein (NS)1 might induce IL-1β and IL-18 expression by activating NLRP3 inflammasomes in AOSD [56]. Jia et al. recently revealed that CMV DNA was found in the plasma of AOSD patients with new-onset disease or relapses, and CMV infection is strongly associated with the initiation/amplification of inflammation in AOSD [57]. Besides, Bamidis et al. reported a patient who suffered from sequelae of COVID-19 manifested as severe AOSD [55]. In consideration of infectious

triggers, innate immunity plays a crucial role in AOSD pathogenesis.

The DAMPs including advanced glycation end products (AGEs), high mobility group box-1 (HMGB1), soluble CD163 (sCD163), macrophage migration inhibitory factor (MIF), and neutrophil extracellular trap (NET) have been implicated in AOSD pathogenesis [1–2, 11, 58]. Accumulating evidence demonstrates a pathogenic role of advanced glycation end products (AGEs) in inflammation [59–60]. Chen et al. revealed that the AGE levels were elevated and correlated with activity scores and ferritin levels in AOSD patients [61], suggesting the involvement of AGEs in AOSD pathogenesis. HMGB1, a member of DAMPs, is released into the extracellular space from macrophages following inflammasome activation [62]. HMGB1 interacts with TLR2, TLR4, or the receptor for AGEs (RAGE) and mediates inflammatory response [63]. Jung et al. demonstrated that elevated HMGB1 levels were correlated with systemic scores and C-reactive protein (CRP) in AOSD patients and associated with skin rash and sore throat [64]. The sCD163, a heme receptor expressed on macrophages, is elevated and related to hyperferritinemia in AOSD patients [65]. MIF, a T lymphocyte-derived cytokine, inhibits random migration of macrophages [66–67] and reduces anti-inflammatory actions of corticosteroids [68]. Increasing evidence indicates that MIF is a proinflammatory cytokine that can upregulate the expression of proinflammatory mediators, including IL-1β, IL-2, IL-6, IL-8, TNF-α, IFN-γ, and prostaglandin E2 [69]. Serum MIF levels were elevated and correlated with disease activity in AOSD patients [70–71]. Zou et al. also revealed highly increased intracellular MIF in monocytes [70], suggesting that macrophages are activated in AOSD and supporting that AOSD is a disease of histiocyte-macrophage system activation [72–73]. Hu et al. showed that NET DNA from AOSD patients exerted a potent capacity to accelerate the activation of macrophages and increased the expression of IL-1β, IL-6, and TNF-α [74]. In summary, PAMPs or DAMPs can trigger an interplay between host genetic factors and macrophage activation, contributing to AOSD pathogenesis [1–2, 11, 58].

3.2.2. The Common Features of Macrophage Activation in COVID-19 and AOSD.

In response to COVID-19 infection, macrophages may be activated and produce proinflammatory cytokines, resulting in the development of systemic hyperinflammation, the so-called cytokine storm [75–76]. A variety of proinflammatory cytokines, such as IL-1β, IL-6, IL-8, and IFN-γ, were elevated in severe COVID-19 patients [77] and active AOSD patients [12–19], suggesting a common link of the cytokine storm in the pathogenesis of both diseases. Although Meng et al. recently revealed higher IL-6 and IL-10 in severe COVID-19 than in AOSD [78], a clear distinction of cytokine profiles between severe COVID-19 and active AOSD is challenging and needs to be explored in future studies.

3.2.3. Activated Macrophage-Related Mediators as the Disease Activity Indicators in AOSD.

PAMPs or DAMPs initiate macrophage activation through PRRs, including TLRs, NLRP3 inflammasomes [79–82], and C-type lectin domain family 5-member A (CLEC5A)/DAP12 complex, and subsequently cause the release of proinflammatory cytokines and activate an adaptive immune response [29, 83]. Virus sensing can trigger TLRs or activate the NLRP3 inflammasome, leading to inflammatory responses in AOSD [56, 84]. Hsieh et al. also revealed elevated expression of NLRP3 inflammasome signaling molecules, which was correlated with disease activity in AOSD patients [85]. Chen et al. demonstrated that the levels of CLEC5A-expressing monocytes were increased and correlated with disease activity and levels of IL-1β and IL-18 in AOSD patients [86].

It is well known that ferritin is a characteristic mediator of AOSD [1–3]. The activated macrophages can stimulate the release of ferritin, and elevated H-ferritin expressions in the lymph nodes and skin were correlated with the severity of AOSD [87–88]. Beyond its iron storage role, ferritin takes a pathogenic role in inflammation [89]. The synthesis of ferritin can be upregulated in response to inflammatory cytokines such as IL-1β and IL-6. Moreover, ferritin can stimulate inflammatory pathways to amplify the inflammatory process, supporting a hypothesis that ferritin may not only act as a bystander of acute-phase reaction [90]. Ferritin could be exported through the gasdermin D pole [91], and full-length gasdermin D is cleaved into the N-terminal p30 fragment upon activation of inflammasomes. The p30 fragment forms a pore in the cell membrane, through which the activated IL-1β and IL-18 are exported from the cell [92]. Recently, Nagai et al. showed that adults or children with Still's disease had elevated serum gasdermin D N-terminal levels correlated with ferritin and IL-18 [93]. Furthermore, the gasdermin D inhibitor could reduce the release of pyroptosis-mediated ferritin by macrophages. In summary, increased ferritin from macrophage activation was correlated with disease activity of AOSD and might serve as an activity indicator of this disease [94].

3.2.4. Inflammatory Reactions and the Related Manifestations of AOSD.

Sustained macrophage activation may lead to tissue inflammation with increased secretion of proinflammatory cytokines. After NLRP3 inflammasome activation, caspase enzymes induce the overproduction of IL-1β and IL-18, the hallmark cytokines of active AOSD [12–14, 16]. IL-1β and IL-18 further promote the secretion of proinflammatory cytokines, including IL-6, IL-8, IL-17A, and tumor necrosis factor- (TNF-) α [95–96]. IL-1β can also activate macrophages that play a crucial role in the cytokine storm or MAS [97–98]. In the skin, IL-18 is produced in keratinocytes, Langerhans cells, and dermal dendritic cells and may be related to the cutaneous manifestation of AOSD [99]. The locally activated macrophages in the liver produce a high amount of IL-18 and contribute to AOSD-related hepatitis [13, 100]. With this unique feature, IL-18 is the first identified diagnostic marker and indicator of disease activity for AOSD [14, 101].

Chemokines such as IL-8 are produced mainly by activated macrophages and act as the chemotactic agents of inflammatory cells. Chen et al. revealed that the serum IL-8 level was a significant predictor of persistent arthritis [13]. Furthermore, IFN-γ-induced chemokines such as C-X-C

motif chemokine 9 (CXCL9), CXCL10, and CXCL11 may contribute to inflammatory responses and cutaneous manifestations in AOSD [102]. IL-6 also enhances immune response and inflammatory reactions and contributes to AOSD pathogenesis [19–20, 103]. As a proinflammatory cytokine, IL-6 may be responsible for fever and skin rash, as well as the production of acute-phase proteins in AOSD [13, 104]. Therefore, biologics targeting IL-6 or its receptor have been proved to be effective in the treatment of AOSD.

MAS or hemophagocytic lymphohistiocytosis (HLH) is characterized by excessive macrophage activation accompanied by the cytokine storm, hemophagocytosis, and hyperferritinemia [105]. The possible trigger factors of MAS include infections, medications used, and uncontrolled AOSD [106–108], and it is associated with high mortality in AOSD [109]. Besides, di Benedetto et al. reported that ferritin levels could be used to predict the emergence of MAS in AOSD patients [110], and AOSD and MAS were both considered hyperferritinemic syndrome [111]. Inflammasome-derived IL-18/IL-1β were suggested to play important roles in MAS-associated rheumatic diseases [112]. AOSD patients having higher IL-18 levels were more likely to develop MAS, and their IL-18 and ferritin levels were further increased at the time of MAS [113].

3.3. Development of New Targeted Therapies.
Because AOSD is a rare disease with a heterogeneity of the clinical course, there is currently no concise consensus for treating AOSD. Although corticosteroids and csDMARDs are the standard-of-care treatment for AOSD [22], a significant proportion of patients showed poor therapeutic response or corticosteroid dependence [21, 114]. Given the pathogenic role of proinflammatory cytokines in AOSD, these inflammatory mediators would become the therapeutic targets.

3.3.1. Anti-IL-1 Therapy.
Given that IL-1 is implicated in the pathogenesis of AOSD [115–116] and its ligands and receptors are secreted mainly by activated macrophages, the administration of IL-1-blocking agents in AOSD patients seems to be a logical therapeutic approach with a corticosteroid-sparing effect [24–25, 117–120]. The IL-1-blocking agents include anakinra (an IL-1R antagonist), rilonacept (a soluble IL-1 trap molecule), and canakinumab (anti-IL-1β monoclonal antibody). The response to anakinra therapy was rapid and sustained in most patients with AOSD [24–25, 117–118]. An open-label randomized study showed that anakinra induced more beneficial responses than DMARDs in corticosteroid-refractory AOSD patients [120]. A meta-analysis revealed that anakinra was effective in treating AOSD with a steroid-sparing effect [121]. Recently, Vastert et al. demonstrated that the use of anakinra could minimize the steroid dose and improve clinical outcomes in children or adults with Still's disease [122]. A systematic review indicated that anakinra treatment was associated with a steroid-sparing effect, and a large proportion of patients could discontinue the use of steroids [123]. A high-dose anakinra has also been successfully used to treat refractory AOSD complicated with life-threatening MAS [124–125]. Rilonacept, an inhibitor of both IL-1α and IL-1β, has a longer

half-life than anakinra. Limited reports revealed that rilonacept effectively treated AOSD patients with the systemic or articular subtype [126–127]. Although a randomized controlled trial was terminated prematurely with the primary endpoint not achieved, canakinumab treatment improved several outcome measures in AOSD [128]. Based on the evidence and consensus, Italian experts recommended that anti-IL-1 therapy was considered relatively safe and effective in treating refractory AOSD patients, especially the systemic subtype patients, as either the first line or a subsequent line of biological treatment [129].

3.3.2. Anti-IL-6 Therapy.
IL-6, a pleiotropic cytokine, binds to IL-6R and a 130 kDa signal-transducing β-receptor subunit (gp130) forms a functioning hexametric structure [130]. The activation of gp130 induces the phosphorylation of the signal transducer and activator of transcription 1 (STAT1), STAT3, and mitogen-activated protein kinase (MAPK) cascade and then activates proinflammatory reactions [131]. The pathogenic role of IL-6 [12–13, 103] is substantiated by the successful treatment with IL-6-blocking agents in AOSD. The IL-6 receptor antagonist, tocilizumab (TCZ), has recently been proposed as a promising biological agent for AOSD patients. In a case series of 14 patients with intractable AOSD, TCZ therapy resulted in complete resolution of the clinical disease activity in 57% of patients and markedly reduced the maintenance dose of corticosteroids [20]. TCZ is effective in treating AOSD patients with either the systemic or chronic articular patterns [132], including those who were refractory to anakinra [133–135] or TNF-α inhibitors [136–137]. Furthermore, TCZ treatment was effective for AOSD patients complicated with MAS [138]. However, macrophage activation syndrome developed following TCZ therapy in one patient with refractory AOSD, implying that caution should be exercised in the very active status of this disease [139]. Based on the previous findings [132–138, 140–141], TCZ treatment is effective and well tolerated in treating refractory AOSD patients.

3.3.3. Anti-IL-17 Therapy.
Given the pathogenic role of IL-17 in AOSD pathogenesis [18], the administration of IL-17 inhibitors in AOSD patients seems to be a logical therapeutic approach with a corticosteroid-sparing effect. The IL-17 inhibitors have recently been proposed as a promising biological agent for rheumatic patients [142–143]. Clinical trials showed that anti-IL-17 antibodies significantly reduced rheumatoid arthritis (RA) signs and symptoms and C-reactive protein levels [144–145]. Several monoclonal antibody-mediated IL-17 inhibition approaches for patients with inflammatory diseases have proceeded to phase III clinical trials.

3.3.4. Anti-IL-18 Therapy.
IL-18, one member of the IL-1 family, is expressed on monocytes, macrophages, and dendritic cells [146]. The binding of IL-18 to its receptors (IL-18Rα and IL-18Rβ) triggers proinflammatory reactions. Previous studies revealed that IL-18 levels were elevated and correlated with disease activity in AOSD [12–14], and markedly increased IL-18 levels were reported in AOSD patients
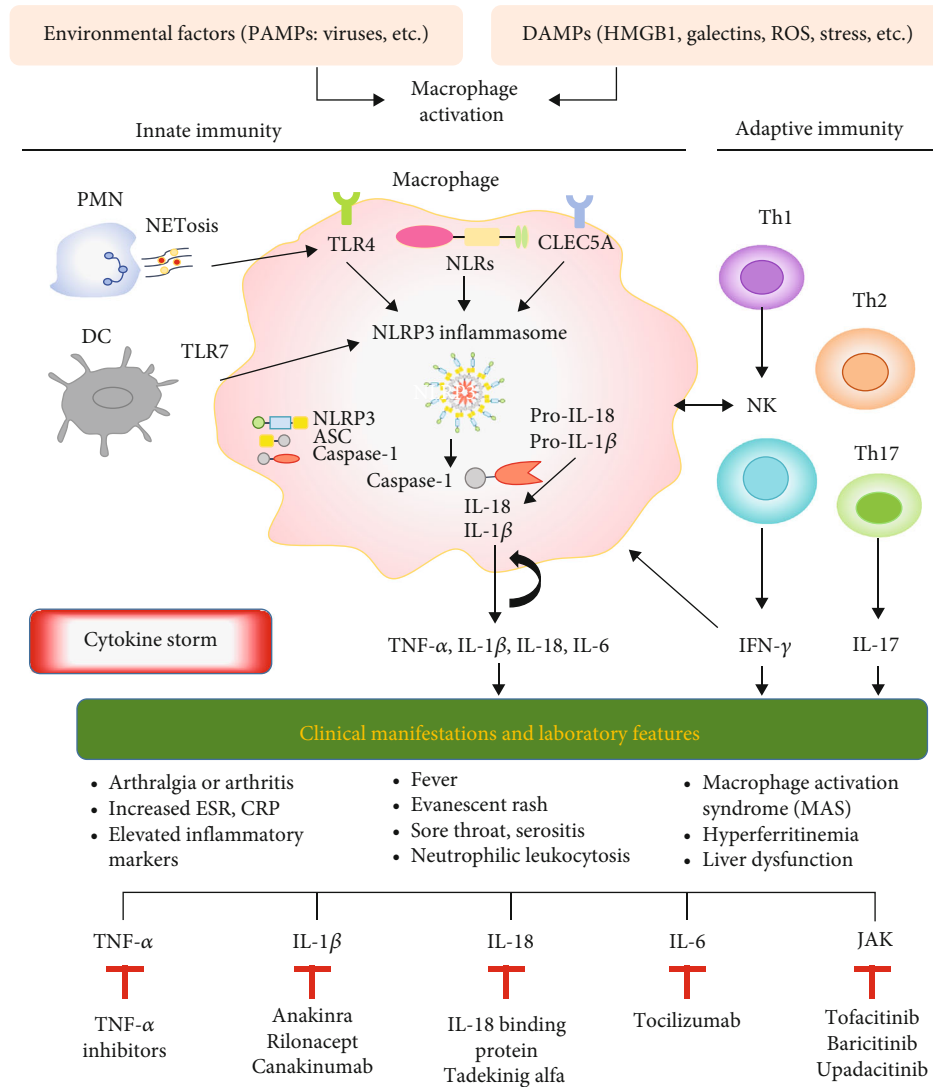
FIGURE 1: The proposed model for the summary of the pathogenic role of macrophages in adult-onset Still's disease and its implication in clinical manifestations and therapeutics. PAMPs: pathogen-associated molecular patterns; DAMPs: damage-associated molecular patterns; HMGB1: high mobility group box-1; ROS: reactive oxygen species; PMN: polymorphonuclear neutrophils; NETs: neutrophil extracellular traps; DC: dendritic cells; TLRs: Toll-like receptors; NLRs: cytosol-expressed nucleotide-binding oligomerization- (NOD-) like receptors; NLRP: nucleotide-binding oligomerization domain, leucine-rich repeat, and pyrin domain; CLEC5A: C-type lectin domain family 5-member A; Th: helper T cells; NK: natural killer cells; IL: interleukin; TNF: tumor necrosis factor; IFN: interferon.

complicated with MAS [112]. Given that IL-18 binding protein (IL-18BP) is an inhibitor of IL-18, a phase II clinical trial demonstrated that IL-18BP (Tadekinig alfa) was effective and well tolerated in treating AOSD [28]. Recently, Tadekinig alfa has been shown to have therapeutic effects with a rapid decrease of disease activity in active AOSD patients who were refractory to csDMARDs [147]. These available results indicate that IL-18 may be a promising therapeutic target in AOSD.

3.3.5. Anti-TNF-α Therapy. TNF-α, an important proinflammatory cytokine, has been reported to be elevated in sera and synovial membranes of AOSD patients compared with osteoarthritis patients or healthy subjects [13, 148]. Although

Kraetsch et al. revealed significant improvement in the clinical and laboratory outcomes in 6 AOSD patients receiving infliximab therapy [149], a recent evidence-based review showed that TNF-α inhibitors might not be effective in AOSD treatment [137].

3.3.6. Anti-IFN-γ Therapy. Given a pathogenic role of interferons such as IFN-γ in AOSD [15], the IFN-γ blockade may effectively treat AOSD with or without concomitant MAS [150]. Recently, Gabr et al. reported that emapalumab, an IFN-γ blockade, effectively eliminated fever and improved laboratory outcomes of a patient with AOSD complicated by MAS [151]. Data regarding the effectiveness of the IFN-γ blockade in treating AOSD remain limited.

3.3.7. Janus Kinase (JAK) Inhibitors. Given that JAK inhibitors can block multicytokines, the use of JAK inhibitors may be feasible for AOSD treatment. Kacar et al. reported that baricitinib, a JAK1/2 inhibitor, was effective in treating two AOSD patients who were refractory to csDMARDs and biological therapy [152]. The combination of baricitinib and anakinra therapy effectively treated a patient with refractory AOSD [153]. A recent report from China revealed the successful use of tofacitinib, a JAK1/3 inhibitor, in 14 patients with AOSD [154]. Besides, tofacitinib therapy was effective in treating a patient with AOSD complicated by MAS [155].

4. Conclusions

The status of hyperinflammation in AOSD, mainly driven by an innate immune response, is characterized by an overproduction of proinflammatory cytokines [1–2, 11, 58]. PAMPs or DAMPs initiate macrophage activation through PRRs and subsequently activate adaptive immune responses [29, 83]. The elevated levels of activated macrophage-related mediators may contribute to the clinical manifestations of AOSD and act as the potential therapeutic targets [156]. Accordingly, the inhibitors to IL-1, IL-6, and IL-18 have been shown to be effective in AOSD treatment. The use of TNF-α inhibitors, such as infliximab, was effective for AOSD patients with the chronic articular subtype. Through the multicytokine blockade, JAK inhibitors were also an effective treatment for AOSD with or without concomitant MAS. Better insights into the pathogenic role of macrophages in AOSD can aid in identifying disease biomarkers and novel therapeutics. Based on the available evidence of the pivotal role of macrophage activation in AOSD pathogenesis and its clinical implication, we summarized the data as in Figure 1.

Data Availability

The data supporting the results cited in the text can be found in the relevant articles cited in the references.

Conflicts of Interest

All authors report no financial interests or potential conflicts of interest.

Authors' Contributions

All authors made substantive intellectual contributions to this review and approved the final manuscript. P-KC and D-YC performed the literature search and appraised the selected articles. P-KC and D-YC drafted the manuscript, and D-YC revised the final manuscript.

Acknowledgments

References

[1] S. Kadavath and P. Efthimiou, "Adult-onset Still's disease-pathogenesis, clinical manifestations, and new treatment options," *Annals of Medicine*, vol. 22, pp. 1–9, 2015.

[2] M. Y. Wang, J. C. Jia, C. D. Yang, and Q. Y. Hu, "Pathogenesis, disease course, and prognosis of adult-onset Still's disease: an update and review," *Chinese medical journal*, vol. 132, pp. 2856–2863, 2019.

[3] Q. Y. Hu, T. Zeng, C. Y. Sun et al., "Clinical features and current treatments of adult-onset Still's disease: a multicenter survey of 517 patients in China," *Clinical and Experimental Rheumatology*, vol. 37, Supplement 121, pp. 52–57, 2019.

[4] A. Lenert and Q. Yao, "Macrophage activation syndrome complicating adult onset Still's disease: a single center case series and comparison with literature," *Seminars in Arthritis and Rheumatism*, vol. 45, pp. 711–716, 2016.

[5] J. G. Larkin and R. D. Sturrock, "Adult Still's disease. A new consideration in pyrexia of unknown origin," *Scottish Medical Journal*, vol. 28, pp. 255–258, 1983.

[6] G. Magadur-Joly, E. Billaud, J. H. Barrier et al., "Epidemiology of adult Still's disease: estimate of the incidence by a retrospective studyin west France," *Annals of the Rheumatic Diseases*, vol. 54, pp. 587–590, 1995.

[7] K. Wakai, A. Ohta, A. Tamakoshi et al., "Estimated prevalence and incidence of adult Still's disease: findings by a nationwide epidemiological survey in Japan," *Journal of Epidemiology*, vol. 7, pp. 221–225, 1997.

[8] K. J. Evensen and H. C. Nossent, "Epidemiology and outcome of adult-onset Still's disease in northern Norway," *Scandinavian Journal of Rheumatology*, vol. 35, pp. 48–51, 2006.

[9] D. L. Kastner, I. Aksentijevich, and R. Goldbach-Mansky, "Autoinflammatory disease reloaded: a clinical perspective," *Cell*, vol. 140, pp. 784–790, 2010.

[10] K. Dolasia, M. K. Bisht, G. Pradhan, A. Udgata, and S. Mukhopadhyay, "TLRs/NLRs: shaping the landscape of host immunity," *International Reviews of Immunology*, vol. 37, pp. 3–19, 2018.

[11] J.-Y. Jung, C. H. Suh, and H. A. Kim, "The role of damage-associated molecular pattern for pathogenesis and biomarkers in adult-onset Still's disease," *Expert Review of Molecular Diagnostics*, vol. 19, pp. 459–468, 2019.

[12] J. H. Choi, C. H. Suh, Y. M. Lee et al., "Serum cytokine profiles in patients with adult onset Still's disease," *The Journal of Rheumatology*, vol. 30, pp. 2422–2427, 2003.

[13] D. Y. Chen, J. L. Lan, F. J. Lin, and T. Y. Hsieh, "Proinflammatory cytokine profiles in the sera and in the pathological tissues of patients with active untreated adult onset Still's disease," *The Journal of Rheumatology*, vol. 31, pp. 2189–2198, 2004.

[14] Y. Kawaguchi, H. Terajima, M. Harigai, M. Hara, and N. Kamatani, "Interleukin-18 as a novel diagnostic marker and indicator of disease severity in adult-onset Still's disease," *Arthritis & Rheumatology*, vol. 44, pp. 1716-1717, 2001.

[15] D. Y. Chen, J. L. Lan, F. J. Lin, T. Y. Hsieh, and M. C. Wen, "A predominance of Th1 cytokine in peripheral blood and pathological tissues of patients with active untreated adult-onset Still's disease," *Annals of the Rheumatic Diseases*, vol. 63, pp. 1300–1306, 2004.

[16] K. H. Jung, J. J. Kim, J. S. Lee et al., "Interleukin-18 as an efficient marker for remission and follow-up in patients with

inactive adult-onset Still's disease," *Scandinavian Journal of Rheumatology*, vol. 43, pp. 162–169, 2014.

[17] C. Girard, J. Rech, M. Brown et al., "Elevated serum levels of free interleukin-18 in adult-onset Still's disease," *Rheumatology (Oxford)*, vol. 55, pp. 2237–2247, 2016.

[18] D. Y. Chen, J. L. Lan, Y. M. Chen, C. C. Lin, H. H. Chen, and C. W. Hsieh, "Potential role of Th17 cells in the pathogenesis of adult-onset Still's disease," *Rheumatology*, vol. 49, no. 12, pp. 2305–2312, 2010.

[19] E. Feist, S. Mitrovic, and B. Fautrel, "Mechanisms, biomarkers and targets for adult-onset Still's disease," *Nature Reviews Rheumatology*, vol. 14, pp. 603–618, 2018.

[20] P. Sfriso, S. Bindoli, and P. Galozzi, "Adult-onset Still's disease: molecular pathophysiology and therapeutic advances," *Drugs*, vol. 78, pp. 1187–1195, 2018.

[21] S. Castañeda, R. Blanco, and M. A. González-Gay, "Adult-onset Still's disease: advances in the treatment," *Best Practice & Research. Clinical Rheumatology*, vol. 30, pp. 222–238, 2016.

[22] D. H. Yoo, "Treatment of adult-onset Still's disease: up to date," *Expert Review of Clinical Immunology*, vol. 13, pp. 849–866, 2017.

[23] A. A. Fitzgerald, S. A. LeClercq, A. Yan, J. E. Homik, and C. A. Dinarello, "Rapid responses to anakinra in patients with refractory adult-onset Still's disease," *Arthritis and Rheumatism*, vol. 52, pp. 1794–1803, 2005.

[24] T. Lequerré, P. Quartier, D. Rosellini et al., "Interleukin-1 receptor antagonist (anakinra) treatment in patients with systemic-onset juvenile idiopathic arthritis or adult onset Still's disease: preliminary experience in France," *Annals of the Rheumatic Diseases*, vol. 67, pp. 302–308, 2008.

[25] K. Laskari, A. G. Tzioufas, and H. M. Moutsopoulos, "Efficacy and long-term follow-up of IL-1R inhibitor anakinra in adults with Still's disease: a case-series study," *Arthritis Research & Therapy*, vol. 13, p. R91, 2011.

[26] X. Puéchal, M. De Bandt, J. M. Berthelot et al., "Tocilizumab in refractory adult Still's disease," *Arthritis Care and Research*, vol. 63, pp. 155–159, 2011.

[27] Y. Ma, M. Wu, X. Zhang et al., "Efficacy and safety of tocilizumab with inhibition of interleukin-6 in adult-onset Still's disease: a meta-analysis," *Modern Rheumatology*, vol. 28, pp. 849–857, 2018.

[28] C. Gabay, B. Fautrel, J. Rech et al., "Open-label, multicentre, dose-escalating, phase II clinical trial on the safety and efficacy of Tadekining alfa (IL-18BP) in adult-onset Still's disease," *Annals of the Rheumatic Diseases*, vol. 77, pp. 840–847, 2018.

[29] S. Frizinsky, S. Haj-Yahia, D. Machnes Maayan et al., "The innate immune perspective of autoimmune and autoinflammatory conditions," *Rheumatology (Oxford)*, vol. 58, pp. vi1–vi8, 2019.

[30] D. Schenten and R. Medzhitov, "The control of adaptive immune responses by the innate immune system," *Advances in Immunology*, vol. 109, pp. 87–124, 2011.

[31] T. S. Kapellos, L. Taylor, H. Lee et al., "A novel real time imaging platform to quantify macrophage phagocytosis," *Biochemical Pharmacology*, vol. 116, pp. 107–119, 2016.

[32] D. Hirayama, T. Iida, and H. Nakase, "The phagocytic function of macrophage-enforcing innate immunity and tissue homeostasis," *International Journal of Molecular Sciences*, vol. 19, p. 92, 2017.

[33] D. M. Mosser and J. P. Edwards, "Exploring the full spectrum of macrophage activation," *Nature Reviews. Immunology*, vol. 8, pp. 958–969, 2008.

[34] S. W. Brubaker, K. S. Bonham, I. Zanoni, and J. C. Kagan, "Innate immune pattern recognition: a cell biological perspective," *Annual Review of Immunology*, vol. 33, pp. 257–290, 2015.

[35] T. Satoh and S. Akira, "Toll-like receptor signaling and its inducible proteins," *Microbiology spectrum*, vol. 4, no. 6, 2016.

[36] J. M. Platnich and D. A. Muruve, "NOD-like receptors and inflammasomes: a review of their canonical and non-canonical signaling pathways," *Archives of Biochemistry and Biophysics*, vol. 670, pp. 4–14, 2019.

[37] N. Kelley, D. Jeltema, Y. Duan, and Y. He, "The NLRP3 inflammasome: an overview of mechanisms of activation and regulation," *International Journal of Molecular Sciences*, vol. 20, p. 3328, 2019.

[38] L. Franchi, R. Muñoz-Planillo, and G. Núñez, "Sensing and reacting to microbes through the inflammasomes," *Nature Immunology*, vol. 13, pp. 325–332, 2012.

[39] F. Martinon, V. Pétrilli, A. Mayor, A. Tardivel, and J. Tschopp, "Gout-associated uric acid crystals activate the NALP3 inflammasome," *Nature*, vol. 440, pp. 237–241, 2006.

[40] T. Salti, K. Khazim, R. Haddad, S. Campisi-Pinto, G. Bar-Sela, and I. Cohen, "Glucose induces IL-1alpha-dependent inflammation and extracellular matrix proteins expression and deposition in renal tubular epithelial cells in diabetic kidney disease," *Frontiers in Immunology*, vol. 11, p. 1270, 2020.

[41] L. Baron, A. Gombault, M. Fanny et al., "The NLRP3 inflammasome is activated by nanoparticles through ATP, ADP and adenosine," *Cell death & disease*, vol. 6, article e1629, 2015.

[42] S. R. Mulay, O. P. Kulkarni, K. V. Rupanagudi et al., "Calcium oxalate crystals induce renal inflammation by NLRP3-mediated IL-1β secretion," *The Journal of Clinical Investigation*, vol. 123, pp. 236–246, 2013.

[43] J. M. G. W. Wouters, J. van der Veen, L. B. A. van de Putte, and D. J. R. A. M. de Rooij, "Adult Still's disease and viral infection," *Annals of the Rheumatic Diseases*, vol. 47, pp. 764–767, 1988.

[44] K. Izumikawa, Y. Morinaga, A. Kondo et al., "Adult Still's disease associated with cytomegalovirus infection," *Journal of Infection and Chemotherapy*, vol. 13, pp. 114–117, 2007.

[45] J. Pouchot, H. Quakil, M. L. Debin, and P. Vinceneux, "Adult Still's disease associated with acute human parvovirus B19 infection," *Lancet*, vol. 341, pp. 1280-1281, 1993.

[46] D. Y. Chen, Y. M. Chen, J. L. Lan, B. S. Tzang, C. C. Lin, and T. C. Hsu, "Significant association of past parvovirus B19 infection with cytopenia and arthritis in patients with adult-onset Still's disease," *Clinica Chimica Acta*, vol. 413, pp. 855–860, 2012.

[47] H. S. K. Huang and W. E. DeCoteau, "Adult-onset Still's disease: an unusual presentation of rubella infection," *Canadian Medical Association Journal*, vol. 122, pp. 1275-1276, 1980.

[48] M. Gallo, A. Calvanese, F. Oscuro et al., "Acute hepatitis in a patient with adult-onset Still's disease," *La Clinica Terapeutica*, vol. 148, pp. 183–187, 1997.

[49] T. Schifter and U. H. Lewinski, "Adult onset Still's disease associated with Epstein-Barr virus infection in a 66-year-old woman," *Scandinavian Journal of Rheumatology*, vol. 27, pp. 458–460, 1998.

[50] K. Yoshioka, S. Fujimoto, H. Oba, M. Minami, and T. Aoki, "Onset of adult-onset-Still's disease following influenza vaccination," *Modern Rheumatology*, vol. 21, pp. 432–435, 2011.

[51] A. S. Luder, V. Naphtali, E. Ben Porat, and N. Lahat, "Still's disease associated with adenovirus infection and defect in adenovirus directed natural killing," *Annals of the Rheumatic Diseases*, vol. 48, pp. 781–786, 1989.

[52] A. Agnihotri, A. Ruff, L. Gotterer, A. Walker, A. H. McKenney, and A. Brateanu, "Adult onset Still's disease associated with mycoplasma pneumonae infection and hemophagocytic lymphohistiocytosis," *Case Reports in Medicine*, vol. 2016, Article ID 2071815, 4 pages, 2016.

[53] M. Pichon, L. P. Claire, P. Genet, F. Caby, Y. Yazdanpanah, and A. M. Menn, "Adult-onset Still's disease associated with human immunodeficiency virus infection," *Rheumatology (Oxford)*, vol. 59, pp. e99–e101, 2020.

[54] J. F. De Carvalho, "COVID-19 in Still's disease," *European Review for Medical and Pharmacological Sciences*, vol. 24, pp. 12627–12629, 2020.

[55] A. D. Bamidis, P. Koehler, V. di Cristanziano et al., "First manifestation of adult-onset Still's disease after COVID-19," *The Lancet Rheumatology*, vol. 3, pp. e319–e321, 2021.

[56] D. Y. Chen, Y. M. Chen, H. H. Chen et al., "Human parvovirus B19 nonstructural protein NS1 activates NLRP3 inflammasome signaling in adult-onset Still's disease," *Molecular Medicine Reports*, vol. 17, no. 2, pp. 3364–3371, 2018.

[57] J. Jia, H. Shi, M. Liu et al., "Cytomegalovirus infection may trigger adult-onset Still's disease onset or relapses," *Frontiers in Immunology*, vol. 10, p. 898, 2019.

[58] M. Gerfaud-Valentin, Y. Jamilloux, J. Iwaz, and P. Sève, "Adult-onset Still's disease," *Autoimmunity Reviews*, vol. 13, pp. 708–722, 2014.

[59] G. Basta, G. Lazzerini, M. Massaro et al., "Advanced glycation end products activate endothelium through signal-transduction receptor RAGE: a mechanism for amplification of inflammatory responses," *Circulation*, vol. 105, no. 7, pp. 816–822, 2002.

[60] J. Li, F. Hou, Z. Guo, Y. Shan, X. Zang, and Z. Liu, "Advanced glycation end products upregulate C-reactive protein synthesis by human hepatocytes through stimulation of monocyte IL-6 and IL-1β production," *Scandinavian Journal of Immunology*, vol. 66, no. 5, pp. 555–562, 2007.

[61] D. Y. Chen, Y. M. Chen, C. C. Lin et al., "The potential role of advanced glycation end products (AGEs) and soluble receptors for AGEs (sRAGE) in the pathogenesis of adult-onset Still's disease," *BMC Musculoskeletal Disorders*, vol. 16, no. 1, p. 111, 2015.

[62] B. Lu, T. Nakamura, K. Inouye et al., "Novel role of PKR in inflammasome activation and HMGB1 release," *Nature*, vol. 488, no. 7413, pp. 670–674, 2012.

[63] B. Lu, H. Wang, U. Andersson, and K. J. Tracey, "Regulation of HMGB1 release by inflammasomes," *Protein & Cell*, vol. 4, no. 3, pp. 163–167, 2013.

[64] J. Y. Jung, C. H. Suh, S. Sohn, J. Y. Nam, and H. A. Kim, "Elevated high-mobility group B1 levels in active adult-onset Still's disease associated with systemic score and skin raash," *Clinical Rheumatology*, vol. 35, pp. 1937–1942, 2016.

[65] S. Colafrancesco, R. Priori, C. Alessandri et al., "sCD163 in AOSD: a biomarker for macrophage activation related to hyperferritinemia," *Immunologic Research*, vol. 60, no. 2-3, pp. 177–183, 2014.

[66] B. R. Bloom and B. Bennett, "Mechanism of a reaction in vitro associated with delayed-type hypersensitivity," *Science*, vol. 153, no. 3731, pp. 80–82, 1966.

[67] R. A. Mitchell, H. Liao, J. Chesney et al., "Macrophage migration inhibitory factor (MIF) sustains macrophage proinflammatory function by inhibiting p53: regulatory role in the innate immune response," *Proceedings of the National Academy of Sciences*, vol. 99, no. 1, pp. 345–350, 2002.

[68] F. F. Wang, L. A. Zhu, Y. Q. Zou et al., "New insights into the role and mechanism of macrophage migration inhibitory factor in steroid-resistant patients with systemic lupus erythematosus," *Arthritis Research & Therapy*, vol. 14, no. 3, p. R103, 2012.

[69] T. Calandra and T. Roger, "Macrophage migration inhibitory factor: a regulator of innate immunity," *Nature Reviews. Immunology*, vol. 3, pp. 791–800, 2003.

[70] Y. Q. Zou, L. J. Lu, S. J. Li et al., "The levels of macrophage migration inhibitory factor as an indicator of disease activity and severity in adult-onset Still's disease," *Clinical Biochemistry*, vol. 41, no. 7-8, pp. 519–524, 2008.

[71] H. Becker, M. Gaubitz, W. Domschke, and P. Willeke, "Potential role of macrophage migration inhibitory factor in adult-onset Still's disease," *Scandinavian Journal of Rheumatology*, vol. 38, pp. 69–71, 2009.

[72] B. Fautrel, "Ferritin levels in adult Still's disease: any sugar?," *Joint, Bone, Spine*, vol. 69, pp. 355–357, 2002.

[73] K. Matsui, T. Tsuchida, K. Hiroishi et al., "High serum level of macrophage-colony stimulating factor (M-CSF) in adult-onset Still's disease," *Rheumatology*, vol. 38, no. 5, pp. 477-478, 1999.

[74] Q. Hu, H. Shi, T. Zeng et al., "Increased neutrophil extracellular traps activate NLRP3 and inflammatory macrophages in adult-onset Still's disease," *Arthritis Research & Therapy*, vol. 21, no. 1, p. 9, 2019.

[75] N. Vaninov, "In the eye of the COVID-19 cytokine storm," *Nature Reviews. Immunology*, vol. 20, no. 5, p. 277, 2020.

[76] S. Bhaskar, A. Sinha, M. Banach et al., "Cytokine storm in COVID-19-immunopathological mechanisms, clinical considerations, and therapeutic approaches: the REPROGRAM consortium position paper," *Frontiers in Immunology*, vol. 11, article 1648, 2020.

[77] Y. Tang, J. Liu, D. Zhang, Z. Xu, J. Ji, and C. Wen, "Cytokine storm in COVID-19: the current evidence and treatment strategies," *Frontiers in Immunology*, vol. 11, p. 1708, 2020.

[78] J. Meng, Y. Ma, J. Jia et al., "Cytokine storm in coronavirus disease 2019 and adult-onset Still's disease: similarities and differences," *Frontiers in Immunology*, vol. 11, article 603389, 2021.

[79] M. F. Tsan and B. Gao, "Pathogen-associated molecular pattern contamination as putative endogenous ligands of Toll-like receptors," *Journal of Endotoxin Research*, vol. 13, pp. 6–14, 2007.

[80] L. A. B. Joosten, S. Abdollahi-Roodsaz, C. A. Dinarello, L. O'Neill, and M. G. Netea, "Toll-like receptors and chronic inflammation in rheumatic diseases: new developments," *Nature Reviews Rheumatology*, vol. 12, pp. 344–357, 2016.

[81] K. Komai, T. Shichita, M. Ito, M. Kanamori, S. Chikuma, and A. Yoshimura, "Role of scavenger receptors as damage-associated molecular pattern receptors in Toll-like receptor activation," *International Immunology*, vol. 29, pp. 59–70, 2017.

[82] Q. Xie, W. W. Shen, J. Zhong, C. Huang, L. Zhang, and J. Li, "Lipopolysaccharide/adenosine triphophate induces IL-1β and IL-18 secretion through the NLRP3 inflammasome in RAW264.7 murine macrophage cells," *International Journal of Molecular Medicine*, vol. 34, pp. 341–349, 2014.

[83] P. W. Dempsey, S. A. Vaidya, and G. Cheng, "The art of war: innate and adaptive immune responses," *Cellular and Molecular Life Sciences*, vol. 60, pp. 2604–2621, 2003.

[84] T. L. Liao, Y. M. Chen, C. W. Hsieh et al., "Upregulation of circulating microRNA-134 in adult-onset Still's disease and its use as potential biomarker," *Scientific Reports*, vol. 7, no. 1, p. 4214, 2017.

[85] C. W. Hsieh, Y. M. Chen, C. C. Lin et al., "Elevated expression of the NLRP3 inflammasome and its correlation with disease activity in adult-onset Still disease," *The Journal of Rheumatology*, vol. 44, no. 8, pp. 1142–1150, 2017.

[86] P. K. Chen, S. L. Hsieh, J. L. Lan, C. C. Lin, S. H. Chang, and D. Y. Chen, "Elevated expression of C-type lectin domain family 5-member A (CLEC5A) and its relation to inflammatory parameters and disease course in adult-onset Still's disease," *Journal of Immunology Research*, vol. 2020, Article ID 9473497, 11 pages, 2020.

[87] P. Ruscitti, F. Ciccia, P. Cipriani et al., "The CD68(+)/H-ferritin(+) cells colonize the lymph nodes of the patients with adult onset Still's disease and are associated with increased extracellular level of H-ferritin in the same tissue: correlation with disease severity and implication for pathogenesis," *Clinical and Experimental Immunology*, vol. 183, no. 3, pp. 397–404, 2016.

[88] P. Ruscitti, P. Cipriani, F. Ciccia et al., "H-ferritin and CD68+/H-ferritin+monocytes/macrophages are increased in the skin of adult-onset Still's disease patients and correlate with the multi-visceral involvement of the disease," *Clinical and Experimental Immunology*, vol. 186, no. 1, pp. 30–38, 2016.

[89] K. Sharif, V. Vieira Borba, G. Zandman-Goddard, and Y. Shoenfeld, "Eppur Si Muove: ferritin is essential in modulating inflammation," *Clinical and Experimental Immunology*, vol. 191, pp. 149-150, 2018.

[90] P. Ruscitti, O. Berardicurti, A. Barile et al., "Severe COVID-19 and related hyperferritinaemia: more than an innocent bystander?," *Annals of the Rheumatic Diseases*, vol. 79, no. 11, pp. 1515-1516, 2020.

[91] D. Wang, S. Yu, Y. Zhang et al., "Caspse-11-GSDMD pathway is required for serum ferritin secretion in sepsis," *Clinical Immunology*, vol. 205, pp. 148–152, 2019.

[92] P. Broz and V. M. Dixit, "Inflammasomes: mechanism of assembly, regulation and signalling," *Nature Reviews. Immunology*, vol. 16, pp. 407–420, 2016.

[93] H. Nagai, Y. Kirino, H. Nakano et al., "Elevated serum gasdermin D N-terminal implicates monocyte and macrophage pyroptosis in adult-onset Still's disease," *Rheumatology (Oxford)*, no. article keaa814, 2021.

[94] Y. Kirino, Y. Kawaguchi, Y. Tada et al., "Beneficial use of serum ferritin and heme oxygenase-1 as biomarkers in adult-onset Still's disease: a multicenter retrospective study," *Modern Rheumatology*, vol. 28, no. 5, pp. 858–864, 2018.

[95] G. Kaplanski, "Interleukin-18: biologic properties and role in disease pathjogenesis," *Immunological Reviews*, vol. 281, pp. 138–153, 2018.

[96] S. Yasin, N. Fall, R. A. Brown et al., "IL-18 as a biomarker linking systemic juvenile idiopathic arthritis and macrophage activation syndrome," *Rheumatology*, vol. 59, no. 2, pp. 361–366, 2020.

[97] P. Mehta, R. Q. Cron, J. Hartwell, J. J. Manson, and R. S. Tattersall, "Silencing the cytokine storm: the use of intravenous anakinra in haemophagocytic lymphohistiocytosis or macrophage activation syndrome," *The Lancet Rheumatology*, vol. 2, no. 6, pp. e358–e367, 2020.

[98] C. B. Crayne, S. Albeituni, K. E. Nichols, and R. Q. Cron, "The immunology of macrophage activation syndrome," *Frontiers in Immunology*, vol. 10, p. 119, 2019.

[99] T. Yamamoto, "Cutaneous manifestations associated with adult-onset Still's disease: important diagnostic values," *Rheumatology International*, vol. 32, pp. 2233–2237, 2012.

[100] R. Priori, F. Barone, C. Alessandri et al., "Markedly increased IL-18 liver expression in adult-onset Still's disease-related hepatitis," *Rheumatology (Oxford, England)*, vol. 50, no. 4, pp. 776–780, 2011.

[101] H. Kudela, S. Drynda, A. Lux, G. Horneff, and J. Kekow, "Comparative study of interleukin-18 (IL-18) serum levels in adult onset Still's disease (AOSD) and systemic onset juvenile idiopathic arthritis (sJIA) and its use as a biomarker for diagnosis and evaluation of disease activity," *BMC Rheumatology*, vol. 3, no. 1, p. 4, 2019.

[102] J. H. Han, C. H. Suh, J. Y. Jung et al., "Elevated circulating levels of the interferon-γ-induced chemokines are associated with disease activity and cutaneous manifestations in adult-onset Still's disease," *Scientific Reports*, vol. 7, no. 1, p. 46652, 2017.

[103] N. Inoue, M. Shimizu, S. Tsunoda, M. Kawano, M. Matsumura, and A. Yachie, "Cytokine profile in adult-onset Still's disease: comparison with systemic juvenile idiopathic arthritis," *Clinical Immunology*, vol. 169, pp. 8–13, 2016.

[104] M. A. Scheinberg, E. Chapira, M. L. Fernandes, and O. Hubscher, "Interleukin-6: a possible marker of disease activity in adult-onset Still's disease," *Clinical and Experimental Rheumatology*, vol. 14, pp. 653–655, 1996.

[105] A. Ravelli, F. Minoia, S. Davì et al., "2016 classification criteria for macrophage activation syndrome complicating systemic juvenile idiopathic arthritis: a European League Against Rheumatism/American College of Rheumatology/-Paediatric Rheumatology International Trials Organisation collaborative initiative," *Arthritis & Rhematology*, vol. 68, no. 3, pp. 566–576, 2016.

[106] A. Stern, R. Riley, and L. Buckley, "Worsening of macrophage activation syndrome in a patient with adult onset Still's disease after initiation of etanercept therapy," *Journal of Clinical Rheumatology*, vol. 7, pp. 252–256, 2001.

[107] Y. Tsuchida, S. Sumitomo, H. Shoda, K. Kubo, K. Fujio, and K. Yamamoto, "Macrophage activation syndrome associated with tocilizumab treatment in adult-onset Still's disease," *Modern Rheumatology*, vol. 7, pp. 556-557, 2017.

[108] R. Wang, T. Li, S. Ye et al., "Macrophage activation syndrome associated with adult-onset Still's disease: a multicenter retrospective analysis," *Clinical Rheumatology*, vol. 39, no. 8, pp. 2379–2386, 2020.

[109] P. Ruscitti, D. Iacono, F. Ciccia et al., "Macrophage activation syndrome in patients affected by adult-onset Still disease: analysis of survival rates and predictive factors in the Gruppo Italiano di Ricerca in Reumatologia Clinica e Sperimentale cohort," *The Journal of Rheumatology*, vol. 45, no. 6, pp. 864–872, 2018.

[110] P. di Benedetto, P. Cipriani, D. Iacono et al., "Ferritin and C-reactive protein are predictive biomarkers of mortality and macrophage activation syndrome in adult onset Still's disease. Analysis of the multicentre Gruppo Italiano di Ricerca in Reumatologia Clinica e Sperimentale (GIRRCS) cohort," *PLoS One*, vol. 15, no. 7, article e0235326, 2020.

[111] C. Rosário, G. Zandman-Goddard, E. G. Meyron-Holtz, D. P. D'Cruz, and Y. Shoenfeld, "The hyperferritinemic syndrome: macrophage activation syndrome, Still's disease, septic shock and catastrophic antiphospholipid syndrome," *BMC Medicine*, vol. 11, no. 1, p. 185, 2013.

[112] J. Maruyama and S. Inokuma, "Cytokine profiles of macrophage activation syndrome associated with rheumatic diseases," *The Journal of Rheumatology*, vol. 37, pp. 967–973, 2010.

[113] E. S. Weiss, C. Girard-Guyonvarc'h, D. Holzinger et al., "Interleukin-18 diagnostically distinguishes and pathogenically promotes human and murine macrophage activation syndrome," *Blood*, vol. 131, no. 13, pp. 1442–1455, 2018.

[114] U. Kalyoncu, D. Solmaz, H. Emmungil et al., "Response rate of initial conventional treatments, disease course, and related factors of patients with adult-onset Still's disease: data from a large multicenter cohort," *Journal of Autoimmunity*, vol. 69, pp. 59–63, 2016.

[115] V. Pascual, F. Allantaz, E. Arce, M. Punaro, and J. Banchereau, "Role of interleukin-1 (IL-1) in the pathogenesis of systemic onset juvenile idiopathic arthritis and clinical response to IL-1 blockade," *The Journal of Experimental Medicine*, vol. 201, pp. 1479–1486, 2005.

[116] C. P. Mavragani, E. G. Spyridakis, and M. Koutsilieris, "Adult-onset Still's disease: from pathophysiology to targeted therapies," *International Journal of Inflammation*, vol. 2012, Article ID 879020, 10 pages, 2012.

[117] I. Kötter, A. Wacker, S. Koch et al., "Anakinra in patients with treatment-resistant adult-onset Still's disease: four case reports with serial cytokine measurements and a review of the literature," *Seminars in Arthritis and Rheumatism*, vol. 37, no. 3, pp. 189–197, 2007.

[118] L. Naumann, E. Feist, A. Natusch et al., "IL1-receptor antagonist anakinra provides long-lasting efficacy in the treatment of refractory adult-onset Still's disease," *Annals of the Rheumatic Diseases*, vol. 69, no. 2, pp. 466-467, 2010.

[119] C. Iliou, C. Papagoras, N. Tsifetaki, P. V. Voulgari, and A. A. Drosos, "Adult-onset Still's disease: clinical, serological, and therapeutic considerations," *Clinical and Experimental Rheumatology*, vol. 31, pp. 47–52, 2013.

[120] D. Nordström, A. Knight, R. Luukkainen et al., "Beneficial effect of interleukin 1 inhibition with anakinra in adult-onset Still's disease. An open, randomized, multicenter study," *The Journal of Rheumatology*, vol. 39, no. 10, pp. 2008–2011, 2012.

[121] D. Hong, Z. Yang, S. Han, X. Liang, K. Ma, and X. Zhang, "Interleukin 1 inhibition with anakinra in adult-onset Still's disease: a meta-analysis of its efficacy and safety," *Drug Design, Development and Therapy*, vol. 8, pp. 2345–2357, 2014.

[122] S. J. Vastert, Y. Jamilloux, P. Quartier et al., "Anakinra in children and adults with Still's disease," *Rheumatology*, vol. 58, Supplement 6, pp. vi9–vi22, 2019.

[123] R. Giacomelli, J. Sota, P. Ruscitti et al., "The treatment of adult-onset Still's disease with anakinra, a recombinant human IL-1 receptor antagonist: a systematic review of liter-

ature," *Clinical and Experimental Rheumatology*, vol. 39, no. 1, pp. 187–195, 2021.

[124] F. Parisi, A. Paglionico, V. Varriano, G. Ferraccioli, and E. Gremese, "Refractory adult-onset Still disease complicated by macrophage activation syndrome and acute myocarditis," *Medicine (Baltimore)*, vol. 96, no. 24, article e6656, 2017.

[125] H. E. Sönmez, S. Demir, Y. Bilginer, and S. Özen, "Anakinra treatment in macrophage activation syndrome: a single center experience and systemic review of literature," *Clinical Rheumatology*, vol. 37, pp. 3329–3335, 2018.

[126] G. Junge, J. Mason, and E. Feist, "Adult onset Still's disease-the evidence that anti-interleukin-1 treatment is effective and well-tolerated (a comprehensive literature review)," *Seminars in Arthritis and Rheumatism*, vol. 47, pp. 295–302, 2017.

[127] O. Petryna, J. J. Cush, and P. Efthimiou, "IL-1 trap rilonacept in refractory adult onset Still's disease," *Annals of the Rheumatic Diseases*, vol. 71, pp. 2056-2057, 2012.

[128] C. Kedor, J. Listing, J. Zernicke et al., "Canakinumab for treatment of adult-onset Still's disease to achieve reduction of arthritic manifestation (CONSIDER): phase II, randomised, double-blind, placebo-controlled, multicentre, investigator-initiated trial," *Annals of the Rheumatic Diseases*, vol. 79, no. 8, pp. 1090–1097, 2020.

[129] AOSD Consensus Group, S. Colafrancesco, M. Manara et al., "Management of adult-onset Still's disease with interleukin-1 inhibitors: evidence- and consensus-based statements by a panel of Italian experts," *Arthritis Research & Therapy*, vol. 21, no. 1, p. 275, 2019.

[130] G. Skiniotis, M. J. Boulanger, K. C. Garcia, and T. Walz, "Signaling conformations of the tall cytokine receptor gp130 when in complex with IL-6 and IL-6 receptor," *Nature Structural & Molecular Biology*, vol. 12, pp. 545–551, 2005.

[131] C. A. Hunter and S. A. Jones, "IL-6 as a keystone cytokine in health and disease," *Nature Immunology*, vol. 16, pp. 448–457, 2015.

[132] F. Vercruysse, T. Barnetche, E. Lazaro et al., "Adult-onset Still's disease biological treatment strategy may depend on the phenotypic dichotomy," *Arthritis Research & Therapy*, vol. 21, no. 1, p. 53, 2019.

[133] M. De Bandt and B. Saint-Marcoux, "Tocilizumab for multi-refractory adult-onset Still's disease," *Annals of the Rheumatic Diseases*, vol. 68, pp. 153-154, 2009.

[134] K. Perdan-Pirkmajer, S. Praprotnik, and M. Tomšič, "A case of refractory adult-onset Still's disease successfully controlled with tocilizumab and a review of the literature," *Clinical Rheumatology*, vol. 29, pp. 1465–1467, 2010.

[135] J. Rech, M. Ronneberger, M. Englbrecht et al., "Successful treatment of adult-onset Still's disease refractory to TNF and IL-1 blockade by IL-6 receptor blockade," *Annals of the Rheumatic Diseases*, vol. 70, no. 2, pp. 390–392, 2011.

[136] R. Suematsu, A. Ohta, E. Matsuura et al., "Therapeutic response of patients with adult Still's disease to biologic agents: multicenter results in Japan," *Modern Rheumatology*, vol. 22, no. 5, pp. 712–719, 2012.

[137] S. Zhou, J. Qiao, J. Bai, Y. Wu, and H. Fang, "Biological therapy of traditional therapy-resistant adult-onset Still's disease: an evidence-baased review," *Therapeutics and Clinical Risk Management*, vol. 14, pp. 167–171, 2018.

[138] E. Watanabe, H. Sugawara, T. Yamashita, A. Ishii, A. Oda, and C. Terai, "Successful tocilizumab therapy for

macrophage activation syndrome associated with adult-onset Still's disease: a case-based review," *Case Reports in Medicine*, vol. 2016, Article ID 5656320, 7 pages, 2016.

[139] M. Kobayashi, Y. Takahashi, H. Yamashita, H. Kaneko, and A. Mimori, "Benefit and a possible risk of tocilizumab therapy for adult-onset Still's disease accompanied by macrophage activation syndrome," *Modern Rheumatology*, vol. 21, pp. 92–96, 2011.

[140] S. Kır, M. Özgen, and S. Zontul, "Adult-onset Still's disease and treatment results with tocilizumab," *International Journal of Clinical Practice*, vol. 75, article e13936, 2020.

[141] S. Castañeda, D. Martínez-Quintanilla, J. L. Martín-Varillas, N. García-Castañeda, B. Atienza-Mateo, and M. A. González-Gay, "Tocilizumab for the treatment of adult-onset Still's disease," *Expert Opinion on Biological Therapy*, vol. 19, pp. 273–286, 2019.

[142] S. Ivanov and A. Linden, "Interleukin-17 as drug target in human disease," *Trends in Pharmacological Sciences*, vol. 30, pp. 95–103, 2009.

[143] W. B. van den Berg and P. Miossec, "IL-17 as a future therapeutic target for rheumatoid arthritis," *Nature Reviews Rheumatology*, vol. 5, pp. 549–553, 2009.

[144] M. C. Genovese, F. van den Bosch, S. A. Roberson et al., "LY2439821, a humanized anti-interleukin-17 monoclonal antibody, in the treatment of patients with rheumatoid arthritis: a phase I randomized, double-blind, placebo-controlled, proof-of-concept study," *Arthritis and Rheumatism*, vol. 62, no. 4, pp. 929–939, 2010.

[145] P. Durez, V. Chindalore, B. Wittmer et al., "AIN457, an anti-IL-17 antibody, shows good safety and induces clinical responses in patients with active rheumatoid arthritis (RA) despite methotrexate therapy in a randomized, double-blind, proof-of-concept trial," *Annals of the Rheumatic Diseases*, vol. 68, Supplement 3, p. 125, 2009.

[146] I. S. Afonina, C. Muller, S. J. Martin, and R. Beyaert, "Proteolytic processing of interleukin-1 family cytokines: variations on a common theme," *Immunity*, vol. 42, pp. 991–1004, 2015.

[147] U. Kiltz, D. Kiefer, J. Braun, E. J. Schiffrin, C. Girard-Guyonvarc'h, and C. Gabay, "Prolonged treatment with Tadekinig alfa in adult-onset Still's disease," *Annals of the Rheumatic Diseases*, vol. 79, article e10, 2020.

[148] T. Fujii, T. Nojima, H. Yasuoka et al., "Cytokine and immunogenetic profiles in Japanese patients with adult Still's disease. Association with chronic articular disease," *Rheumatology (Oxford, England)*, vol. 40, no. 12, pp. 1398–1404, 2001.

[149] H. G. Kraetsch, C. Antoni, J. R. Kalden, and B. Manger, "Successful treatment of a small cohort of patients with adult onset of Still's disease with infliximab: first experiences," *Annals of the Rheumatic Diseases*, vol. 60, pp. iii55–iii57, 2001.

[150] I. Di Cola, P. Ruscitti, R. Giacomelli, and P. Cipriani, "The pathogenic role of interferons in the hyperinflammatory response on adult-onset Still's disease and macrophage activation syndrome: paving the way towards new therapeutic targets," *Journal of Clinical Medicine*, vol. 10, p. 1164, 2021.

[151] J. B. Gabr, E. Liu, S. Mian et al., "Successful treatment of secondary macrophage activation syndrome with emapalumab in a patient with newly diagnosed adult-onset Still's disease: case report and review of the literature," *Annals of Translational Medicine*, vol. 8, no. 14, p. 887, 2020.

[152] M. Kacar, J. Fitton, A. K. Gough, M. H. Buch, D. G. McGonagle, and S. Savic, "Mixed results with baricitinib in biological-resistant adult-onset Still's disease and undifferentiated systemic autoinflammatory disease," *RMD Open*, vol. 6, article e001246, 2020.

[153] C. Ladhari, C. Jorgensen, and Y. M. Pers, "Treatment of refractory adult onset Still's disease with combination anakinra and baricitinib therapy," *Rheumatology (Oxford, England)*, vol. 58, pp. 736-737, 2019.

[154] Q. Hu, M. Wang, J. Jia, J. Teng, H. Chi, and T. Liu, "Tofacitinib in refractory adult-onset Still's disease: 14 cases from a single center in China," *Annals of the Rheumatic Diseases*, vol. 79, pp. 842–844, 2020.

[155] M. Honda, M. Moriyama, M. Kondo, S. Kumakura, and Y. Murakawa, "Tofacitinib-induced remission in refractory adult-onset Still's disease complicated by macrophage activation syndrome," *Scandinavian Journal of Rheumatology*, vol. 49, no. 4, pp. 336–338, 2020.

[156] S. Li, S. Zheng, S. Tang et al., "Autoinflammatory pathogenesis and targeted therapy for adult-onset Still's disease," *Clinical Reviews in Allergy and Immunology*, vol. 58, no. 1, pp. 71–81, 2020.